Electronic Supplementary Material (ESI) for Dalton Transactions.

SUPPORTING INFORMATION

The core of the matter – arene substitution determines the coordination and catalytic behaviour of tris(1-phosphanyl-1'-ferrocenylene)arene gold(I) complexes

Axel Straube,[a] Peter Coburger,[b] Marvin Michak,[a] Mark Ringenberg,[c] and Evamarie Hey-Hawkins *[a]

Changing the aromatic core of C_3-symmetric tris(ferrocenyl)arene-based tris-phosphanes has profound effects on their coordination behaviour towards gold(I). Depending on the arene (*s*-triazine, benzene, or trifluorobenzene), four different coordination modes can be distinguished and their preference has been rationalised using computational methods. The corresponding 1:1 ligand-to-metal complexes, studied by variable-temperature NMR spectroscopy, revealed fluctional behaviour in solution. Given the presence of up to three or six ferrocenylene spacers per complex, their electrochemistry was investigated. The redox-responsive nature of the complexes can be advantageously exploited in the catalytic ring-closing isomerisation of *N*-(2-propyn-1-yl)benzamide, where the benzene-based 2:3 ligand-to-metal complex has been shown to display multiple activity states depending on the degree of (reversible) oxidation in a preliminary trial.

Table of Contents

1. Syntheses and characterisation ... 3
   1.1. General information ... 3
      Materials and methods ... 3
      Crystallography ... 3
      Electrochemistry ... 3
      Computational methods ... 4
   1.2. Synthetic procedures ... 4
   1.2.1. {1,3,5-Tris(1-diphenylphosphanyl-κ²*P¹*,*P²*-1'-ferrocenylene)benzene}gold(I) triflate (**[1b(Au)]OTf**) ... 4
   1.2.2. {2,4,6-Tris(1-diphenylphosphanyl-κ²*P¹*,*P²*-1'-ferrocenylene)-1,3,5-trifluorobenzene}gold(I) triflate (**[1c(Au)]OTf**) and *catena*-{[μ₃-2,4,6-Tris(1-diphenylphosphanyl-1κ¹*P¹*,2κ¹*P²*,3κ¹*P³*-1'-ferrocenylene)-1,3,5-trifluorobenzene]trigold(I)} triflate (**{[(1c)₂(Au)₃](OTf)₃}ₙ**) ... 8
   1.2.3. Bis{μ-1,3-bis(1-diphenylphosphanyl-2κ²*P¹*,*P²*-1'-ferrocenylene)-5-(1-diphenylphosphanyl-1κ¹*P³*-1'-ferrocenylene)benzene}trigold(I) triflate (**[(1b)₂(Au)₃](OTf)₃**) ... 13
   1.2.4. Bis{μ-4,6-bis(1-diphenylphosphanyl-2κ²*P¹*,*P²*-1'-ferrocenylene)-2-(1-diphenylphosphanyl-1κ¹*P³*-1'-ferrocenylene)-1,3,5-triazine}trigold(I) triflate (**[(1a)₂(Au)₃](OTf)₃**) ... 16
   1.2.5. 2,4,6-Tris{1-bis(pentafluorophenyl)phosphanyl-1'-ferrocenylene}-1,3,5-triazine (**1a^F**) ... 19
   1.2.6. [2,4,6-Tris{1-bis(pentafluorophenyl)phosphanyl-κ²*P¹*,*P²*-1'-ferrocenylene}-1,3,5-triazine]gold(I) triflate (**[1a^F(Au)]OTf**) ... 21
   1.2.7. [2,4,6-Tris{1-bis(pentafluorophenyl)phosphanyl-κ²*P¹*,*P²*-1'-ferrocenylene}-1,3,5-triazine]silver(I) triflate (**[1a^F(Ag)]OTf**) ... 24
   1.3. Catalytic tests ... 27
2. Single Crystal X-Ray Diffraction Analyses ... 28
   2.1. Crystallographic data ... 28
   2.2. Structural parameters ... 29
3. Variable-temperature NMR Spectra ... 32
4. DFT Calculations ... 38
5. Electrochemistry ... 40
   5.1. Scanning Speed Dependence of **[1b(Au)]OTf** and Decamethylferrocene – (Quasi)Reversibility ... 40
   5.2. Electrochemical Data of **1a^F**, **[1a^F(Ag)]OTf**, and **[1a^F(Au)]OTf** ... 40
6. Spectroelectrochemistry ... 43
7. Catalysis ... 45
   7.1. NMR Spectrum Stacks, Linear Fitting Plots, and Turn-Over Frequencies (TOF) ... 45
   7.2. Steric Characterisation of the Gold(I) Complexes by %Vol_{bur} ... 52
   7.3. Stoichiometric Oxidation of Gold(I) Complexes – NMR-spectroscopic Studies ... 54

Autor Contributions ... 58

References ... 58

DFT Coordinates of Optimised Structures ... 60

1. Syntheses and characterisation

1.1. General information

Materials and methods

All reactions and manipulations were carried out under an atmosphere of either nitrogen or argon using standard Schlenk line techniques unless stated otherwise. Thin-layer chromatography (TLC) with silica gel 60 F254 on glass or aluminium sheets available from Merck KGaA was used for monitoring the ligand synthesis. Column chromatography was performed using a Biotage Isolera 1 automatic purification system with SNAP Ultra cartridges (silica, spherical particle, diameter: 0.025 mm) using solvents purged with nitrogen prior to use. The fractions were detected by an integrated UV/Vis detector.
Molecular sieves (4 Å) were activated at 300 °C in vacuo for a minimum of 3 h. Dry, oxygen-free solvents (THF, CH_2Cl_2, Et_2O, hexanes, and toluene) were obtained from an MBraun Solvent Purification System MB SPS-800 and directly stored over 4 Å molecular sieves, except for THF, which was further distilled from potassium/benzophenone and stored over 4 Å molecular sieves. 1,2-Dichloroethane was degassed using the freeze-pump-thaw method and stored over 4 Å molecular sieves. CD_2Cl_2 and $CDCl_3$ were dried by stirring over P_2O_5 at room temperature for several days, followed by vacuum transfer into a storage flask, degassing by the freeze-pump-thaw method, and storage over 4 Å molecular sieves.
$(C_6F_5)_2PCl$,[1] (nBu$_4$N)[B{3,5-$C_6H_3(CF_3)_2$}$_4$] (= (nBu$_4$N)BAr$^F_4$),[2] [Fe(C_5H_4{C(O)CH_3})$_2$]BF_4 (= [Ac$_2$fc]BF_4, **5b**),[3] and *N*-prop-2-ynylbenzamide (**2**)[4] were synthesised as described in the literature. Ph_2PCl was distilled and stored under nitrogen prior to use. 2,4,6-Tris(1-bromo-1'-ferrocenylene)-1,3,5-triazine (**4a**), tris-phosphanes **1a**, **1b**, and **1c**, [Fe(C_5H_4{C(O)CH_3})$_2$][Al(OC{CF_3}$_4$)] (= [Ac$_2$fc][Teflonate], **5a**), **[1a(Au)]** as well as [Au(η^2-nbe)$_3$]OTf (nbe = norbornene) were prepared according to our previously published procedures.[5,6] All other chemicals were used as purchased.

NMR spectra were recorded with a BRUKER Avance III HD 400 MHz NMR spectrometer at 25 °C (frequencies of ^{1}H: 400.13 MHz; ^{11}B 128.38 MHz; ^{13}C 100.63 MHz; ^{19}F: 376.53 MHz; ^{31}P: 161.99 MHz). Pseudo-triplets and -quadruplets (due to additional coupling to heteronuclei like ^{19}F and ^{31}P) of ferrocenyl protons are abbreviated as pt/pq and their observable coupling constants *J* are given. Quintuplets are abbreviated as "quint". Assignment of ^{1}H and ^{13}C signals to the respective chemical entities are based on ^{1}H,^{1}H COSY, phase-sensitive ^{1}H,^{13}C HSQC and ^{1}H,^{13}C HMBC NMR experiments. TMS was used as the internal standard in the ^{1}H and ^{13}C{^{1}H}/^{13}C{^{31}P,^{1}H} NMR spectra, and spectra of all other nuclei were referenced to TMS using the Ξ scale.[7]
Electrospray ionisation (ESI) mass spectrometry was performed with an ESI ESQUIRE 3000 PLUS spectrometer with an IonTrap analyser from Bruker Daltonics, or a MicroTOF spectrometer from Bruker Daltonics with a ToF analyser in positive mode. As solvents for the measurements, pure CH_2Cl_2 or mixtures of CH_2Cl_2 and CH_3CN were used. Dry, oxygen-free solvents were used for air-sensitive species. Elemental analyses were performed with a VARIO EL elemental analyser from Heraeus. Melting points were determined with a Gallenkamp MPD350·BM2.5 melting point device and are reported uncorrected. FTIR spectra were obtained with a PerkinElmer FT-IR spectrometer Spectrum 2000 as KBr pellets and with a Thermo Scientific Nicolet iS5 with an ATR unit in the range from 4000 to 400 cm^{-1}. UV/Vis spectra were recorded on a PerkinElmer UV/Vis-NIR Lambda 900 spectrometer in quartz cuvettes (d = 10 mm). The sample concentration was $3\cdot10^{-5}$ mol·L^{-1}.

Crystallography

The data were collected on a Gemini-CCD diffractometer (RIGAKU INC.) using Mo-K_α radiation (λ=0.71073 Å), ω-scan rotation. Data reduction was performed with CrysAlis Pro[8] including the program SCALE3 ABSPACK[9] for empirical absorption correction. The structure solutions for **[1b(Au)]OTf**, **{[(1c)$_2$(Au)$_3$](OTf)$_3$}$_n$**, **[(1a)$_2$(Au)$_3$](OTf)$_3$**, **[(1b)$_2$(Au)$_3$](OTf)$_3$**, **[1a^F(Au)]OTf**, and **[1a^F(Ag)]OTf** were performed with SHELXS-97 (direct methods).[10] The anisotropic full-matrix least-squares refinement on F^2 of all non-hydrogen atoms was performed with SHELXL-97.[10] All non-hydrogen atoms were refined with anisotropic thermal parameters and the HFIX command was used to locate all hydrogen atoms for non-disordered regions of the structure. Structure figures were generated with Mercury (versions 3.8 and 3.10)[11] and POV-Ray (Version 3.7).[12] CCDC 2021517 (**[1a^F(Au)]OTf**), 2021518 (**[1a^F(Ag)]OTf**), 2021519 (**[1b(Au)]OTf**), 2021520 (**[(1a)$_2$(Au)$_3$](OTf)$_3$**), 2021521 (**[(1b)$_2$(Au)$_3$](OTf)$_3$**), 2021522 (**{[(1c)$_2$(Au)$_3$](OTf)$_3$}$_n$**) contain the supplementary crystallographic data for this paper. These data are provided free of charge by The Cambridge Crystallographic Data Centre.

Electrochemistry

Cyclic voltammetry (CV) measurements on 1.0 mmol·L^{-1} analyte solutions in dry, oxygen-free dichloromethane containing 0.1 mol·L^{-1} (nBu$_4$N)BF_4 or (nBu$_4$N)BAr$^F_4$ as supporting electrolyte have been conducted in a three-electrode setup (GAMRY Instruments, SP-50 potentiostat by BioLogic Science Instruments) under a blanket of nitrogen at room temperature. The glassy-carbon working electrode (ALS; surface area 0.07 cm^2) and the counter electrode (neoLab; platinum wire, 99.9%) were immersed in the analyte solution, while the reference electrode (ALS; Ag/$AgNO_3$ (0.01 mol·L^{-1}) in 0.1 mol·L^{-1} tetrabutylammonium hexafluorophosphate in dry, oxygen-free CH_3CN) was connected to the cell via a bridge tube (filled with the supporting electrolyte) through Vycor

tips. The reference electrode was calibrated against decamethylferrocene as an internal standard at the end of the CV experiment,[13] and the results were converted to the FcH/[FcH]$^+$ scale in accordance with the IUPAC requirements.[14]
Spectroelectrochemistry was performed using an optically transparent thin-layered electrode (OTTLE) cooled using a liquid nitrogen cryostat as described previously.[15]

Computational methods

All calculations were carried out with the ORCA program package.[16,17] All geometry optimisations were performed at the BP86-D3BJ/def2-TZVP[18–22] level of theory in the gas phase. For calculations involving gold, the respective effective core potentials, namely def2-ECP,[23] were used. Frequency calculations were carried out to confirm the nature of stationary points found by geometry optimisations. Density fitting techniques, also called resolution-of-identity approximation (RI),[24] were used for GGA calculations. Energy decomposition analyses (EDA) were conducted at the M06L-D3(0)/def2-TZVP[25] level of theory using the CPCM model for DCM.[26] Mulliken spin densities for **[1a]$^+$** and **[1a^F]$^+$** were calculated at the same level of theory by removing one electron from the optimised geometries. Starting geometries were derived from available solid-state molecular structures of **1a**, **1b**, **[1a(Au)]OTf**, and **[1b(Au)]OTf**; structures for **1c** and its gold(I) complexes were modelled from **1b**, and structures involving **1a^F** were modelled from **1a**, respectively. Cartesian coordinates of all structures are listed at the end of this document.

1.2. Synthetic procedures

1.2.1. {1,3,5-Tris(1-diphenylphosphanyl-κ^2*P*^{1},*P*^{2}-1'-ferrocenylene)benzene}gold(I) triflate ([1b(Au)]OTf)

In a Schlenk flask protected from direct light, 100 mg **1b** (84.6 µmol, 1.15 eq.) and 46.0 mg [Au(η^2-nbe)$_3$]OTf (73.5 µmol, 1.00 eq.) were dissolved in 15 mL CH_2Cl_2 under stirring. Stirring was continued overnight after which subjecting the reaction mixture to ^{31}P{^{1}H} NMR spectroscopy showed formation of the desired product. The reaction mixture was filtered *via* cannula and the volatiles were removed *in vacuo*. The solid orange residue was dried *in vacuo* for 20 min and washed with hexanes (2x 5 mL), yielding a fine yellow powder after drying. The raw product was completely dissolved in 25 mL THF, the solvent volume reduced to approx. ⅓ of the original volume and placed in the freezer (−25 °C) overnight. Filtration *via* cannula afforded the product as a crystalline orange solid which upon prolonged drying *in vacuo* at 40 °C turned into a fine yellow powder (69 mg, 62%). Crystals suitable for single-crystal X-ray diffraction analysis were obtained by tempering part of the polycrystalline solid obtained from the THF recrystallisation step at 70 °C followed by slowly cooling to 25 °C for two days.
Initial isolation attempts by removing excess **1b** and displaced norbornene by extraction with diethyl ether and crystallisation from CH_2Cl_2/toluene or hexanes did only result in the retrieval of an ill-defined amorphous substance. NMR spectra of this material (Fig. S6), indicative of at least two different *P,P*'-dicoordinated gold(I) centres and dynamic solution processes, suggested by severely broadened NMR spectral features, differed from those of the reaction mixture (Fig. S5).[27] This material could be a (mixture of) coordination polymer(s) containing **1b** in μ$_3$:κ^1*P*,κ^1*P*',κ^1*P*'' coordination mode; in a CHN analysis, the experimentally determined values were best fitted when assuming a 1:1 mixture of **[1b(Au)]OTf** and hypothetical **{[(1b)$_2$(Au)$_3$](OTf)$_3$}$_n$**, and mass spectrometric and NMR spectroscopic features resemble those of **{[(1c)$_2$(Au)$_3$](OTf)$_3$}$_n$** (*vide infra*).

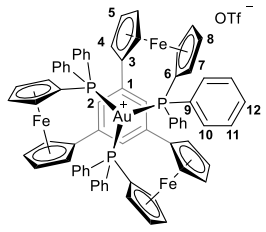

(Apparent high-temperature form, C_{3v})

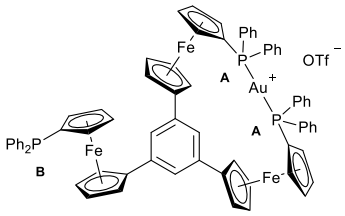

(Low-temperature and solid-state form, C_s)

Mp: 183–185 °C (from THF). Anal. calcd. for $C_{73}H_{57}AuF_3Fe_3O_3P_3S$: C 57.35, H 3.76, found: C 56.86, H 3.55%. UV/Vis (CH_2Cl_2), λ_{max} (ε): 447 (1500); 347sh (6200), 285sh (35800) nm (dm^3·mol^{-1}·cm^{-1}). IR (ATR, ṽ): 3054 (w), 2976 (w), 2856 (w, all ν(C–H)), 1595 (m), 1480 (m), 1435 (m, both ν(C–P)), 1386 (w), 1309 (w), 1257 (s), 1222 (s), 1150 (s), 1099 (s), 1063 (m), 1027 (s), 998 (m), 923 (m), 889 (m), 869 (m), 825 (m), 743 (s), 693 (vs), 636 (vs), 595 (m), 572 (m), 542 (m), 529 (s), 498 (vs), 475 (vs), 423 (s) cm^{-1}. ^{1}H NMR (CD_2Cl_2, 25 °C, δ): 7.58 (3 H, s, H2), 7.55–7.40 (30 H, m, H10–12), 4.84 (6 H, pt, J_{HH} = 2.0 Hz, H4), 4.60 (6 H, s(br), H7/8), 4.15 (6 H, pt, J_{HH} = 2.0 Hz, H5), 4.05 (6 H, s(br), H7/8).ppm. ^{13}C{^{1}H} NMR (CD_2Cl_2, 25 °C, δ): 138.3 (s, C1), 133.5 (m, C11), 131.2 (s, C12), 129.1 (s, C10), 122.6 (s, C2), 86.7 (s, C3), 75.9 (s (br), C7/8), 73.7 (s (br), C7/8), 70.8 (s, C5), 68.4 (s, C4) ppm[1]. ^{19}F{^{1}H} NMR (CD_2Cl_2, δ): −78.8 (s, O_3SCF_3) ppm. ^{31}P{^{1}H} NMR (CD_2Cl_2, 25 °C, δ): 24.6 (s(br), $\omega_{1/2}$ = 2000 Hz) ppm; (CD_2Cl_2, −60 °C, δ): 41.8 (2 P, s(br), $\omega_{1/2}$ = 89 Hz, P_A), −19.5 (1 P, s(br), $\omega_{1/2}$ = 138 Hz, P_B) ppm. HRMS (ESI-TOF, m/z): Calcd. for $C_{72}H_{52}AuFe_3P_3$ 1379.1388; found 1379.1368 [M−OTf]$^+$.

[1] The signals for quaternary carbon atoms C6 and C9 are not distinguishable from the baseline, owing to a combination of $^1J_{CP}$ coupling and the dynamics of the complex.

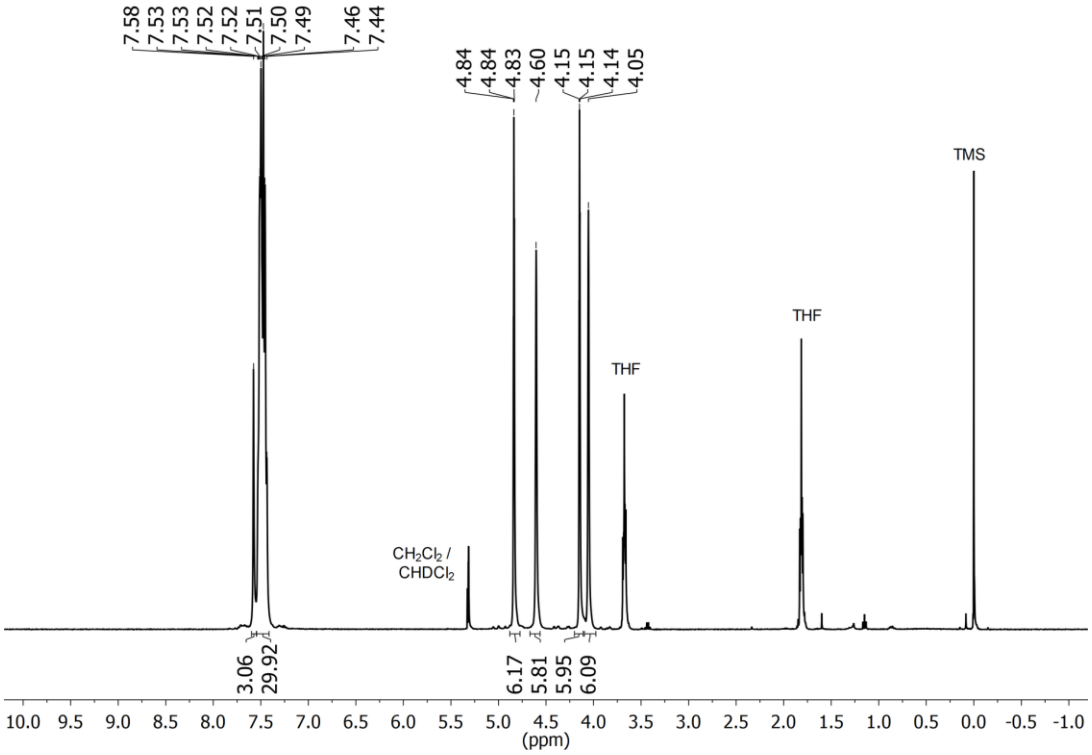

Figure S1 ^{1}H NMR spectrum of **[1b(Au)]OTf** in CD_2Cl_2 recorded at 25 °C. Residual solvent of crystallisation, THF, is correspondingly labelled.

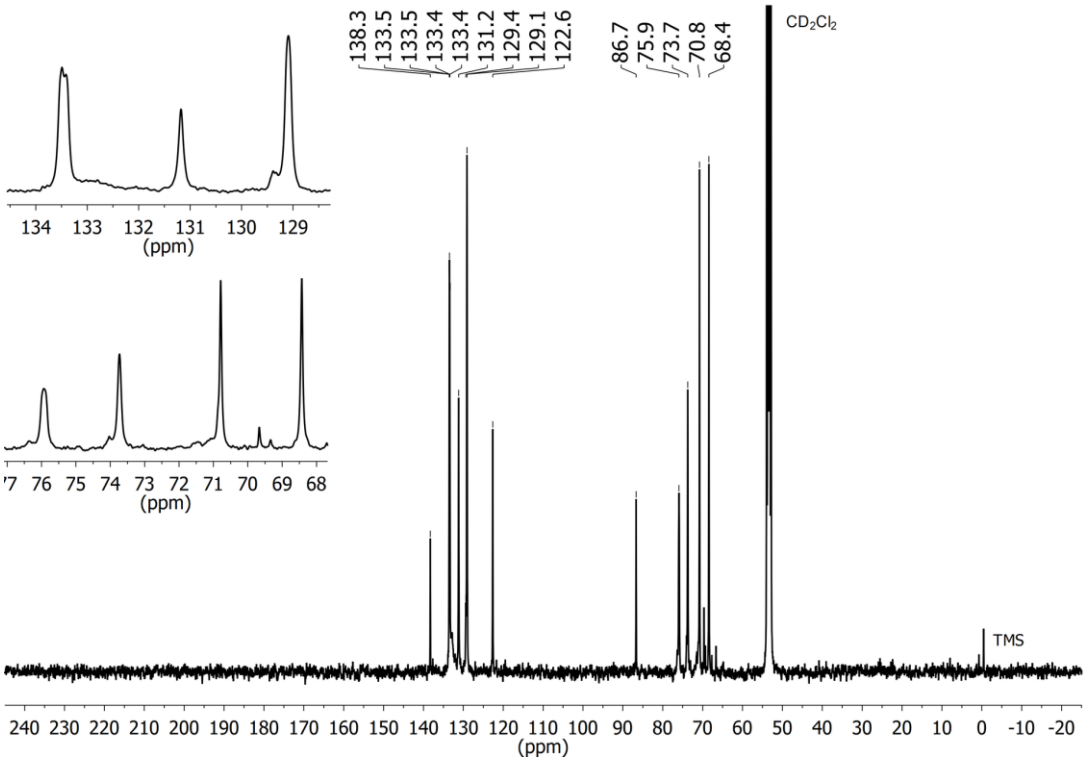

Figure S2 $^{13}C\{^{1}H\}$ NMR spectrum of **[1b(Au)]OTf** in CD_2Cl_2 recorded at 25 °C. The two inserts show magnifications of the spectral regions of the *P*-bound phenyl rings (top) and the ferrocenylene moieties (bottom).

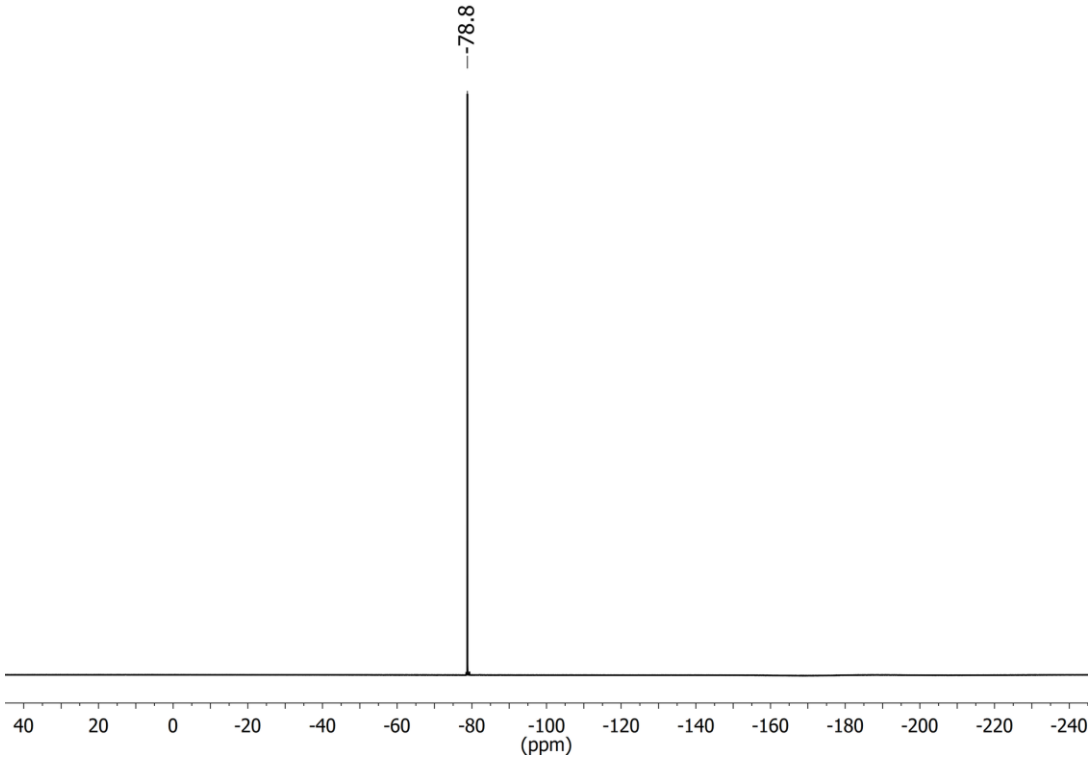

Figure S3 $^{19}F\{^{1}H\}$ NMR spectrum of **[1b(Au)]OTf** in CD_2Cl_2 recorded at 25 °C.

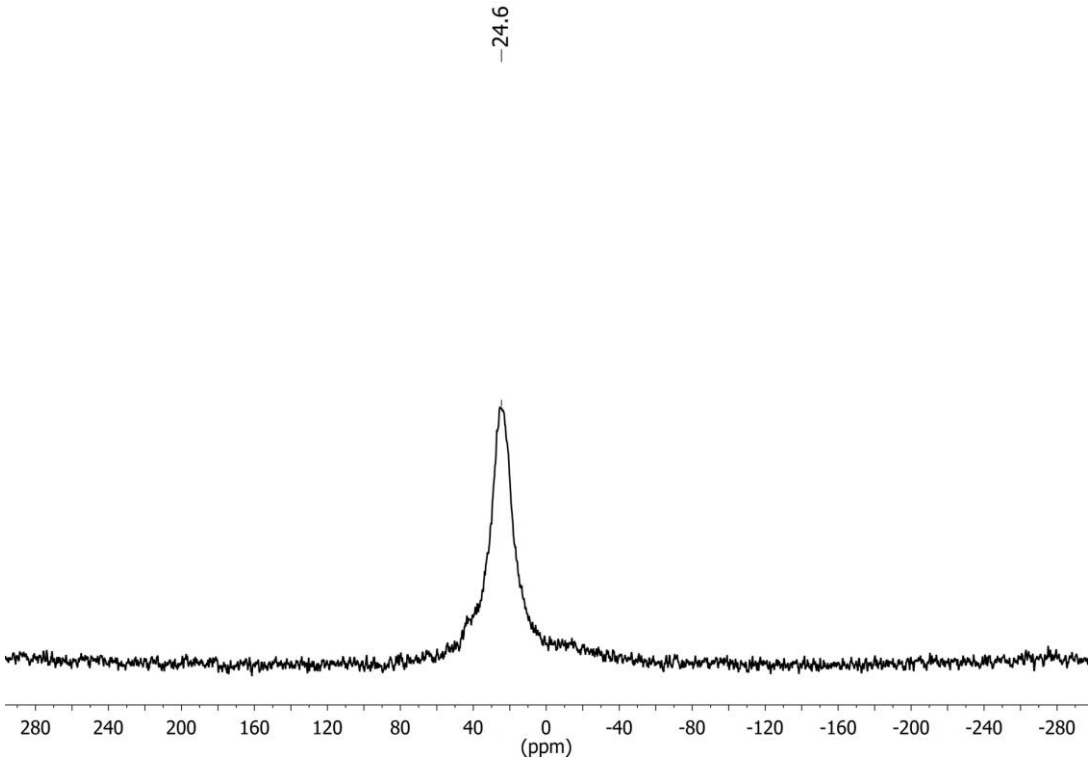

Figure S4 $^{31}P\{^{1}H\}$ NMR spectrum of **[1b(Au)]OTf** in CD_2Cl_2 recorded at 25 °C. For the graphic representation, exponential line broadening of lb = 50 Hz has been applied.

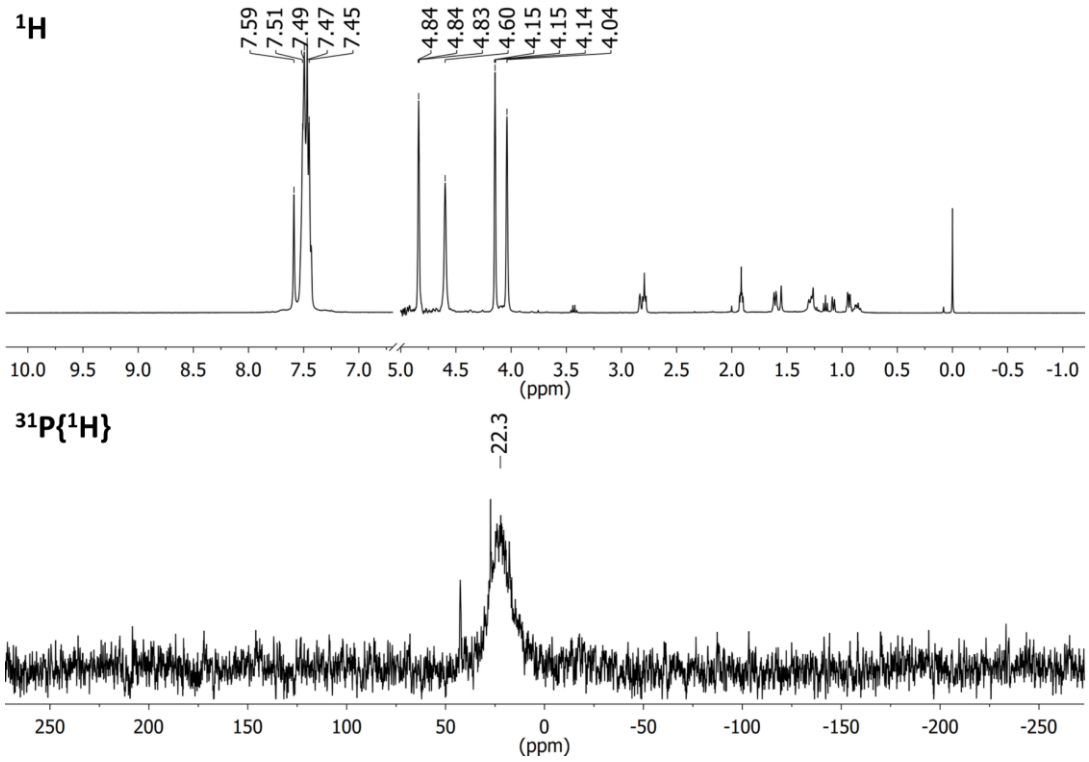

Figure S5 ^{1}H (top) and ^{31}P{^{1}H} (bottom) NMR spectra of the reaction mixture of **1b** and [Au(η^{2}-nbe)$_{3}$]OTf in CH_2Cl_2/CD_2Cl_2 (corresponding resonances not shown) recorded at 25 °C.

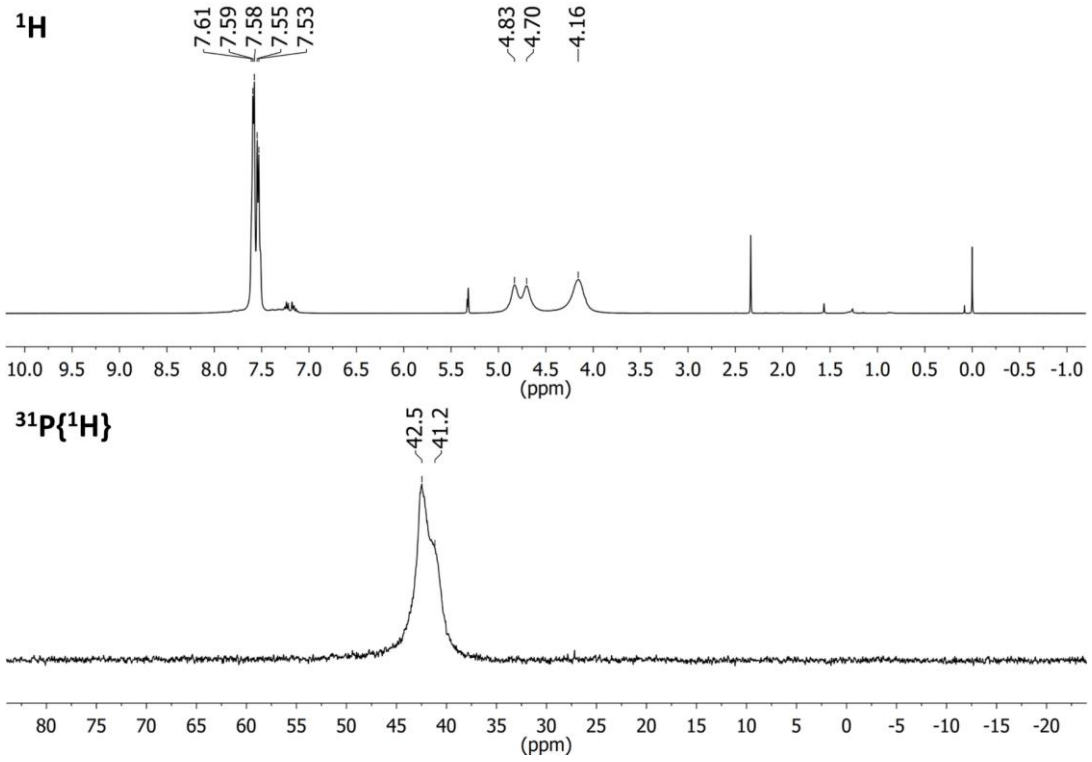

Figure S6 ^{1}H (top) and ^{31}P{^{1}H} (bottom) NMR spectra of the ill-defined precipitate obtained from attempted purification of **[1b(Au)]OTf** by crystallisation from CH_2Cl_2/toluene in CD_2Cl_2 recorded at 25 °C (compare to NMR spectra of **{[(1c)$_2$(Au)$_3$](OTf)$_3$}$_n$** (*vide infra*)).

1.2.2. {2,4,6-Tris(1-diphenylphosphanyl-κ²*P*¹,*P*²-1'-ferrocenylene)-1,3,5-trifluorobenzene}gold(I) triflate ([1c(Au)]OTf) and *catena*-{[μ₃-2,4,6-Tris(1-diphenylphosphanyl-1κ¹*P*¹,2κ¹*P*²,3κ¹*P*³-1'-ferrocenylene)-1,3,5-trifluorobenzene]trigold(I)} triflate ({[(1c)₂(Au)₃](OTf)₃}ₙ)

[1c(Au)]OTf was prepared by the same procedure as **[1b(Au)]OTf**, reacting 90.0 mg **1c** (72.8 µmol, 1.20 eq.) and 38.0 mg [Au(η²-nbe)₃]OTf (60.6 µmol, 1.00 eq.) in 6 mL CH_2Cl_2. Layering half of the filtered reaction mixture (diluted to 4 mL with CH_2Cl_2) with toluene (10 mL) and storing it at 7 °C overnight yielded an orange oil. After washing with hexanes (2 mL) and drying *in vacuo*, a sample of **[1c(Au)]OTf** sufficiently pure for NMR was obtained (no yield was determined).
Attempting the crystallisation of **[1c(Au)]OTf** by removing the volatiles of half of the filtered reaction *in vacuo* and re-dissolution in 9 mL THF (storage at 7 °C and −25 °C) did not yield any solid. Concentrating the sample *in vacuo* to about a third of its original volume, heating it to 70 °C in a closed Schlenk flask and slowly cooling it to 25 °C over two days yielded crystals suitable for single-crystal X-ray diffraction analysis which were found to be the newly formed coordination polymer **{[(1c)₂(Au)₃](OTf)₃}ₙ**.

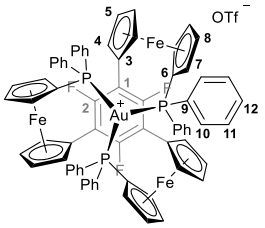

(Apparent high-temperature form, C_{3v})

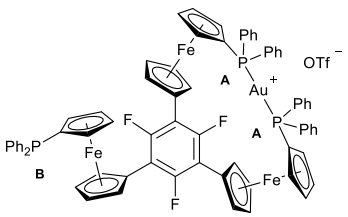

(Low-temperature form, *Cs*)

^{1}H NMR (CD_2Cl_2, δ): 7.56–7.23 (30 H, m, H10–12), 4.79 (6 H, s, H4), 4.68 (6 H, s, H7/8), 4.27 (6 H, s, H7/8), 4.21 (6 H, m, H5) ppm. ^{13}C{^{1}H} NMR (CD_2Cl_2, δ): 155.5 (dt, $^1J_{CF}$ = 253.6 Hz, $^4J_{CF}$ = 10.2 Hz, C2), 133.4 (m, C11), 132.9 (m(br), C9), 131.0 (s, C12), 129.0 (m, C10), 111.8 (m, C1), 75.3 (m, C7/8), 75.0 (s, C3), 73.9 (s, C7/8), 72.0 (m(br), C6), 71.4 (t, $^4J_{CF}$ = 4.7 Hz, C4), 70.5 (s, C5) ppm. ^{19}F{^{1}H} NMR (CD_2Cl_2, δ): −78.8 (3 F, s, O_3SCF_3), −106.4 (3 F, s(br), $\omega_{1/2}$ = 97 Hz, C_6F_3) ppm. ^{31}P{^{1}H} NMR (CD_2Cl_2, 25 °C, δ): 24.2 (s(br), $\omega_{1/2}$ = 1530 Hz); (CD_2Cl_2, −50 °C, δ): 40.5 (2 P, s(br), $\omega_{1/2}$ = 130 Hz, P_A), −19.6 (1 P, s(br), $\omega_{1/2}$ = 252 Hz, P_B) ppm. HRMS (ESI-TOF, m/z): Calcd. for $C_{72}H_{54}F_3Fe_3P_3$ 1433.1106; found 1433.1142 [M−OTf]$^+$.

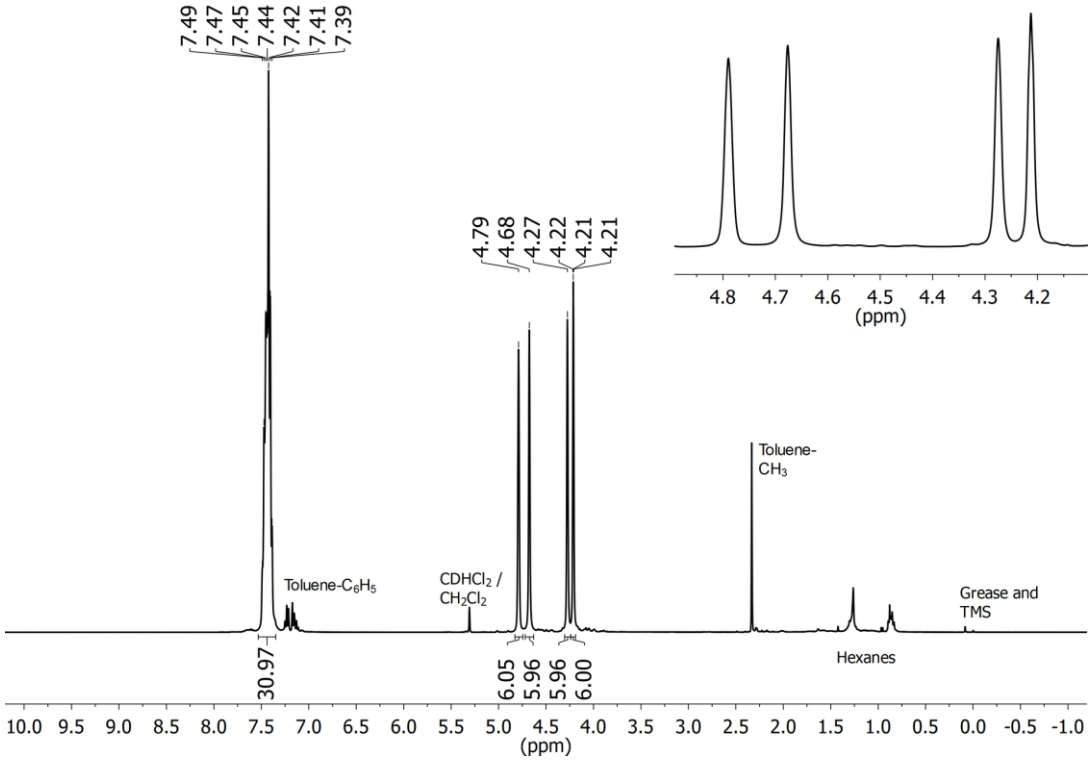

Figure S7 ^{1}H NMR spectrum of **[1c(Au)]OTf** in CD_2Cl_2 recorded at 25 °C. The insert shows a magnification of the ferrocenylene resonances.

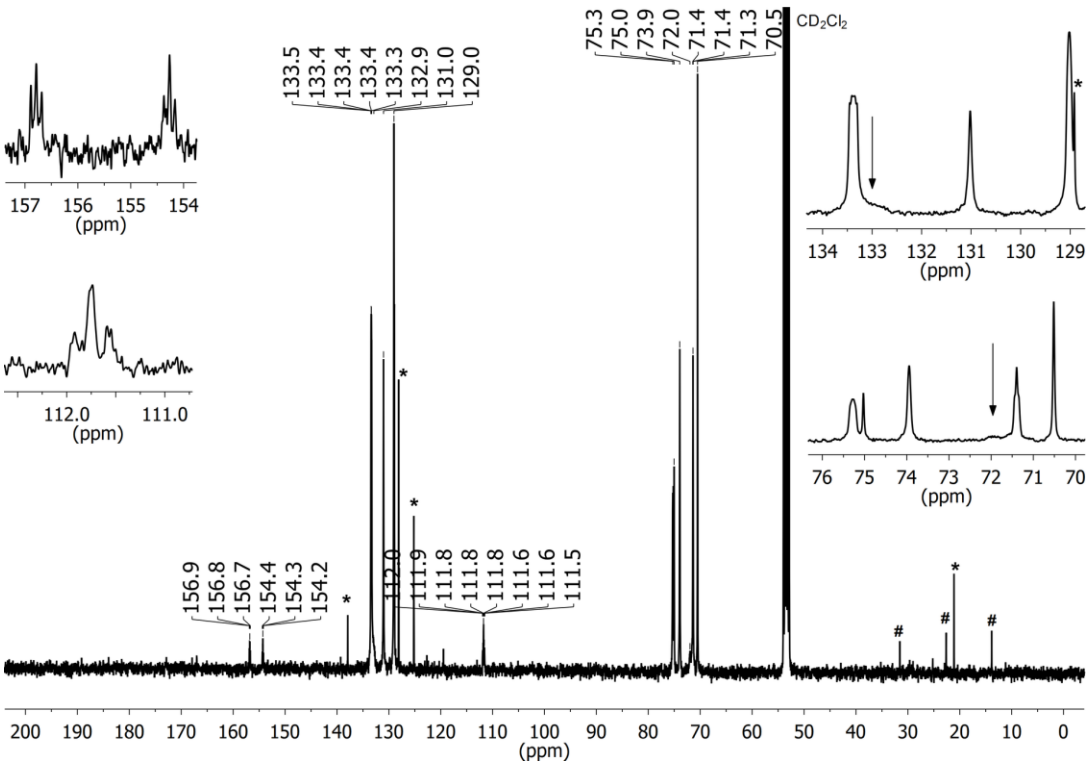

Figure S8 $^{13}C\{^{1}H\}$ NMR spectrum of **[1c(Au)]OTf** in CD_2Cl_2 recorded at 25 °C. The inserts show magnifications of the spectral regions of the C_6F_3 core (left), of the *P*-bound phenyl rings (top right) and of the ferrocenylene moieties (bottom right). Signals marked with an asterisk (*) correspond to toluene, signals marked with the hashtag symbol (#) correspond to hexanes. The two arrows point towards severely broadened resonances of quaternary carbon atoms.

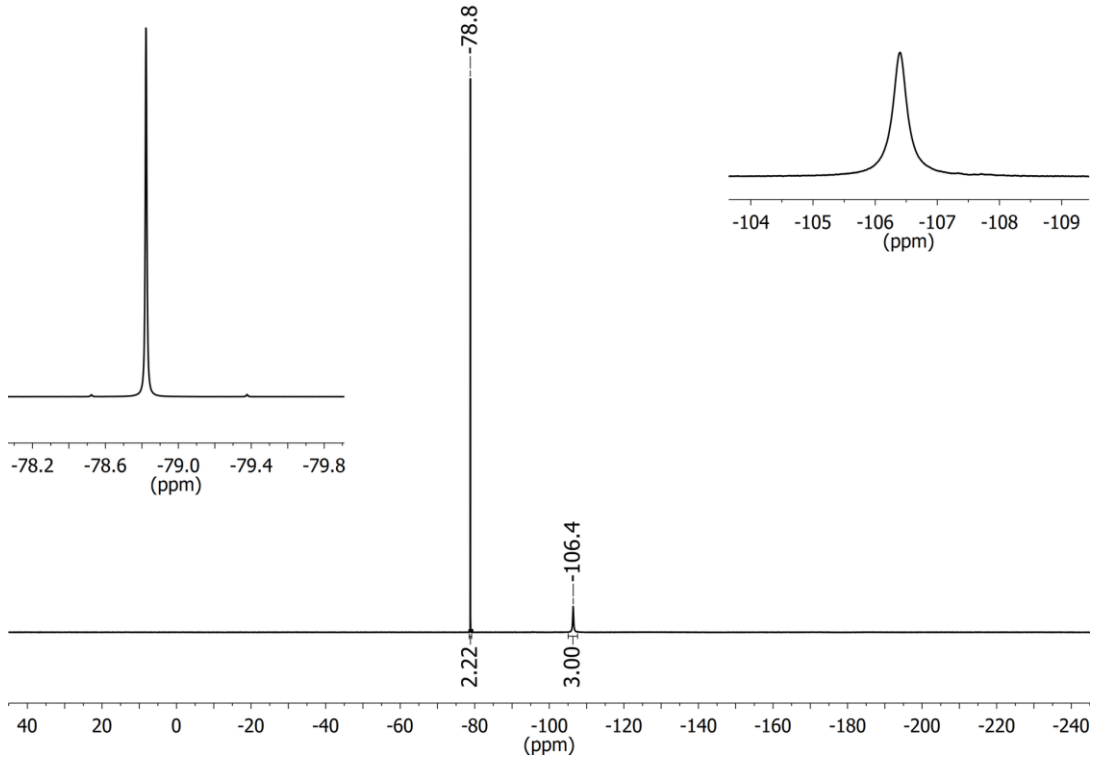

Figure S9 $^{19}F\{^{1}H\}$ NMR spectrum of **[1c(Au)]OTf** in CD_2Cl_2 recorded at 25 °C. The inserts show magnifications of the triflate CF_3 (left) and the trifluorobenzene core (right) resonances. The triflate integral is slightly underestimated with respect to the expected relative value of 3.00.

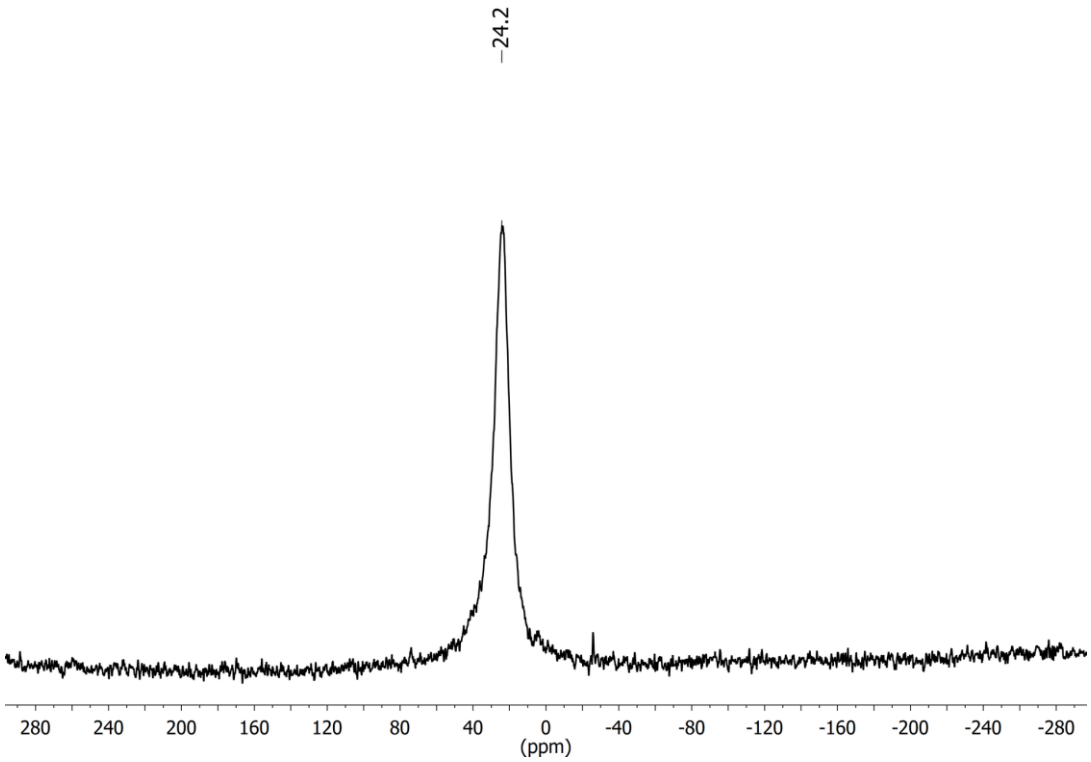

Figure S10 $^{31}P\{^{1}H\}$ NMR spectrum of **[1c(Au)]OTf** in CD_2Cl_2 recorded at 25 °C. For the graphic representation, exponential line broadening of lb = 50 Hz has been applied.

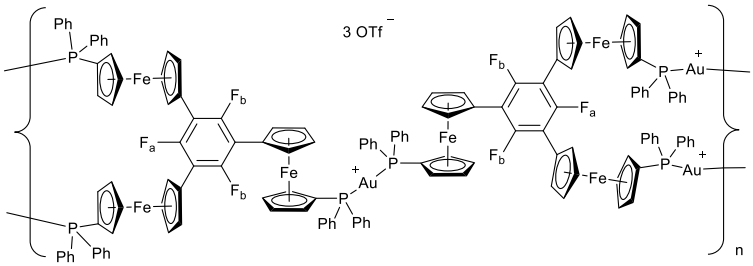

^{1}H NMR (CD_2Cl_2, δ): 8.23–7.06 (30 H, m, $P(C_6H_5)_2$), 4.79 (6 H, s(br), $\omega_{1/2}$ = 13.5 Hz, C_5H_4), 4.40 (12 H, m, C_5H_4), 4.18 (6 H, s(br), $\omega_{1/2}$ = 29.1 Hz, C_5H_4) ppm. $^{13}C\{^{1}H\}$ NMR (CD_2Cl_2, δ): 155.6 (d, $^{1}J_{CF}$ = 254.6 Hz, *C*F_b), *141.1* (s, C_6F_3)[2], 133.5 (s, $P(C_6H_5)_2$), 132.4 (s, $P(p\text{-}C_6H_5)_2$), 130.0 (s(br), $P(i\text{-}C_6H_5)_2$), 129.6 (s, $P(C_6H_5)_2$), *121.1* (d, $^{1}J_{CF}$ = 321.0 Hz, *C*F_a)[2], 111.6 (m, C_6F_3), 75.6 (m(br), C_5H_4)[3], 75.4 (s, C_5H_4), 74.8 (m(br), C_5H_4), 71.6 (s, C_5H_4), 70.9 (s, C_5H_4) ppm. $^{19}F\{^{1}H\}$ NMR (CD_2Cl_2, δ): −78.7 (3 F, s, O_3SCF_3), −101.7 (1 F, s(br), $\omega_{1/2}$ = 268 Hz, F_a), −108.1 (2 F, s(br), $\omega_{1/2}$ = 135 Hz, F_b) ppm. $^{31}P\{^{1}H\}$ NMR (CD_2Cl_2, δ): 41 (s(br), $\omega_{1/2}$ = 262 Hz) ppm. HRMS (ESI-TOF, m/z): Calcd. for $C_{144}H_{108}F_6Fe_6P_6$ 1021.3969; found 1021.3969 $[Au_3(1c)_2]^{3+}$; calcd. for $C_{145}H_{108}F_9Fe_6O_3P_6S$ 1606.5716, found 1606.5745 $[Au_3(1c)_2(OTf)]^{3+}$.

[2] Two of the four expected ^{13}C NMR signals for the C_6F_3 core of the coordination polymer are not unambiguously identifiable and are hence given in italics.

[3] Only five ^{13}C NMR resonances have been identified; given the possible dynamic of the structure, they are just listed and not assigned to specific carbon atoms.

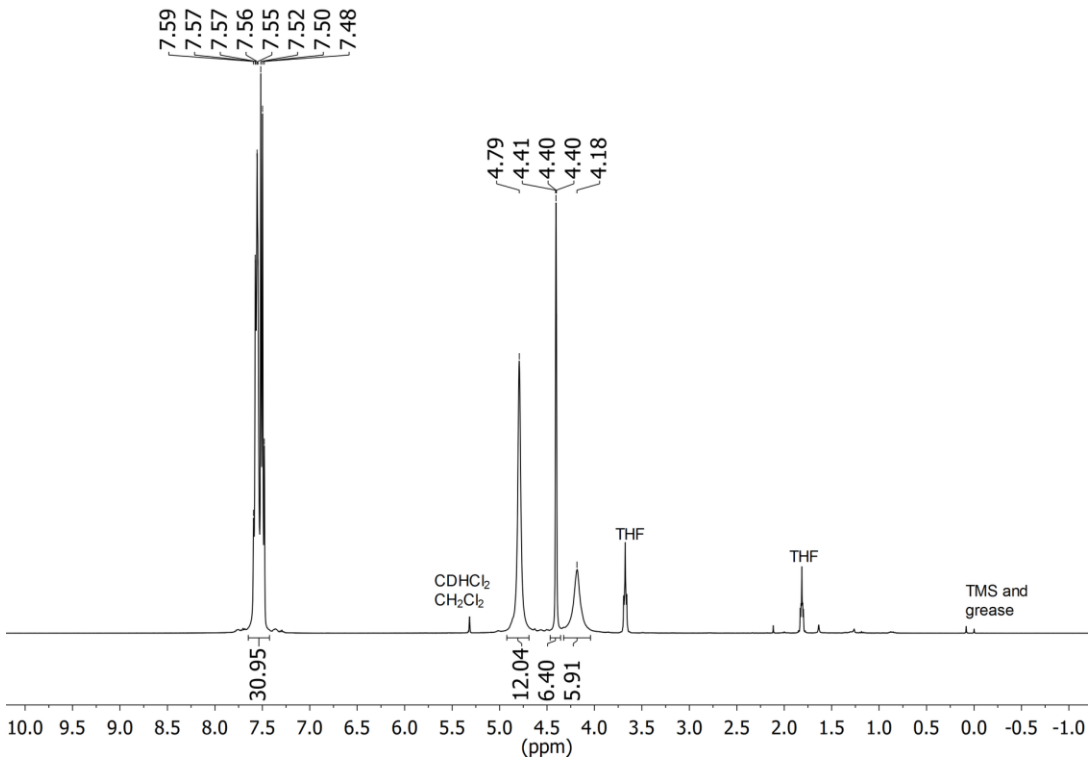

Figure S11 ^{1}H NMR spectrum of the solution of **{[(1c)$_2$(Au)$_3$](OTf)$_3$}$_n$** in CD_2Cl_2 recorded at 25 °C.

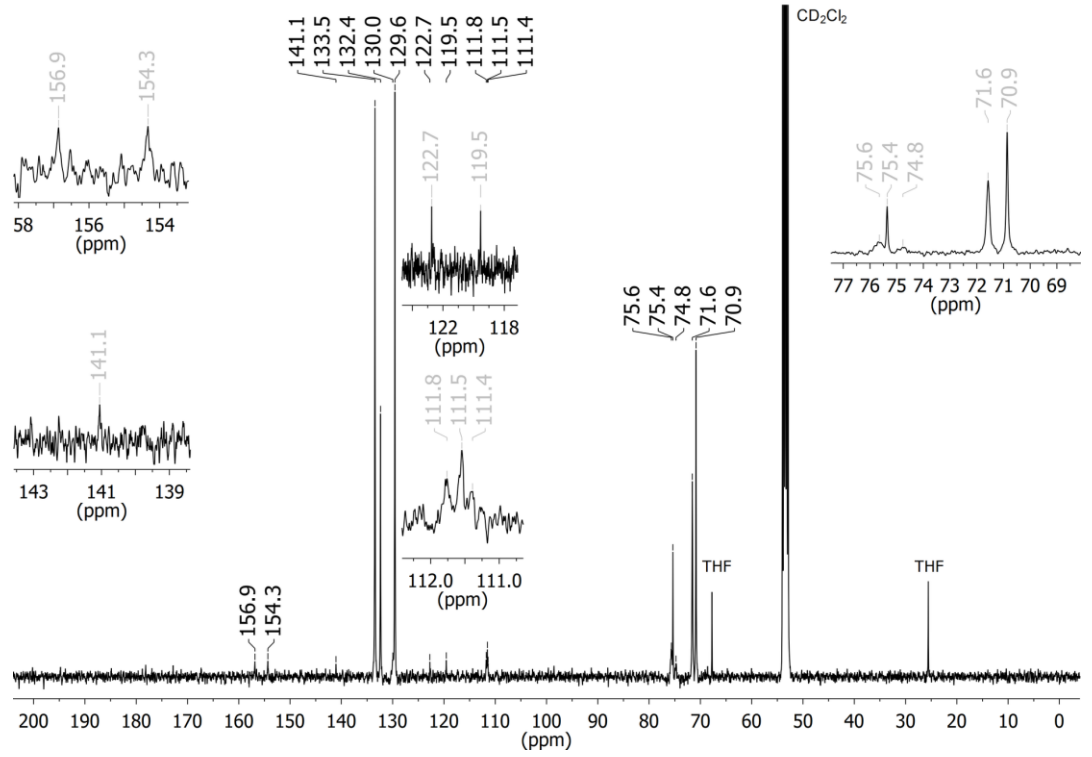

Figure S12 $^{13}C\{^{1}H\}$ NMR spectrum of the solution of **{[(1c)$_2$(Au)$_3$](OTf)$_3$}$_n$** in CD_2Cl_2 recorded at 25 °C. The inserts show magnifications of the spectral regions of the C_6F_3 cores (left and centre) and of the ferrocenylene moieties (right).

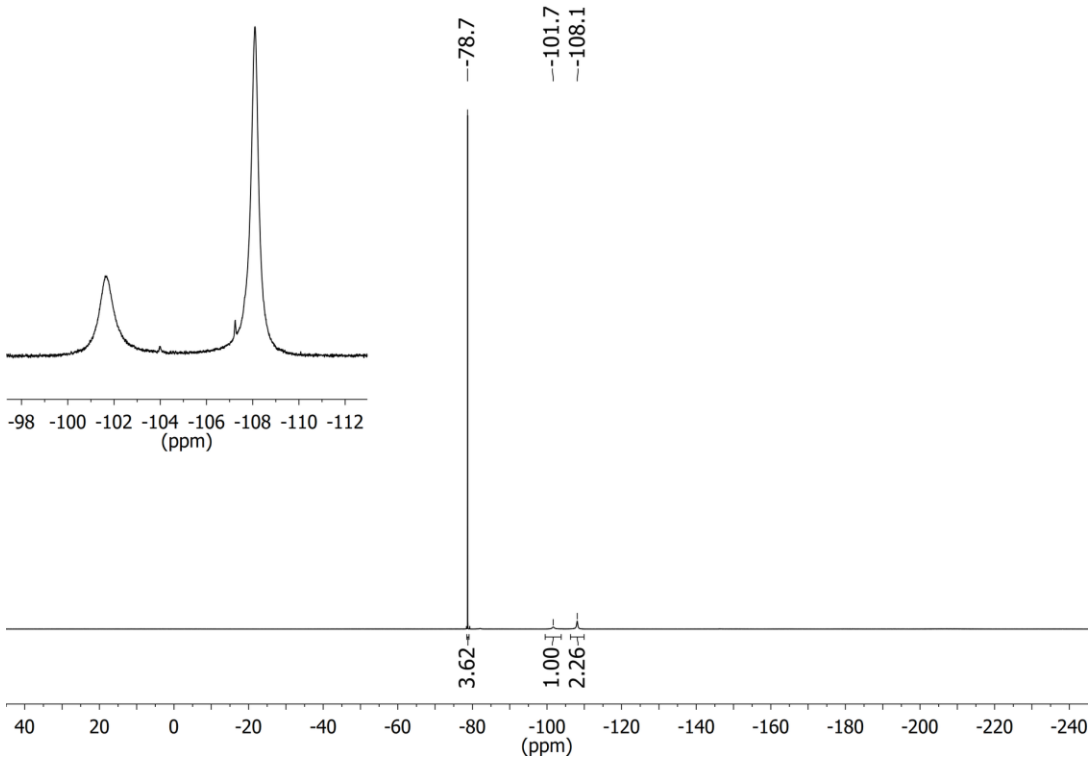

Figure S13 $^{19}F\{^{1}H\}$ NMR spectrum of the solution of **{[(1c)$_2$(Au)$_3$](OTf)$_3$}$_n$** in CD_2Cl_2 recorded at 25 °C. The insert shows a magnification of the spectral region corresponding to the C_6F_3 cores.

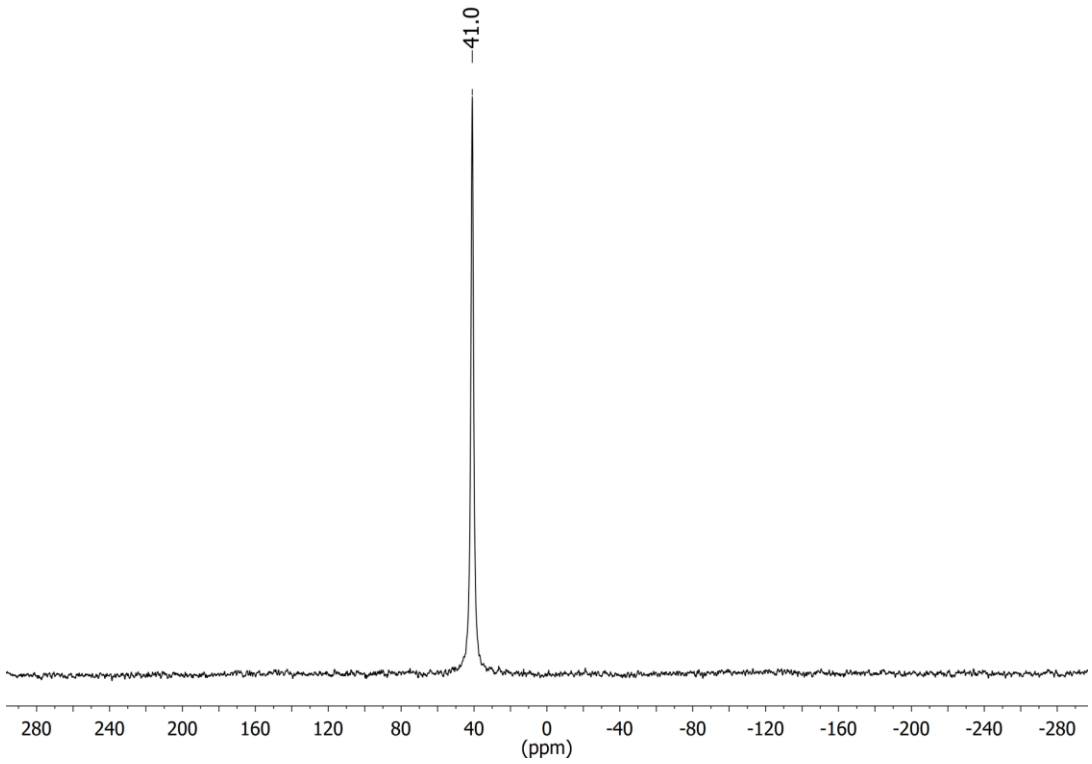

Figure S14 $^{31}P\{^{1}H\}$ NMR spectrum of the solution of **{[(1c)$_2$(Au)$_3$](OTf)$_3$}$_n$** in CD_2Cl_2 recorded at 25 °C. For graphic representation, exponential line broadening of lb = 50 Hz has been applied (no splitting or fine structure is recognisable at lower apodisation values).

1.2.3. Bis{μ-1,3-bis(1-diphenylphosphanyl-2κ²*P*¹,*P*²-1'-ferrocenylene)-5-(1-diphenylphosphanyl-1κ¹*P*³-1'-ferrocenylene)benzene}trigold(I) triflate ([(1b)₂(Au)₃](OTf)₃)

In a Schlenk flask protected from direct light, 94.0 mg **1b** (79.5 µmol, 1.00 eq.) and 75.0 mg [Au(η²-nbe)₃]OTf (119 µmol, 1.50 eq.) were dissolved in 10 mL CH_2Cl_2 under stirring. Stirring was continued overnight after which subjecting the reaction mixture to $^{31}P\{^1H\}$ NMR spectroscopy showed formation of **[(1b)₂(Au)₃](OTf)₃**. The reaction mixture was filtered *via* cannula and the volatiles were removed *in vacuo*. The solid orange residue was washed with diethyl ether (2x 5 mL), re-dissolved in 2 mL CH_2Cl_2, layered with 10 mL toluene, and stored at 7 °C for two days. So-obtained crystals proved suitable for single-crystal X-ray diffraction analysis. Prolonged drying *in vacuo* at 40 °C yielded **[(1b)₂(Au)₃](OTf)₃** as a fine orange powder (100 mg, 74%).

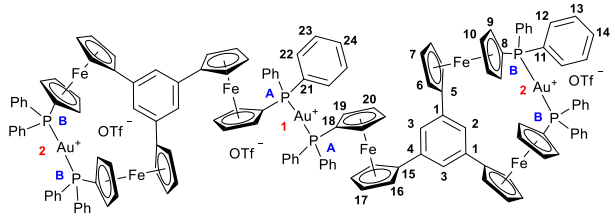

Mp: >230 °C (decomp.; from CH_2Cl_2/toluene). Anal. calcd. for $C_{147}H_{114}Au_3F_9Fe_6O_9P_3S_3$: C 51.88, H 3.38, found: C 51.90, H 3.35%. UV/Vis (CH_2Cl_2), λ_{max} (ε): 445 (3100), 352sh (11800), 286 (71400) nm ($dm^3 \cdot mol^{-1} \cdot cm^{-1}$). IR (KBr, $\tilde{\nu}$): 3094 (w), 3053 (w), 2929 (w), 2850 (w, all ν(C–H)), 2000–1700 (aromatic overtones), 1632 (w), 1595 (m), 1480 (w), 1435 (m, ν(C–P)), 1387 (w), 1308 (w), 1264 (vs), 1222 (m), 1150 (s), 1100 (m), 1029 (s), 998 (m), 922 (w), 870 (w), 827 (m), 748 (m), 694 (s), 636 (s), 571 (w), 544 (w), 515 (m), 500 (s), 477 (m), 426 (w) cm^{-1}. ^1H NMR (CD_2Cl_2, δ): 7.92 (2 H, t, $^4J_{HH}$ = 1.6 Hz, H2), 7.70–7.48 (60 H, m, H12–14+H22–24), 7.19 (4 H, d, $^4J_{HH}$ = 1.6 Hz, H3), 4.90 (8 H, pt, J_{HH} = 1.9 Hz, H6/7), 4.78 (8 H, pt, J_{HH} = 1.9 Hz, H9), 4.66 (4 H, pt, J_{HH} = 1.8 Hz, H16/17), 4.54 (4 H, pt, J_{HH} = 1.8 Hz, H20), 4.43 (4 H, m, H19), 4.35 (4 H, pt, J_{HH} = 1.8 Hz, H16/17), 4.12 (8 H, m, H10), 4.06 (8 H, pt, J_{HH} = 1.9 Hz, H6/7) ppm. $^{13}C\{^{31}P,^1H\}$ NMR (CD_2Cl_2, δ): 138.7 (s, C1), 138.4 (s, C4), 133.4 (s, C13), 133.3 (s, C23), 132.5 (s, C24), 132.3 (s, C14), *131.0* (m, C21)[4], *130.7* (m, C11)[4], 129.6 (s, C22), 129.4 (s, C12), 123.3 (s, C2), 123.2 (s, C3), 87.6 (s, C5), 87.5 (s, C15), 77.3 (s, C20), 77.2 (s, C10), 75.2 (s, C19), 74.8 (s, C9), 71.9 (s, C16/17), 71.7 (s, C6/7), *69.5* (m, C8)[5],

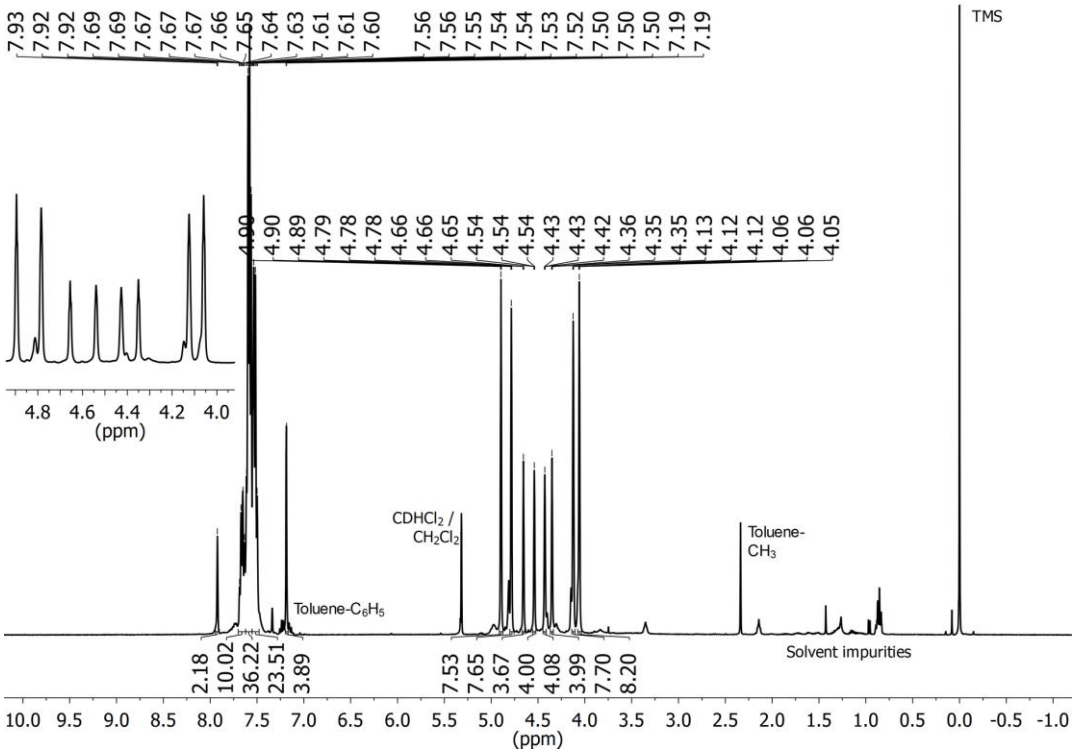

Figure S15 ^1H NMR spectrum of **[(1b)₂(Au)₃](OTf)₃** in CD_2Cl_2 recorded at 25 °C. The insert shows a magnification of the ferrocenylene resonances.

[4] The signals attributable to quaternary carbon atoms C11 and C21 have been assigned using the *P*-coupled $^{13}C\{^1H\}$ NMR spectrum in which their intensities are greater than in the corresponding $^{13}C\{^{31}P,^1H\}$ NMR spectrum.

[5] The signals for quaternary, *P*-bound carbon atoms C8 and C18 have been assigned using the *P*-coupled $^{13}C\{^1H\}$ NMR spectrum in which their intensities are greater than in the corresponding $^{13}C\{^{31}P,^1H\}$ NMR spectrum as well as making use of correlations found in the $^1H,^{13}C$ HMBC experiment through their coupling to protons H9 and H19.

69.2 (s, C6/7), 68.9 (s, C16/17), *68.2* (m, C18)[5] ppm. $^{19}F\{^1H\}$ NMR (CD_2Cl_2, δ): −78.6 (s, O_3SCF_3) ppm. $^{31}P\{^1H\}$ NMR (CD_2Cl_2, δ): 42.5 (2 P, P_B), 41.1 (1 P, P_A) ppm. HRMS (ESI-TOF, m/z): Calcd. for $C_{144}H_{114}Au_3Fe_6P_3$ 985.4157; found 985.4163 $[M-3OTf]^{3+}$.

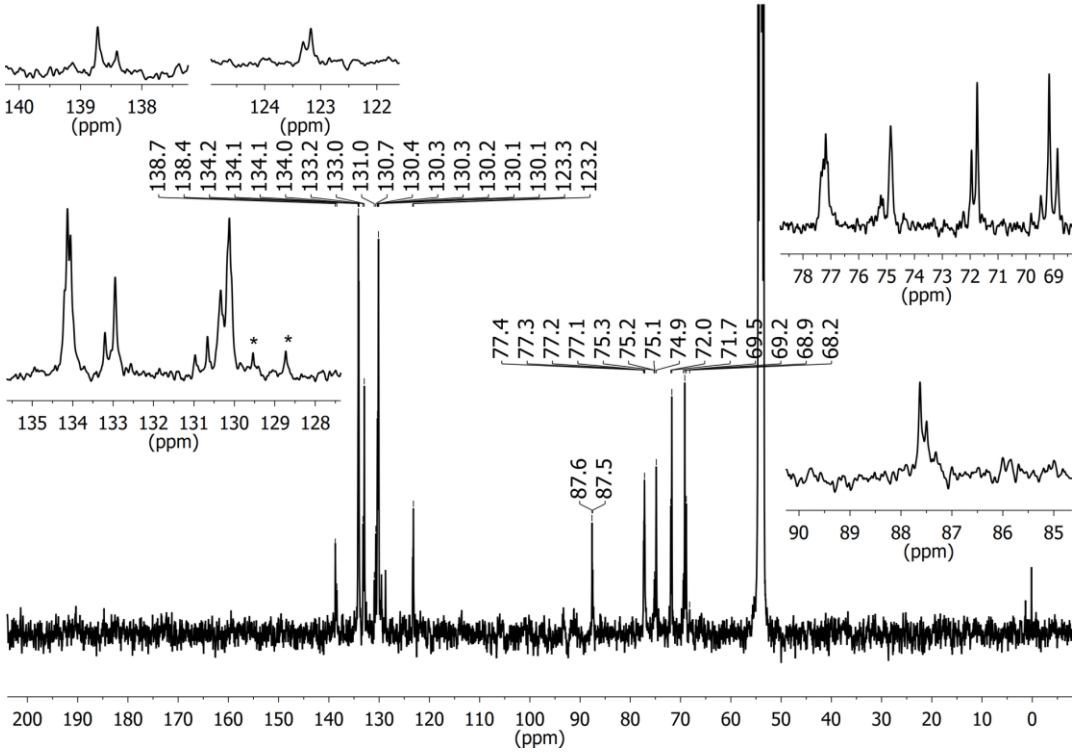

Figure S16 $^{13}C\{^1H\}$ NMR spectrum of **[(1b)$_2$(Au)$_3$](OTf)$_3$** in CD_2Cl_2 recorded at 25 °C. The inserts show magnifications of the benzene core regions (top left), of the *P*-bound phenyl rings (bottom left, signals labelled by asterisk (*) are presumably not part of **[(1b)$_2$(Au)$_3$](OTf)$_3$**), and of the ferrocenylene regions (right).

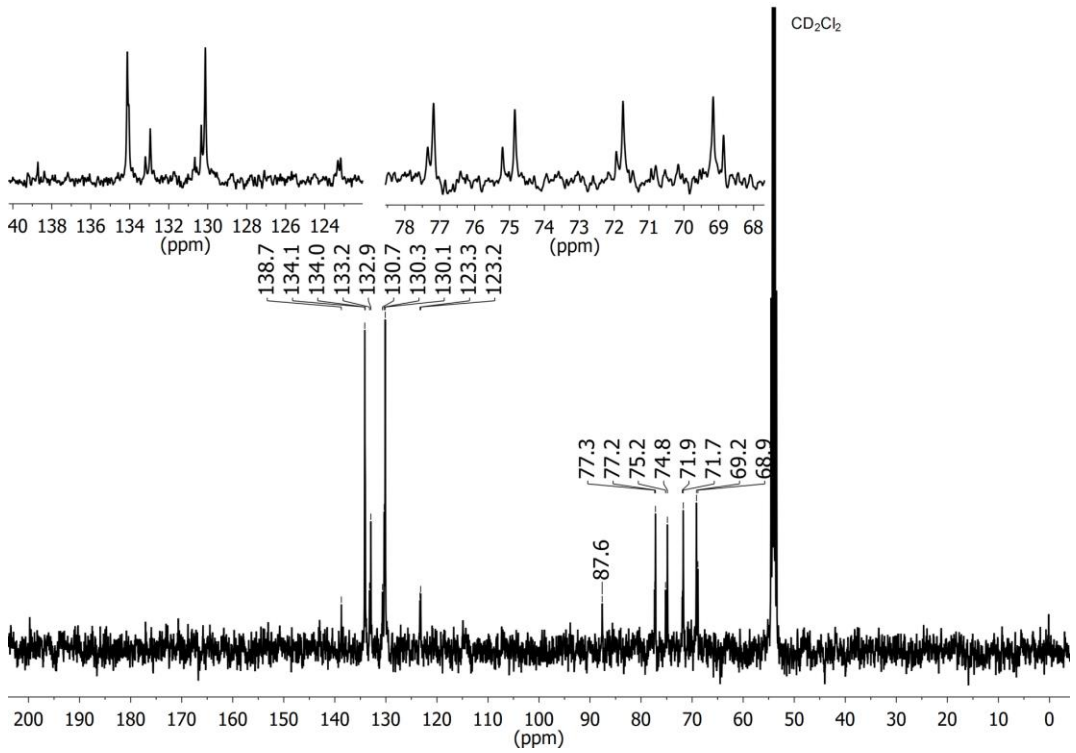

Figure S17 $^{13}C\{^{31}P,^1H\}$ NMR spectrum of **[(1b)$_2$(Au)$_3$](OTf)$_3$** in CD_2Cl_2 recorded at 25 °C. The inserts show magnifications of the *P*-bound phenyl rings (left) and of the ferrocenylene region (right).

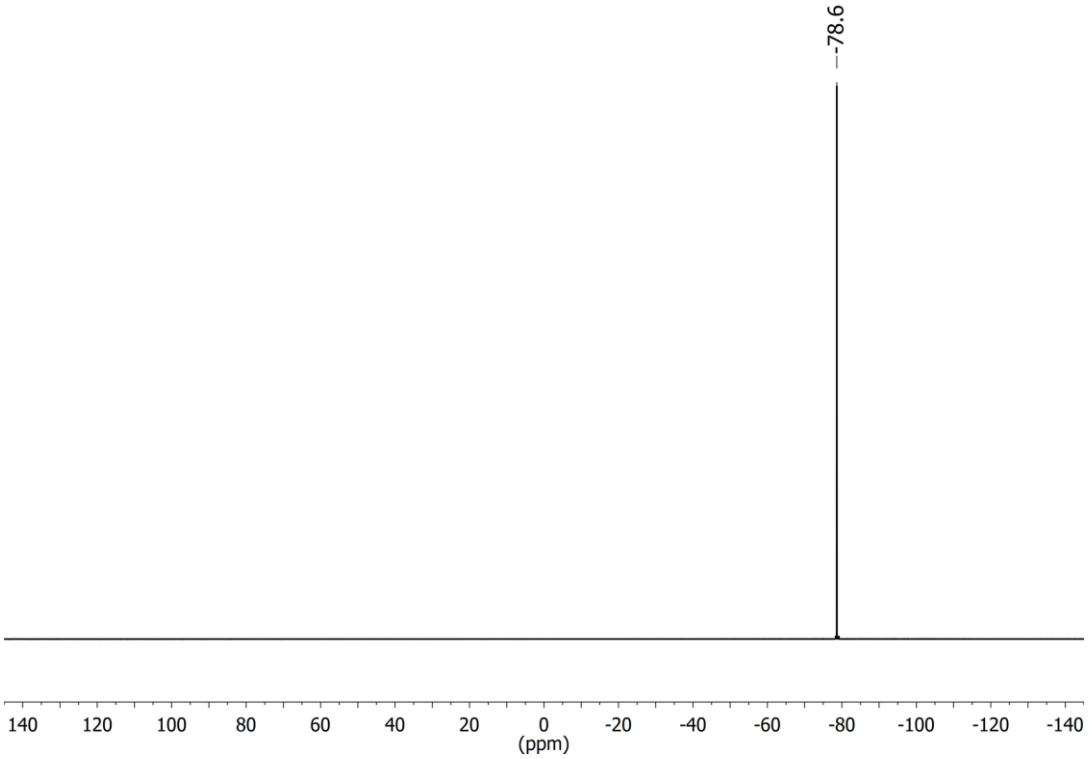

Figure S18 $^{19}F\{^{1}H\}$ NMR spectrum of **$[(1b)_2(Au)_3](OTf)_3$** in CD_2Cl_2 recorded at 25 °C.

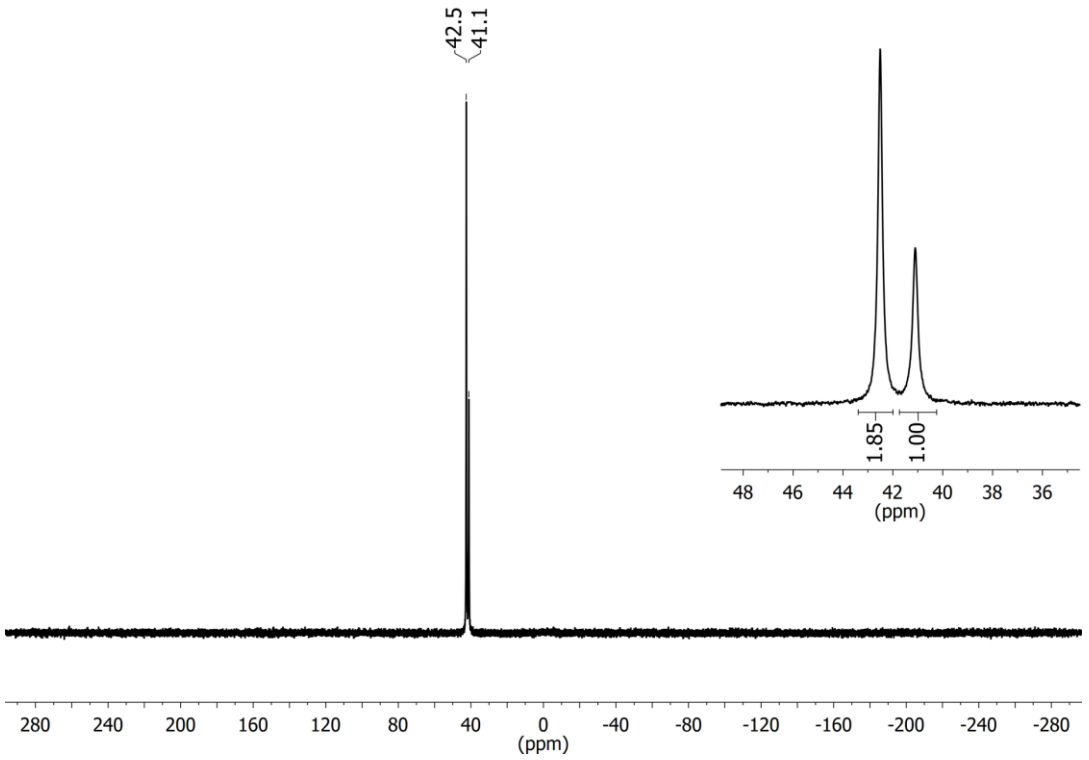

Figure S19 $^{31}P\{^{1}H\}$ NMR spectrum of **$[(1b)_2(Au)_3](OTf)_3$** in CD_2Cl_2 recorded at 25 °C using an inverse-gated pulse sequence ($z_g$ig) to allow for integration of the signals. The insert shows a magnification of the signals and their relative integrals.

1.2.4. Bis{μ-4,6-bis(1-diphenylphosphanyl-2κ²*P*¹,*P*²-1'-ferrocenylene)-2-(1-diphenylphosphanyl-1κ¹*P*³-1'-ferrocenylene)-1,3,5-triazine}trigold(I) triflate ([(1a)₂(Au)₃](OTf)₃)

[(1a)₂(Au)₃](OTf)₃, including crystals suitable for single-crystal X-ray diffraction analysis, was obtained by the same method as **[(1b)₂(Au)₃](OTf)₃**, using 100 mg (79.3 μmol, 1.00 eq.) **1a** and 75.0 mg [Au(η²-nbe)₃]OTf (119 μmol, 1.50 eq.). **[(1a)₂(Au)₃](OTf)₃** was isolated as a fine red powder (105 mg, 77%) after prolonged drying at 40 °C *in vacuo*.

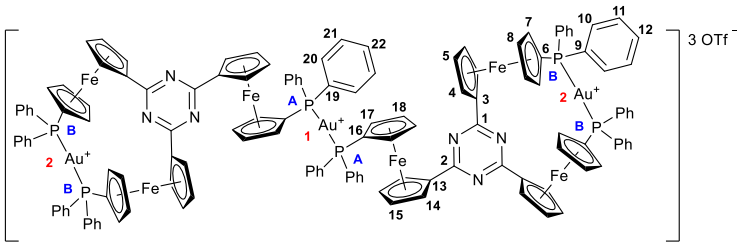

Mp: >240 °C (decomp.; from CH_2Cl_2/toluene). Anal. calcd. for $C_{141}H_{108}Au_3F_9Fe_6O_9N_6P_3S_3$: C 49.67, H 3.19, N 2.46 found: C 49.67, H 2.94, N2.38%. UV/Vis (CH_2Cl_2), λ_{max} (ε) 463 (5600); 379sh (10200), 348 (15400), 288 (76900) nm ($dm^3 \cdot mol^{-1} \cdot cm^{-1}$). IR (KBr, $\tilde{\nu}$): 3088 (m), 3053 (m), 3014 (w), 2921 (w), 2851 (w, all ν(C–H)), 1631 (w), 1513 (vs), 1436 (m, ν(C–P)), 1383 (m), 1361 (m), 1319 (m), 1264 (s), 1222 (m), 1151 (s), 1101 (m), 1058 (m), 1029 (s), 998 (m), 927 (w), 832 (m), 747 (m), 694 (s), 636 (s), 572 (w), 559 (w), 544 (w), 505 (s), 478 (s), 429 (m) cm^{-1}. ^1H NMR (CD_2Cl_2, δ): 7.79–7.39 (60 H, m, H10–12+H20–22), 5.35 (8 H, pt, J_{HH} = 2.0 Hz, H4), 5.20 (4 H, pt, J_{HH} = 2.0 Hz, H14), 4.81 (8 H, pt, J_{HH} = 2.0 Hz, H7/8), 4.55 (4+4 H, m, H15+H17/18), 4.49 (4 H, m, H17/18), 4.22 (8 H, m, H7/8), 4.05 (8 H, s(br), $\omega_{1/2}$ = 14.5 Hz, H5) ppm. $^{13}C\{^{31}P,^1H\}$ NMR (CD_2Cl_2, δ): 175.6 (s, C1), 175.4 (s, C2), 134.1 (s, C11), 134.0 (C21), 133.4 (s, C22), 133.1 (s, C12), *130.9* (s, C19)[6], 130.5 (s, C20), 130.2 (s, 10), 129.7 (s, C9), 82.5 (s, C3), 82.4 (s, C13), 77.1 (s, C17/18), 76.4 (s (br), $\omega_{1/2}$ = 36 Hz, C7/8), 75.6 (s, C7/8), 75.3 (s, C17/18) 74.3 (s, C15), 74.1 (s, C5) 72.1 (s, C4), 72.0 (s, C14), 70.3 (s, C6), 69.4 (s, C16) ppm. $^{19}F\{^1H\}$ NMR (CD_2Cl_2, δ): −78.7 (s, O_3SCF_3) ppm. $^{31}P\{^1H\}$ NMR (CD_2Cl_2, δ): 41.9 (2 P, P_B), 40.7 (1 P, P_A) ppm. HRMS (ESI-TOF, m/z): Calcd. for $C_{138}H_{108}Au_3Fe_6N_6P_3$ 987.4061; found 987.4051 $[M-3OTf]^{3+}$.

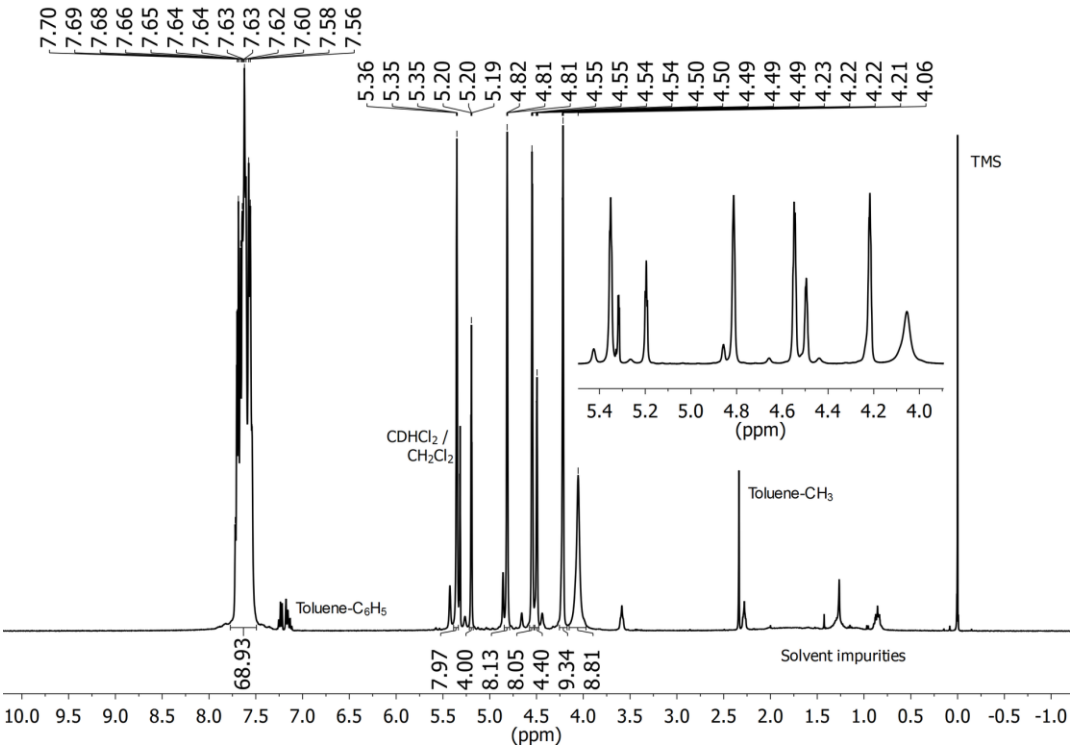

Figure S20 ^1H NMR spectrum of **[(1a)₂(Au)₃](OTf)₃** in CD_2Cl_2 recorded at 25 °C. The insert shows a magnification of the ferrocenylene resonances.

[6] The signal attributable to quaternary carbon atom C19 has been assigned using the *P*-coupled $^{13}C\{^1H\}$ (z_gp_g) NMR spectrum in which its intensity is greater than in the corresponding $^{13}C\{^{31}P,^1H\}$ NMR spectrum.

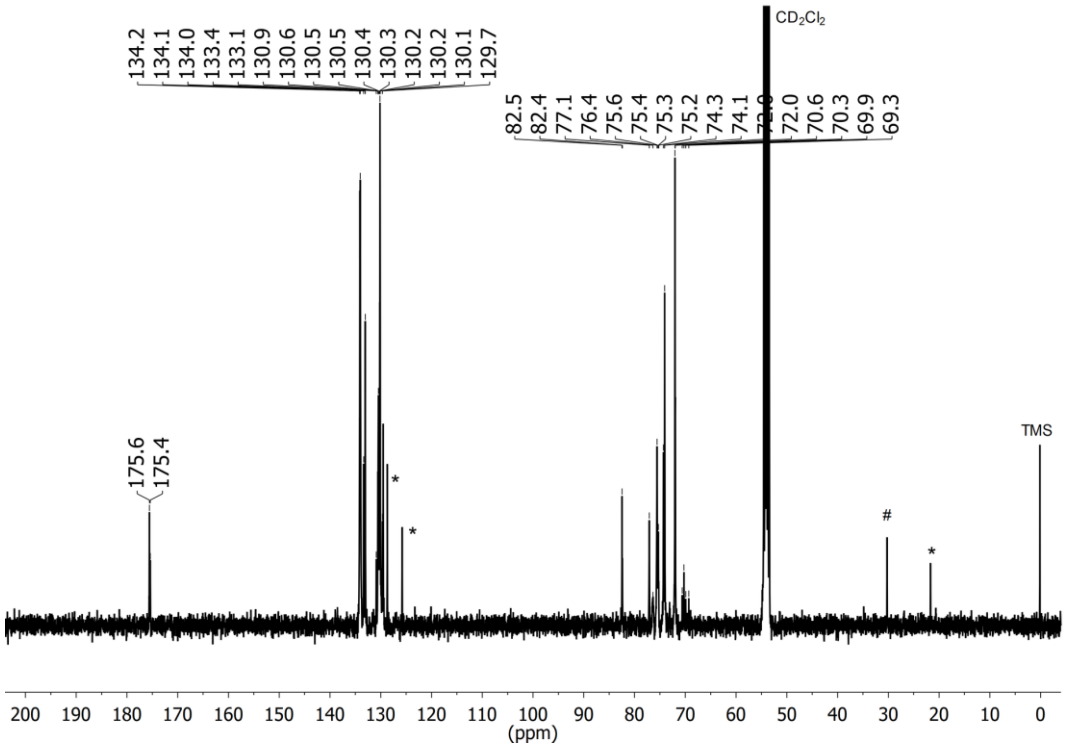

Figure S21 $^{13}C\{^{1}H\}$ NMR spectrum of **[(1a)$_2$(Au)$_3$](OTf)$_3$** in CD_2Cl_2 recorded at 25 °C using the z_gp_g pulse sequence for fast-relaxing nuclei. Signals labelled by asterisk (*) are attributable to toluene, the signal labelled with the hashtag symbol (#) is attributable to grease.

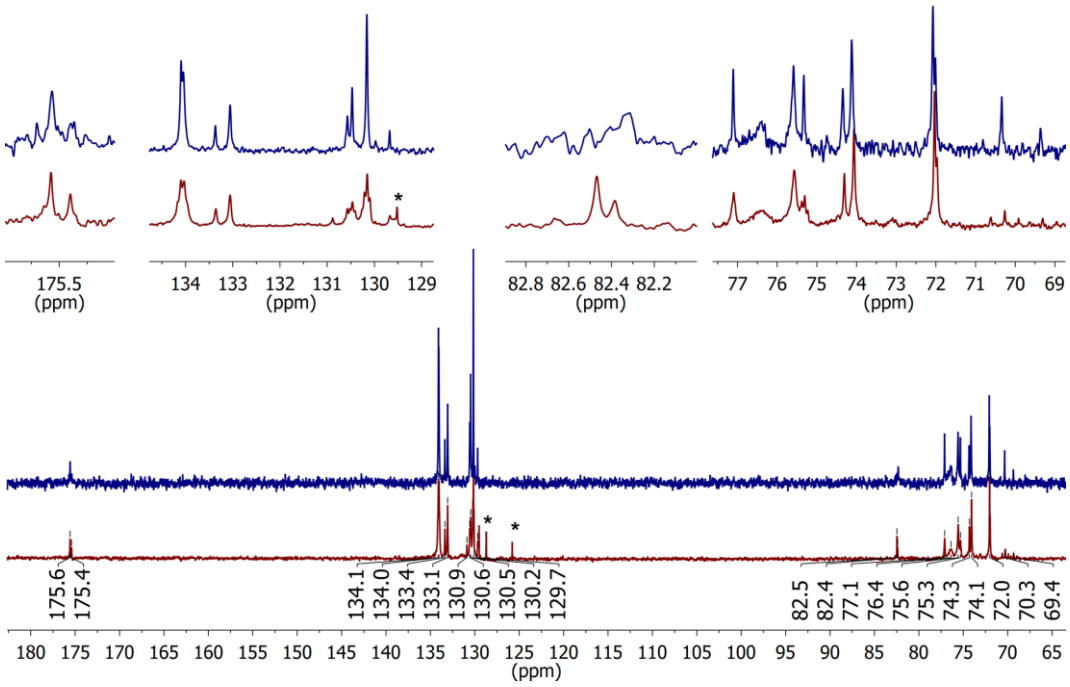

Figure S22 Stacked $^{13}C\{^{1}H\}$ (maroon, bottom) and $^{13}C\{^{31}P,^{1}H\}$ (navy, top) spectra of **[(1a)$_2$(Au)$_3$](OTf)$_3$** in CD_2Cl_2 recorded at 25 °C The inserts are magnifications of the C_3N_3 core (left), of the *P*-bound phenyl rings (centre left), of the *ipso* carbon atoms of the C_3N_3-bound cyclopentadienyl ring (centre right), and of the ferrocenylene region (right). Signals labelled by an asterisk (*) are attributable to toluene.

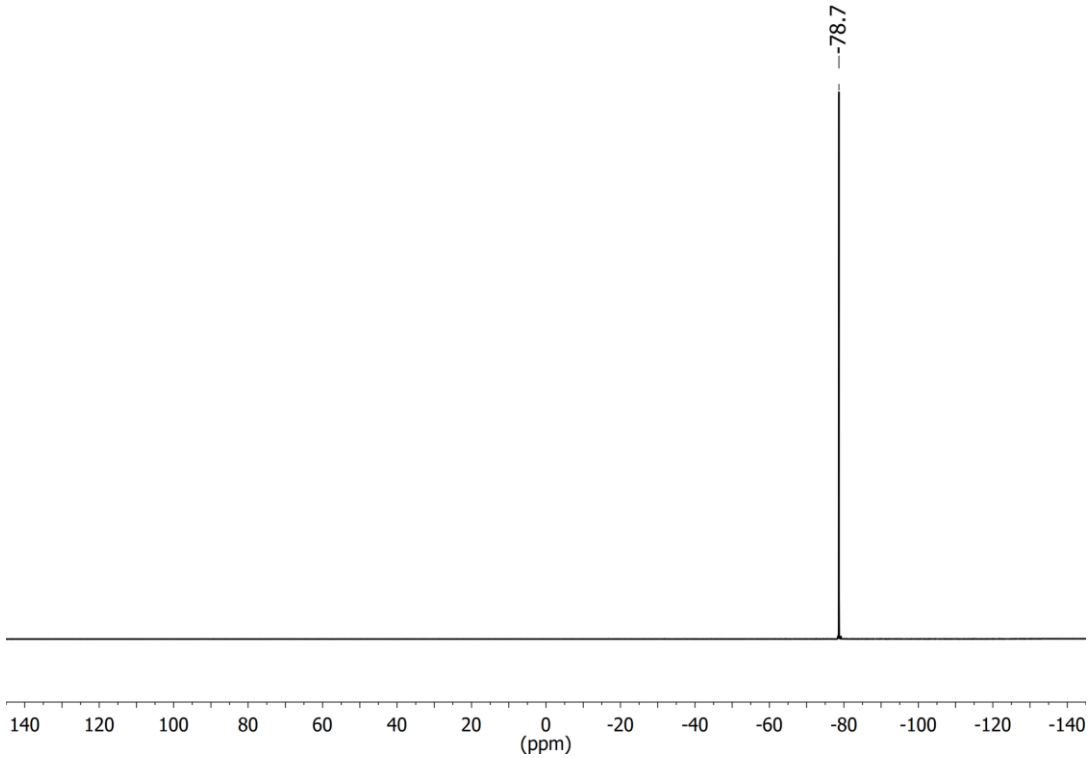

Figure S23 $^{19}F\{^{1}H\}$ NMR spectrum of **$[(1a)_2(Au)_3](OTf)_3$** in CD_2Cl_2 recorded at 25 °C.

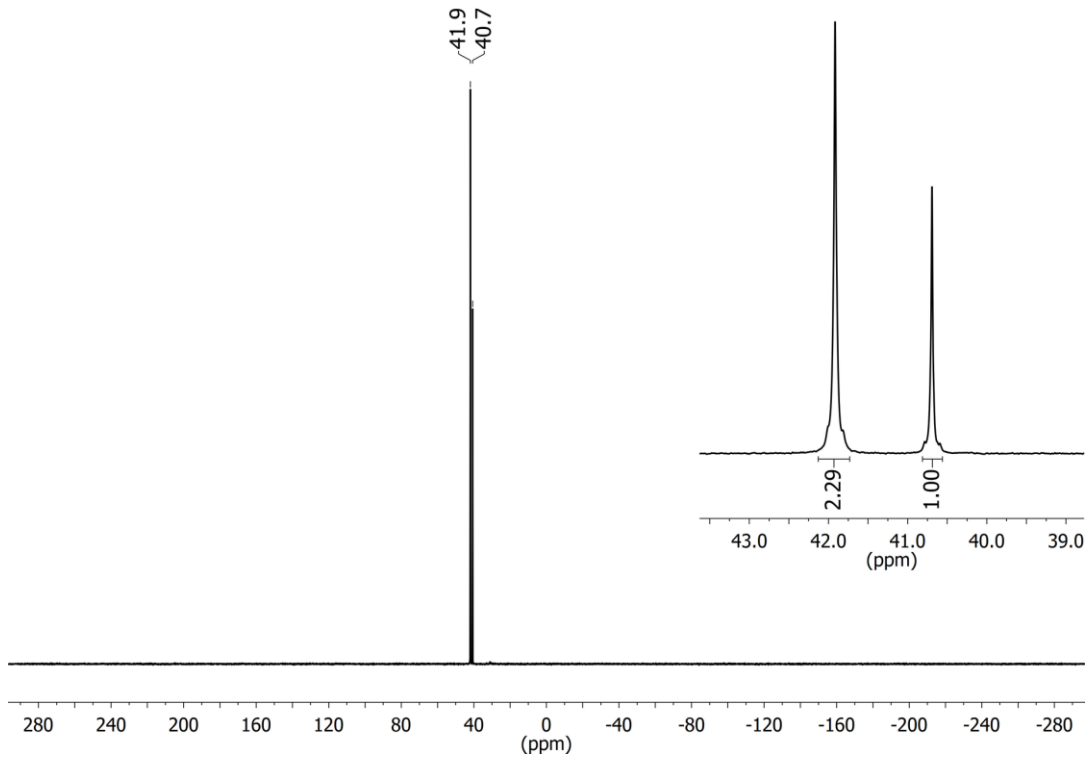

Figure S24 $^{31}P\{^{1}H\}$ NMR spectrum of **$[(1a)_2(Au)_3](OTf)_3$** in CD_2Cl_2 recorded at 25 °C using an inverse-gated pulse sequence (z_{ig}) to allow for integration of the signals. The insert shows a magnification of the signals and their relative integrals.

1.2.5. 2,4,6-Tris{1-bis(pentafluorophenyl)phosphanyl-1'-ferrocenylene}-1,3,5-triazine ($1a^F$)

A stirred solution of 940 mg (10.8 mmol, 1.00 eq.) **4a** in 35 mL THF was cooled to −80 °C (ethyl acetate/$N_{2(l)}$) and 2.35 mL (1.52 mol·L^{-1}, 35.7 mmol, 3.30 eq.) *n*-BuLi in *n*-hexane were added dropwise over the course of 10 min, resulting in a strong intensification of the red colour. The mixture was kept stirring for 1.5 hours at −80 °C, followed by the dropwise addition of 1.49 g (37.3 mmol, 3.45 eq.) chlorobis(pentafluorophenyl)phosphane dissolved in 20 mL THF at the same temperature. After warming to room temperature over the course of 2 hours and stirring at 60 °C for 1 hour, $^{31}P\{^1H\}$ NMR spectroscopy and TLC (hexanes/CH_2Cl_2, 1:1) indicated formation of the desired product and full conversion of **4a**. For quenching, a degassed saturated aqueous solution of NH_4Cl (30 mL) was added to the fervently stirred mixture *via* cannula. The phases were separated, and the aqueous phase was extracted with diethyl ether (2x 10 mL). The combined organic phases were dried over degassed $MgSO_4$, filtered, the drying agent extracted (2x 10 mL CH_2Cl_2), and then the product mixture was adsorbed on Celite® and subjected to column chromatography (degassed hexanes/CH_2Cl_2, gradient 12% to 95% CH_2Cl_2). The fractions were combined, and the solvent was removed under reduced pressure. The residue was filtered over degassed silica using CH_2Cl_2, and the solvent was removed *in vacuo*, yielding $\mathbf{1a^F}$ (270 mg, 15% yield) as a red foam.

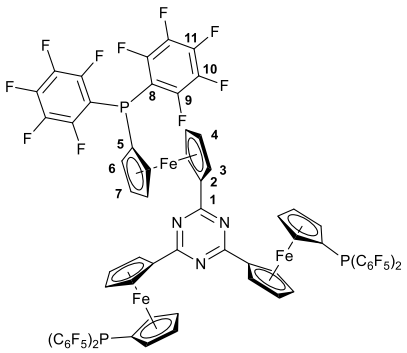

Mp: 98–100 °C (from CH_2Cl_2). R_f: 0.47 (hexanes/CH_2Cl_2 7:5). Anal. calcd. for $C_{69}H_{24}F_{30}Fe_3N_3P_3$: C 48.03, H 1.40, N 2.44, found: C 48.50, H 1.38, N 2.35%. IR (ATR, $\tilde{\nu}$): 2925 (w), 2855 (w, both ν(C–H)), 1639 (m), 1517 (s), 1473 (s, ν(C–P)), 1383 (m), 1362 (w), 1321 (w), 1289 (w), 1262 (w), 1202 (w), 1162 (w), 1141 (w), 1089 (s, ν(C–F)), 1030 (m), 977 (s), 833 (m, broad), 763 (w), 743 (w), 727 (w), 638 (w), 503 (m), 415 (w) cm^{-1}. ^1H NMR (CD_2Cl_2, δ): 5.22 (6 H, pt, J_{HH} = 2.0 Hz, H3), 4.44 (6 H, m, H7), 4.43 (6 H, pt, J_{HH} =2.0 Hz, H4), 4.29 (6 H, m, H6) ppm. $^{13}C\{^1H\}$ NMR (CD_2Cl_2, δ): 174.9 (s, C1), 147.2 (d, $^1J_{CF}$ = 247.8 Hz, C9/10), 142.3 (d, $^1J_{CF}$ = 256.6 Hz, C11), 137.3 (d, $^1J_{CF}$ = 255.6 Hz, C9/10), 109.6 (m, C8), 81.2 (s, C2), 75.2 (d, $^2J_{CP}$ = 20.7 Hz, C6), 74.4 (d, $^3J_{CP}$ = 5.6 Hz, C7), 72.5 (s, C4), 70.7 (s, C3), 68.3 (m, C5) ppm. $^{19}F\{^1H\}$ NMR (CD_2Cl_2, δ): −129.9 (12F, m, F9), −150.9 (6F, t, $^3J_{FF}$ = 20.4 Hz, F11), −161.0 (12F, pseudo-td, J_{FF} = 23.2, 8.6 Hz, F10) ppm. $^{31}P\{^1H\}$ NMR (CD_2Cl_2, δ): −57.7 (p, $^3J_{PF}$ = 29.6 Hz) ppm. HRMS (ESI-TOF, m/z): Calcd. for $C_{69}H_{24}F_{30}Fe_3N_3P_3$ 1725.8831; found 1725.8838 $[M]^+$.

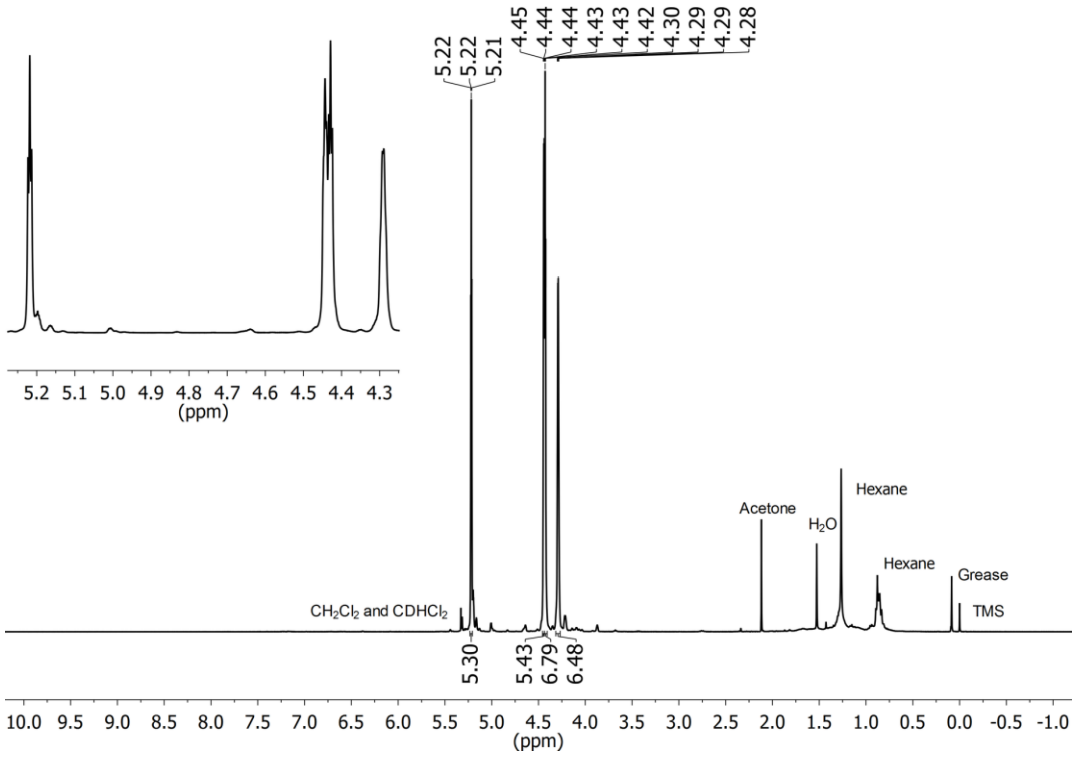

Figure S25 ^1H NMR spectrum of $\mathbf{1a^F}$ in CD_2Cl_2 recorded at 25 °C. The insert shows a magnification of the ferrocenylene resonances.

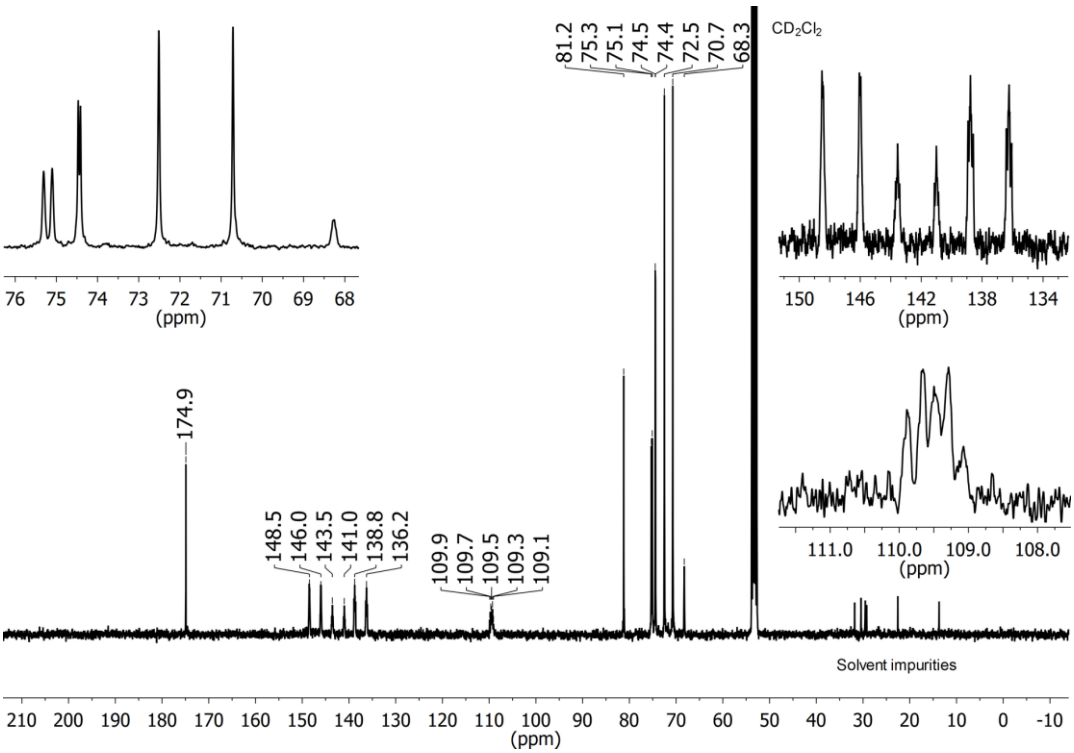

Figure S26 $^{13}C\{^{1}H\}$ NMR spectrum of **1a^{F}** in CD_2Cl_2 recorded at 25 °C. The inserts show magnifications of the spectral regions corresponding to the ferrocenylene (top left) and to the pentafluorophenyl groups (top right) as well as the signal corresponding to the *P*-bound *ipso* carbon atom (C8) of the pentafluorophenyl rings (bottom right).

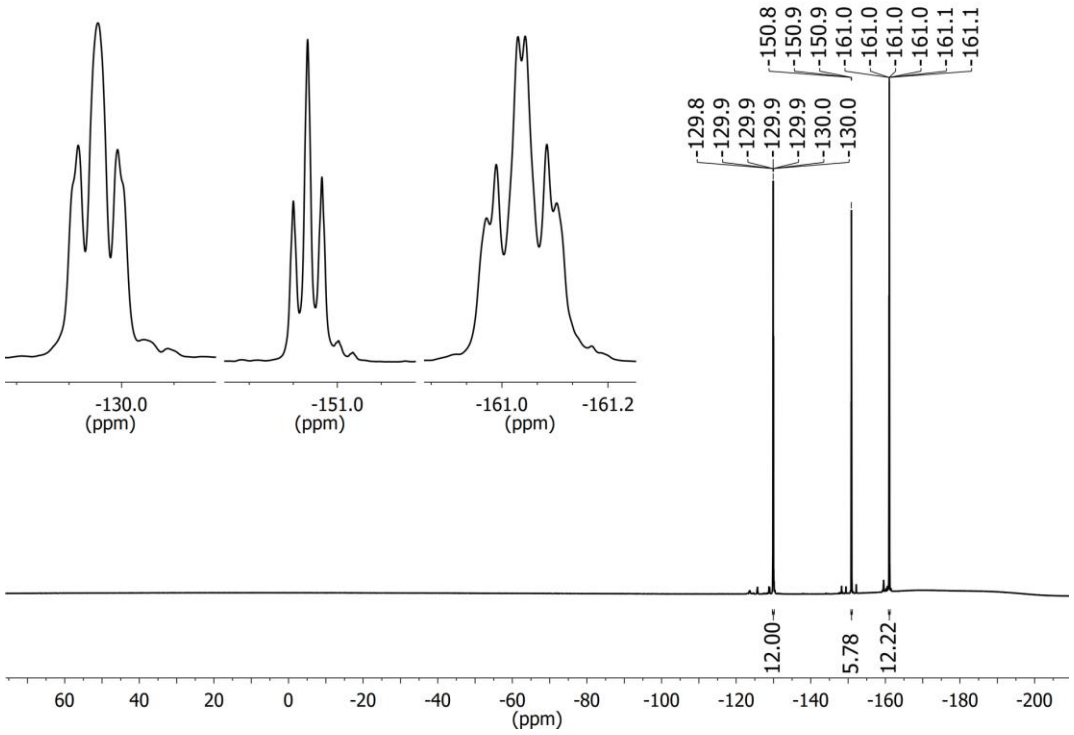

Figure S27 $^{19}F\{^{1}H\}$ NMR spectrum of **1a^{F}** in CD_2Cl_2 recorded at 25 °C. The inserts show magnifications of the individual resonances of the *ortho* (left), the *para* (centre), and the *meta* (right) fluorine atoms of the pentafluorophenyl rings.

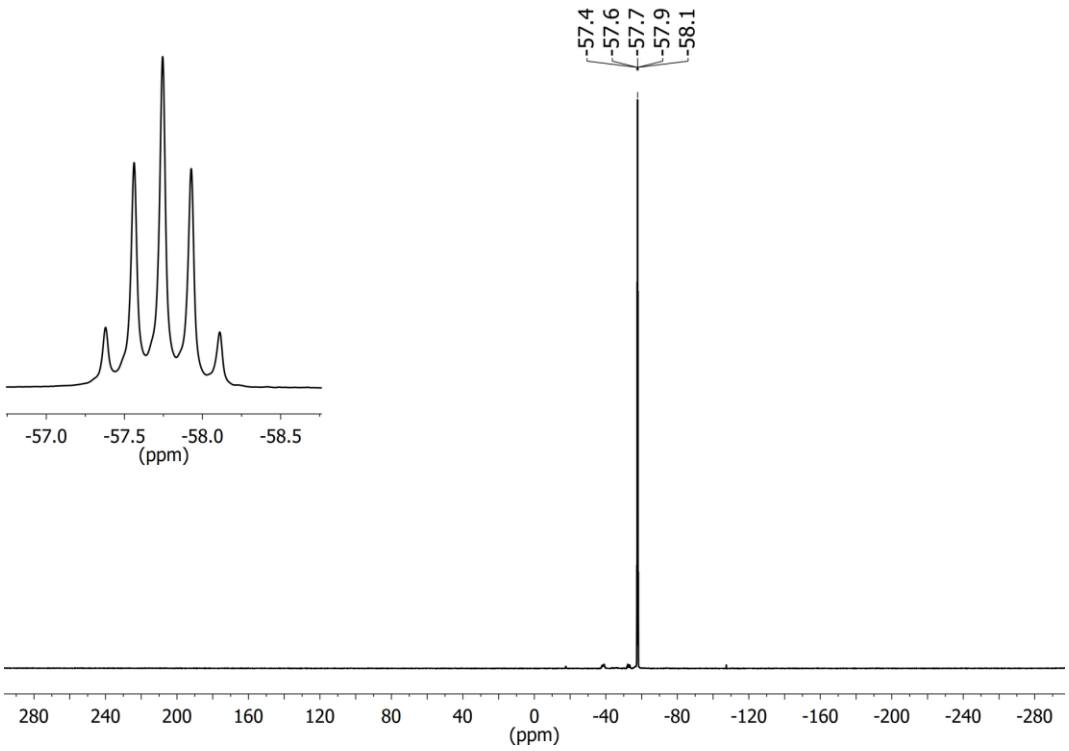

Figure S28 $^{31}P\{^{1}H\}$ NMR spectrum of **1a^{F}** in CD_2Cl_2 recorded at 25 °C. The insert shows a magnification of the resonance for a closer inspection of the ^{31}P-^{19}F coupling.

1.2.6. [2,4,6-Tris{1-bis(pentafluorophenyl)phosphanyl-κ²*P¹*,*P²*-1'-ferrocenylene}-1,3,5-triazine]gold(I) triflate ([1a^{F}(Au)]OTf)

In a Schlenk flask protected from direct light, 93.0 mg **1a^{F}** (53.9 µmol, 1.10 eq.) and 31.0 mg [Au(η²-nbe)$_3$]OTf (49.0 µmol, 1.00 eq.) were dissolved in 6 mL CH_2Cl_2 under stirring. Stirring was continued overnight, the reaction mixture was filtered *via* cannula, and the volatiles were removed *in vacuo*. The brown residue was washed with hexanes (2x 5 mL), re-dissolved in 3 mL CH_2Cl_2, and again precipitated with 6 mL hexanes. Layering a CH_2Cl_2 solution of this precipitate with toluene and storing it at 7 °C yielded **[1a^{F}(Au)]OTf** as small red prisms after several weeks, suitable for X-ray diffraction analysis, NMR spectroscopy, electrochemical studies (CV and SWV), and ESI mass spectrometry. No yield or melting point could be determined and not enough material for CHN and $^{13}C\{^{1}H\}$ NMR spectroscopic analyses could be collected.

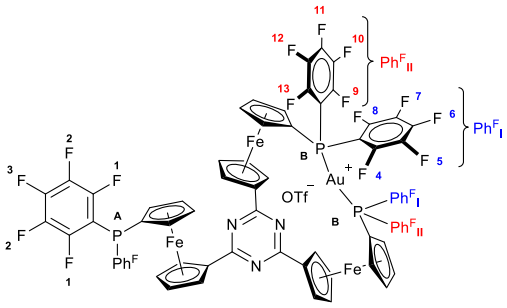

^{1}H NMR (CD_2Cl_2, 25 °C, δ): 5.46 (4 H, pt, J_{HH} = 1.7 Hz), 5.26 (2 H, s), 5.00 (4 H, m), 4.63 (6 H, s(br)), 4.47 (2 H, s), 4.46 (2 H, s), 4.27 (4 H, s(br)) ppm. ^{1}H NMR (CD_2Cl_2, −60 °C, δ): 5.52 (2 H, s), 5.50 (2 H, s), 5.30 (2 H, s), 5.08 (2 H, s), 5.01 (2 H, s), 4.74 (2 H, s), 4.63 (2 H, s), 4.60 (2 H, s), 4.49 (4 H, s), 4.29 (2 H, s), 3.60 (2 H, s) ppm. $^{19}F\{^{1}H\}$ NMR (CD_2Cl_2, 25 °C, δ):[7] −78.9 (s, O_3SCF_3), −126.5 (m(br), $\omega_{1/2}$ = 650 Hz, F4/8/9/13), −129.7 (t, $^{3}J_{FF}$ = 27 Hz, F1), −130.0 (m(br), $\omega_{1/2}$ = 770 Hz, F4/8/9/13), −142.7 (m(br), $\omega_{1/2}$ = 820 Hz, F6/11), −145.9 (m(br), $\omega_{1/2}$ = 760 Hz, F6/11), −150.8 (t, $^{3}J_{FF}$ = 21 Hz, F3), −156.3 (m(br), $\omega_{1/2}$ = 420 Hz, F5/7/10/12), −160.4 (m(br), $\omega_{1/2}$ = 400 Hz, F5/7/10/12), −161.0 (m, F2) ppm; (CD_2Cl_2, −60 °C, δ):[8] −79.4 (3 F, s, O_3SCF_3), −125.3 (4 F, s, $\omega_{1/2}$ = 62 Hz, F4+8), −129.1 (2 F, s(br), $\omega_{1/2}$ = 150 Hz, F13), −129.9 (4 F, s, $\omega_{1/2}$ = 76 Hz, F1), −131.8 (2 F, s(br), $\omega_{1/2}$ = 150 Hz, F9), −140.7 (2 F, s, $\omega_{1/2}$ = 63 Hz, F6), −145.5 (2 F, s, $\omega_{1/2}$ = 65 Hz, F11), −149.8 (2 F, t, $^{3}J_{FF}$ = 21 Hz, F3), −154.7 (4 F, m, F5+7), −158.6 (2 F, s(br), $\omega_{1/2}$ = 180 Hz, F12), −160.0 (4 F, s,

[7] Due to the signal width and the (pulse sequence-induced) complicated baseline, no meaningful integrals could be determined. The number of equivalent nuclei has hence been omitted.

[8] The assignment of the $^{19}F\{^{1}H\}$ NMR signals at −60 °C to either Ph^{F}_{I} or Ph^{F}_{II} and, more specifically, to either F9/13 // F10/12 is arbitrary and solely intended to illustrate the fact that one of the two pentafluorophenyl rings shows a hindered rotation about the P–C axis at this temperature while the other still rotates freely. The correlation between the signals of either ring has been established by a ^{19}F,^{19}F COSY NMR experiment at −60 °C.

$\omega_{1/2}$ = 58 Hz, F2), −161.5 (2 F, s(br), $\omega_{1/2}$ = 160 Hz, F10) ppm. $^{31}P\{^{1}H\}$ NMR (CD_2Cl_2, 25 °C, δ): −2.1 (2 P, s(br), $\omega_{1/2}$ = 41 Hz, P_B), −58.4 (1 P, quint, $^{3}J_{PF}$ = 31 Hz, P_A) ppm. HRMS (ESI-TOF, m/z): Calcd. for $C_{69}H_{24}AuF_{30}Fe_3N_3P_3$ 1921.8419; found 1921.8407 $[M-OTf]^+$.

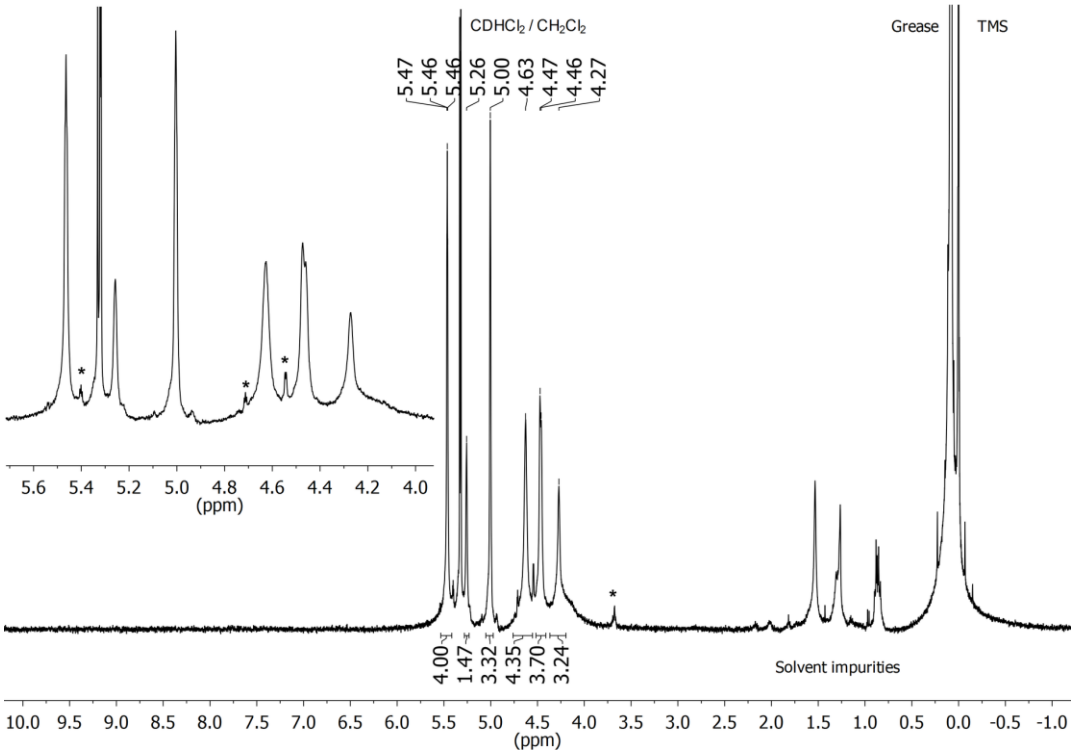

Figure S29 ^{1}H NMR spectrum of **[1a^{F}(Au)]OTf** in CD_2Cl_2 recorded at 25 °C. The insert shows a magnification of the ferrocenylene resonances. Signals marked by asterisks (*) arise from residual **1a^{F}**. The TMS/grease signals had to be cropped, since they outweighed the signals of interest of **[1a^{F}(Au)]OTf** of which only a very limited amount was available.

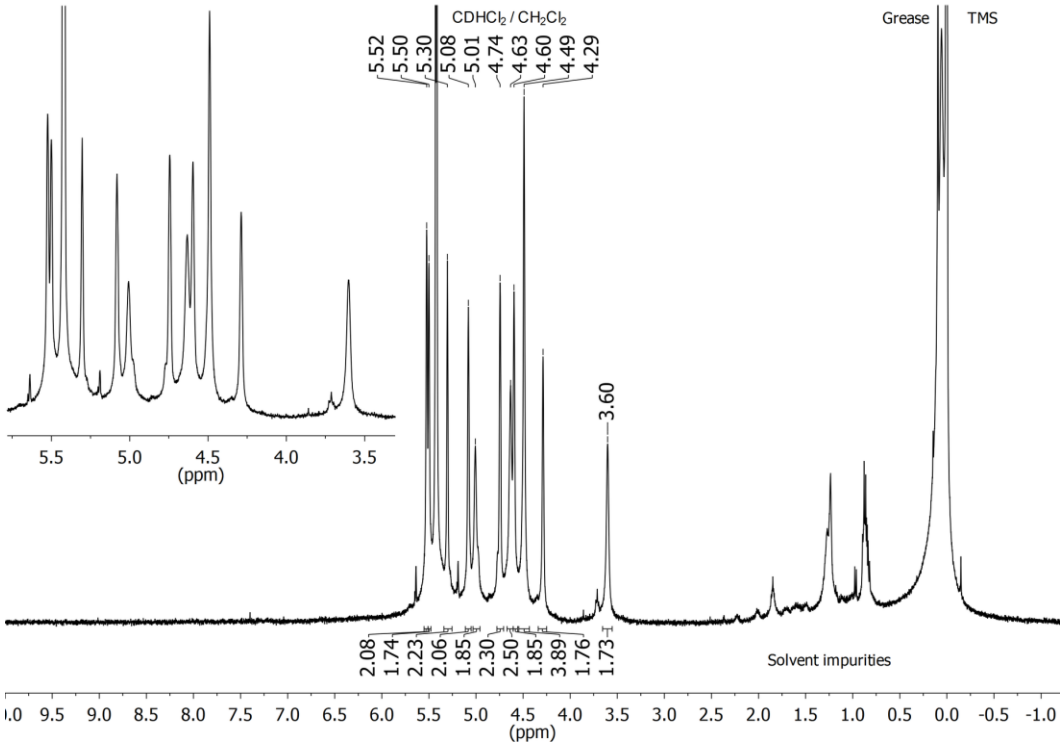

Figure S30 ^{1}H NMR spectrum of **[1a^{F}(Au)]OTf** in CD_2Cl_2 recorded at −60 °C. The insert shows a magnification of the ferrocenylene resonances. The TMS/grease signals had to be cropped, since they outweighed the signals of interest of **[1a^{F}(Au)]OTf** of which only a very limited amount was available.

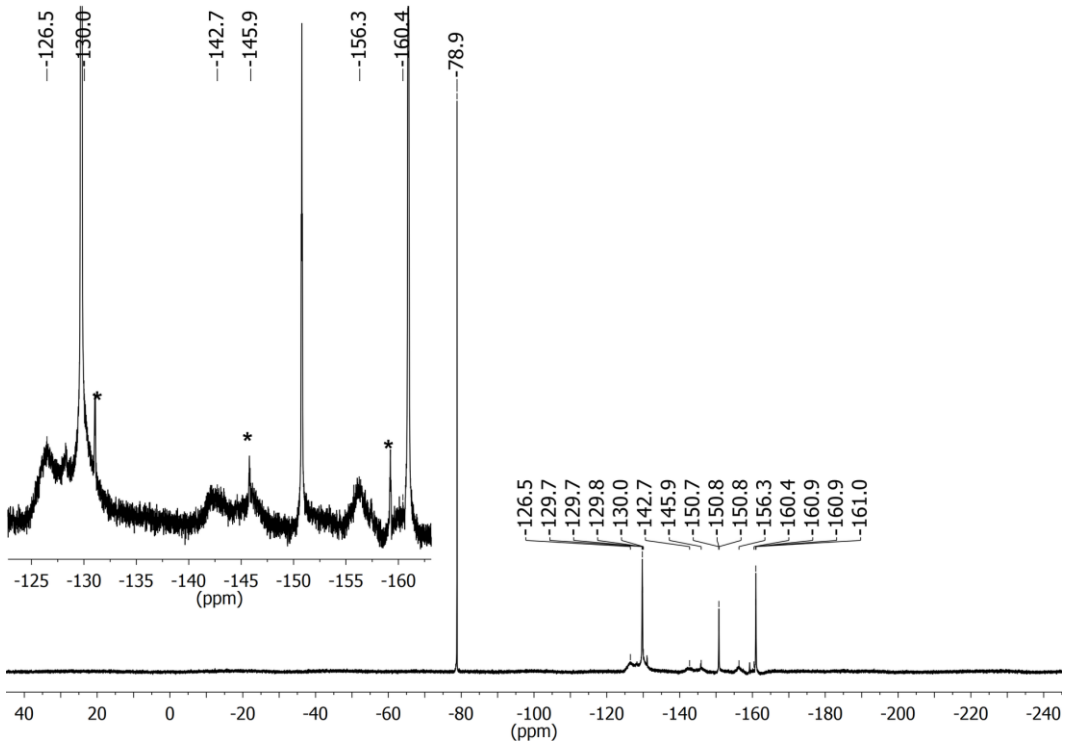

Figure S31 $^{19}F\{^{1}H\}$ NMR spectrum of **[1a^{F}(Au)]OTf** in CD_2Cl_2 recorded at 25 °C. The insert shows a magnification of the pentafluorophenyl resonances. Signals labelled by an asterisk (*) correspond to residual **1a^{F}**.

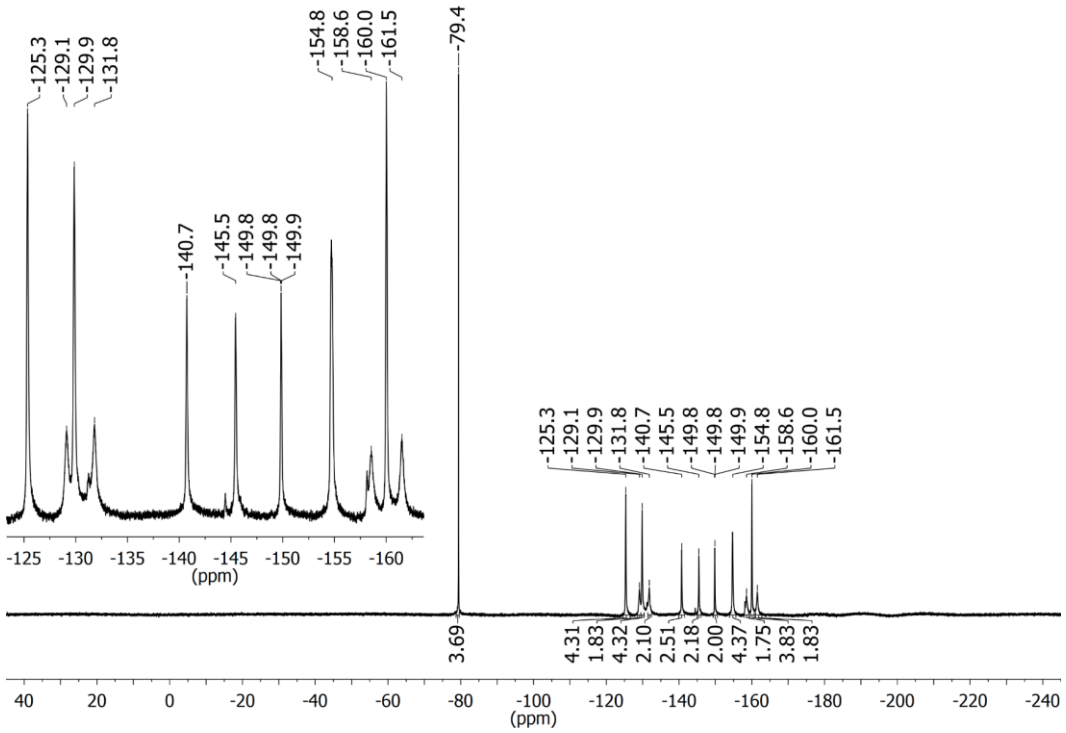

Figure S32 $^{19}F\{^{1}H\}$ NMR spectrum of **[1a^{F}(Au)]OTf** in CD_2Cl_2 recorded at −60 °C. The insert shows a magnification of the pentafluorophenyl resonances.

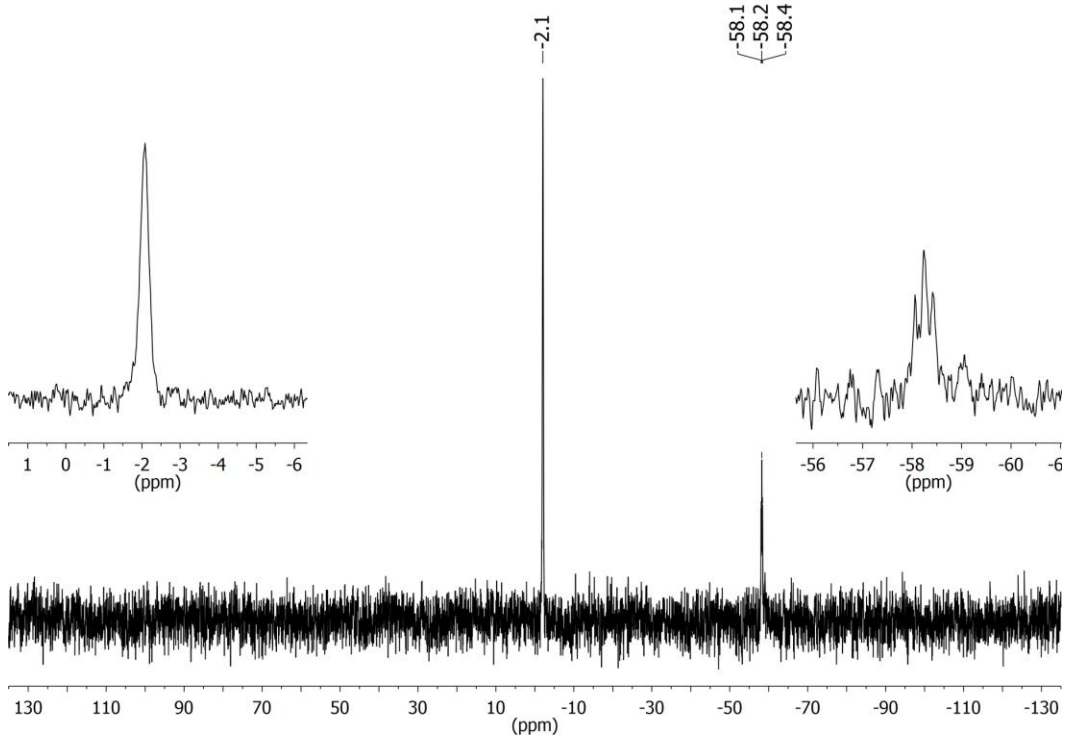

Figure S33 $^{31}P\{^{1}H\}$ NMR spectrum of **[1a^{F}(Au)]OTf** in CD_2Cl_2 recorded at 25 °C. The insert shows a magnification of the pentafluorophenyl resonances.

1.2.7. [2,4,6-Tris{1-bis(pentafluorophenyl)phosphanyl-κ²*P*¹,*P*²-1'-ferrocenylene}-1,3,5-triazine]silver(I) triflate ([1a^{F}(Ag)]OTf)

In a Schlenk flask protected from direct light, 120 mg **1a^{F}** (69.5 µmol, 1.15 eq.) and 15.5 mg silver(I) triflate (60.5 µmol, 1.00 eq.) were suspended in 5 mL CH_2Cl_2 under stirring. The reaction mixture was stirred overnight, filtered, and the volatiles were removed *in vacuo*. Full dissolution of the red precipitate was only achieved in 10 mL 1,2-dichloroethane, and this solution was layered with 20 mL hexanes and stored at 7 °C overnight. So-obtained crystals of **[1a^{F}(Ag)]OTf** were found suitable for X-ray diffraction analysis and further analyses (after prolonged drying; isolated yield 40 mg, 33%).

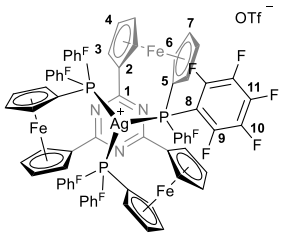

(Apparent high-temperature form, C_{3v})

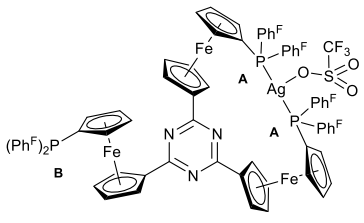

(Low-temperature and solid-state form, C_s)

Mp: >220 °C (decomp.; from $C_2H_4Cl_2$/hexanes). Anal. calcd. for $C_{70}H_{24}AgF_{33}Fe_3O_3N_3P_3S$: C 42.41, H 1.22, N 2.12 found: C 42.39, H 1.08, N2.16%. IR (KBr, $\tilde{\nu}$): 2966 (w), 2919 (w), 2857 (w, all ν(C–H)), 1723 (w), 1642 (m), 1518 (s), 1478 (s, ν(C–P)), 1385 (m), 1366 (w), 1321 (w), 1291 (m), 1262 (m), 1231 (m), 1172 (m), 1143 (w), 1093 (s), 1062 (w), 1027 (m), 978 (s), 831 (m), 807 (m), 763 (w), 638 (m), 506 (m), 477 (w), 421 (w) cm^{-1}. ^{1}H NMR (CD_2Cl_2, δ): 5.33 (6 H, s(br), $\omega_{1/2}$ = 5.6 Hz, H3), 4.81 (6 H, s(br), $\omega_{1/2}$ = 13.7 Hz, H6/7), 4.59 (6 H, s(br), $\omega_{1/2}$ = 23.6 Hz, H6/7), 4.35 (6 H, s(br), $\omega_{1/2}$ = 15.2 Hz, H4) ppm.[9] $^{19}F\{^{1}H\}$ NMR (CD_2Cl_2, δ): −78.7 (3 F, s, O_3SCF_3), −127.6 (12 F, m(br), $\omega_{1/2}$ = 587 Hz, F9), −146.4 (6 F, m(br), $\omega_{1/2}$ = 986 Hz, F11), −158.2 (12 F, m(br), $\omega_{1/2}$ = 500 Hz, F10) ppm. $^{31}P\{^{1}H\}$ NMR (CD_2Cl_2, 25 °C, δ): −47.8 (m(br), $\omega_{1/2}$ = 1495 Hz); (CD_2Cl_2, −50 °C, δ): −44.8 (2 P, d of m, $^{1}J_{PAg} \approx 630$ Hz, P_A), −61.0 (1 P, quint, $^{3}J_{PF} \approx 28$ Hz, P_B)[10] ppm. HRMS (ESI-TOF, m/z): Calcd. for $C_{69}H_{24}AgFe_3N_3P_3$ 1833.7816; found 1833.7844 $[M-OTf]^+$.

[9] No $^{13}C\{^{1}H\}$ NMR signals could be detected in either the $^{13}C\{^{1}H\}$ or the $^{13}C\{^{31}P,^{1}H\}$ NMR experiment, probably owing to the high fluxionality and additional coupling to further NMR-active nuclei (^{19}F, $^{107/109}Ag$).

[10] The coupling in both $^{31}P\{^{1}H\}$ NMR signals is not fully resolved, hence only approximate values are given. In case of the pendant $P(C_6F_5)_2$ group, only a triplet-like structure is resolved instead of the expected quintet; however, the measurable $^{3}J_{PF}$ coupling constant is in good agreement with that of the free ligand.

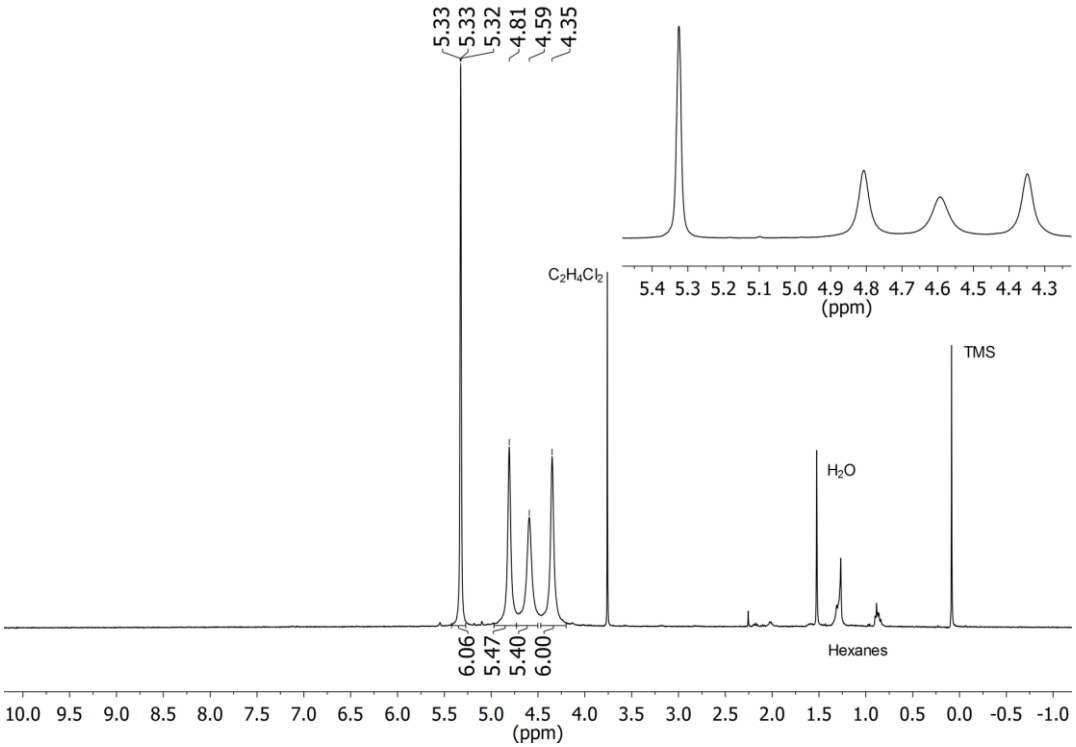

Figure S34 ^{1}H NMR spectrum of **[1a^{F}(Ag)]OTf** in CD_2Cl_2 recorded at 25 °C. The insert shows a magnification of the ferrocenylene resonances. The signal centred at 5.33 ppm is a superposition of the $CHDCl_2$/CH_2Cl_2 signals and the signal of protons H3 of **[1a^{F}(Ag)]OTf**.

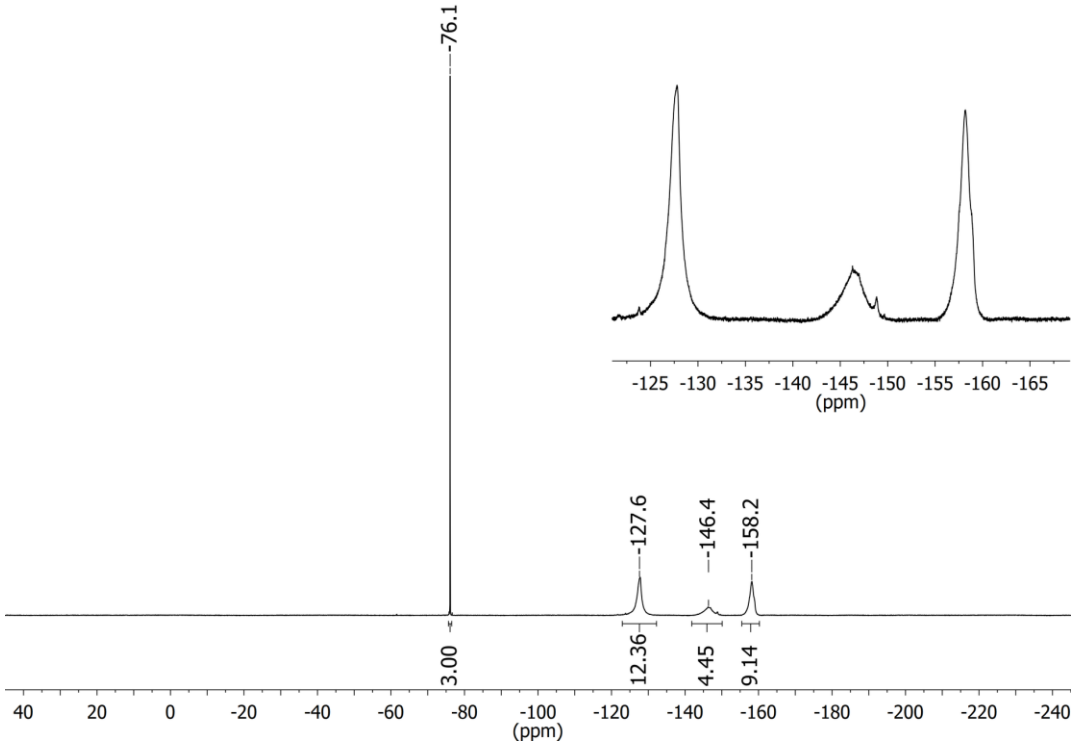

Figure S35 ^{19}F{^{1}H} NMR spectrum of **[1a^{F}(Ag)]OTf** in CD_2Cl_2 recorded at 25 °C. The insert shows a magnification of the pentafluorophenyl resonances. The integrals for the *para* and *meta* fluorine substituents are underestimated, possibly due to a poor, pulse sequence-induced baseline.

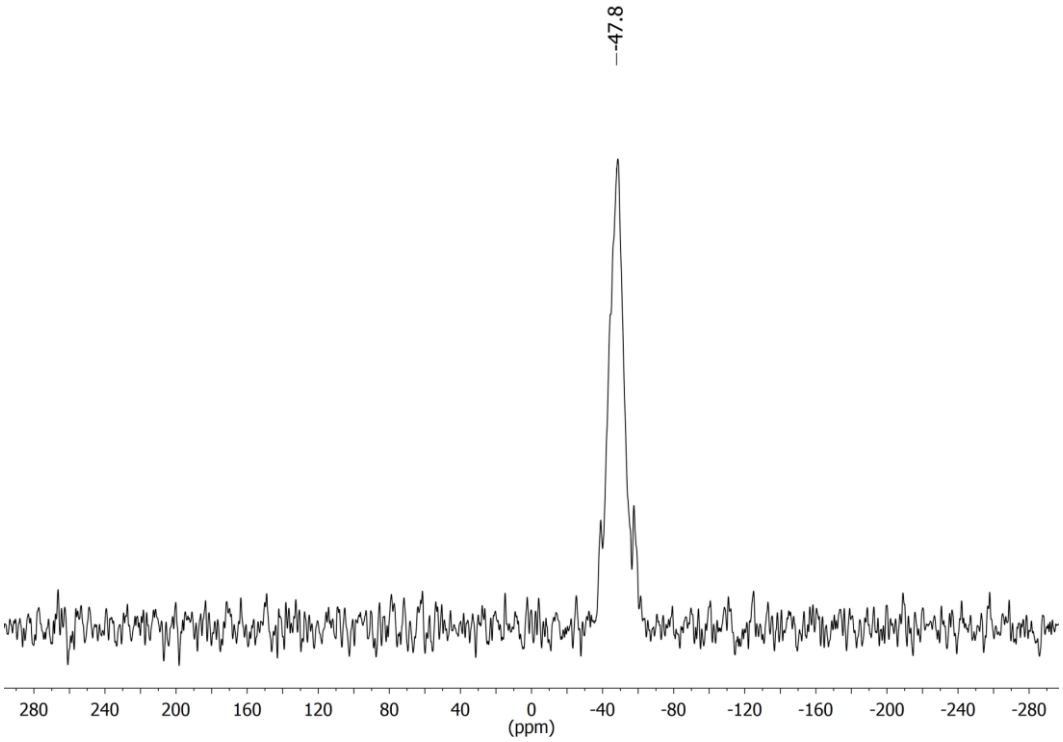

Figure S36 $^{31}P\{^{1}H\}$ NMR spectrum of **[1a^{F}(Ag)]OTf** in CD_2Cl_2 recorded at 25 °C. For graphic representation, exponential line broadening of lb = 150 Hz has been applied.

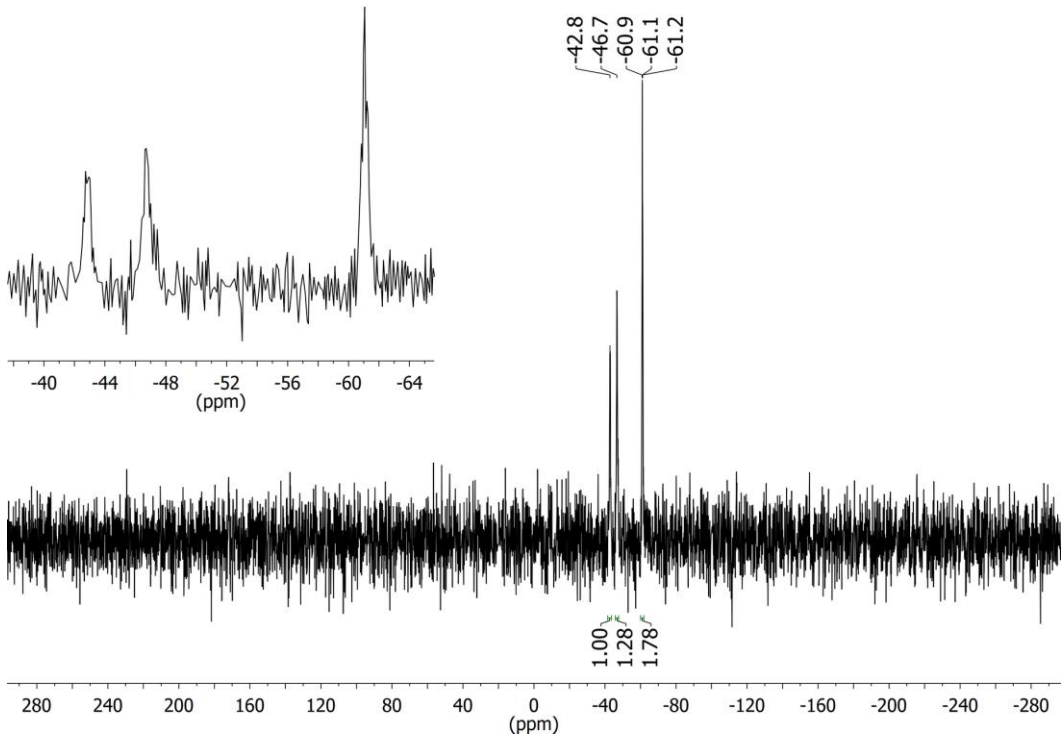

Figure S37 $^{31}P\{^{1}H\}$ NMR spectrum of **[1a^{F}(Ag)]OTf** in CD_2Cl_2 recorded at −50 °C. The insert shows a magnification of the spectral region of interest.

1.3. Catalytic tests

Catalytic experiments were run on the NMR scale under argon in inert-gas NMR tubes, using 0.5 mL of a stock solution of *N*-prop-2-ynylbenzamide (**2**) (72.0 mmol·L^{-1}) and 1,3,5-trimethoxybenzene (7.2 mmol·L^{-1}) in dry CD_2Cl_2 (containing TMS as an internal chemical shift standard) and 0.1 mL of a stock solution of the respective (pre-)catalyst (10.8 mmol·L^{-1} for **[1a(Au)]OTf** and **[1b(Au)]OTf**, 3.6 mmol·L^{-1} for **[(1a)$_2$(Au)$_3$](OTf)$_3$** and **[(1b)$_2$(Au)$_3$](OTf)$_3$**, corresponding to 3 mol% Au with respect to **2**) in CD_2Cl_2, leading to an effective substrate concentration of [**5**]$_0$ = 60 mmol·L^{-1} and [1,3,5-trimethoxybenzene] = 6.0 mmol·L^{-1}. Stock solutions were stored at −25 °C and protected from light.

For redox-switching experiments involving **[(1a)$_2$(Au)$_3$](OTf)$_3$** and **[(1b)$_2$(Au)$_3$](OTf)$_3$**, stock solutions of oxidant **5a** (36.0 mmol·L^{-1}) and reductant **6** (39.6 mmol·L^{-1}) were freshly prepared for each set of runs and added to the inert-gas NMR tubes at the chosen points in time in steps of 20 µL corresponding to 1.0 eq. **5a** or 1.1 eq. **6** *via* microliter syringes. After each addition of **5a** or **6**, the NMR tube was closed again under argon and shaken vigorously. For experiments involving **[1a(Au)]OTf** and **[1b(Au)]OTf**, 30 µL of the stock solution of **5a** correspond to 1.0 eq. of complex. The catalytic inactivity of pure **5a** and **5a** + **6** has been demonstrated previously.[5]

All reactions were followed by time-resolved ^{1}H NMR spectroscopy at 25 °C, using 12 scans and d = 10 s. For evaluation of the conversion/yield, spectra were stacked and jointly subjected to auto phase correction and baseline correction (polynomial fit) by MestReNova (version 12.0.0-20080). Spectra which had not been properly shimmed were removed from further analyses. Using the "Concentration Graph" function of MestReNova's built-in data analysis suite, signals of interest were integrated against the signal from the internal standard's methoxy protons (9 H, 3.71–3.79 ppm). As best suited (least affected by paramagnetic additives) for determining the yield, the *ortho*-phenyl protons (H_O) of **3a** (2 H, 7.93–7.99 ppm) were chosen. Cross-checking against other ^{1}H NMR signals of both **2** and **3a** gave similar yields, conversions, and TOF as those reported. For an exemplary stack, s. Figs. S73 and S74.

2. Single Crystal X-Ray Diffraction Analyses

2.1. Crystallographic data

Table S1 Crystallographic data of gold(I) complexes **[1b(Au)]OTf**, **{[(1c)$_2$(Au)$_3$](OTf)$_3$}$_n$**, **[(1a)$_2$(Au)$_3$](OTf)$_3$**, **[(1b)$_2$(Au)$_3$](OTf)$_3$**, **[1a^F(Au)]OTf**, and silver complex **[1a^F(Ag)]OTf**.

	[1b(Au)]OTf	**{[(1c)$_2$(Au)$_3$](OTf)$_3$}$_n$**	**[(1a)$_2$(Au)$_3$](OTf)$_3$**	**[(1b)$_2$(Au)$_3$](OTf)$_3$**	**[1a^F(Au)]OTf**	**[1a^F(Ag)]OTf**
Empirical formula[a]	$C_{72}H_{57}AuFe_3P_3 \cdot CF_3SO_3 \cdot 5\ C_4H_8O$ [b]	$C_{144}H_{108}Au_3F_6Fe_6P_6 \cdot 3\ CF_3SO_3$ [c]	$C_{138}H_{108}Au_3Fe_6N_3P_6 \cdot CF_3SO_3 \cdot 2.5\ C_7H_8$ [d]	$C_{144}H_{114}Au_3Fe_6P_6 \cdot C_7H_8$ [e]	$C_{69}H_{24}AuF_{30}Fe_3N_3P_3 \cdot CF_3O_3S$ [f]	$C_{69}H_{24}AgF_{30}Fe_3N_3P_3 \cdot CF_3O_3S \cdot 0.5\ C_2H_4Cl_2$ [g]
Formula weight [g·mol^{-1}]	1889.19	3511.33	3341.02	3346.44	2071.41	2031.53
T [K]	130	130	130	130	130	130
Crystal system	Monoclinic	Triclinic	Triclinic	Triclinic	Triclinic	Triclinic
Space group	$P2_1/n$	$P\bar{1}$	$P\bar{1}$	$P\bar{1}$	$P\bar{1}$	$P\bar{1}$
a,	23.1998(4),	14.1852(2),	12.4778(2),	12.6182(2),	12.6634(9),	12.7215(7),
b,	16.4337(2),	19.1612(3),	23.4172(6),	23.5315(4),	15.1030(9),	15.1519(9),
c [Å]	23.6527(3)	31.3978(6)	27.2317(7)	27.2516(7)	19.188(1)	19.199(1)
α,	90,	80.713(2),	70.125(2),	69.340(2),	93.198(5),	93.368(5),
β,	107.834(2),	84.878(1),	84.260(2),	83.591(2),	97.777(6),	98.006(5),
γ [°]	90	85.819(1)	89.076(2)	66.260(1)	103.745(6)	103.392(5)
V [Å^3]	8584.5(2)	8372.1(2)	7444.1(3)	7523.6(3)	3517.1(4)	3549.0(4)
Z	4	2	2	2	2	2
ρ_{calc} [g·cm^{-3}]	1.462	1.393	1.491	1.477	1.956	1.901
Θ_{max} [°]	30.507	28.347	30.220	28.282	26.710	26.369
F(000)	4016	3456	3317	3314	2008	1499
Reflns collected	60373	118656	125800	89742	23124	21465
Independent reflns	26202	37788	40508	37318	11822	13499
R_1/wR_2 {$I > 2\sigma(I)$}	0.0397 / 0.0788	0.0436 / 0.0905	0.0760 / 0.1612	0.0590 / 0.1168	0.0987 / 0.1491	0.1018 / 0.1686
R_1/wR_2 (all data)	0.0743 / 0.0922	0.0665 / 0.0970	0.1285 / 0.1861	0.1062 / 0.1341	0.2352 / 0.1973	0.2439 / 0.2267
Largest diff. peak/hole [e·Å^{-3}]	1.514 / −1.568	1.605 / −1.828	5.010 / −3.427	2.644 / −1.729	1.098 / −0.21	1.565 / −0.827

[a] Given as Compound·Solvent(s) or Cation·Anion(s)·Solvent(s) for clarity. [b] One molecule of THF could not be properly modelled and was hance removed using the SQUEEZE routine implemented in SHELX-97. [c] Nine molecules of THF per asymmetric unit were removed using the SQUEEZE routine implemented in SHELX-97. [d] None of the three triflate anions could be properly located and/or described in the solid-state structure, as large channels filled with heavily disordered solvent molecules and smaller channels with disordered anions are present. Thus, 1500 electrons/asymmetric unit have been removed using the SQUEEZE routine implemented in SHELX-97, corresponding to three triflate ions (3·74 e$^-$) and an unspecified number of dichloromethane (52 e$^-$)/toluene (50 e$^-$) molecules as co-crystallised solvents. [e] Two of the three triflate anions could not be located in the solid-state structure, as large channels filled with heavily disordered solvent molecules and smaller channels with disordered anions are found. Thus, 560 electrons/asymmetric unit have been removed using the SQUEEZE routine implemented in SHELX-97, corresponding to two triflate ions (2·74 = 148 e$^-$) and an unspecified number of dichloromethane (52 e$^-$)/toluene (50 e$^-$) molecules as co-crystallised solvents. One equivalent of toluene crystallised on the inversion centre of the unit cell. [f] Half an equivalent of co-crystallised 1,2-dichloroethane is present in the unit cell but could not be properly modelled. It was hence removed using the SQUEEZE routine implemented in SHELX-97. [g] Co-crystallised 1,2-dichloroethane is present in two different positions in the unit cell, each with 0.25 occupancy.

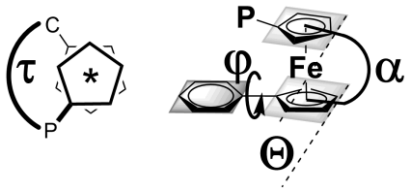

Fig. S38 Schematic representation of key structural parameters for the compounds under investigation (τ: torsion about the Cp^P(centroid)···Fe···Cp^C(centroid) axes; φ: torsion between the central arene and the directly bound cyclopentadienyl rings; Θ: angle between the mean planes through the substituted cyclopentadienyl rings; α: angle between Ct^C–Fe–Ct^P, Ct^C denotes the calculated centre of gravity of the *C*-substituted cyclopentadienyl ring; Ct^P denotes the calculated centre of gravity of the *P*-substituted cyclopentadienyl ring). Parameters chosen and named following reference [28].

2.2. Structural parameters

Table S2 Selected bond lengths [Å], distances [Å], and angles [°] of mononuclear complexes **[1b(Au)]OTf**, **[1a^F(Au)]OTf**, and **[1a^F(Ag)]OTf**; numbering scheme according to Fig. S38, ferrocenylene geometric parameters according to Fig. S39.

	[1b(Au)]OTf	[1a^F(Au)]OTf	[1a^F(Ag)]OTf		[1b(Au)]OTf	[1a^F(Au)]OTf	[1a^F(Ag)]OTf
M(1)–P(1) / **M(1)–P(2)**[a]	2.3025(8) / 2.3017(8)	2.300(4) / 2.286(4)	2.429(3) / 2.417(3)	**∢(P(1)–M(1)–P(2))** / **∢(P(1)–M(1)–O(1))** / **∢(P(2)–M(1)–O(1))**[a]	161.31(4) / 101.04(5) / 94.99(5)	165.4(2) / 77.5(2) / 103.2(3)	156.7(1) / 88.2(2) / 105.0(2)
C$^P_{ips}$(fc$_1$)–P(1) /	1.781(4)	1.77(1)	1.78(1)	**α(fc(1))** /	177.02	176.0	174.7
C$^P_{ips}$(fc$_2$)–P(2) /	1.786(3)	1.76(2)	1.78(1)	**α(fc(2))** /	177.50	176.8	176.5
C$^P_{ips}$(fc$_3$)–P(3)[b]	1.808(3)	1.84(2)	1.82(1)	**α(fc(3))**	176.52	178.0	177.4
C$^C_{ips}$(fc$_1$)–C^{Link}(1) /	1.483(4)	1.49(3)	1.45(2)	**Θ(fc(1))** /	2.33	4.6	5.6
C$^C_{ips}$(fc$_2$)–C^{Link}(2) /	1.473(4)	1.44(2)	1.49(1)	**Θ(fc(2))** /	2.01	2.8	3.2
C$^C_{ips}$(fc$_3$)–C^{Link}(3)[c]	1.473(6)	1.50(3)	1.45(2)	**Θ(fc(3))**	4.03	4.0	3.5
Ct^C(1)–Fe(1) /	1.647	1.634	1.638	**τ(fc(1))** /	−88.02	−88.9	−86.1
Ct^C(2)–Fe(2) /	1.654	1.637	1.662	**τ(fc(2))** /	87.10	82.4	79.8
Ct^C(3)–Fe(3)[d]	1.648	1.629	1.636	**τ(fc(3))**	−126.19	87.2	88.0
Ct^P(1)–Fe(1) /	1.638	1.616	1.649	**φ(fc(1))** /	11.61	13.9	16.0
Ct^P(2)–Fe(2) /	1.646	1.639	1.644	**φ(fc(2))** /	13.15	4.1	6.2
Ct^P(3)–Fe(3)[e]	1.649	1.647	1.624	**φ(fc(3))**	8.32	11.2	14.1
M(1)–O(1)[a,f]	3.813(3)	3.08(1)	2.57(1)				

[a] M(1) = Au for **[1b(Au)]OTf** and **[1a^F(Au)]OTf**, M(1) = Ag for **[1a^F(Ag)]OTf**; [b] C$^P_{ips}$(fc$_n$) corresponds to the respective *ipso* carbon atom of the *P*-substituted cyclopentadienyl ring (**[1b(Au)]OTf**: C(12), C(34), C(56); **[1a^F(Au)]OTf** and **[1a^F(Ag)]OTf**: C(9), C(31), C(53)); [c] C^{Link}(n) refers to the C atom to which the *C*-substituted cyclopentadienyl is bound (**[1b(Au)]OTf**: C(1), C(3), C(5); **[1a^F(Au)]OTf** and **[1a^F(Ag)]OTf**: C(1), C(2), C(3)); [d] Ct^C denotes the calculated centre of gravity of the *C*-substituted cyclopentadienyl ring; [e] Ct^P denotes the calculated centre of gravity of the *P*-substituted cyclopentadienyl ring; [f] Closest distance between the oxygen atom of a triflate anion and any metal atom (sum of van-der-Waals radii of gold and oxygen: 3.82 Å,[29] sum of atomic radii: 2.02 Å;[30] silver and oxygen: 4.03 Å,[29] 2.11 Å[30]).

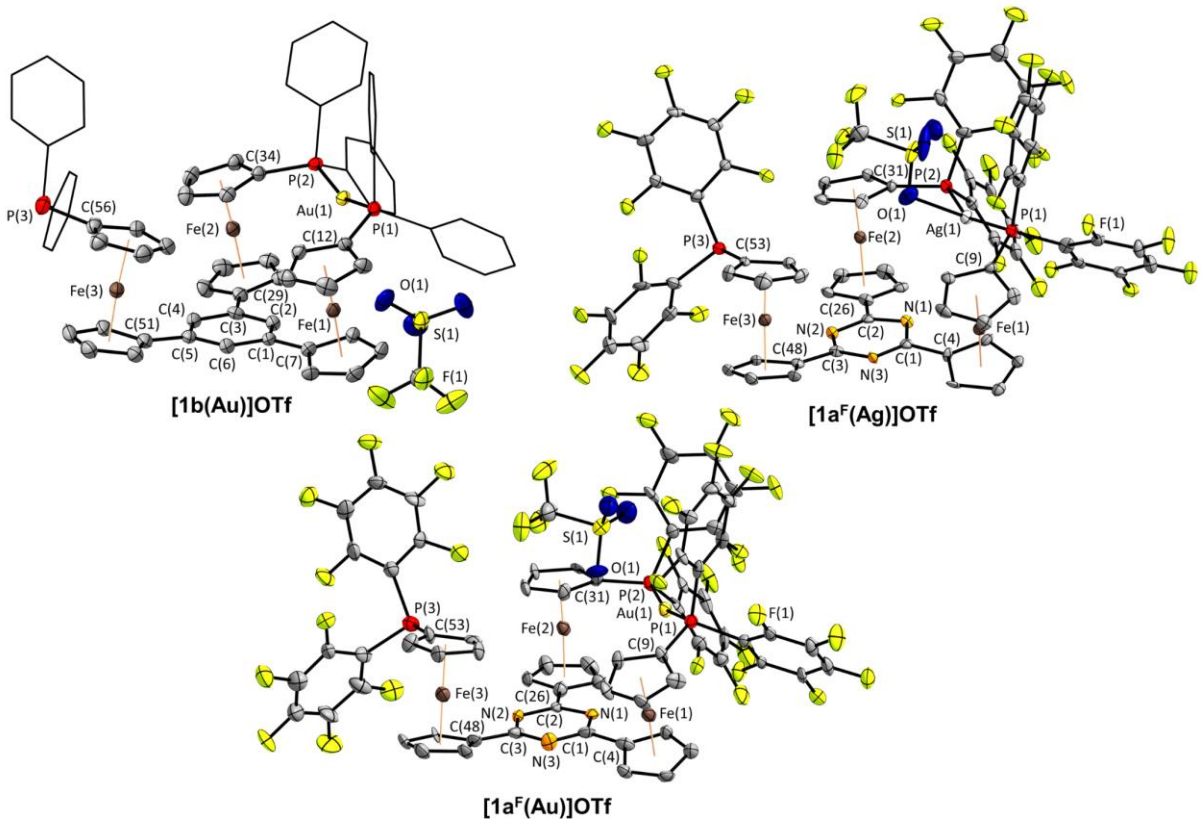

Fig. S39 Molecular structures of mononuclear complexes **[1b(Au)]OTf**, **[1a^F(Ag)]OTf**, and **[1a^F(Au)]OTf** including part of their atom-numbering scheme. Thermal ellipsoids are set at the 50% (**[1b(Au)]OTf**) and 30% (**[1a^F(Ag)]OTf**, **[1a^F(Au)]OTf**) probability levels. Co-crystallised solvents and hydrogen atoms have been omitted for clarity, and the *P*-bound phenyl rings of **[1b(Au)]OTf** are depicted in wireframe style.

Table S3 Selected bond lengths [Å], distances [Å], and angles [°] of ligands of polynuclear complexes **{[(1c)$_2$(Au)$_3$](OTf)$_3$}$_n$**, **[(1a)$_2$(Au)$_3$](OTf)$_3$**, and **[(1b)$_2$(Au)$_3$](OTf)$_3$**; numbering scheme according to Figs. S40–42, ferrocenylene geometric parameters according to Fig. S38.

	{[(1c)$_2$(Au)$_3$](OTf)$_3$}$_n$	[(1b)$_2$(Au)$_3$](OTf)$_3$	[(1a)$_2$(Au)$_3$](OTf)$_3$		{[(1c)$_2$(Au)$_3$](OTf)$_3$}$_n$	[(1b)$_2$(Au)$_3$](OTf)$_3$	[(1a)$_2$(Au)$_3$](OTf)$_3$
Au(1)–P(1) /	2.303(1)	2.295(2)	2.301(2)				
Au(1)–P(4) /	2.304(1)	2.298(2)	2.302(2)				
Au(2)–P(2) /	2.305(3)	2.299(2)	2.303(2)	**∢(P(1)–Au(1)–P(4)) /**	170.45(5)	173.33(6)	171.96(8)
Au(2)–P(3) /	2.320(3)	2.298(2)	2.303(2)	**∢(P(2)–Au(2)–P(3)) /**	171.4(1)	162.44(7)	164.05(8)
Au(3)–P(5) /	2.296(1)	2.302(2)	2.302(3)	**∢(P(5)–Au(3)–P(6))**	172.72(5)	164.85(6)	162.92(8)
Au(3)–P(6)	2.299(1)	2.300(1)	2.304(3)				
C$^P_{ips}$(fc$_1$)–P(1) /	1.780(4)	1.779(6)	1.78(1)	**α(fc(1)) /**	175.20	177.47	177.43
C$^P_{ips}$(fc$_2$)–P(2) /	1.781(5)	1.771(8)	1.77(1)	**α(fc(2)) /**	176.23	176.97	176.22
C$^P_{ips}$(fc$_3$)–P(3) /	1.795(4)	1.778(6)	1.78(1)	**α(fc(3)) /**	177.27	176.08	176.11
C$^P_{ips}$(fc$_4$)–P(4) /	1.785(4)	1.782(7)	1.779(7)	**α(fc(4)) /**	175.50	177.51	176.83
C$^P_{ips}$(fc$_5$)–P(5) /	1.770(6)	1.768(7)	1.782(8)	**α(fc(5)) /**	176.37	174.95	177.01
C$^P_{ips}$(fc$_6$)–P(6)[a]	1.767(4)	1.773(7)	1.76(1)	**α(fc(6))**	177.58	176.21	175.65
C$^C_{ips}$(fc$_1$)–C^{Link}(1) /	1.472(6)	1.475(9)	1.47(1)	**Θ(fc(1)) /**	5.65	2.91	3.06
C$^C_{ips}$(fc$_2$)–C^{Link}(2) /	1.469(6)	1.49(1)	1.47(1)	**Θ(fc(2)) /**	3.19	2.97	3.91
C$^C_{ips}$(fc$_3$)–C^{Link}(3) /	1.479(6)	1.47(1)	1.45(1)	**Θ(fc(3)) /**	1.66	4.85	3.73
C$^C_{ips}$(fc$_4$)–C^{Link}(4) /	1.488(7)	1.46(1)	1.47(1)	**Θ(fc(4)) /**	5.26	3.27	3.16
C$^C_{ips}$(fc$_5$)–C^{Link}(5) /	1.491(6)	1.478(8)	1.46(1)	**Θ(fc(5)) /**	2.78	4.88	3.73
C$^C_{ips}$(fc$_6$)–C^{Link}(6)[b]	1.483(6)	1.47(1)	1.48(1)	**Θ(fc(6))**	0.47	3.98	4.33
Ct^C(1)–Fe(1) /	1.655	1.655	1.659	**τ(fc(1)) /**	134.57	142.06	144.72
Ct^C(2)–Fe(2) /	1.644	1.654	1.646	**τ(fc(2)) /**	71.59	92.98	91.95
Ct^C(3)–Fe(3) /	1.653	1.647	1.649	**τ(fc(3)) /**	69.27	−95.16	−98.65
Ct^C(4)–Fe(4) /	1.661	1.662	1.650	**τ(fc(4)) /**	122.6	146.58	141.55
Ct^C(5)–Fe(5) /	1.645	1.641	1.646	**τ(fc(5)) /**	75.99	−98.38	−98.39
Ct^C(6)–Fe(6)[c]	1.649	1.652	1.646	**τ(fc(6))**	74.86	91.97	90.08
Ct^P(1)–Fe(1) /	1.639	1.652	1.652	**φ(fc(1)) /**	34.09	5.33	8.59
Ct^P(2)–Fe(2) /	1.643	1.649	1.654	**φ(fc(2)) /**	33.41	7.59	7.93
Ct^P(3)–Fe(3) /	1.642	1.631	1.631	**φ(fc(3)) /**	31.77	3.58	4.62
Ct^P(4)–Fe(4) /	1.642	1.642	1.655	**φ(fc(4)) /**	27.38	9.99	5.47
Ct^P(5)–Fe(5) /	1.636	1.635	1.639	**φ(fc(5)) /**	31.33	6.59	3.16
Ct^P(6)–Fe(6)[d]	1.626	1.655	1.649	**φ(fc(6))**	27.55	11.76	5.80
Shortest Au–O$_{Tf}$[e]	3.421(4)	–	3.46(2)	**φ(Arene(1)–Arene(2))**	78.24	33.26	35.16

[a] C$^P_{ips}$(fc$_n$) corresponds to the respective *ipso* carbon atom of the *P*-substituted cyclopentadienyl ring ({**[(1c)$_2$(Au)$_3$](OTf)$_3$}$_n$** and **[(1b)$_2$(Au)$_3$](OTf)$_3$**: C(12), C(34), C(56), C(84), C(106), C(128); **[(1a)$_2$(Au)$_3$](OTf)$_3$**: C(9), C(31), C(53), C(78), C(100), C(122)). [b] C^{Link}(n) refers to the C atom to which the *C*-substituted cyclopentadienyl is bound ({**[(1c)$_2$(Au)$_3$](OTf)$_3$}$_n$** and **[(1b)$_2$(Au)$_3$](OTf)$_3$**: C(1), C(3), C(5), C(73), C(75), C(77); **[(1a)$_2$(Au)$_3$](OTf)$_3$**: C(1), C(2), C(3), C(70), C(71), C(72)). [c] Ct^C denotes the calculated centre of gravity of the *C*-substituted cyclopentadienyl ring. [f] Ct^P denotes the calculated centre of gravity of the *P*-substituted cyclopentadienyl ring. [e] Closest distance between the oxygen atom of a triflate anion and any gold atom (sum of van-der-Waals radii of gold and oxygen: 3.82 Å,[29] sum of atomic radii: 2.02 Å[30]).

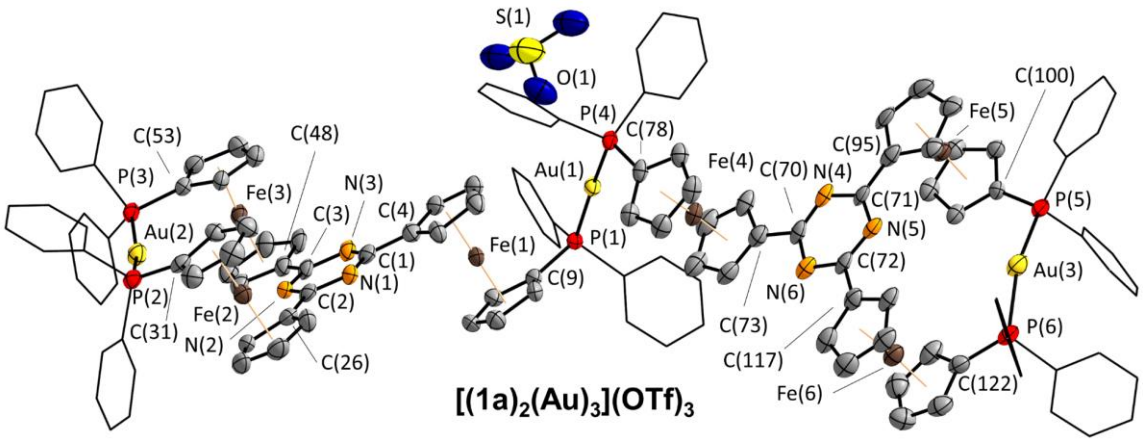

Fig. S40 Molecular structure of trinuclear complex **[(1a)$_2$(Au)$_3$](OTF)$_3$** including part of its atom-numbering scheme. Thermal ellipsoids are set at the 50% probability level. For clarity, hydrogen atoms and co-crystallised solvent molecules have been omitted and *P*-bound phenyl rings are depicted in wireframe style. The SO_3^- group of the sole triflate anion which for which refinement was possible is shown, while the disordered CF_3 group has been omitted for clarity.

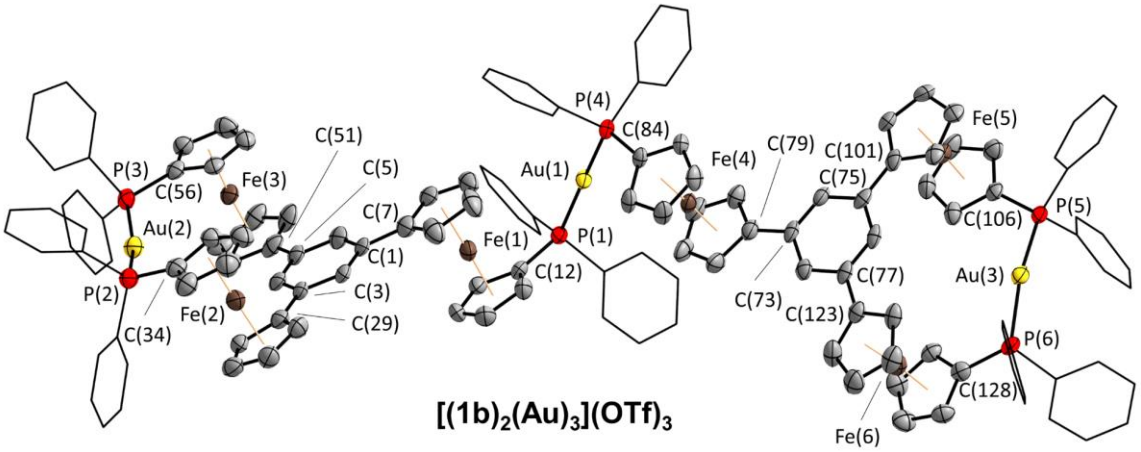

Fig. S41 Molecular structure of trinuclear complex **[(1b)$_2$(Au)$_3$](OTF)$_3$** including part of its atom-numbering scheme. Thermal ellipsoids are set at the 50% probability level. For clarity, hydrogen atoms and co-crystallised solvent molecules have been omitted and *P*-bound phenyl rings are depicted in wireframe style. None of the three triflate anions could be refined.

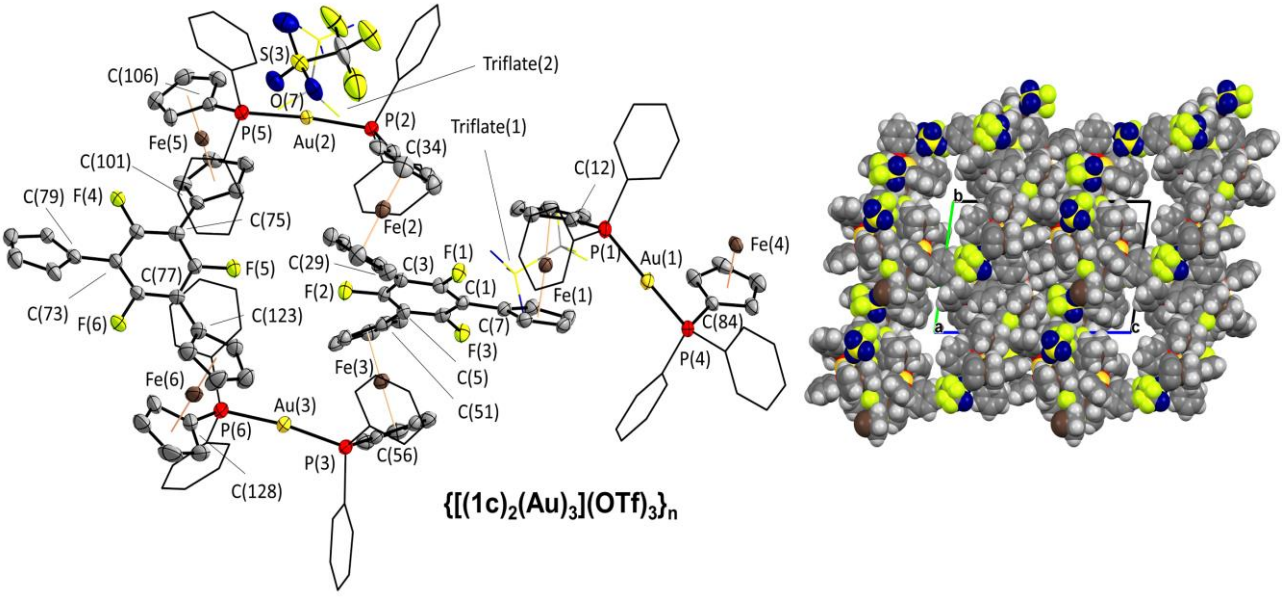

Fig. S42 Left: Section of the molecular structure of coordination polymer **{[(1c)$_2$(Au)$_3$](OTf)$_3$}$_n$** including part of its atom-numbering scheme. Only the asymmetric unit is shown (*i.e.* the ferocenylene moiety around Fe(4) is comprised of C(79)–C(88)). Thermal ellipsoids are set at the 50% probability level. For clarity, hydrogen atoms and disorder of Au(2) (occupancy 0.79[shown]/0.21) have been omitted and *P*-bound phenyl rings are depicted in wireframe style. Triflate anions 1 and 2 are depicted in wireframe style and only triflate anion 3, involved in the shortest O–Au interaction, is shown in ellipsoid style. **Right:** Space-filling model of the polymeric structure of **{[(1c)$_2$(Au)$_3$](OTf)$_3$}$_n$** viewed along the crystallographic *a* axis, highlighting the small channels along *a*, including (partly disordered) anions and hydrogen atoms.

Only one (in **[(1b)$_2$(Au)$_3$](OTf)$_3$**) and 2.5 (in **[(1a)$_2$(Au)$_3$](OTf)$_3$**) equivalents of toluene per unit cell could be located and refined, while the majority of solvent molecules had to be removed by the SQUEEZE routine implemented in PLATON.[10] For coordination polymer (CP) **{[(1c)$_2$(Au)$_3$](OTf)$_3$}$_n$**, nine molecules of THF per asymmetric unit (18 molecules of THF per unit cell) are present in the structure but could not be satisfactorily modelled from the data. The corresponding electron count of 720 electrons/unit cell (40 e^-/THF) has been removed using the SQUEEZE routine implemented in PLATON.[10] The asymmetric unit (Fig. S42) of **{[(1c)$_2$(Au)$_3$](OTf)$_3$}$_n$** consists of the three gold(I) ions and two crystallographically independent tris-phosphane ligands, one of which (Fe/P(1) to Fe/P(3)) is located completely within the asymmetric unit, while the other (Fe/P(4) to Fe/P(6)) lies partly (P–C_5H_4 ring of Fe(4)) within the next asymmetric unit.

3. Variable-temperature NMR Spectra

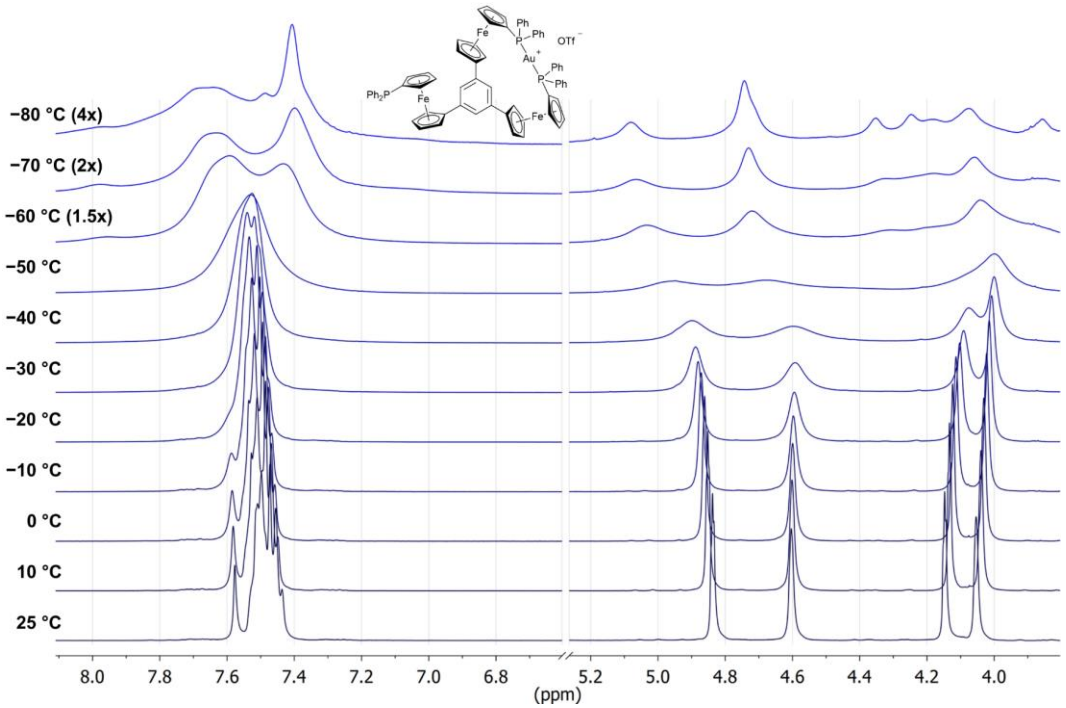

Fig. S43 Stacked VT ^{1}H NMR spectra of **[1b(Au)]OTf** in CD_2Cl_2 recorded over a temperature range from 25 °C to −80 °C. Only the relevant regions are shown, and the excised region only contains the signal for $CHDCl_2/CH_2Cl_2$. Scaling has been changed as indicated for better visibility.

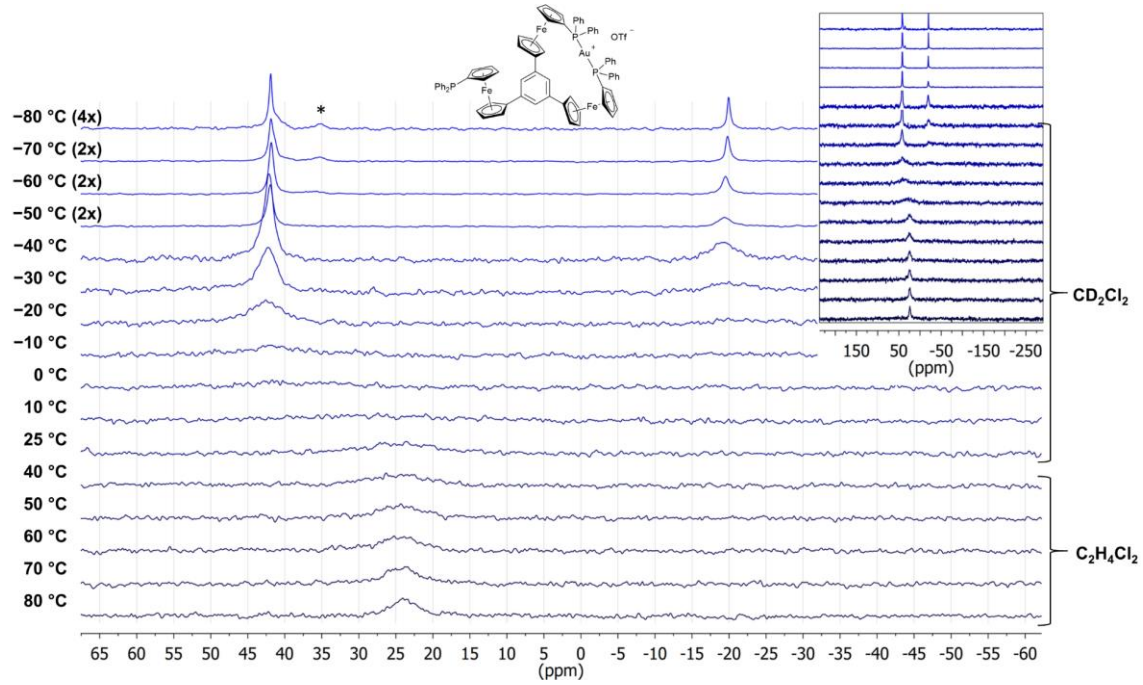

Fig. S44 Stacked VT $^{31}P\{^{1}H\}$ NMR spectra of **[1b(Au)]OTf** in CD_2Cl_2 recorded over a temperature range from 25 °C to −80 °C, and in $C_2H_4Cl_2$ recorded over a temperature range from 40 °C to 80 °C (THF-d_8 for locking). The insert aims to give an enhanced perspective on the relevant signals. Scaling has been applied as indicated for better visibility. The signal at about 35 ppm (*) probably originates from a small impurity.

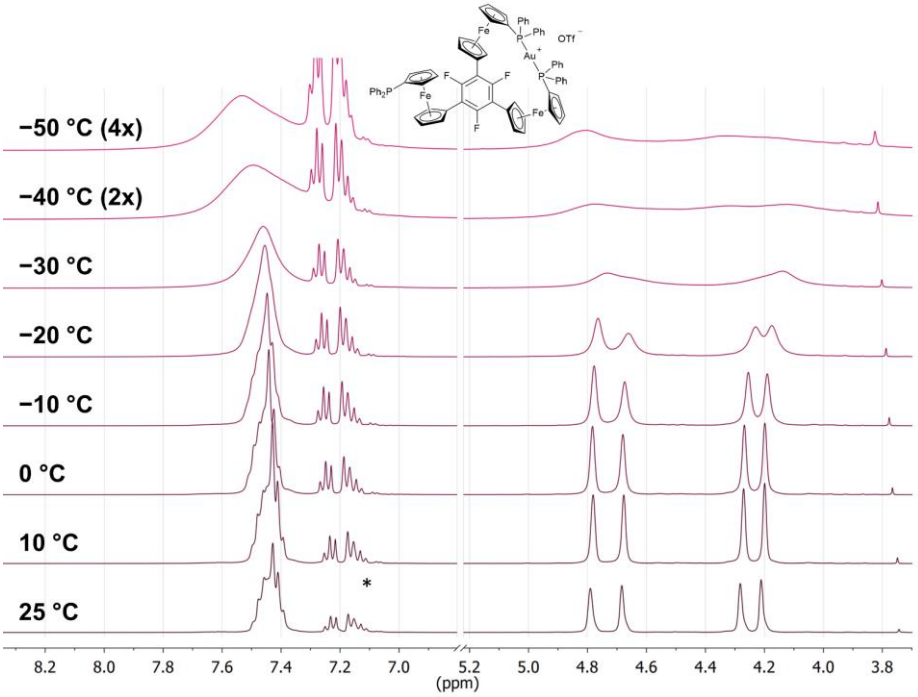

Fig. S45 Stacked VT ^{1}H NMR spectra of **[1c(Au)]OTf** in CD_2Cl_2 recorded over a temperature range from 25 °C to −50 °C. Only the relevant regions are shown, and the excised region only contains the signal for $CHDCl_2/CH_2Cl_2$. Scaling has been adapted for better visibility as indicated. The signals marked by the asterisk (*) correspond to the arene protons of toluene which has been used in the purification process.

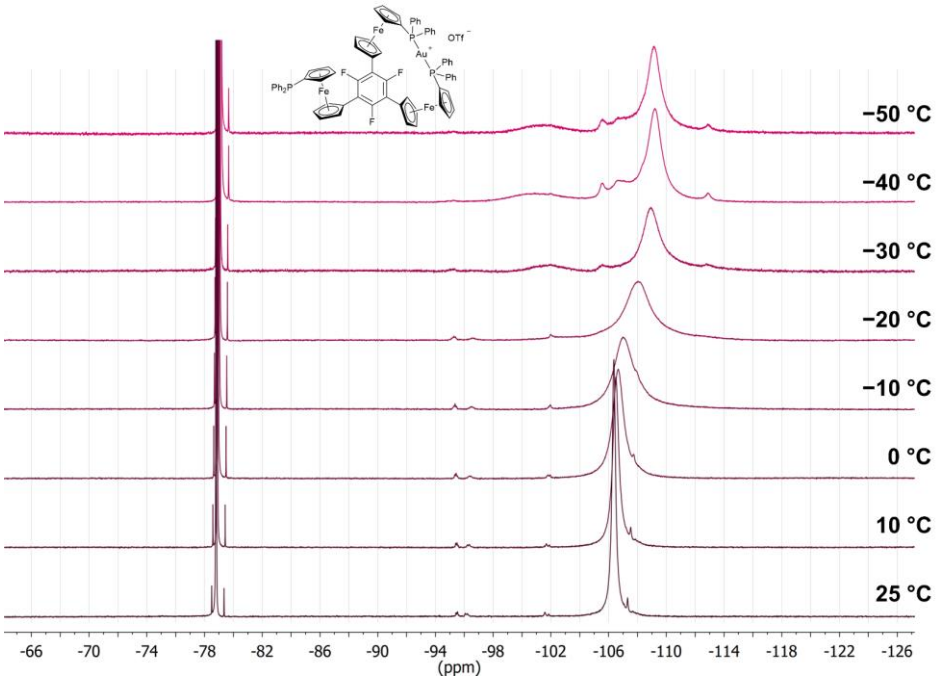

Fig. S46 Stacked VT $^{19}F\{^{1}H\}$ NMR spectra of **[1c(Au)]OTf** in CD_2Cl_2 recorded over a temperature range from 25 °C to −50 °C. The cropped signal at about −79 ppm corresponds to the triflate anion.

While the loss of apparent C_{3v} symmetry is comparatively easy to discern in the VT $^{31}P\{^{1}H\}$ NMR spectra of **[1c(Au)]OTf** (Fig. S47), this effect is less prominent in the corresponding $^{19}F\{^{1}H\}$ NMR spectra (Fig. S46). However, the appearance of a broad signal centred at about −101 ppm and the upfield shift of the original C_6F_3 resonance at −106 ppm to −109 ppm can be linked to an inequivalence of the fluorine substituents at the arene core, the broader resonance connected to the fluorine atom closest to gold. Below −50 °C, no satisfying spectra could be recorded anymore, most likely due to lowered solubility.

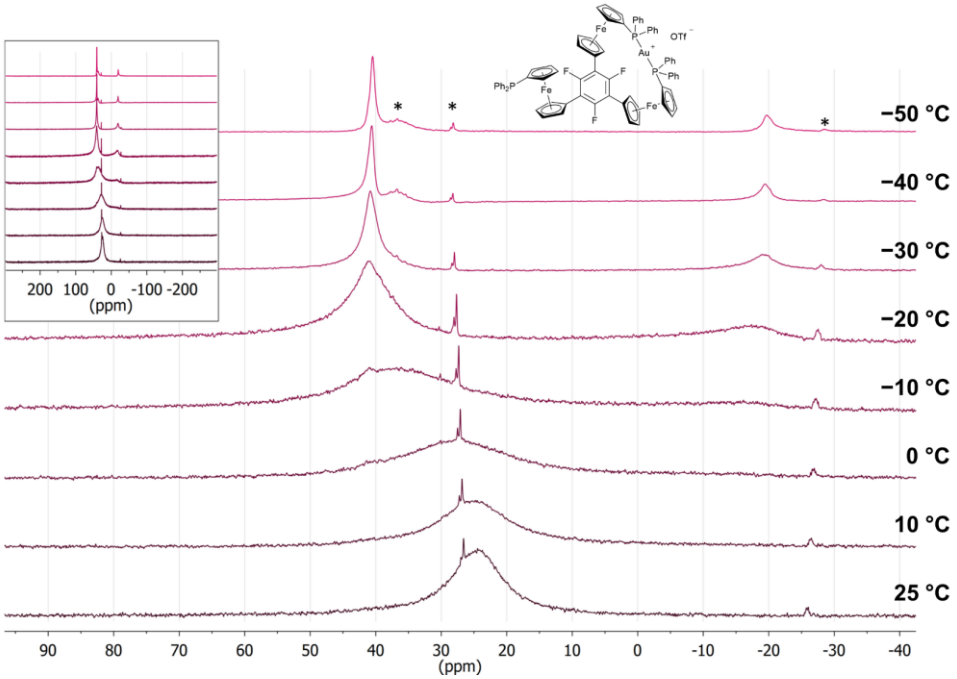

Fig. S47 Stacked VT $^{31}P\{^{1}H\}$ NMR spectra of **[1b(Au)]OTf** in CD_2Cl_2 recorded over a temperature range from 25 °C to −50 °C. The insert aims to give an enhanced perspective on the relevant signals. Signals marked by asterisks (*) originate from one or several unknown impurities.

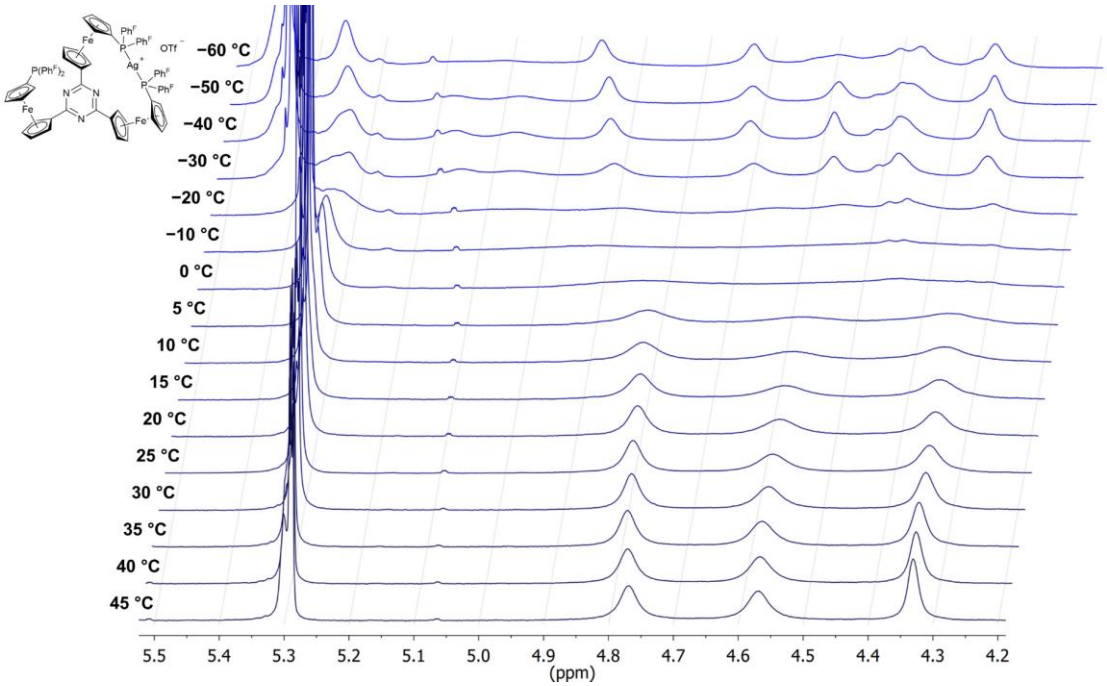

Fig. S48 Stacked VT ^{1}H NMR spectra of **[1a^{F}(Ag)]OTf** in CD_2Cl_2 recorded over a temperature range from 45 °C to −60 °C. Only the relevant spectral region is shown. A stacking angle of 10° has been applied to allow an easier discrimination of the $CHDCl_2/CH_2Cl_2$ signal and the decoalescing **[1a^{F}(Ag)]OTf** ferrocenylene resonance.

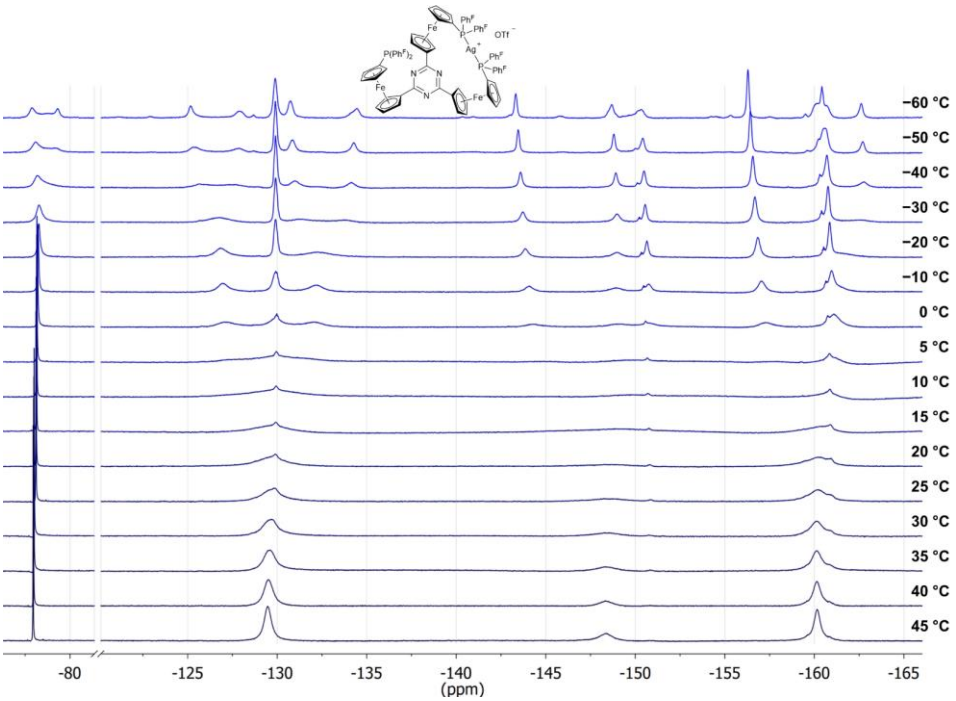

Fig. S49 Stacked VT $^{19}F\{^{1}H\}$ NMR spectra of **[1a^{F}(Ag)]OTf** in CD_2Cl_2 recorded over a temperature range from 45 °C to −60 °C. Only the relevant spectral regions are shown.

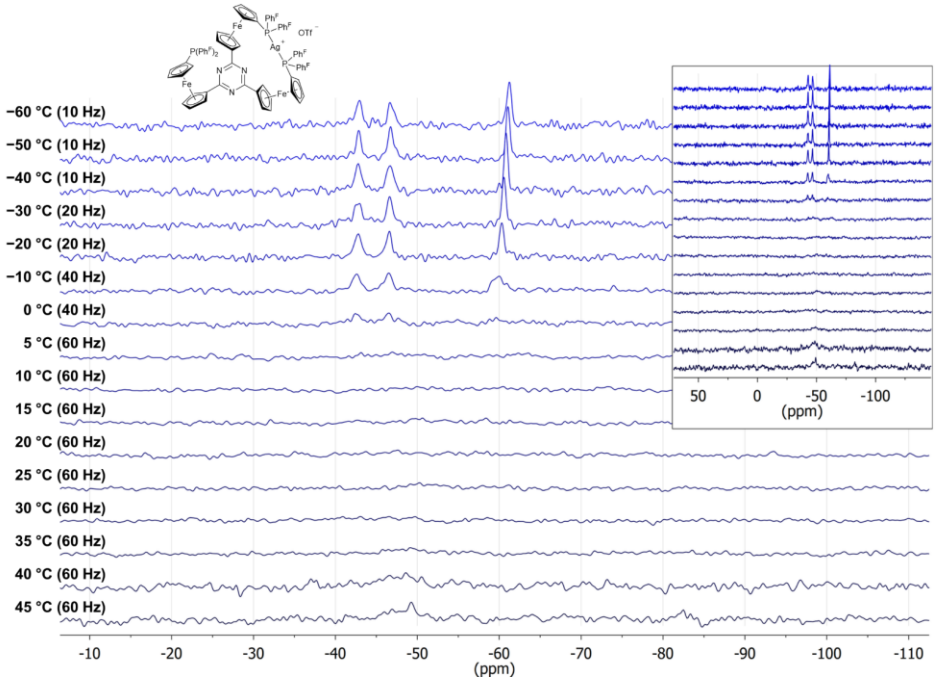

Fig. S50 Stacked VT $^{31}P\{^{1}H\}$ NMR spectra of **[1a^{F}(Ag)]OTf** in CD_2Cl_2 recorded over a temperature range from 45 °C to −60 °C. The insert aims to give an enhanced perspective on the relevant signals. Different exponential line broadening has been applied to the spectra as indicated next to the temperature.

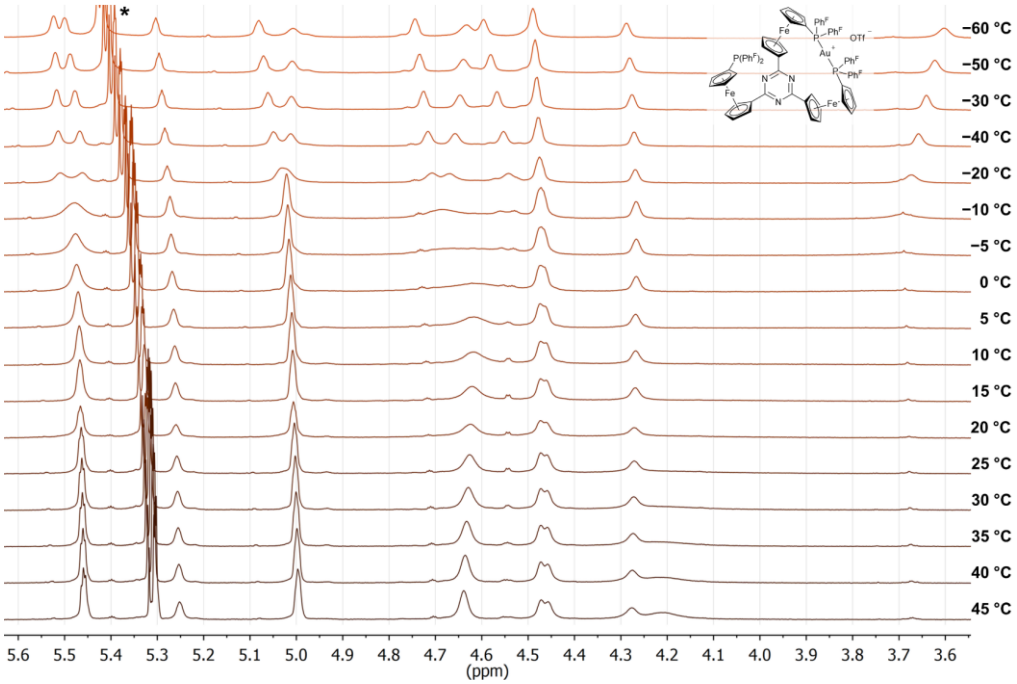

Fig. S51 Stacked VT ^{1}H NMR spectra of **[1a^{F}(Au)]OTf** in CD_2Cl_2 recorded over a temperature range from 45 °C to −60 °C. Only the relevant spectral region is shown. The $CHDCl_2/CH_2Cl_2$ signal is marked by an asterisk (*).

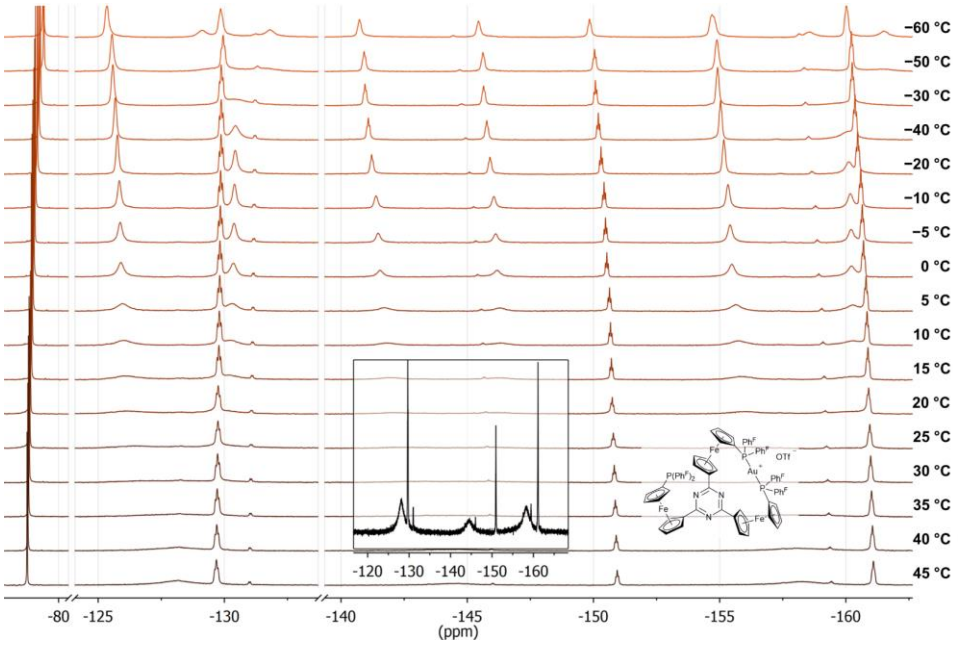

Fig. S52 Stacked VT $^{19}F\{^{1}H\}$ NMR spectra of **[1a^{F}(Au)]OTf** in CD_2Cl_2 recorded over a temperature range from 45 °C to −60 °C. Only the relevant spectral regions are shown. The insert depicts the spectrum at 45 °C aiming to show the very broad resonances for the bis(pentafluorophenyl)phosphanyl groups involved in the (fluctional) coordination of gold.

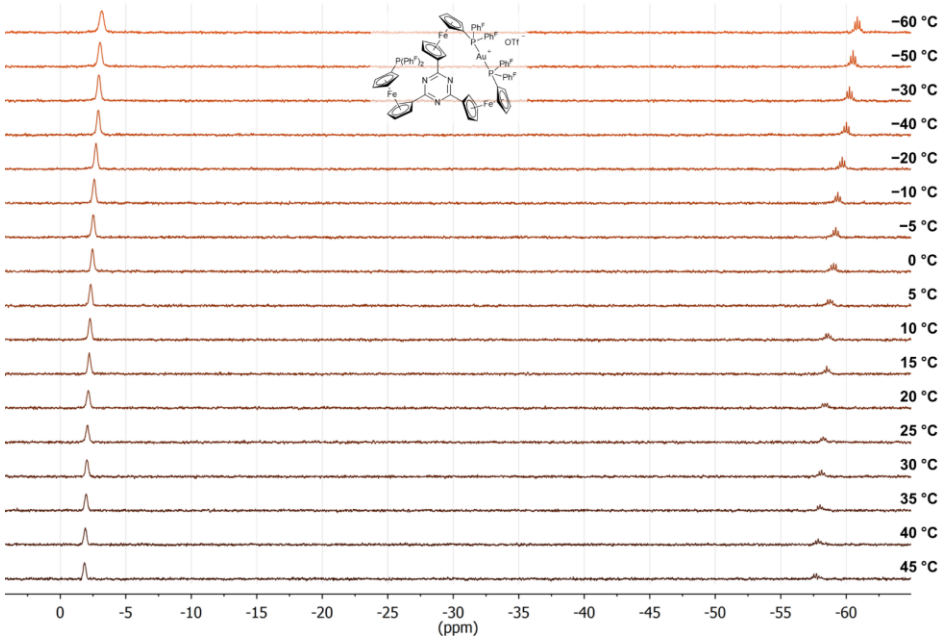

Fig. S53 Stacked VT $^{31}P\{^{1}H\}$ NMR spectra of **[1a^{F}(Au)]OTf** in CD_2Cl_2 recorded over a temperature range from 45 °C to −60 °C.

4. DFT Calculations

Table S4 Calculated absolute energies [E_h] of free tris-phosphanes **1a–c**, of pre-formed ligand fragments **[1a–c()]$_{open/closed}$**, of the gold(I) ion, and of the open as well as of the closed complexes **[1a$^{(F)}$–c(Au)]$^+$** (DFT level of theory, CPCM solvent model [CH_2Cl_2]).

Entity	E [E_h]	Entity	E [E_h]	Entity	E [E_h]
Au$^+$	−135.5798901	**[1a()]$_{open}$**	−7642.1280764107	**[1a(Au)]$^+_{open}$**	−7777.90785157186
1a	−7642.14632015548	**[1b()]$_{open}$**	−7593.9725218511	**[1b(Au)]$^+_{open}$**	−7729.75310335655
1b	−7593.97938626378	**[1c()]$_{open}$**	−7891.76291230438	**[1c(Au)]$^+_{open}$**	−8027.54257377607
1c	−7891.77253597254	**[1a()]$_{closed}$**	−7642.12862215758	**[1a^F(Au)]$^+_{open}$**	−10755.727617087268
		[1b()]$_{closed}$	−7593.96413062434	**[1a(Au)]$^+_{closed}$**	−7777.92095451187
1b$_{rotated}$	−7593.97179978259	**[1c()]$_{closed}$**	−7891.74910992938	**[1b(Au)]$^+_{closed}$**	−7729.75320456070
[1b()]$_{open,rotated}$	−7593.95791438302			**[1c(Au)]$^+_{closed}$**	−8027.53961852385
[1b(Au)]$^+_{open,rotated}$	−7729.73395335248			**[1a^F(Au)]$^+_{closed}$**	−10755.648973570896

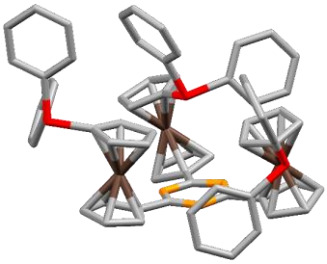

Fig. S54 Calculated structure of free tris-phosphane **1a**.

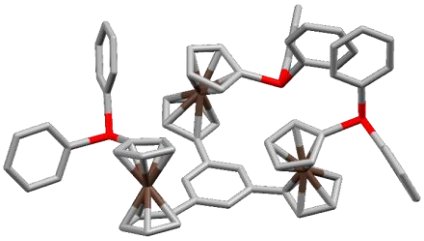

Fig. S55 Calculated structure of free tris-phosphane **1b**.

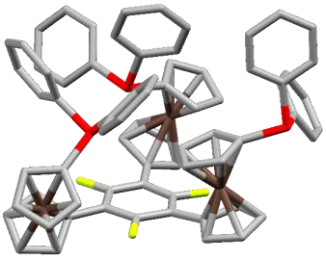

Fig. S56 Calculated structure of free tris-phosphane **1c**.

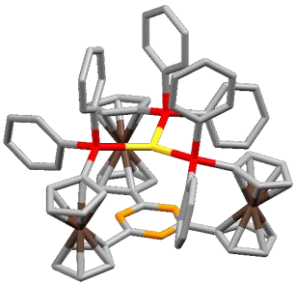

Fig. S57 Calculated structure of closed complex cation **[1a(Au)]$^+_{closed}$**.

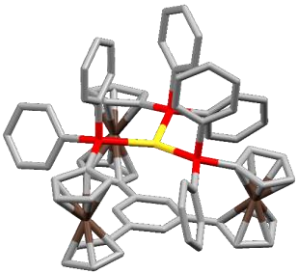

Fig. S58 Calculated structure of closed complex cation **[1b(Au)]$^+_{closed}$**.

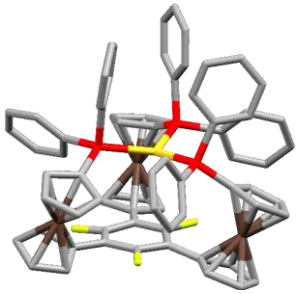

Fig. S59 Calculated structure of closed complex cation **[1c(Au)]$^+_{closed}$**.

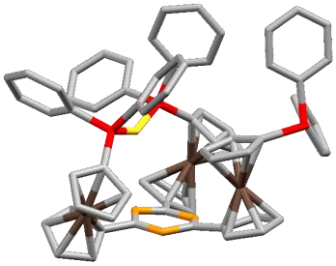

Fig. S60 Calculated structure of open complex cation **[1a(Au)]$^+_{open}$**.

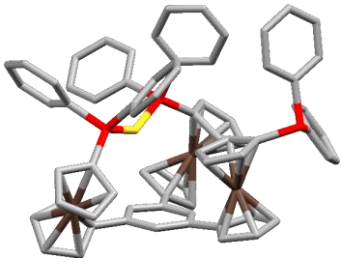

Fig. S61 Calculated structure of open complex cation **[1b(Au)]$^+_{open}$**.

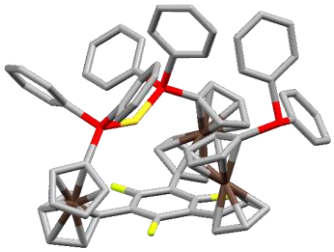

Fig. S62 Calculated structure of open complex cation **[1c(Au)]$^+_{open}$**.

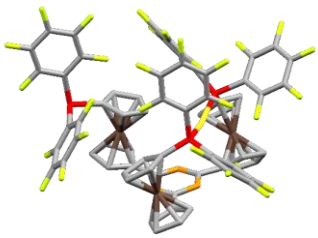

Fig. S63 Calculated structure of open complex cation **[1a^F(Au)]$^+_{open}$**.

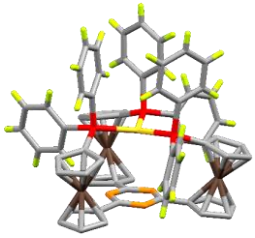

Fig. S64 Calculated structure of closed complex cation **[1a^F(Au)]$^+_{closed}$**.

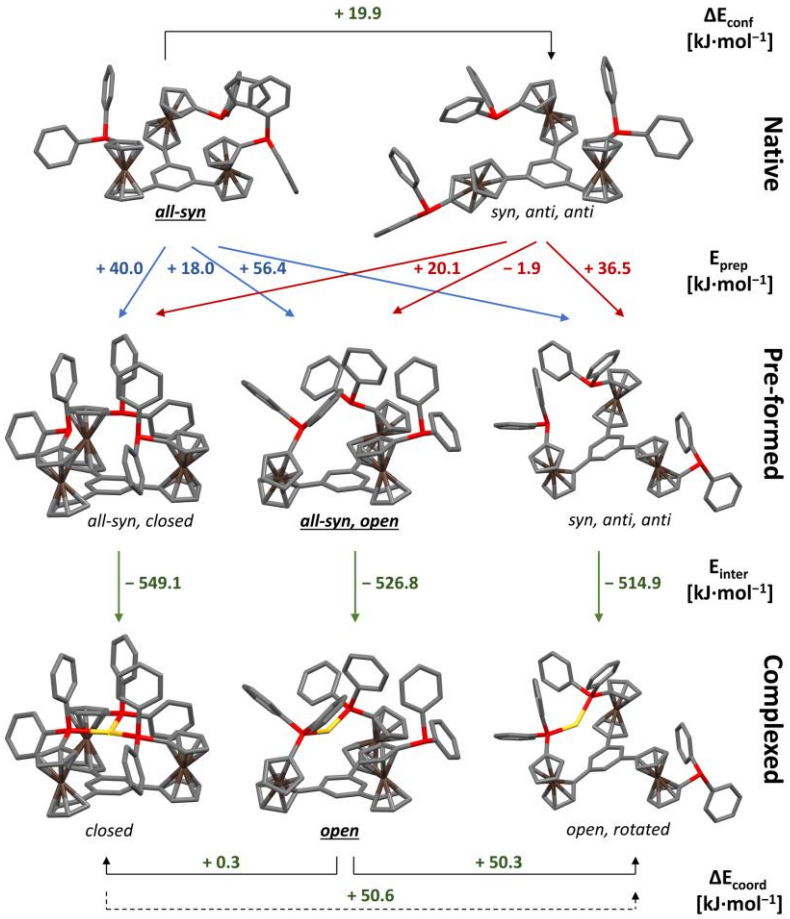

Fig. S65 – Investigation of the conformational influence of benzene-based tris-phosphane **1b** on the relative stabilities of closed tricoordinate *vs*. open dicoordinate gold(I) complexes. All energies are given in kJ·mol^{-1} and refer to the energy of the calculated structure at the origin of the respective arrow. The most stable structure in each row is indicated in bold and underlined print.

Different conformations of the free tris-phosphanes and the open, dicoordinate gold(I) complexes might contribute to the balance of steric and electronic factors. For this reason, benzene-based **1b**, showing the most delicate balance of both factors, was chosen as a model system (Fig S65). The energies of a second, "extreme" conformation in which the non-coordinated ferrocenylphosphane was rotated to the opposite face of the central arene (*syn*,*anti*,*anti* conformation) were calculated for **1b**, the pre-formed ligand fragment **[1b()]**$^+$, and for the corresponding complex **[1b(Au)]**$^+$ (Table S4) on the same level of theory (checking the whole conformational space of both the tris-phosphanes and the resulting dicoordinate gold complexes is out of the scope of this study). Geometry optimisations of the free tris-phosphane and the dicoordinate gold complex in this conformation have identified these structures as local minima, however with higher absolute energies than the all-*syn* conformers by about 20 kJ·mol^{-1} (free tris-phosphane) and 50 kJ·mol^{-1} (gold complex). These energy differences seem reasonable in light of the apparently unhindered rotation of native **1b** and the hindered rotation of **[1b(Au)]OTf** in (VT) NMR spectroscopy. Starting from the *syn*,*anti*,*anti* conformer does not change the all-*syn* ligand conformation from being the energetically most favourable one. Furthermore, the interaction energy between the two different dicoordinate forms also favours the all-*syn* conformer by about 12 kJ·mol^{-1}.

These findings do not take the role of the anion into account which, especially for the dicoordinate form, might exert stabilising influences. While the relative orientation of the pendant ferrocenylphosphane has been found to play an important role in determining the relative stabilities of the resulting complexes, the clear preference for the open, all-*syn* ligand conformation is observable irrespective of the starting conformation of native **1b** and is most likely the decisive factor in favouring the open over the closed geometry.

5. Electrochemistry

5.1. Scanning Speed Dependence of [1b(Au)]OTf and Decamethylferrocene – (Quasi)Reversibility

Table S5 Peak potentials $E_p^{an/ca}$ and separation ΔE_p as well as half-wave potentials $E_{1/2}$, peak currents $i_{a/c}$, peak current ratios and scanning speed-normalised currents for **[1b(Au)]OTf** and decamethylferrocene (**6**) in 0.1 mmol·L^{-1} (nBu$_4$N)BF$_4$ in CH_2Cl_2, reported *vs.* the reference electrode (Ag/AgCl) prior to internal referencing of **[1b(Au)]OTf** *vs.* [FcH]/[FcH]$^+$. All values are given as the average of three (voltages) or two (currents, first cycle ignored) consecutive scans.

Scanning speed v	[1b(Au)]OTf							[Fe(C$_5$Me$_5$)$_2$] (6)						
	E_p^a	E_p^c	$E_{1/2}$ (ΔE_p)	i_a	i_c	i_a/i_c	$i_c/\sqrt{v}$	E_p^{an}	E_p^{ca}	$E_{1/2}$ (ΔE_p)	i_a	i_c	i_a/i_c	$i_c/\sqrt{v}$
[mV·s^{-1}]	mV			µA			µA·s$^{0.5}$·mV$^{-0.5}$	mV			µA			µA·s$^{0.5}$·mV$^{-0.5}$
50	693	511	602 (182)	28	20	1.35	2.89	−220	−375	−297 (155)	40	42	0.96	5.94
100	706	504	605 (202)	35	29	1.21	2.90	−203	−394	−298 (191)	54	58	0.94	5.76
200	729	489	609 (240)	42	38	1.09	2.71	−181	−416	−298 (234)	70	79	0.89	5.56

Due to the larger-than-expected peak separation ΔE_p between the anodic (oxidation, E_p^a) and cathodic (reduction, E_p^c) peaks in the cyclic voltammogram of **[1b(Au)]OTf** (and related compounds, cf. Table 4 in main article) which deviates from the 59 mV/z (z = number of electrons involved, 25 °C) of a perfectly reversible, that is, Nernstian, redox process, we investigated the scanning speed dependence of peak potentials and separation (Table S5). Given the low polarity of the SE and the uncompensated Ohmic drop of the CV setup, these values have been compared to the chosen internal standard, decamethylferrocene (**6**) at v = 50, 100, and 200 mV·s^{-1}.

As apparent from the assembled data, the positions of both peak maxima shift with increasing scanning speed, thereby enlarging the respective peak separation from 182 to 240 mV. This behaviour is typical for so-called quasireversible redox processes where the rate of electron transfer (eT) between the electrode and the electrochemical layer around it becomes comparable to the rate of diffusion to that interface. Thus, the measured currents do not only depend on the mass transfer anymore (in contrast, the rate of eT for a completely reversible process in the Nernstian sense is much higher than that of mass transfer). Identical to the reversible case where peak positions and separations are independent of scanning speed, the peak current ratio i_a/i_c is still unity. In both cases, the ratio of i_c and the square root of the scanning speed, $\sqrt{v}$ should also be constant.[31,32]

For **[1b(Au)]OTf**, the peak current ratio i_a/i_c is significantly greater than unity at lower scanning speed, as the anodic current outweighs its cathodic counterpart, hinting at a partly irreversible process. When v becomes higher, the ratio approaches 1. When comparing all values to those obtained for **6** under very similar conditions (differing but comparable sample concentration), comparable trends particularly with respect to $E_p^{a/c}$ and ΔE_p are found, with the absolute values of ΔE_p for **6** being slightly smaller than for **[1b(Au)]OTf**. Peak current ratios are closer to unity especially for slower scanning speed, while $i_c/\sqrt{v}$ varies to only a comparatively small extent for both compounds.

Assuming ideal/Nernstian behaviour for reference compound **6**,[13] an exact classification of **[1b(Au)]OTf** as either reversible or quasireversible in its oxidation is thus hampered not so much by the peak potential shifts and large peak separation – as this behaviour is found for both samples – but due to the stark deviation of i_a/i_c for smaller scanning speeds. Therefore, the oxidation of **[1b(Au)]OTf** (and corresponding processes for the other gold complexes for which similar measurements have been conducted) is termed quasireversible in the context of this study.

5.2. Electrochemical Data of 1a^F, [1a^F(Ag)]OTf, and [1a^F(Au)]OTf

For free perfluorophenyl tris-phosphane **1a^F** in the BF$_4$-based SE (Fig. S66), three closely spaced oxidations, none of which is reversible, can be discerned. While the sample does not yield cathodic currents on an initial scan, a weak reduction event at about −500 mV *vs.* FcH/[FcH]$^+$ (for potentials, cf. Table S6) results from addressing the first oxidation already (pink trace in Fig. S66). This reduction in turn also entails a matching oxidation and intensifies with shifting the anodic vertex potential to higher voltages (cf. pink *vs.* purple *vs.* blue trace). Taken together, these observations indicate the presence of one or several electron-transfer induced chemical reactions (EC mechanism).[33] At higher anodic potentials, more unstructured and/or broad, irreversible oxidation events appear. Changing the SE to the much less coordinating BAr$^F{}_4^-$ anion, three separate and well-resolved oxidation steps result, in line with a stepwise oxidation of the three ferrocenylene groups without interference from the lone pairs of electrons on the phosphorus atoms. This stands in stark contrast to the results obtained for non-fluorinated **1a** under the same conditions, for which only the first of three oxidations is partly reversible (cf. main article).[6] Compared to **1a**, the oxidation potentials of **1a^F** are shifted to more anodic values (Table S6), in line with stronger electron-withdrawing effect of the PPh$^F{}_2$ *vs.* the PPh$_2$ group.[34,35]

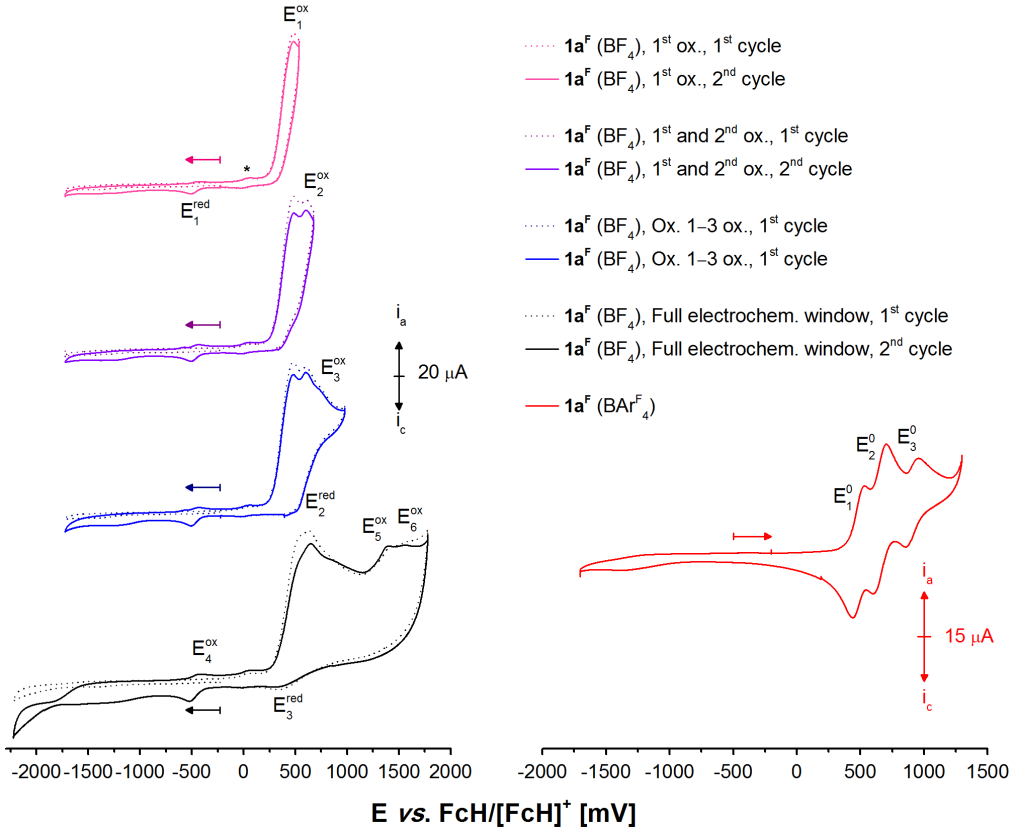

Fig. S66 Cyclic voltammograms of tris-phosphane **1a^F** in the BF_4- (left) and BAr^F_4-based (right) supporting electrolytes (SE). Horizontal arrows indicate the starting potential and initial scan direction (100 mV·s^{-1}). For **1a^F** in the BAr^F_4-based SE (red trace), the second of three consecutively measured cycles are shown. For all measurements in the BF_4-based SE, dotted lines refer to the first, solid lines to the second of three consecutively measured cycles. The redox event marked with an asterisk (*) is likely due to an impurity. Peak potentials have been labelled for Table S6.

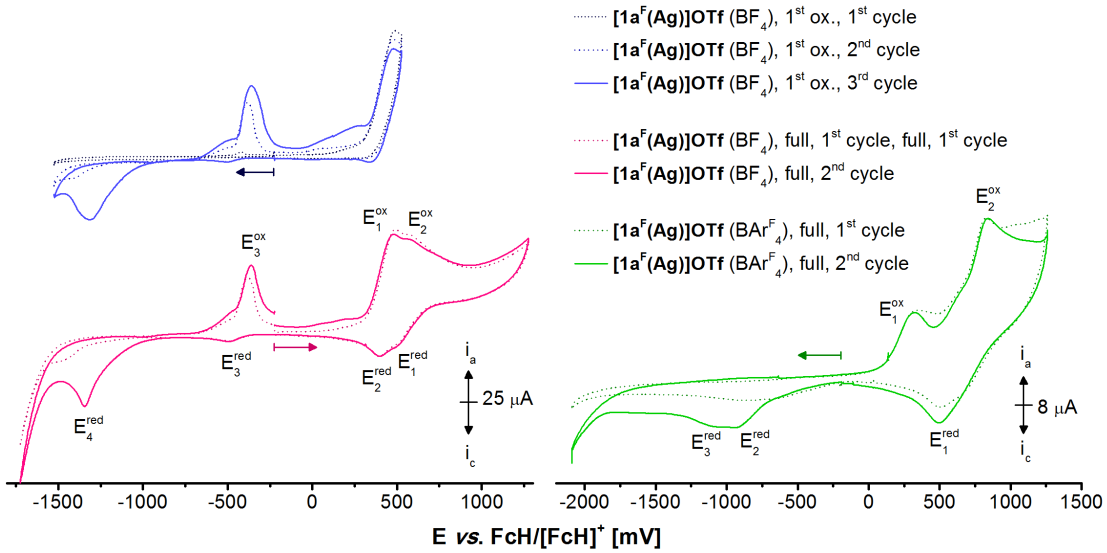

Fig. S67 Cyclic voltammograms of **[1a^F(Ag)]OTf** in the BF_4- (left) and BAr^F_4-based (right) supporting electrolytes (SE). Horizontal arrows indicate the starting potential and initial scan direction (100 mV·s^{-1}). Peak potentials have been labelled for Table S6 and refer to the second of three consecutively measured cycles (solid lines).

For silver(I) complex **[1a^F(Ag)]OTf**, the cyclic voltammograms recorded in the BF_4-based SE (Fig. S67) show clear signs of several chemical reactions occurring after the first oxidation already. While reduction-silent on the first scan in cathodic direction (dark blue dotted trace), the first, irreversible oxidation leads to the appearance of a small reduction event at very negative potentials

(−1.5 V *vs.* FcH/[FcH]$^+$) and, quite unexpectedly, an intense re-oxidation at around −370 mV *vs.* FcH/[FcH]$^+$. In a following third cycle, the reductive current at about −980 mV *vs.* FcH/[FcH]$^+$ increases significantly. This behaviour is also found when the anodic vertex potential is increased (pink traces), and analysing **[1a^F(Ag)]OTf** in the BAr$^F_4$-based SE (green traces) also gives clear indications of one/several EC mechanisms operating, even though the re-oxidation peak at −370 mV *vs.* FcH/[FcH]$^+$ is now absent. Furthermore, the first and second oxidation are more separated, and the oxidation-induced reductions split into two broad events. The first oxidation E_1^{ox} (BAr$^F_4$), when addressed on its own, is also irreversible.

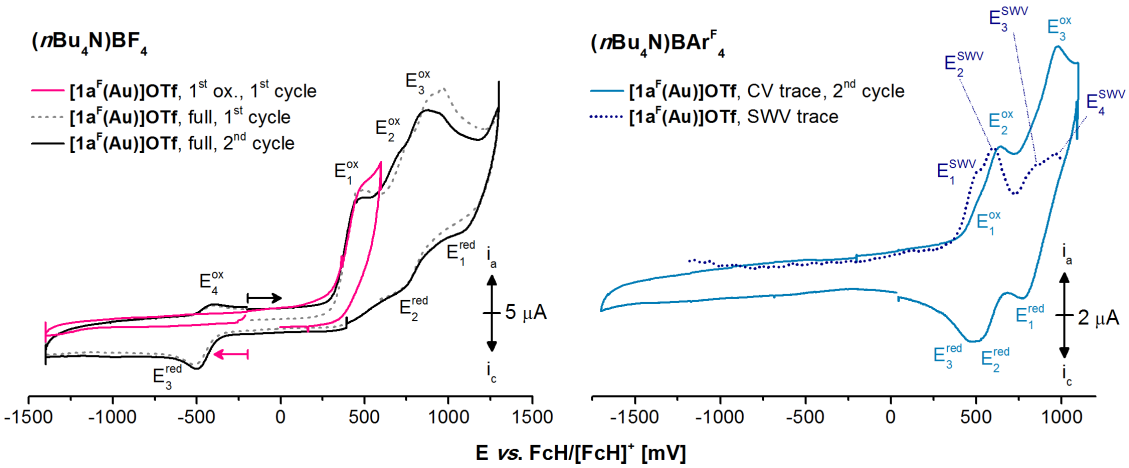

Fig. S68 Cyclic voltammograms of **[1a^F(Au)]OTf** in the BF_4^- (left) and BAr$^F_4$-based (right) supporting electrolytes (SE). Horizontal arrows indicate the starting potential and initial scan direction (100 mV·s^{-1}). For the measurement in the BAr$^F_4$-based SE, the dotted dark blue trace represents the result of square-wave voltammetry (SWV) at 100 mV·s^{-1}, revealing the oxidation processes to consist of four individual steps of similar anodic current. Only a very small amount of **[1a^F(Au)]OTf** has been available for measurement, resulting in very small currents and noisy traces. Peak potentials have been labelled for Table S6 and refer to the second of three consecutively measured cycles.

Even though only very little sufficiently pure material of **[1a^F(Au)]OTf** was available after crystallisation, cyclic voltammograms in both SE could be recorded (Fig. S68). The so-obtained traces show clear differences to those of **[1a^F(Ag)]OTf** in both SE as we have previously observed for the coinage metal complexes of non-fluorinated **1a**.[6] Perhaps unsurprisingly, **[1a^F(Au)]OTf** is not reversibly oxidisable in the BF_4^--based SE (black and pink traces) and shows clear indications of electron transfer-induced chemical reactivity with a delayed reduction E_3^{red} (BF_4^-) originating from the first, irreversible oxidation. In the BAr$^F_4$-based SE (blue traces), the oxidation processes – two at first glance, the "first" peak actually preceded by a small shoulder – seem to be more reversible, but square-wave voltammetry (SWV) actually reveals four oxidation processes to take place, even though only three ferrocenylene moieties are available in the molecule. Further analyses are warranted to elucidate whether this behaviour is connected to a gold(I)-centred oxidation or to ligand-centred reactivity.

Table S6 Oxidation and reduction peak potentials of perfluorophenyl tris-phosphane **1a^F** and corresponding complexes **[1a^F(Ag)]OTf** and **[1a^F(Au)]OTf** in the two different supporting electrolytes (SE) determined by cyclic voltammetry as well as formal redox potentials of **1a^F** in the BAr$^F_4$-based SE (bottom row). Assignment of the corresponding processes according to Figs. S66–68.

Potentials [mV]	E_1^{ox}	E_2^{ox}	E_3^{ox}	E_4^{ox}	E_5^{ox}	E_6^{ox}	E_1^{red}	E_2^{red}	E_3^{red}	E_4^{red}
	0.1 mmol·L^{-1} (*n*Bu$_4$N)BF$_4$ in CH$_2$Cl$_2$									
1a^F	485	605	767	−432	1390	1567	−502	506	418	–
[1a^F(Ag)]OTf	484	575	−370	--	--	--	495	397	−494	−1388
[1a^F(Au)]OTf	492	740	894	−397.4	--	--	726	−505	1097	–
	0.1 mmol·L^{-1} (*n*Bu$_4$N)BAr$^F_4$ in CH$_2$Cl$_2$									
[1a^F(Ag)]OTf	317	838	--	--	--	--	500	−979	--	--
[1a^F(Au)]OTf	506	644	977	--	--	--	439	520	769	--

Potentials [mV]	E_1^0 (ΔE_p) [a]	E_2^0 (ΔE_p)	E_3^0 (ΔE_p)	$\Delta E_{1/2}^0$ [b]	$\Delta E_{2/3}^0$ [b]
1a^F	487 (91)	653 (107)	907 (99)	166	254

[a] Redox potential with the splitting between the anodic (oxidation) and cathodic (reduction) peaks given in brackets. [b] Peak-to-peak separation of the first and second / second and third redox process, respectively.

6. Spectroelectrochemistry

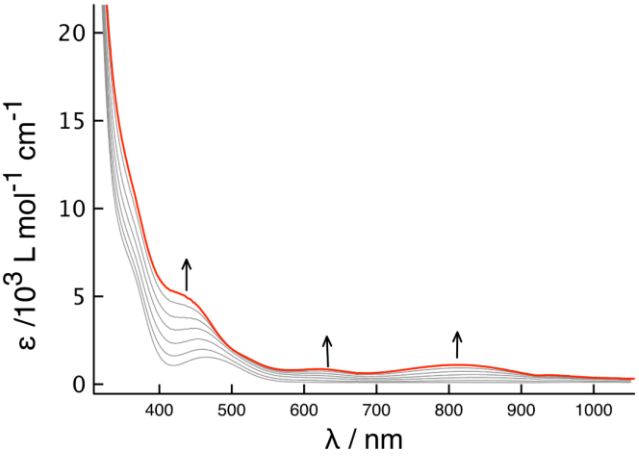

Fig. S69 Time-dependent UV/Vis spectra recorded during the oxidation of **[1b(Au)]OTf** at 25 °C in 0.1 mol·L^{-1} (nBu$_4$N)BAr$^F_4$ in CH_2Cl_2. The grey line represents the starting point and the red line represents the product obtained after oxidation. Arrows indicate the direction of intensity changes. Reduction regenerates the initial spectrum.

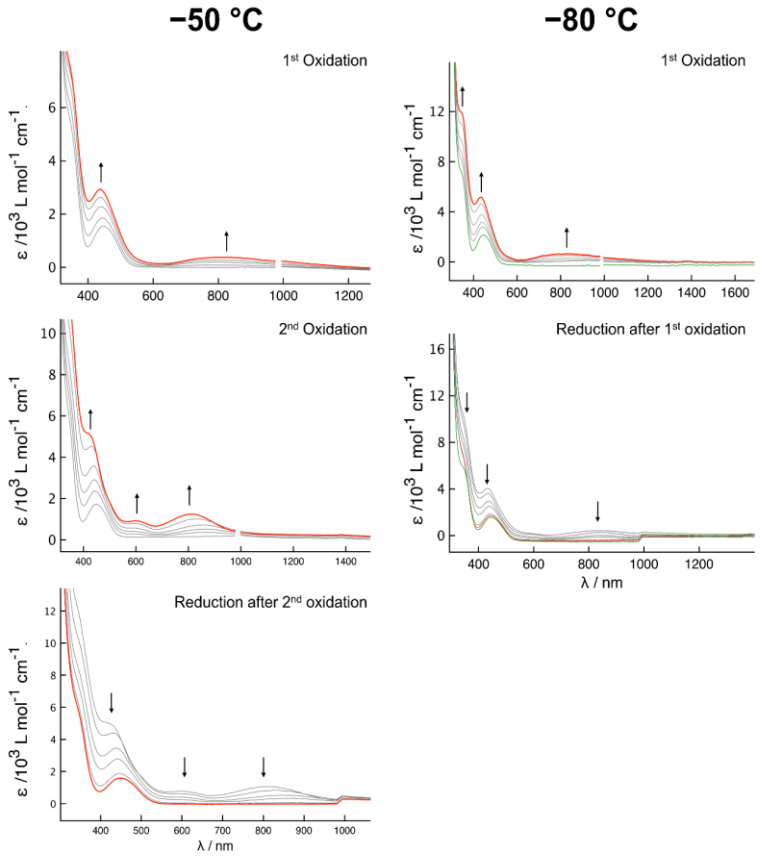

Fig. S70 Time-dependent UV/Vis spectra recorded during the oxidation and reduction of **[1b(Au)]OTf** at −50 °C (left) and −80 °C (right) in 0.1 mol·L^{-1} (nBu$_4$N)BAr$^F_4$ in CH_2Cl_2. The green lines represent the starting points, the red line represents the product obtained after oxidation or reduction, respectively. Arrows indicate the direction of intensity changes.

In contrast to the cyclic voltammograms of **[1b(Au)]OTf** in the BAr$^F_4$-based SE (Fig. 8, main article) showing the first oxidation to be irreversible under these conditions, following the oxidations by spectroelectrochemistry (SEC) paints a different picture. At 25 °C (Fig. S69), the first oxidation, showing a UV/Vis spectroscopic trace in accordance with an iron(II)-centred oxidation,[36–38] appears reversible in that the spectrum obtained after reduction of the previously oxidised species matches the initial UV/Vis spectrum of **[1b(Au)]OTf**. The second oxidation (not shown), in contrast, leads to decomposition of the material.

While triazine-based **[1a(Au)]OTf** did show a marked change in SEC behaviour upon decreasing the temperature,[6] the cool-down (Fig. S70) has less impact on the SEC response of **[1b(Au)]OTf**. The UV/Vis spectral changes for the first oxidations at 25 °C, −50 °C, and −80 °C are virtually identical. However, when cooled down to −50 °C, the second oxidation of **[1b(Au)]OTf** also becomes reversible. Notably, reducing the material obtained from the second oxidation restores the initial spectra characteristics of **[1b(Au)]OTf** without allowing the isolation of the mono-oxidised species. At all three temperatures, the first oxidation brings about a broad and weak absorption band centred at about 800 nm which Lang and co-workers have assigned to a ligand-to-metal charge-transfer (LMCT) event for the 1,3,5-tris(1-ferrocenyl)benzene parent structure of **1b**.[39] No intervalence charge-transfer band (which for the oxidation of 1,3,5-tris(1-ferrocenyl)benzene appears between 1300 and 1800 nm), can be discerned, speaking against **[1b(Au)]OTf** forming mixed-valent species upon oxidation.

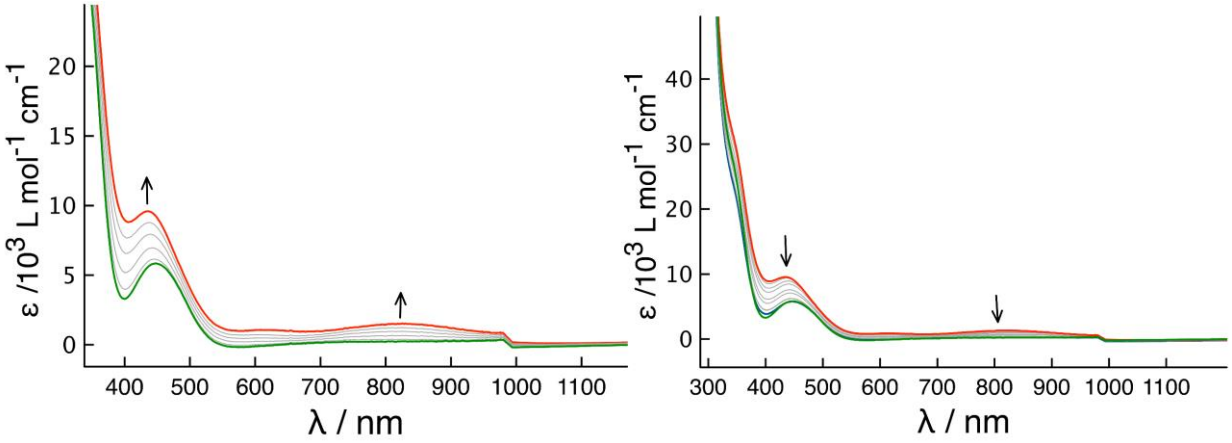

Fig. S71 Time-dependent UV/Vis spectra recorded during the oxidation (left) and reduction (right) of **[(1b)$_2$(Au)$_3$](OTf)$_3$** at 25 °C in 0.1 mol·L^{-1} (nBu$_4$N)BAr$^F{}_4$ in CH_2Cl_2. For the oxidation, the green line represents the starting point and the red line represents the product obtained. For the reduction, the starting point is the red spectrum, and the spectrum obtained after reduction is shown in blue. The green spectrum corresponds to the spectrum of native **[(1b)$_2$(Au)$_3$](OTf)$_3$**. Arrows indicate the direction of intensity changes. These plots are magnified versions of the SEC plots in Fig. 12, main article.

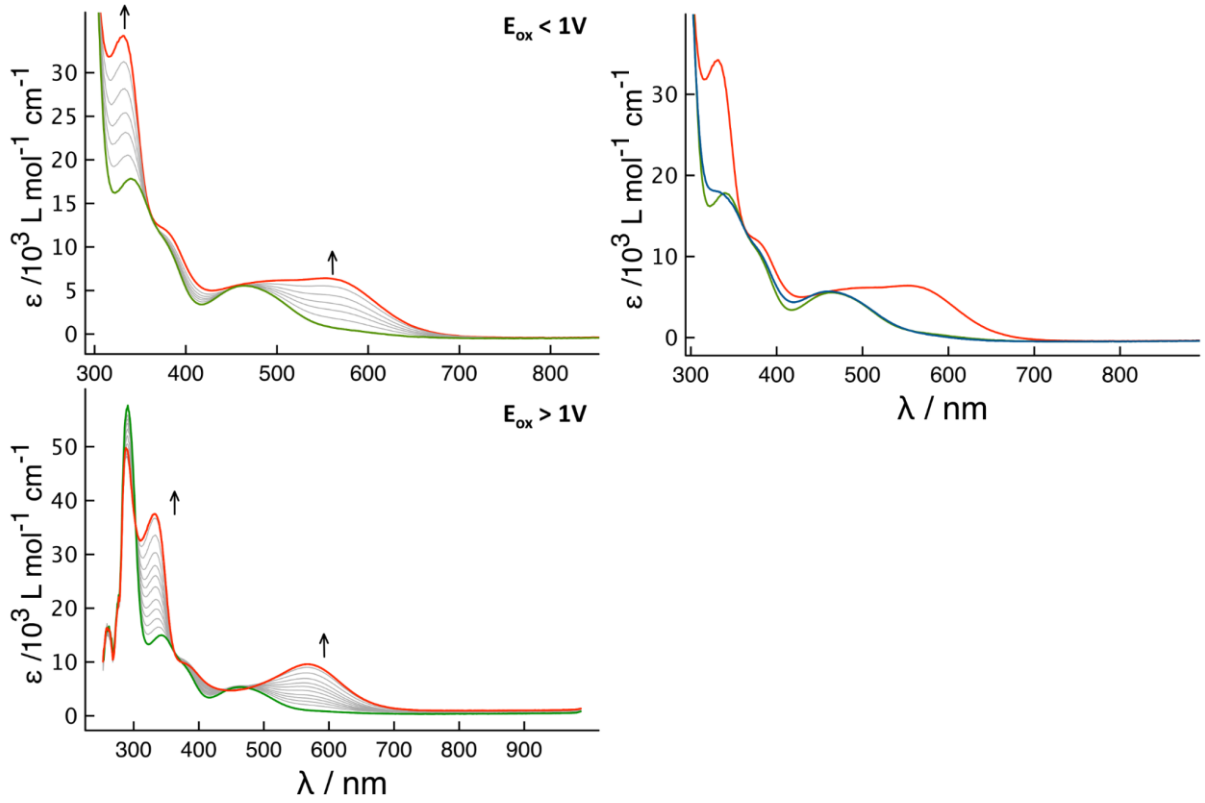

Fig. S72 Time-dependent UV/Vis spectra recorded during the oxidation (left) and reduction (right) of **[(1a)$_2$(Au)$_3$](OTf)$_3$** at 25 °C in 0.1 mol·L^{-1} (nBu$_4$N)BAr$^F{}_4$ in CH_2Cl_2. For the oxidations below (top) and above (bottom) 1 V *vs*. FcH/[FcH]$^+$, the green line represents the starting point and the red line represents the product obtained. For the reduction, the starting point is the red spectrum, and the spectrum obtained after reduction is shown in blue. The green spectrum corresponds to the spectrum of native **[(1a)$_2$(Au)$_3$](OTf)$_3$**. Arrows indicate the direction of intensity changes. These plots are magnified versions of the SEC plots in Fig. 12, main article.

7. Catalysis

7.1. NMR Spectrum Stacks, Linear Fitting Plots, and Turn-Over Frequencies (TOF)

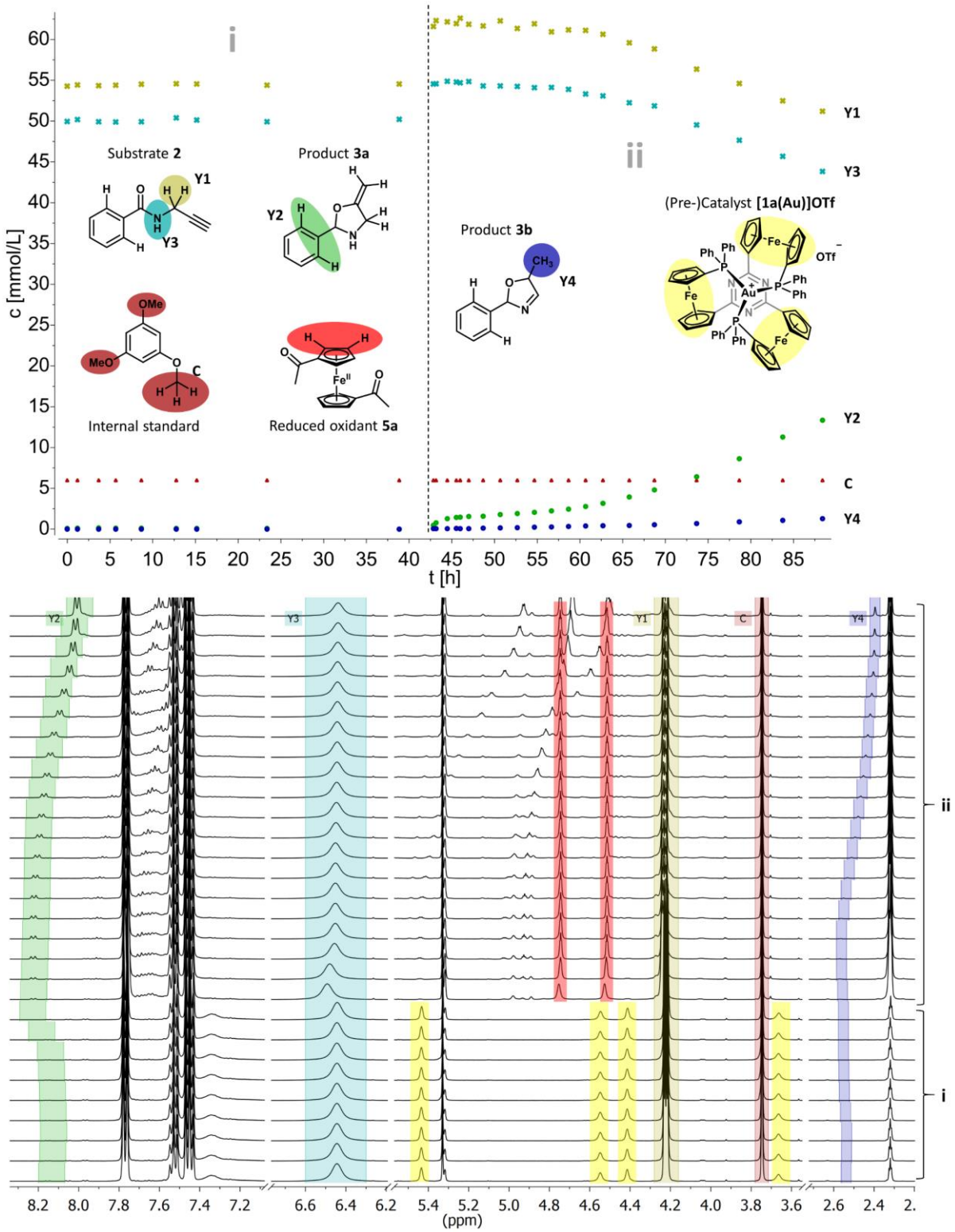

Figure S73 Top: Reaction profile determined for different ^{1}H resonances of substrate **2** (light blue and golden crosses), product **3a** (green circles), and aromatic follow-up product **3b** (navy circles) for redox-switched gold(I)-catalysed cyclisation of **2** to **3a**/**3b** (3 mol% Au as **[1a(Au)]OTf**, $[\mathbf{2}]_0$ = 60 mmol·L^{-1}, CD_2Cl_2, 25 °C), concentrations determined *vs.* internal standard 1,3,5-trimethoxybenzene (dark red triangles). Phases **i** and **ii** refer to Fig. 10, main article, and correspond to native **[1a(Au)]OTf** (**i**) and after oxidation with two equivalents of **5a** (**ii**). **Bottom:** Stacked ^{1}H NMR spectra (only regions of interest are shown) forming the basis for the concentration profiles. Spectral regions Y1–Y4 which have been integrated *vs.* the internal standard C are highlighted in the corresponding colour. ^{1}H resonances attributable to **[1a(Au)]OTf** during phase **i** are highlighted in yellow, and resonances attributable to 1,1'-diacetylferrocene (reduced oxidant **5a**) are highlighted in bright red during phase **ii**. The apparent concentration "jump" upon addition of **5a** is due to a shortening of the relaxation time arising from the presence of paramagnetic species.

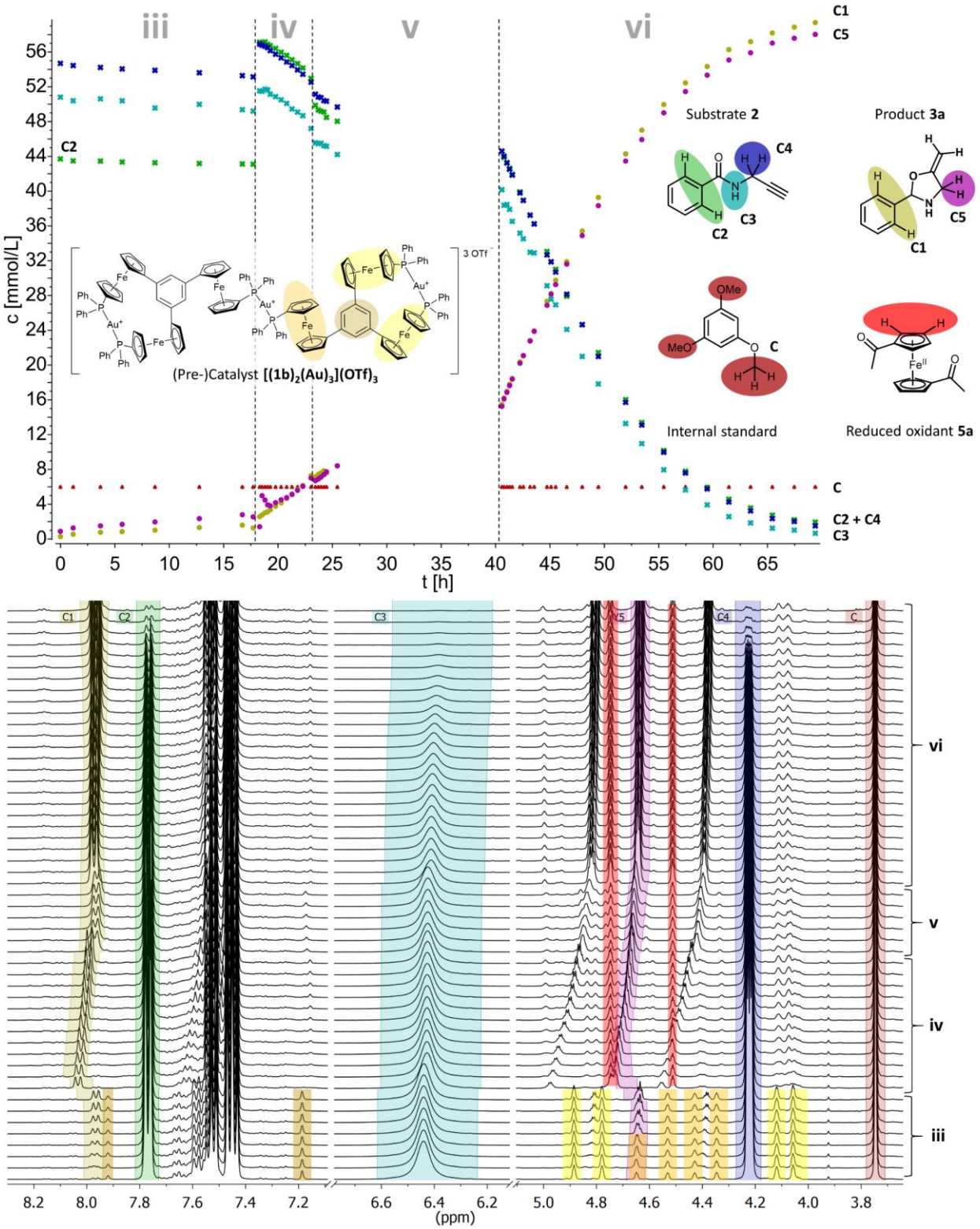

Figure S74 Top: Reaction profile determined for different ^{1}H resonances of substrate **2** (navy, light blue, and green crosses) and product **3a** (golden and lilac circles) for redox-switched gold(I)-catalysed cyclisation of **2** to **3a** (3 mol% Au as **[(1b)$_2$(Au)$_3$](OTf)$_3$**, **[2]$_0$** = 60 mmol·L^{-1}, CD_2Cl_2, 25 °C), concentrations being determined *vs.* internal standard 1,3,5-trimethoxybenzene (dark red triangles). Phases **iii**–**vi** refer to Fig. 11, main article, and correspond to native **[(1b)$_2$(Au)$_3$](OTf)$_3$** (**iii**), after oxidation with two equivalents of **5a** (**iv**), after reduction with 2.2 equivalents of **6** (**v**), and after re-oxidation with 2.2 equivalents of **5a** (**vi**). Between 25 h and 40 h, no spectra were recorded. **Bottom:** Stacked ^{1}H NMR spectra (only regions of interest are shown) forming the basis for the concentration profiles. Spectral regions C1–C5 which have been integrated *vs.* the internal standard C are highlighted in the corresponding colour. ^{1}H resonances attributable to the **[(1b)$_2$(Au)$_3$](OTf)$_3$** during phase **iii** are highlighted in yellow, orange, and brown, and resonances attributable to 1,1'-diacetylferrocene (reduced oxidant **5a**) are highlighted in bright red starting from phase **iv**. The apparent concentration "jump" upon addition of **5a** is due to a shortening of the relaxation time arising from the presence of paramagnetic species.

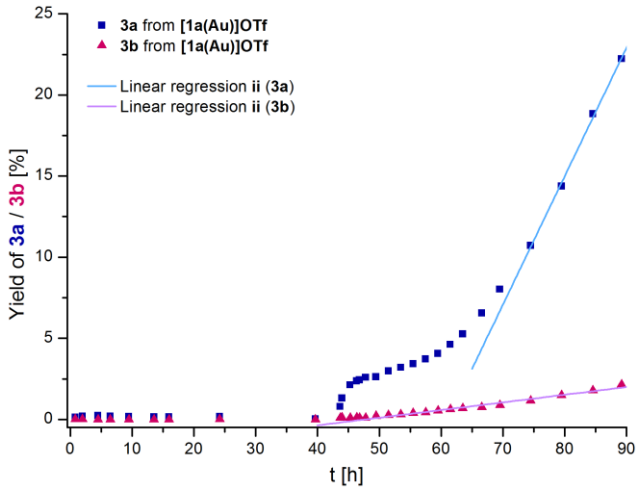

Figure S75 Reaction profile, including linear regressions, for 3 mol% Au catalyst loading of **[1a(Au)]OTf** in the catalytic conversion of **2** to **3a** (navy) and **3b** (grape). Concentrations were determined by integration of protons Y2 of **3a** and Y4 of **3b** (Fig. S73) *vs.* internal standard 1,3,5-trimethoxybenzene (^{1}H NMR). For resulting a (TOF), b, and R_{corr}^2, cf. Table S7.

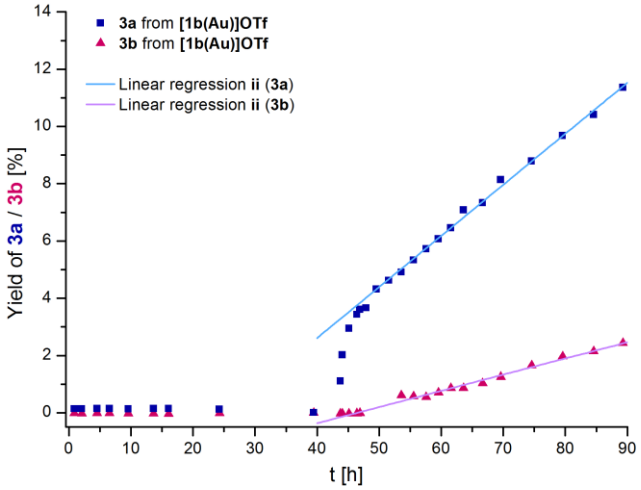

Figure S76 Reaction profile, including linear regressions, for 3 mol% Au catalyst loading of **[1b(Au)]OTf** in the catalytic conversion of **2** to **3a** (navy) and **3b** (grape). Concentrations were determined by integration of protons Y2 of **3a** and Y4 of **3b** (Fig. S73) *vs.* internal standard 1,3,5-trimethoxybenzene (^{1}H NMR). For resulting a (TOF), b, and R_{corr}^2, cf. Table S7.

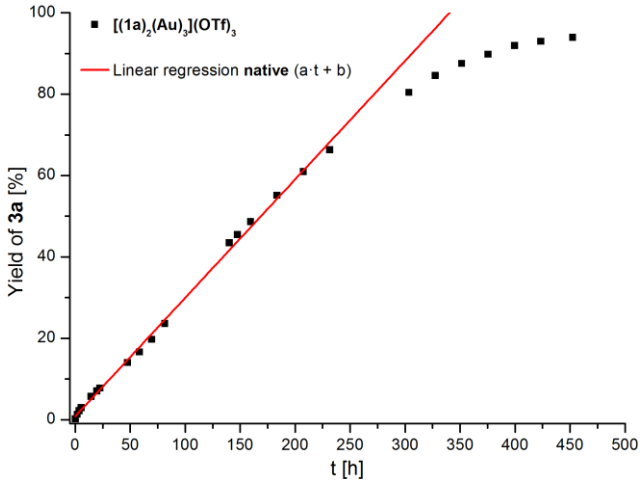

Figure S77 Reaction profile, including linear regression, for 3 mol% Au catalyst loading of **[(1a)$_2$(Au)$_3$](OTf)$_3$** in the catalytic conversion of **2** to **3a**. Concentrations were determined by integration of protons C4 of **3a** (Fig. S74) *vs.* internal standard 1,3,5-trimethoxybenzene (^{1}H NMR). For resulting a (TOF), b, and R_{corr}^2, cf. Table S7.

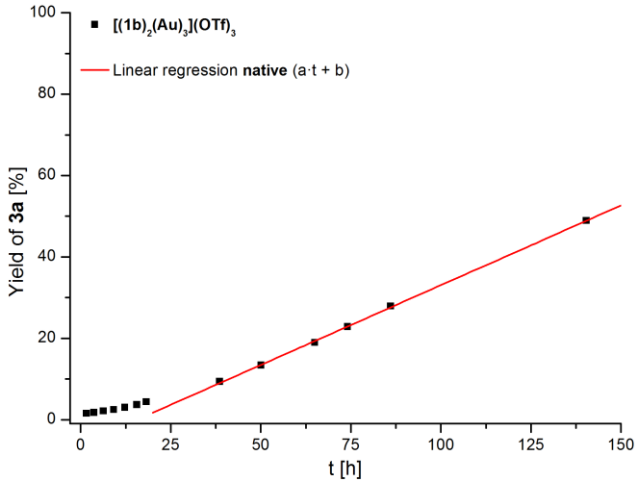

Figure S78 Reaction profile, including linear regression, for 3 mol% Au catalyst loading of **[(1b)$_2$(Au)$_3$](OTf)$_3$** in the catalytic conversion of **2** to **3a**. Concentrations were determined by integration of protons C4 of **3a** (Fig. S74) *vs.* internal standard 1,3,5-trimethoxybenzene (^{1}H NMR). For resulting a (TOF), b, and R_{corr}^2, cf. Table S7.

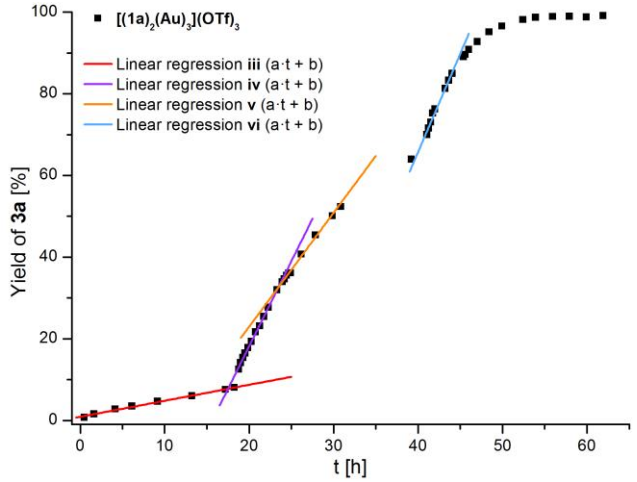

Figure S79 Reaction profile, including linear regressions, for 3 mol% Au catalyst loading of **[(1a)$_2$(Au)$_3$](OTf)$_3$** before (red) and after (purple) the addition of 2 eq. of **5a**, after the addition of 2.2 eq. of **6** (orange), and after the addition of 2.2 eq. of **5a** (light blue) in the catalytic conversion of **2** to **3a**. Concentrations were determined by integration of protons C2 of **3a** (Fig. S74) *vs.* internal standard 1,3,5-trimethoxybenzene (^{1}H NMR). For resulting a (TOF), b, and R_{corr}^2, cf. Table S7.

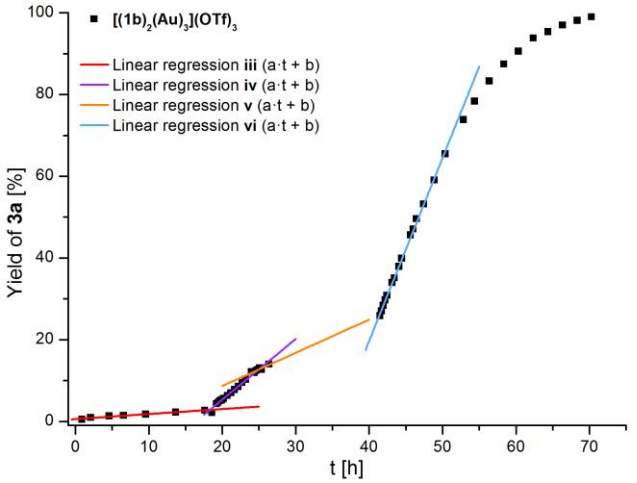

Figure S80 Reaction profile, including linear regressions, for 3 mol% Au catalyst loading of **[(1b)$_2$(Au)$_3$](OTf)$_3$** before (red) and after (purple) the addition of 2 eq. of **5a**, after the addition of 2.2 eq. of **6** (orange), and after the addition of 2.2 eq. of **5a** (light blue) in the catalytic conversion of **2** to **3a**. Concentrations were determined by integration of protons C2 of **3a** (Fig. S74) *vs.* internal standard 1,3,5-trimethoxybenzene (^{1}H NMR). For resulting a (TOF), b, and R_{corr}^2, cf. Table S7.

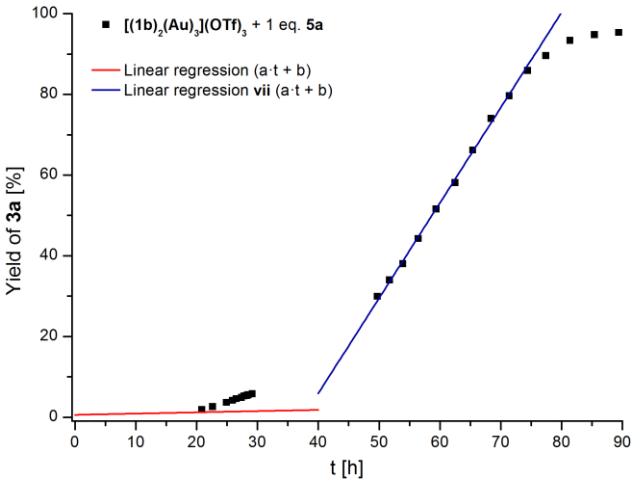

Figure S81 Reaction profile, including linear regressions, for 3 mol% Au catalyst loading of **[(1b)$_2$(Au)$_3$](OTf)$_3$** before (red) and after (navy) the addition of 1 eq. of **5a** in the catalytic conversion of **2** to **3a**. Concentrations were determined by integration of protons C2 of **3a** (Fig. S74) *vs.* internal standard 1,3,5-trimethoxybenzene (^{1}H NMR). For resulting a (TOF), b, and R_{corr}^2, cf. Table S7.

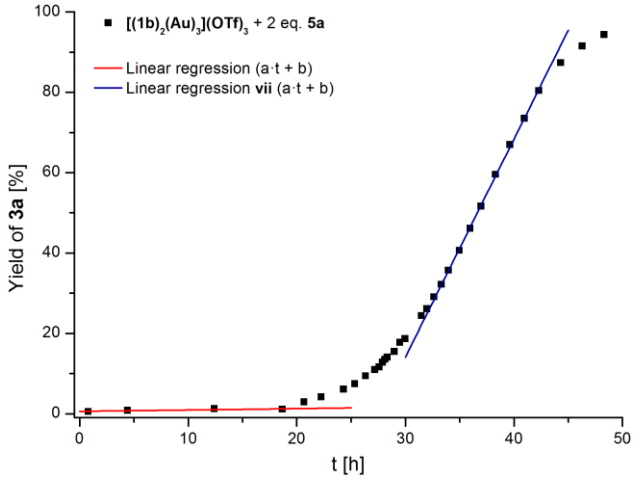

Figure S82 Reaction profile, including linear regressions, for 3 mol% Au catalyst loading of **[(1b)$_2$(Au)$_3$](OTf)$_3$** before (red) and after (navy) the addition of 2 eq. of **5a** in the catalytic conversion of **2** to **3a**. Concentrations were determined by integration of protons C2 of **3a** (Fig. S74) *vs.* internal standard 1,3,5-trimethoxybenzene (^{1}H NMR). For resulting a (TOF), b, and R_{corr}^2, cf. Table S7.

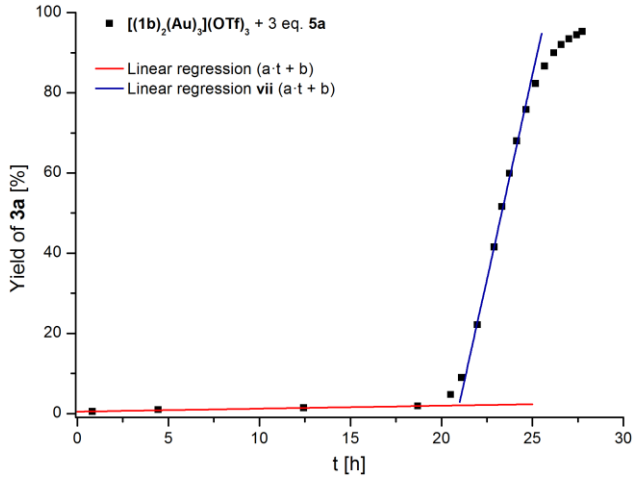

Figure S83 Reaction profile, including linear regressions, for 3 mol% Au catalyst loading of **[(1b)$_2$(Au)$_3$](OTf)$_3$** before (red) and after (navy) the addition of 3 eq. of **5a** in the catalytic conversion of **2** to **3a**. Concentrations were determined by integration of protons C2 of **3a** (Fig. S74) *vs.* internal standard 1,3,5-trimethoxybenzene (^{1}H NMR). For resulting a (TOF), b, and R_{corr}^2, cf. Table S7.

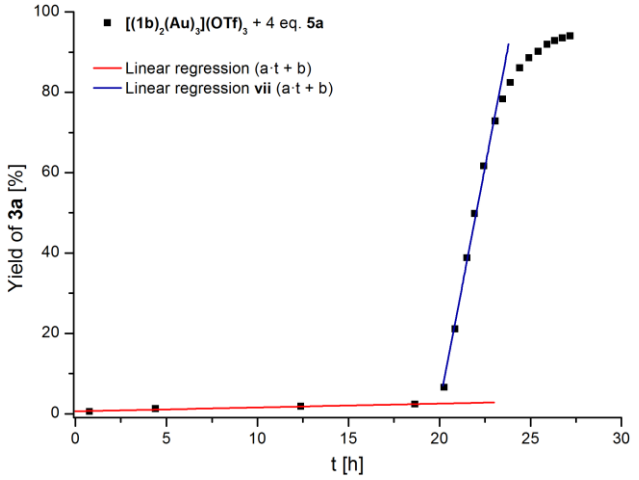

Figure S84 Reaction profile, including linear regressions, for 3 mol% Au catalyst loading of **[(1b)$_2$(Au)$_3$](OTf)$_3$** before (red) and after (navy) the addition of 4 eq. of **5a** in the catalytic conversion of **2** to **3a**. Concentrations were determined by integration of protons C2 of **3a** (Fig. S74) *vs.* internal standard 1,3,5-trimethoxybenzene (^{1}H NMR). For resulting a (TOF), b, and R_{corr}^2, cf. Table S7.

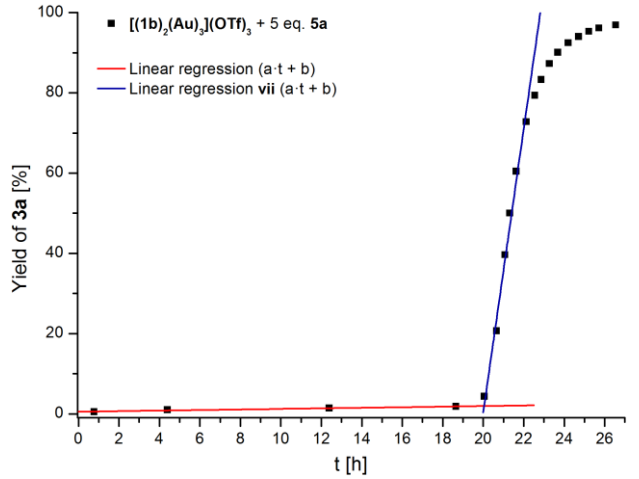

Figure S85 Reaction profile, including linear regressions, for 3 mol% Au catalyst loading of **[(1b)$_2$(Au)$_3$](OTf)$_3$** before (red) and after (navy) the addition of 5 eq. of **5a** in the catalytic conversion of **2** to **3a**. Concentrations were determined by integration of protons C2 of **3a** (Fig. S74) *vs.* internal standard 1,3,5-trimethoxybenzene (^{1}H NMR). For resulting a (TOF), b, and R_{corr}^2, cf. Table S7.

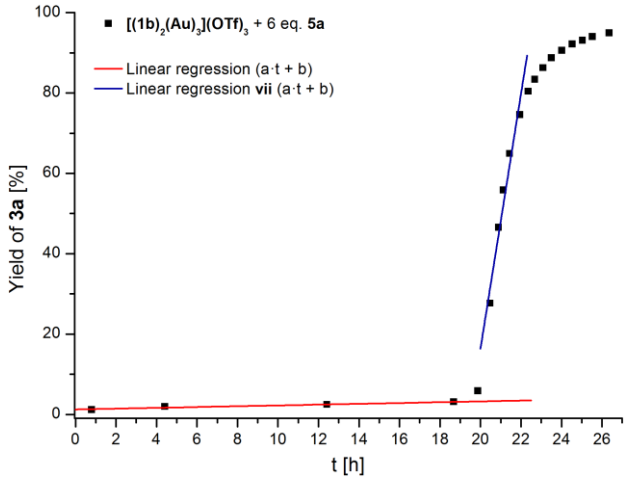

Figure S86 Reaction profile, including linear regressions, for 3 mol% Au catalyst loading of **[(1b)$_2$(Au)$_3$](OTf)$_3$** before (red) and after (navy) the addition of 6 eq. of **5a** in the catalytic conversion of **2** to **3a**. Concentrations were determined by integration of protons C2 of **3a** (Fig. S74) *vs.* internal standard 1,3,5-trimethoxybenzene (^{1}H NMR). For resulting a (TOF), b, and R_{corr}^2, cf. Table S7.

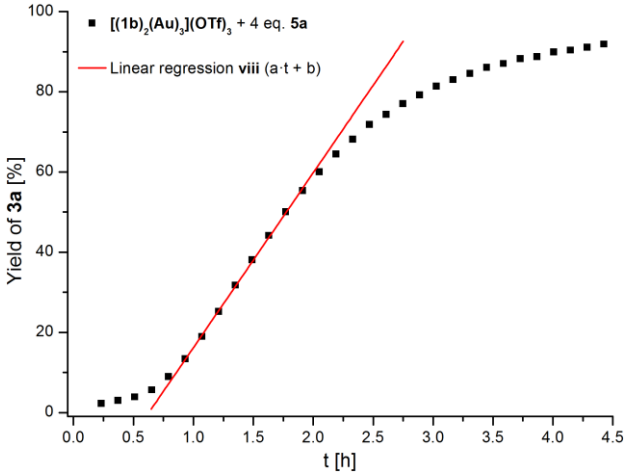

Figure S87 Reaction profile, including linear regression (red), for 3 mol% Au catalyst loading of **[(1b)$_2$(Au)$_3$](OTf)$_3$** and 4 eq. of **5a**, added before the measurement, in the catalytic conversion of **2** to **3a**. Concentrations were determined by integration of protons C2 of **3a** (Fig. S74) *vs.* internal standard 1,3,5-trimethoxybenzene (^{1}H NMR). For resulting a (TOF), b, and R_{corr}^2, cf. Table S7.

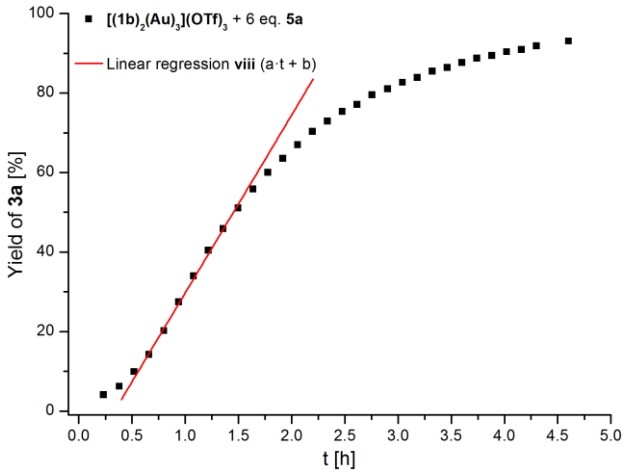

Figure S88 Reaction profile, including linear regression (red), for 3 mol% Au catalyst loading of **[(1b)$_2$(Au)$_3$](OTf)$_3$** and 6 eq. of **5a**, added before the measurement, in the catalytic conversion of **2** to **3a**. Concentrations were determined by integration of protons C2 of **3a** (Fig. S74) *vs.* internal standard 1,3,5-trimethoxybenzene (^{1}H NMR). For resulting a (TOF), b, and R_{corr}^2, cf. Table S7.

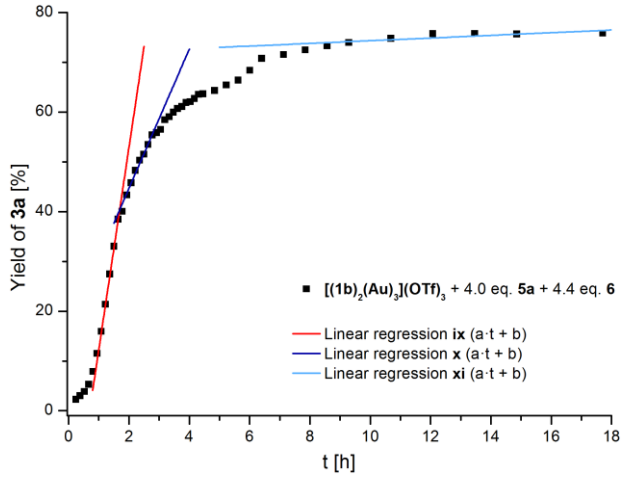

Figure S89 Reaction profile, including linear regressions, for 3 mol% Au catalyst loading of **[(1b)$_2$(Au)$_3$](OTf)$_3$** and 4 eq. of **5a**, added before the measurement (red), and immediately after the addition of 4.4 eq. of **6** (purple) as well as with a delay of 6 h (light blue) in the catalytic conversion of **2** to **3a**. Concentrations were determined by integration of protons C2 of **3a** (Fig. S74) *vs.* internal standard 1,3,5-trimethoxybenzene (^{1}H NMR). For resulting a (TOF), b, and R_{corr}^2, cf. Table S7.

Table S7 Turn-over-frequencies (TOF, parameter a of linear fit), intersections b, and coefficients of determination R_{corr}^2 derived from linear regressions of conversion-over-time plots employing **[1a(Au)]OTf**, **[1b(Au)]OTf**, **[(1a)$_2$(Au)$_3$](OTf)$_3$**, and **[(1b)$_2$(Au)$_3$](OTf)$_3$** as (pre-)catalysts for the gold(I)-catalysed ring-closing isomerisation of **2** to **3a** and **3b** with a 3 mol% Au^I loading referring to substrate **2**. TOF are listed with three significant digits except for TOF < 0.1 h^{-1}.

(Pre-)Catalyst	Additives[a]	Phase[b]		TOF (±error) [h^{-1}]	b (±error)	R_{corr}^2	Time span [h]	Comments
[1a(Au)]OTf	--	**i**		--	--	--	--	
	2.0 eq. **5a**	**ii**	**3a**	0.792 (±0.020)	−48.4 (±1.7)	0.998	74.5 – 89.2	
			3b	0.047 (±0.002)	−2.25 (±0.15)	0.972	49.5 – 89.2	
[1b(Au)]OTf	--	**i**		--	--	--	--	
	2.0 eq. **5a**	**ii**	**3a**	0.178 (±0.003)	−4.53 (±0.18)	0.997	49.6 – 89.3	
			3b	0.057 (±0.002)	−2.63 (±0.11)	0.988	45.1 – 89.3	
[(1a)$_2$(Au)$_3$](OTf)$_3$	--	native		0.291 (±0.004)	0.825 (±0.548)	0.997	5.7 – 232	Followed through ring-methylene protons of **3a** by ^{1}H NMR spectroscopy
	--	**iii**		0.392 (±0.011)	0.899 (±0.119)	0.995	0.5 – 18.3	
	2.0 eq. **5a**	**iv**		4.17 (±0.06)	−65.1 (±1.3)	0.998	18.8 – 23.3	
	2.2. eq. **6**	**v**		2.79 (±0.08)	−32.7 (±2.0)	0.995	23.9 – 29.9	
	2.2 eq. **5a**	**vi**		4.83 (±0.22)	−127 (±9)	0.986	41.1 – 44.1	
[(1b)$_2$(Au)$_3$](OTf)$_3$	--	native		0.392 (±0.004)	−6.13 (±0.33)	0.9995	10.3 – 45.2	Followed through ring-methylene protons of **3a** by ^{1}H NMR spectroscopy
	--	**iii**		0.122 (±0.001)	0.565 (±0.084)	0.970	0.9 – 17.6	
	2.0 eq. **5a**	**iv**		1.48 (±0.03)	−24.3 (±0.6)	0.996	19.2 – 23.2	
	2.2. eq. **6**	**v**		0.813 (±0.138)	−7.61 (±3.44)	0.850	24.0 – 26.4	
	2.2 eq. **5a**	**vi**		4.48 (±0.04)	−159 (±2)	0.999	41.5 – 50.4	
	--	--		0.031 (±0.016)	0.575 (±0.177)	0.492	0.8 – 18.4	Prior to oxidation, no phase assigned
	1.0 eq. **5a**	**vii**		2.36 (±0.05)	−88.6 (±2.7)	0.997	49.7 – 68.4	
	--	--		0.034 (±0.014)	0.588 (±0.164)	0.607	0.8 – 18.7	Prior to oxidation, no phase assigned
	2.0 eq. **5a**	**vii**		5.42 (±0.05)	−149 (±2)	0.9993	32.6 – 41.0	
	--	--		0.073 (±0.009)	0.483 (±0.100)	0.959	0.8 – 18.7	Prior to oxidation, no phase assigned
	3.0 eq. **5a**	**vii**		20.4 (±0.6)	−426 (±15)	0.995	22.0 – 24.7	
	--	**--**		0.096 (±0.014)	0.597 (±0.161)	0.939	0.8 – 18.7	Prior to oxidation, no phase assigned
		vii		23.6 (±1.3)	−470 (±28)	0.989	20.9 – 23.1	
	4.0 eq. **5a**	**viii**		43.6 (±0.5)	−27.5 (±0.7)	0.9992	0.9 – 1.9	Oxidation of pre-catalyst prior to start of ^{1}H NMR experiment; closer sampling interval compared to run **vii**
	--	**--**		0.071 (±0.010)	0.518 (±0.108)	0.949	0.8 – 18.7	
	5.0 eq. **5a**	**vii**		35.3 (±3.1)	−706 (±65)	0.971	20.7 – 22-1	
	--	**--**		0.100 (±0.016)	1.23 (±0.18)	0.930	0.8 – 18.7	
		vii		31.7 (±3.8)	−617 (±80)	0.946	20.5 – 22.0	
	6.0 eq. **5a**	**viii**		44.7 (±1.0)	−15.0 (±1.1)	0.997	0.7 – 1.5	Oxidation of pre-catalyst prior to start of ^{1}H NMR experiment; closer sampling interval compared to run **vii**
	4.0 eq. **5a**	**ix**		40.6 (±0.4)	−28.3 (±0.6)	0.9996	1.1 – 1.6	Oxidation of pre-catalyst prior to start of ^{1}H NMR experiment; closer sampling interval compared to run **vii**
	4.4 eq. **6**	**x**		14.0 (±0.6)	16.7 (±1.4)	0.989	1.9 – 2.8	Phase immediately after addition of **6**
		xi		0.268 (±0.076)	71.7 (±1.0)	0.652	8.6 – 17.7	Phase with long delay after addition of **6**

[a] Equivalents are given with respect to the amount of the (pre-)catalyst used in the corresponding run; [b] With respect to Figs. 10 (main article) and S75–76 (**i**, **ii**), and to Figs. 11 and 12 (main article) and S77–89 (**iii–xi**).

7.2. Steric Characterisation of the Gold(I) Complexes by %Vol_{bur}

In line with the procedure described by Cavallo and co-workers, the first coordination sphere of the gold(I) ion in all complexes but the coordination polymer was characterised by the buried volume (%Vol_{bur}), creating a simple descriptor for the steric demand of the tris-phosphanes in the respective coordination mode.[40–42]

Table S8 Buried volume (%Vol_{bur}) for all discrete 1:1 and 2:3 ligand-to-gold complexes, calculated by the SambVca web application.[41] The labelling scheme of the 2:3 complexes refers to the corresponding solid-state molecular structures (Figs. S40 and S41).

Compound	[1a(Au)]OTf	[1b(Au)]OTf	[1a^F(Au)]OTf	[(1a)$_2$(Au)$_3$](OTf)$_3$	[(1b)$_2$(Au)$_3$](OTf)$_3$
%Vol_{bur} [%]	89.5	67.2	75.8	Au(1): 73.2 Au(2): 66.3 Au(3): 65.7	Au(1): 73.0 Au(2): 66.2 Au(3): 65.4

For the calculations, XYZ files containing the coordinates of the cationic part of the complexes (*i.e.*, omitting anions and co-crystallised solvent) were created from the CIF files. Using the web-based SambVca application (https://www.molnac.unisa.it/OMtools/sambvca2.1/, last checked 20.07.2020)[41] and the standard parameters pre-set therein (omission of hydrogen atoms, scaling of Bondi radii by 1.17, sphere radius 3.5 Å, mesh spacing 0.10 Å), the Cartesian coordinate system was created in analogy to the tutorial examples on the websites (*e.g.* for "Chelating Phosphines" and "Unsymmetric"). Different relative orientations of the Cartesian axes were tested and found to not change the outcome concerning the value of %Vol_{bur} (steric maps will change, based on which direction the atom is viewed from). Resulting %Vol_{bur} values are presented in Table S8 and the corresponding steric maps are shown in Figs. S90 (1:1 ligand-to-metal complexes) and S91 (2:3 ligand-to-metal complexes, exemplarily shown for **[(1a)$_2$(Au)$_3$](OTf)$_3$**).

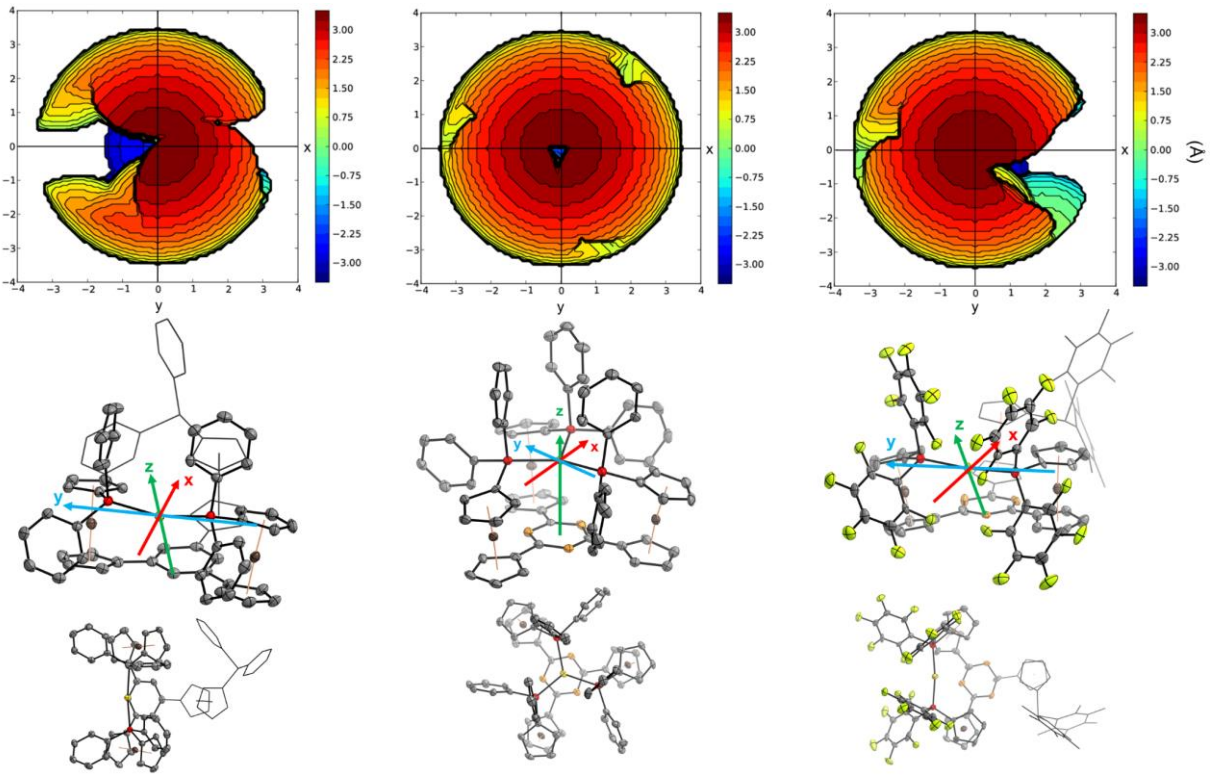

Figure S90 Topographic steric maps of **[1b(Au)]OTf** (left), **[1a(Au)]OTf** (centre), and **[1a^F(Au)]OTf** (right) calculated by SambVca 2.1 based on the respective solid-state molecular structures. Isocontour schemes and axes are given in units of Å. The steric maps are viewed down the z axis which has been defined as shown below the individual maps. Both the Cartesian system (centre) and the resulting molecular orientation (bottom) are shown. The solid-state molecular structure of **[1a(Au)]OTf** has been published before.**Fehler! Verweisquelle konnte nicht gefunden werden.**

As can be seen from both the calculated buried volume %Vol_{bur} and from the steric maps, the κ^3*P*,*P*',*P*'' coordination mode found for **1a** in **[1a(Au)]OTf** shields the gold(I) ion the most from its surrounding, effectively preventing any substrate from approaching. Only the κ^2*P*,*P*' coordination mode in **[1b(Au)]OTf** and **[1a^F(Au)]OTf** results in less steric congestion around the gold(I) centres, while the fluorination of the phenyl rings significantly increases their steric bulk. The latter finding is in line with the notion of

Saunders and co-workers who stated that "C–F is isosteric with C–OH or C=O not C–H […] and polyfluorinated organic molecules are much bulkier than their perprotio analogues."[35]

For 2:3 ligand-to-metal complexes **[(1a)$_2$(Au)$_3$](OTf)$_3$** and **[(1b)$_2$(Au)$_3$](OTf)$_3$** (as their steric parameters are close to identical, only **[(1a)$_2$(Au)$_3$](OTf)$_3$** is shown in Fig. S91), the chelated outer gold(I) ions Au(2) and Au(3) have similar steric characteristics as the gold(I) centre of **[1b(Au)]OTf**, while the central gold(I) ion Au(1) is slightly more sterically protected by its first coordination sphere. With respect to catalytic applications, it is thus possible that the outer gold(I) ions play a larger role for the overall catalytic activity, assuming the steric characteristics to not be changed significantly by solution dynamics.

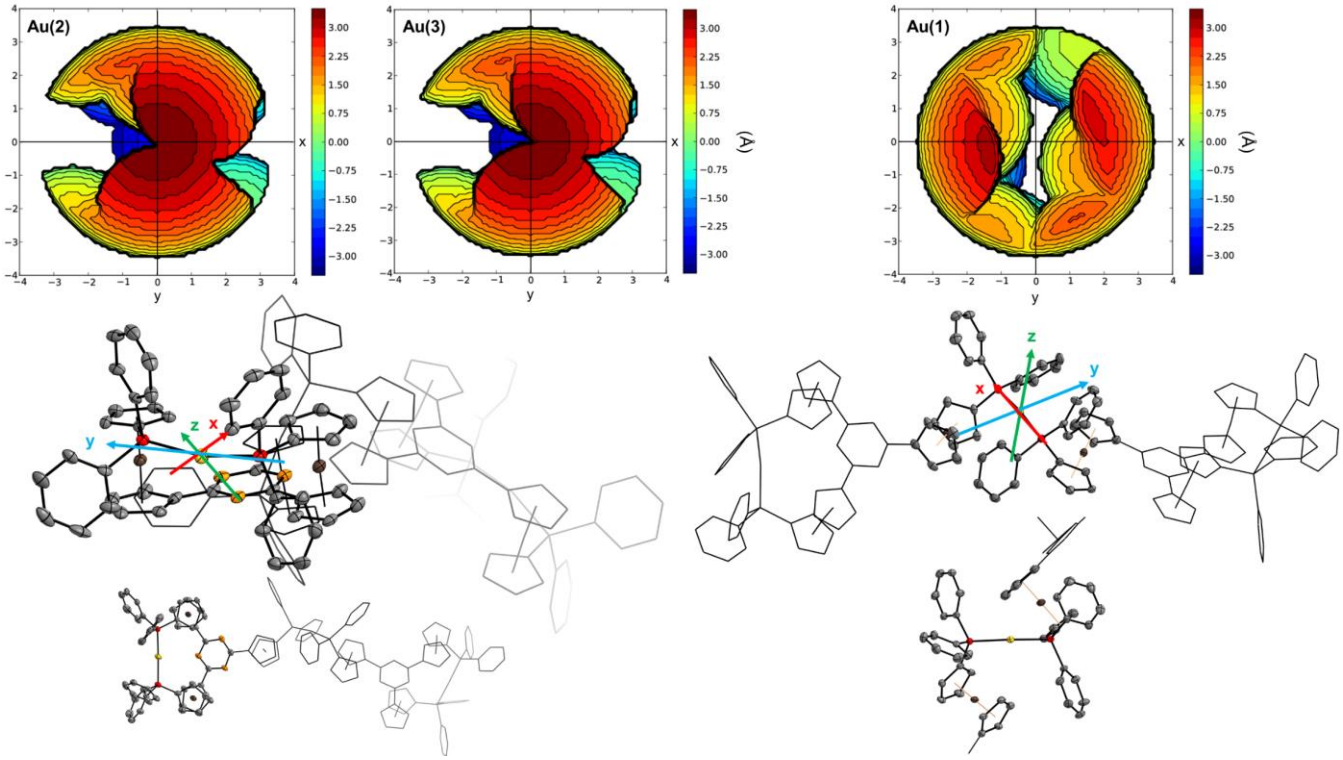

Figure S91 Topographic steric maps of the three gold(I) centres of **[(1a)$_2$(Au)$_3$](OTf)$_3$** calculated by SambVca 2.1 based on the solid-state molecular structures. Isocontour schemes and axes are given in units of Å. The steric maps are viewed down the z axis which has been defined as shown below the individual maps. Outer gold(I) ions Au(2) and Au(3) share a close-to-identical environment, hence only the respective orientation of Au(3) is given. Both the Cartesian system (centre) and the resulting molecular orientation (bottom) are depicted.

7.3. Stoichiometric Oxidation of Gold(I) Complexes – NMR-spectroscopic Studies

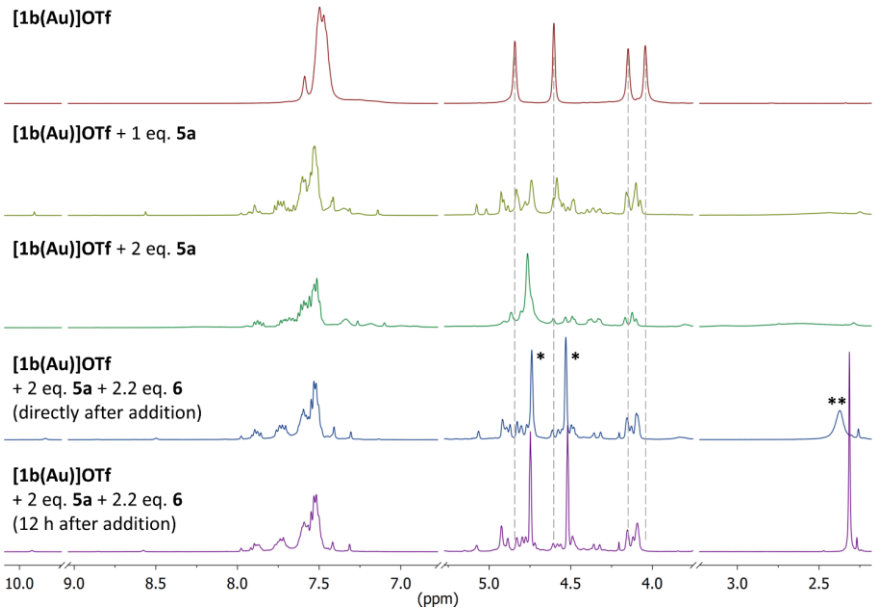

Figure S92 Stepwise oxidation of **[1b(Au)]OTf** by 2 equivalents of **5a**, followed by reduction with 2.2 equivalents of **6**, traced by ^{1}H NMR spectroscopy in CD_2Cl_2 (only regions of interest are shown, all spectra recorded at 25 °C using the same parameters). Dashed lines signify the peak positions of **[1b(Au)]OTf** and signals marked by asterisks (*) correspond to 1,1'-diacetylferrocene (reduced **5a**, *: ferrocenylene protons, **: acetyl-CH_3).

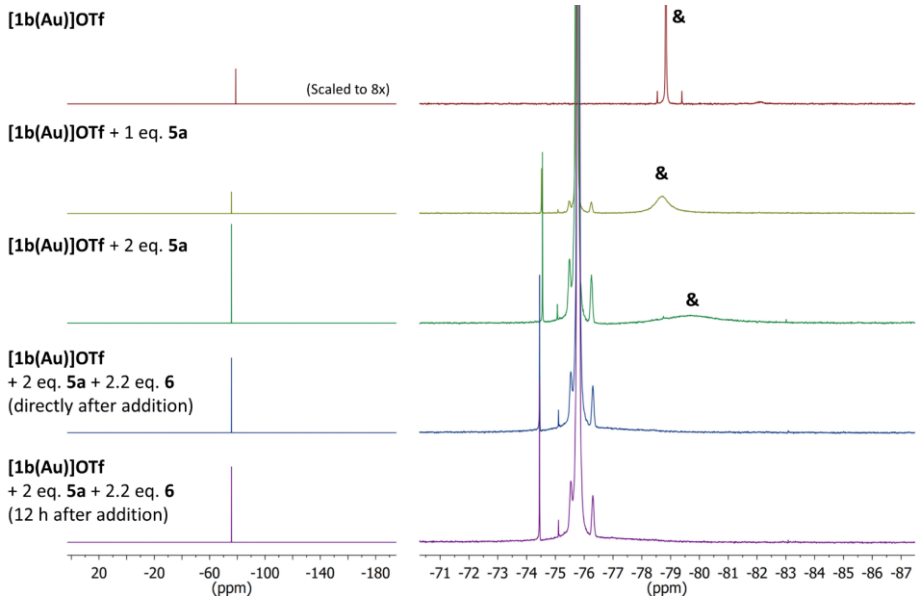

Figure S93 Stepwise oxidation of **[1b(Au)]OTf** by 2 equivalents of **5a**, followed by reduction with 2.2 equivalents of **6**, traced by ^{19}F{^{1}H} NMR spectroscopy in CD_2Cl_2 (left: overview, right: detail of spectral region of interest; all spectra recorded at 25 °C using the same parameters). The ampersand (&) marks the triflate-CF_3 resonance.

When **[1b(Au)]OTf** is reacted with two equivalents of teflonate-based oxidant **5a**, the spectral characteristics of all nuclei (^{1}H, ^{19}F, ^{31}P) change significantly and cannot be restored by the addition of 2.2 equivalents of reductant **6**. Notably, signals for reduced **5a** (*i.e.*, 1,1'-diacetylferrocene, signals marked by asterisks (*****) in Fig. S92) are largely absent from the ^{1}H NMR spectra after the addition of one (yellow-green) and two (green) equivalents of **5a**, while the addition of **6** results in their immediate appearance, suggesting that **5a** and **[1b(Au)]OTf** might be involved in redox equilibria at the NMR timescale.

Furthermore, the ^{19}F{^{1}H} NMR signal of the triflate anion (**&** in Fig. S93) broadens significantly ($\omega_{1/2}$(native) = 3.6 Hz; $\omega_{1/2}$(1 eq. **5a**) = 220 Hz; $\omega_{1/2}$(2 eq. **5a**) = 830 Hz) and does not re-appear upon addition of **6**, hinting at possible involvement in the follow-up chemistry of the oxidised complex cation. In the corresponding ^{31}P{^{1}H} NMR spectra, addition of the first equivalent of **5a** leads to the immediate loss of the broad signal for fluctional **[1b(Au)]OTf**. Instead, several signals centred at 43 ppm (possibly attributable

to *P,P'*-dicoordinate species), a signal at 5.4 ppm and smaller signals at lower field appear. The most distinct effect of adding another equivalent of **5a** is the disappearance of the resonance at 5.4 ppm, coupled to a broad singlet emerging at 42 ppm. Reduction with 2.2 equivalents of **6** mainly restores the $^{31}P\{^{1}H\}$ NMR spectrum obtained from the first oxidation, and no indication of delayed reaction over time was found after either 12 or 20 h.

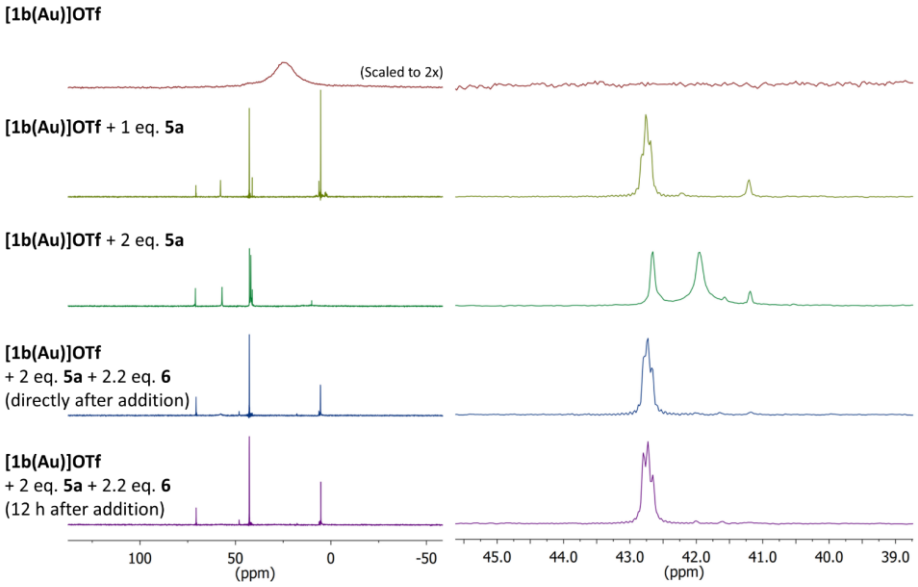

Figure S94 Stepwise oxidation of **[1b(Au)]OTf** by 2 equivalents of **5a**, followed by reduction with 2.2 equivalents of **6**, traced by $^{31}P\{^{1}H\}$ NMR spectroscopy in CD_2Cl_2 (left: overview, right: detail of spectral region of interest; all spectra recorded at 25 °C using the same parameters).

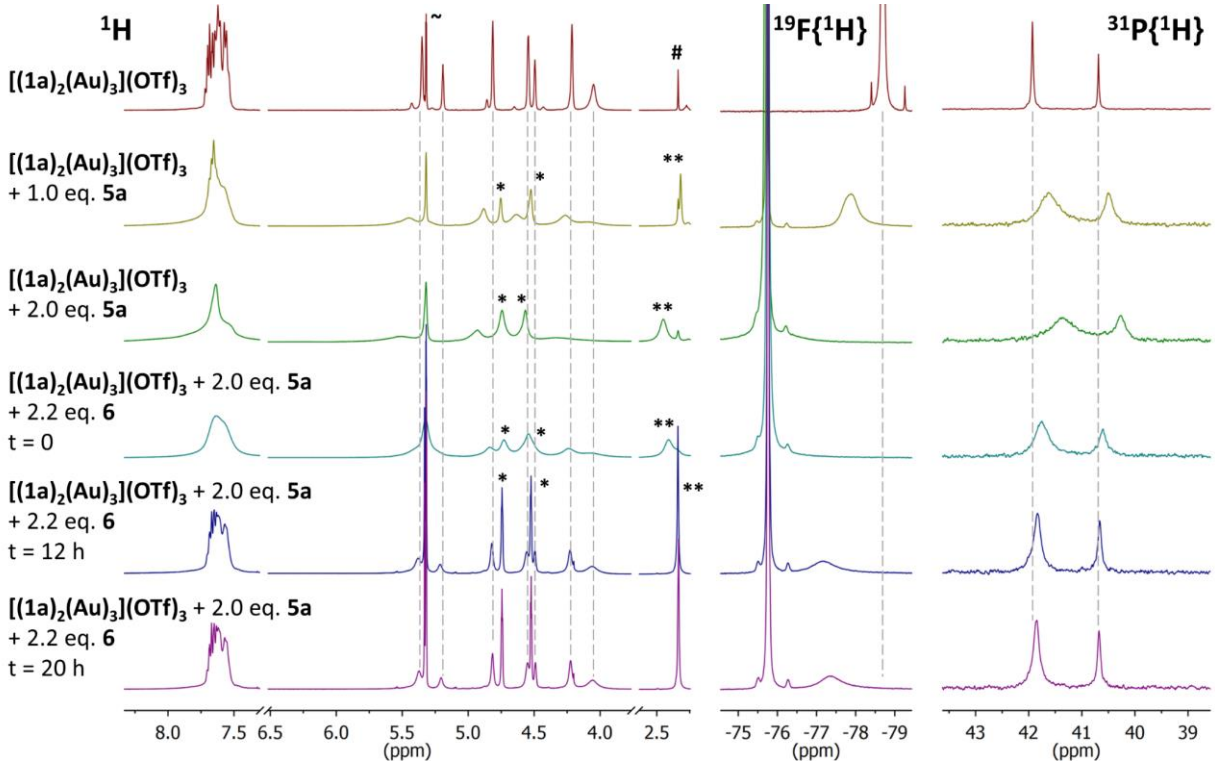

Figure S95 Stepwise oxidation of $[(1a)_2(Au)_3](OTf)_3$ by 2 equivalents of **5a**, followed by reduction with 2.2 equivalents of **6**, traced by ^{1}H (left), $^{19}F\{^{1}H\}$ (centre), and $^{31}P\{^{1}H\}$ (right) NMR spectroscopy in CD_2Cl_2 (all spectra recorded at 25 °C using the same parameters respectively). Dashed lines signify relevant peak positions of native $[(1a)_2(Au)_3](OTf)_3$. ^{1}H NMR signals marked by asterisks (*) correspond to 1,1'-diacetylferrocene (reduced **5a**, *: ferrocenylene protons, **: acetyl-CH_3). The hashtag symbol (#) marks the CH_3 resonance of toluene, and the tilde symbol (~) marks the combined $CHDCl_2/CH_2Cl_2$ signals.

Oxidising **[(1a)$_2$(Au)$_3$](OTf)$_3$** with two equivalents of **5a** (Fig. S95) results in stepwise disappearance of the triflate-CF_3 signal and only surprisingly little changes (as slight shielding and broadening of the signals) in the $^{31}P\{^1H\}$ NMR spectra, maintaining the 2:1 two-peak structure of the native complex. As expected, the ferrocenylene resonances mostly vanish from the ^1H NMR spectrum, particularly after the addition of the second equivalent of **5a**, while signals attributable to reduced **5a** appear. Addition of **6** does immediately restore the spectral fingerprint of native **[(1a)$_2$(Au)$_3$](OTf)$_3$** in the ^1H NMR spectrum in a very broadened form. With delay, relatively sharp signals are recovered. Similarly, the $^{31}P\{^1H\}$ NMR resonances re-appear and sharpen over time. Even though the $^{19}F\{^1H\}$ NMR peak of the triflate CF_3 group does not fully return to its original position and sharpness even after extended waiting, its re-appearance in general speaks for the triflate anion's inertness in the process.

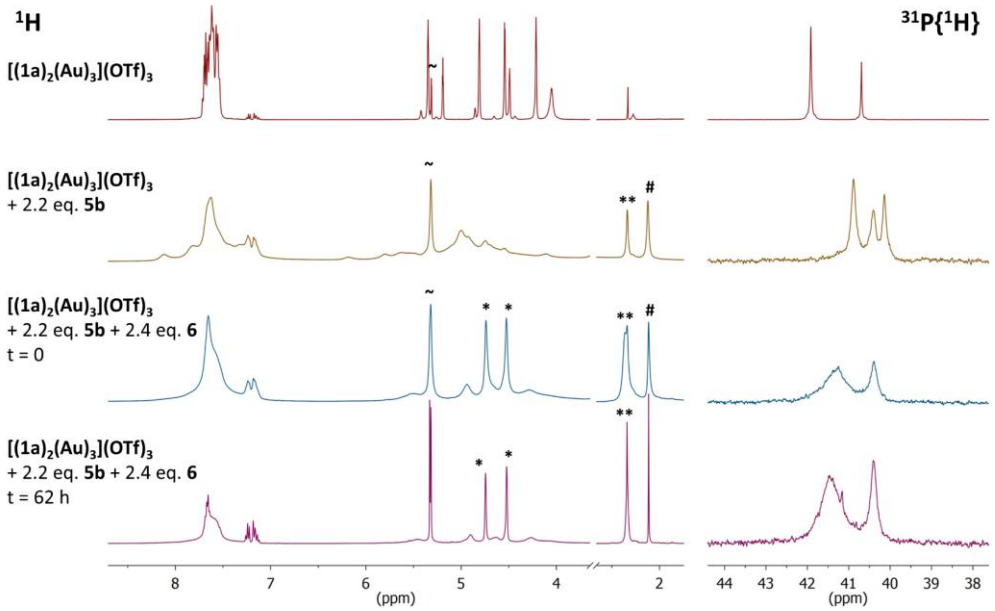

Figure S96 Oxidation of **[(1a)$_2$(Au)$_3$](OTf)$_3$** by 2.2 equivalents of **5b**, followed by reduction with 2.4 equivalents of **6**, traced by ^1H (left) and $^{31}P\{^1H\}$ (right) NMR spectroscopy in CD_2Cl_2 (all spectra recorded at 25 °C using the same parameters). ^1H NMR signals marked by asterisks (*) correspond to 1,1'-diacetylferrocene (reduced **5b**, *: ferrocenylene protons, **: acetyl-CH_3). The hashtag symbol (#) marks the CH_3 resonance of toluene, and the tilde symbol (~) marks the combined $CHDCl_2$/CH_2Cl_2 signals.

Conducting the same reaction with BF_4-based oxidant **5b** (Fig. S96) leads to markedly different results, both with respect to the outcome of the oxidation itself and to the reducibility by **6**. While the $^{31}P\{^1H\}$ resonances are shifted to higher field, too, a third signal appears. The ferrocenylene ^1H NMR signals for 1,1'-diacetylferrocene are not discernible after oxidation and only appear after addition of the reductant, which, however, does not restore the initial spectral properties of **[(1a)$_2$(Au)$_3$](OTf)$_3$** in either the ^1H or the $^{31}P\{^1H\}$ NMR spectrum. This is particularly surprising in so far as the very same procedure, using **5b**, does indeed work for benzene-based **[(1b)$_2$(Au)$_3$](OTf)$_3$** (Fig. **Fehler! Verweisquelle konnte nicht gefunden werden.**). Although the complete regeneration of the signals in both the ^1H and $^{31}P\{^1H\}$ NMR spectra can be observed after addition of first **5b** (golden trace in Fig. **Fehler! Verweisquelle konnte nicht gefunden werden.**) followed by **6** (blue and purple traces in Fig. **Fehler! Verweisquelle konnte nicht gefunden werden.**), a strong deshielding of the $^{31}P\{^1H\}$ NMR signals to about 10 ppm upon oxidation can be observed, contrasting the small chemical shift changes observed during the oxidation of **[(1a)$_2$(Au)$_3$](OTf)$_3$** by both oxidants (Figs. S95 and S96).

This larger oxidation-induced deshielding is also observed during the stepwise oxidation of **[(1b)$_2$(Au)$_3$](OTf)$_3$** using up to six equivalents of TEF-based oxidant **5a** in the corresponding $^{31}P\{^1H\}$ NMR spectra (Fig. S99), even though the overall peak shape and exact shift values (depending on the amount of **5a**) differ to some extent from those observed for **5b**. In the ^1H NMR spectra (Fig. S98), no ferrocenylene signals can be distinguished anymore following the addition of the third equivalent of **5a**. Upon addition of 6.6 equivalents of **6**, the $^{31}P\{^1H\}$ NMR signals of **[(1b)$_2$(Au)$_3$](OTf)$_3$** reappear quite quickly, while its ^1H NMR spectroscopic trace needs more time for returning to what appears to be a spectral trace close to the native state. Some minor changes in peak position might originate from the strongly paramagnetic nature of the sample, containing six equivalents of decamethylferrocenium as **[6](TEF)** and/or **[6]OTf**.

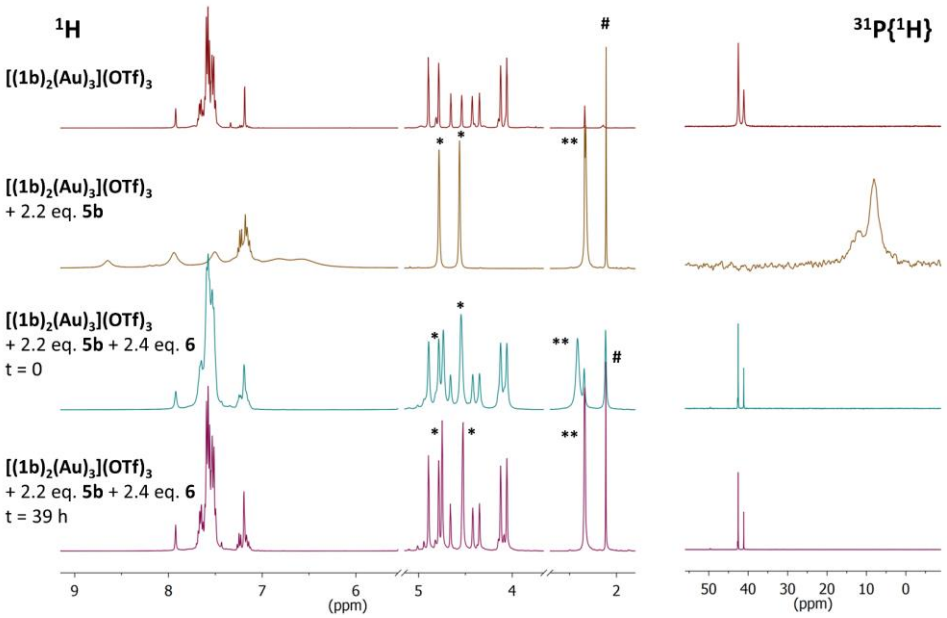

Figure S97 Oxidation of **[(1b)$_2$(Au)$_3$](OTf)$_3$** by 2.2 equivalents of **5b**, followed by reduction with 2.4 equivalents of **6**, traced by ^{1}H (left) and ^{31}P{^{1}H} (right) NMR spectroscopy in CD_2Cl_2 (all spectra recorded at 25 °C using the same parameters). ^{1}H NMR signals marked by asterisks (*) correspond to 1,1'-diacetylferrocene (reduced **5b**, *: ferrocenylene protons, **: acetyl-CH_3). The hashtag symbol (#) marks the CH_3 resonance of toluene.

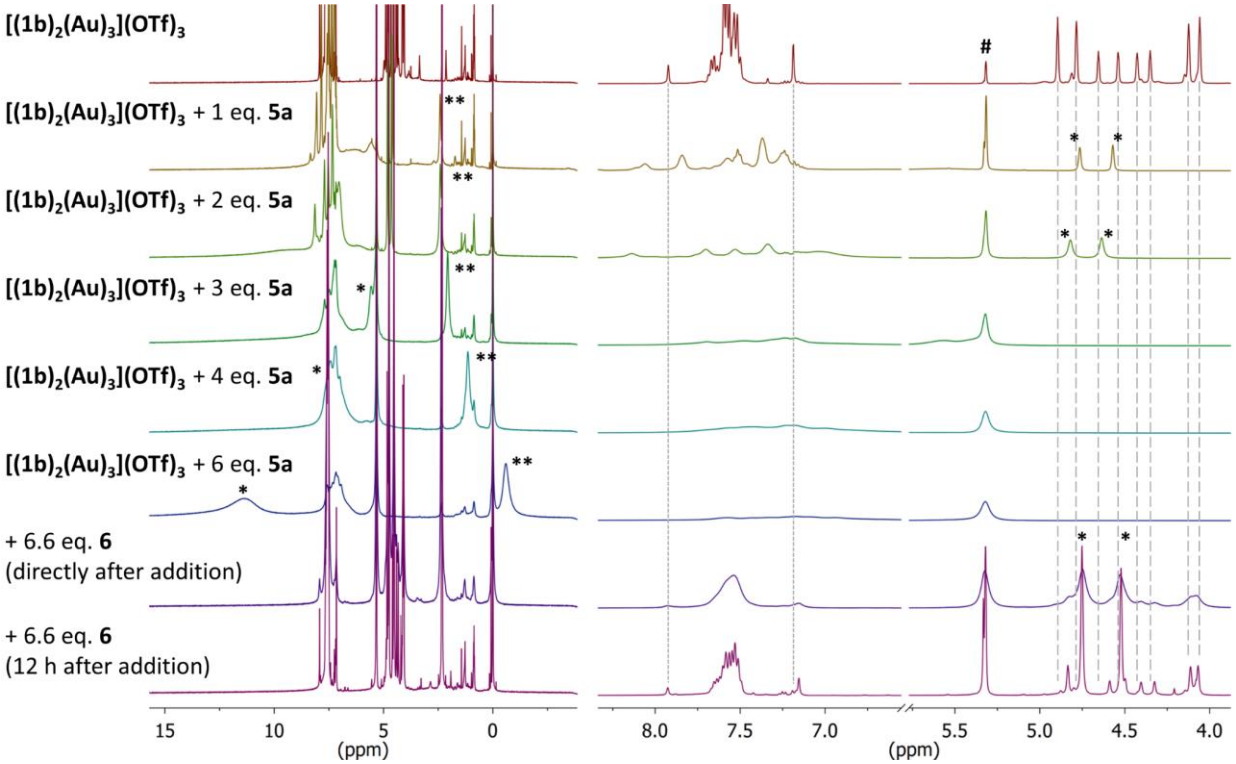

Figure S98 Stepwise oxidation of **[(1b)$_2$(Au)$_3$](OTf)$_3$** by 6 equivalents of **5a**, followed by reduction with 6.6 equivalents of **6**, traced by ^{1}H NMR spectroscopy in CD_2Cl_2 (left: overview, right: regions of interest; all spectra recorded at 25 °C using the same parameters). Dashed lines signify the peak positions of native **[(1b)$_2$(Au)$_3$](OTf)$_3$** and signals marked by asterisks (*) correspond to 1,1'-diacetylferrocene (reduced **5a**, *: ferrocenylene protons, **: acetyl-CH_3). The hashtag symbol (#) marks the $CDHCl_2$/CH_2Cl_2 resonances.

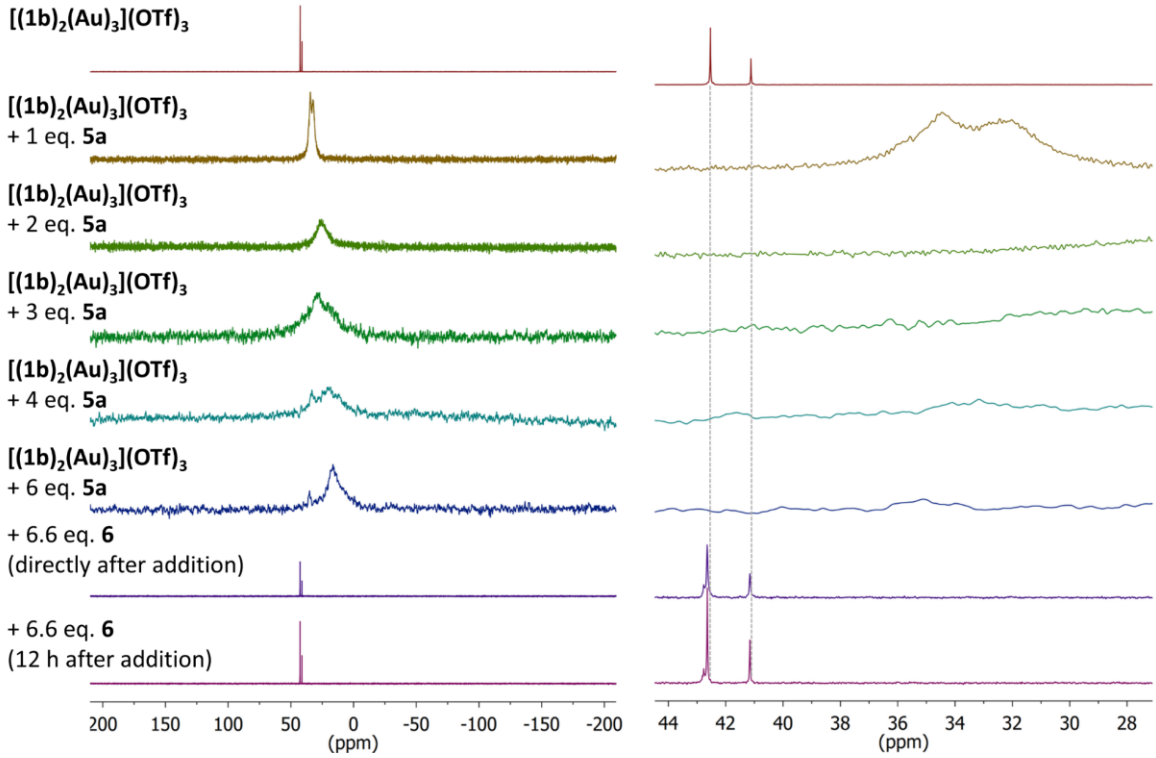

Figure S99 Stepwise oxidation of **[(1b)$_2$(Au)$_3$](OTf)$_3$** by 6 equivalents of **5a**, followed by reduction with 6.6 equivalents of **6**, traced by $^{31}P\{^1H\}$ NMR spectroscopy in CD_2Cl_2 (left: overview, right: regions of interest; all spectra recorded at 25 °C using the same parameters). Dashed lines signify the peak positions of native **[(1b)$_2$(Au)$_3$](OTf)$_3$**.

Autor Contributions

AS has carried out the syntheses and characterisation of the compounds (including the electrochemical characterisation except for spectroelectrochemistry), the calculation of the buried volumes, the catalysis studies, and the NMR experiments, and has written the original draft.
PC has acquired and solved the solid-state structures of all compounds and conducted and evaluated the computational DFT-level calculations.
MRR has conducted the spectroelectrochemical measurements and aided in their interpretation.
MM has carried out the attempted syntheses of defined 2:3 ligand-to-metal complexes of **1c** and conducted preliminary catalytic studies, including the oxidation of the 2:3 ligand-to-metal complexes of **1a** and **1b** using oxidant **5b**. These experiments have been part of MM's Bachelor's project and have been summarised in a corresponding thesis.
EHH has supervised and administered the project, helped in acquiring funding for AS and PC and supported AS in the writing of the draft.

References

1 G. Mancino, A. J. Ferguson, A. Beeby, N. J. Long and T. S. Jones, *J. Am. Chem. Soc.*, 2005, **127**, 524.
2 R. Taube and S. Wache, *J. Organomet. Chem.*, 1992, **428**, 431.
3 A. B. McQuarters, J. W. Kampf, E. E. Alp, M. Hu, J. Zhao and N. Lehnert, *Inorg. Chem.*, 2017, **56**, 10513.
4 P. Wipf, Y. Aoyama and T. E. Benedum, *Org. Lett.*, 2004, **6**, 3593.
5 A. Straube, P. Coburger, L. Dütsch and E. Hey-Hawkins, *Chem. Sci.*, **2020**, DOI: 10.1039/D0SC03604H.
6 A. Straube, P. Coburger, M. R. Ringenberg and E. Hey-Hawkins, *Chem. Eur. J.*, 26, **2020**, 5758.
7 R. K. Harris, E. D. Becker, S. M. Cabral de Menezes, R. Goodfellow and P. Granger, *Pure Appl. Chem.*, 2001, **73**, 1795.
8 CrysAlis Pro, Agilent Technologies.
9 SCALE3 ABSPACK, Oxford Diffraction, 2006.

10 G. M. Sheldrick, *Acta Crystallogr. Sect. A*, 2008, **64**, 112.
11 C. F. Macrae, I. J. Bruno, J. A. Chisholm, P. R. Edgington, P. McCabe, E. Pidcock, L. Rodriguez-Monge, R. Taylor, J. van de Streek and P. A. Wood, *J. Appl. Crystallogr.*, 2008, **41**, 466.
12 C. Cason, T. Fröhlich and C. Lipka, Persistence of Vision Raytracer (3.7), Persistence of Vision Pty. Ltd., 2013.
13 I. Noviandri, K. N. Brown, D. S. Fleming, P. T. Gulyas, P. A. Lay, A. F. Masters and L. Phillips, *J. Phys. Chem. B*, 1999, **103**, 6713.
14 G. Gritzner and J. Kuta, *Pure Appl. Chem.*, 1984, **56**, 461.
15 T. Mahabiersing, H. Luyten, R. C. Nieuwendam and F. Hartl, *Collect. Czech. Chem. Commun.*, 2003, **68**, 1687.
16 F. Neese, *Wiley Interdiscip. Rev. Comput. Mol. Sci.*, 2018, **8**, e1327.
17 F. Neese, *Wiley Interdiscip. Rev. Comput. Mol. Sci.*, 2012, **2**, 73.
18 A. D. Becke, *Phys. Rev. A*, 1988, **38**, 3098.
19 J. P. Perdew, *Phys. Rev. B*, 1986, **33**, 8822.
20 S. Grimme, J. Antony, S. Ehrlich and H. Krieg, *J. Chem. Phys.*, 2010, **132**, 154104.
21 S. Grimme, S. Ehrlich and L. Goerigk, *J. Comput. Chem.*, 2011, **32**, 1456.
22 F. Weigend and R. Ahlrichs, *Phys. Chem. Chem. Phys.*, 2005, **7**, 3297.
23 D. Andrae, U. Häußermann, M. Dolg, H. Stoll and H. Preuß, *Theor. Chim. Acta*, 1990, **77**, 123.
24 R. A. Kendall and H. A. Früchtl, *Theor. Chim. Acta*, 1997, **97**, 158.
25 Yan Zhao and Donald G. Truhlar, *J. Chem. Phys.*, 2006, **125**, 194101.
26 M. Cossi, N. Rega, G. Scalmani and V. Barone, *J. Comput. Chem.*, 2003, **24**, 669.
27 M. C. Gimeno, A. Laguna, C. Sarroca and P. G. Jones, *Inorg. Chem.*, 1993, **32**, 5926.
28 A. Dolmella and G. Bandoli, *Coord. Chem. Rev.*, 2000, **209**, 161.
29 S. Alvarez, *Dalton Trans.*, 2013, **42**, 8617.
30 B. Cordero, V. Gómez, A. E. Platero-Prats, M. Revés, J. Echeverría, E. Cremades, F. Barragán and S. Alvarez, *Dalton Trans.*, 2008, 2832.
31 H. Baumgärtel, *Electrochemistry. A Guide for Newcomers*, De Gruyter, Berlin/Boston, 2019.
32 M. V. Mirkin, *Determination of Electrode Kinetics* in *Handbook of Electrochemistry*, ed. C. G. Zoski, Elsevier, Oxford, 2007, pp. 639–660.
33 P. H. Rieger, *Electrochemistry*, Springer Netherlands, Dordrecht, 1994.
34 B. G. Anderson and J. L. Spencer, *Chem. Eur. J.*, 2014, **20**, 6421.
35 C. L. Pollock, G. C. Saunders, E.C.M. S. Smyth and V. I. Sorokin, *J. Fluor. Chem.*, 2008, **129**, 142.
36 H. B. Gray, Y. S. Sohn and N. Hendrickson, *J. Am. Chem. Soc.*, 1971, **93**, 3603.
37 D. M. Duggan and D. N. Hendrickson, *Inorg. Chem.*, 1975, **14**, 955.
38 S. Hartmann, R. F. Winter, B. M. Brunner, B. Sarkar, A. Knödler and I. Hartenbach, *Eur. J. Inorg. Chem.*, 2003, **2003**, 876.
39 U. Pfaff, A. Hildebrandt, D. Schaarschmidt, T. Hahn, S. Liebing, J. Kortus and H. Lang, *Organometallics*, 2012, **31**, 6761.
40 A. Poater, B. Cosenza, A. Correa, S. Giudice, F. Ragone, V. Scarano and L. Cavallo, *Eur. J. Inorg. Chem.*, 2009, **2009**, 1759.
41 L. Falivene, Z. Cao, A. Petta, L. Serra, A. Poater, R. Oliva, V. Scarano and L. Cavallo, *Nature Chem.*, 2019, **11**, 872.
42 A. Poater, F. Ragone, S. Giudice, C. Costabile, R. Dorta, S. P. Nolan and L. Cavallo, *Organometallics*, 2008, **27**, 2679.

DFT Coordinates of Optimised Structures

1c				1b			
C	7.3886332	4.6369677	15.405051	**C**	17.449984	−0.208684	10.167475
H	7.5031536	3.5658876	15.576625	**Fe**	14.056581	6.072687	4.231686
C	10.304275	3.0250535	14.357463	**Fe**	14.65612	−0.321591	5.965012
H	10.736747	4.0275196	14.313068	**Fe**	19.11587	2.629052	2.107667
C	10.945164	2.0265716	15.089248	**P**	19.086506	−0.343632	3.800388
H	11.87538	2.2501148	15.614127	**P**	16.186796	−2.077411	8.410751
C	4.8736892	−0.55207	12.876648	**P**	16.789278	6.947343	2.437501
H	4.687929	0.0370428	13.7744	**C**	17.355225	2.511088	1.076797
C	0.682191	5.1648921	13.520205	**C**	15.223583	3.46836	1.933911
C	0.25075	−1.182778	10.521583	**H**	15.50337	4.425975	1.49484
H	−0.186778	−1.843578	11.263755	**C**	13.759813	2.168165	3.350438
C	3.4894441	1.0602345	15.990763	**H**	12.886543	2.103157	3.998637
C	0.3332326	−2.850552	15.367622	**C**	15.91003	5.399885	4.701153
H	−0.097938	−3.503401	16.127765	**H**	16.320513	4.472912	4.30995
C	−0.051209	4.141294	12.90324	**C**	18.03327	3.751541	0.788418
C	5.8986842	0.7507643	16.170119	**H**	17.647585	4.745469	1.002093
H	6.9026115	1.1770511	16.183753	**C**	14.293276	0.114419	7.929501
C	5.3851334	−2.002773	10.548424	**H**	13.484889	−0.296068	8.525928
H	5.5826482	−2.563991	9.6334157	**C**	19.501	1.420352	3.694925
C	1.1193076	0.9745185	18.071707	**C**	15.736434	1.153983	2.40252
H	2.166245	0.8943007	18.366829	**H**	16.415914	0.30561	2.327493
C	3.2811935	4.7273609	15.783127	**C**	14.074759	3.385786	2.740559
H	3.5577883	4.7191145	14.733131	**C**	18.246165	1.446176	0.692816
C	−1.227536	0.6195377	18.558754	**H**	18.040849	0.3859	0.797848
H	−2.009702	0.2700327	19.234199	**C**	19.319649	3.446717	0.240479
C	1.5737786	0.4481199	9.5375648	**H**	20.075557	4.171012	−0.048661
H	2.307475	1.2357012	9.4035899	**C**	18.584268	2.472402	4.058882
C	6.1311022	−1.112415	12.666329	**H**	17.562446	2.316379	4.394366
H	6.9080268	−0.978331	13.418632	**C**	13.295812	4.595127	3.040133
C	2.5672878	3.6759282	16.46477	**C**	14.246075	1.306397	7.137004
C	0.7938009	1.5140011	16.818088	**H**	13.388258	1.96364	7.023178
C	5.178673	2.2171185	10.979575	**C**	14.325363	−0.186512	3.953001
H	4.7025357	1.6708715	10.171243	**C**	13.351154	5.847224	2.330491
C	0.2693496	3.5656496	11.664414	**H**	13.919825	6.024443	1.422891
C	1.475529	−1.152225	13.439982	**C**	20.5305	−1.059477	2.906257
C	1.4335837	4.0528629	11.05968	**C**	15.5952	−0.483963	7.766763
C	0.3321995	5.705974	14.842936	**C**	16.072439	2.367835	1.77728
C	3.845562	−0.73589	11.937447	**C**	20.716192	2.052265	3.240146
C	5.4317404	5.5015856	9.5933835	**H**	21.592569	1.528934	2.871107
H	6.0847433	5.343303	8.7401983	**C**	19.227362	3.729302	3.836803
C	1.8102678	5.5951125	12.803528	**H**	18.793729	4.710766	3.99347
C	−1.404656	1.5752008	11.685037	**C**	15.988062	6.683699	4.04672
H	−1.320088	1.3020076	12.730305	**C**	16.2885	8.691612	2.120096
C	1.3249013	−0.25981	10.768485	**C**	19.452777	2.020082	0.181714
C	0.2588697	7.0252782	16.766667	**H**	20.32266	1.467021	−0.160457
H	0.4248307	7.8431823	17.461959	**C**	13.108987	−0.522758	4.652398
C	−0.395136	4.9986604	15.871719	**H**	12.192514	0.059658	4.652364
H	−0.814924	4.007399	15.78489	**C**	14.593022	1.045091	3.200802
C	5.525744	3.3011013	12.992553	**C**	13.316853	−1.748896	5.360877
H	5.3658184	3.7415994	13.969558	**H**	12.595267	−2.244301	6.003862
C	2.2760556	5.0418843	11.600051	**C**	21.796311	−1.206815	3.493775
C	8.5591406	1.4683889	13.744347	**H**	21.939476	−0.927436	4.538652
H	7.6212771	1.2486707	13.233323	**C**	20.540715	3.470258	3.323552
C	−0.152401	−1.047259	9.1549532	**H**	21.258712	4.227897	3.024524
H	−0.965216	−1.584524	8.6737492	**C**	15.158808	8.910561	1.316537
C	0.3740546	−0.734221	14.201309	**H**	14.645402	8.058519	0.868666

H	−0.00582	0.278507	14.068904	**C**	15.51447	1.459659	6.488361
C	−0.634436	2.5961641	11.022872	**H**	15.770127	2.240776	5.777325
C	4.7913442	1.5884121	16.023801	**C**	14.716591	6.918196	5.983353
H	4.9408925	2.6655536	15.946978	**H**	14.088401	7.343184	6.761234
C	3.5731872	5.4178885	11.010255	**C**	18.54901	7.144861	2.932609
C	1.9955028	−2.438053	13.652075	**C**	12.564541	6.812178	3.035897
H	2.8611614	−2.770438	13.078837	**H**	12.435673	7.854025	2.757643
C	−2.293558	0.9844051	10.735049	**C**	14.190626	−2.237029	10.462661
H	−2.984599	0.1698702	10.931556	**H**	14.797824	−1.530637	11.030536
C	−1.04449	2.5993975	9.6393869	**C**	16.960183	9.797843	2.661258
H	−0.637959	3.2425524	8.8655351	**H**	17.847081	9.642299	3.276877
C	−1.563633	1.1534437	17.312164	**C**	19.534834	−0.697946	5.549219
H	−2.608963	1.2218804	17.006786	**C**	15.13478	5.548549	5.894008
C	3.3257684	−0.331537	16.108293	**H**	14.880252	4.752899	6.588693
H	2.3272352	−0.766964	16.082286	**C**	16.346728	0.35841	6.865557
C	6.7559002	3.368063	12.246478	**H**	17.360142	0.169138	6.525836
C	10.400399	0.7386738	15.144232	**C**	16.499889	11.093551	2.41729
H	10.903662	−0.046011	15.710767	**H**	17.032137	11.945764	2.843059
C	4.1129734	−1.46793	10.771497	**C**	15.243009	7.620516	4.852667
H	3.3235502	−1.618855	10.034465	**H**	15.09192	8.668702	4.614718
C	−2.07431	1.6211521	9.4714351	**C**	14.634694	−2.675333	9.205706
H	−2.571499	1.3769832	8.5368529	**C**	20.355638	−1.442026	1.568177
C	3.5061524	5.796767	16.703588	**H**	19.367898	−1.359406	1.111745
H	3.9931265	6.7373675	16.469463	**C**	14.659353	−2.181866	5.106294
C	6.9205947	5.4592702	16.429564	**H**	15.146638	−3.054151	5.532504
H	6.6518832	5.0259371	17.393846	**C**	17.15854	−1.548825	9.87951
C	2.3537614	4.1211646	17.820475	**C**	20.078272	0.263249	6.416763
H	1.8134573	3.5711643	18.584427	**H**	20.29551	1.264503	6.043426
C	0.6720224	−0.046231	8.5442275	**C**	15.28222	−1.226372	4.244791
H	0.5964953	0.3068767	7.5195317	**H**	16.32071	−1.242096	3.921228
C	6.396512	−1.83081	11.496812	**C**	19.519635	7.038902	1.923149
H	7.3882466	−2.251553	11.32465	**H**	19.203268	6.882703	0.889388
C	0.7309848	6.9733066	15.418383	**C**	21.428004	−1.932736	0.82039
H	1.30712	7.7442846	14.922345	**H**	21.277109	−2.222492	−0.220687
C	4.0895393	5.0269956	9.7132202	**C**	13.848592	−3.592384	8.491526
H	3.5591866	4.4560557	8.9630146	**H**	14.198081	−3.955435	7.523443
C	1.4292138	−3.279009	14.611826	**C**	19.243854	−1.977327	6.051183
H	1.8504539	−4.272391	14.775496	**H**	18.790567	−2.723959	5.39528
C	2.9329782	5.4229705	17.962652	**C**	14.691059	10.204731	1.081991
H	2.906898	6.036826	18.858972	**H**	13.808823	10.358619	0.458691
C	−0.199146	−1.576159	15.155032	**C**	19.508619	−2.294643	7.383035
H	−1.035378	−1.22102	15.757921	**C**	21.284773	7.290503	3.558152
C	4.6438413	6.1391866	11.675125	**H**	22.346804	7.338077	3.802623
H	4.6211751	6.5475441	12.676492	**C**	18.967003	7.319959	4.260921
C	7.5907904	6.5564645	13.953308	**H**	18.221394	7.387146	5.054601
H	7.8716675	6.9877771	12.990931	**C**	12.456065	4.807627	4.193819
C	6.7878592	6.8352176	16.217839	**H**	12.238962	4.073607	4.963809
H	6.4329939	7.4794052	17.02366	**C**	20.048613	−1.331791	8.2408
C	7.1195375	7.3828553	14.976816	**H**	20.220954	−1.570095	9.29063
H	7.0246816	8.4566547	14.807765	**C**	12.979945	−2.696128	10.985264
C	4.4333327	−1.166033	16.261804	**H**	12.645882	−2.348004	11.96419
H	4.2823041	−2.243062	16.345998	**C**	22.867076	−1.706807	2.750485
C	−0.432208	5.8049443	17.047102	**H**	23.846639	−1.81701	3.218769
H	−0.884266	5.5219899	17.993031	**C**	20.327126	−0.053104	7.754851
C	6.5288612	2.6915005	10.991952	**H**	20.73438	0.706621	8.423805
H	7.2609952	2.5751057	10.197953	**C**	12.008284	6.167663	4.188881
C	7.7241713	5.1752921	14.151766	**H**	11.379868	6.634535	4.941721
C	−0.556697	1.5857314	16.447364	**C**	12.194822	−3.595015	10.256865

H	−0.818047	1.9717087	15.46036	**H**	11.248492	−3.951593	10.66616
C	5.7239386	−0.630182	16.291035	**C**	12.631954	−4.043427	9.007593
H	6.5892192	−1.284755	16.403749	**H**	12.029706	−4.753615	8.438659
C	0.1164246	0.5265908	18.933489	**C**	22.687618	−2.064148	1.410624
H	0.3847821	0.1049941	19.90362	**H**	23.525677	−2.454133	0.831162
C	9.0965973	2.7618317	13.687329	**C**	15.360995	11.30009	1.633735
C	4.55982	2.6022851	12.211299	**H**	15.002267	12.31293	1.445312
H	3.5255396	2.4137108	12.490609	**C**	18.87111	−0.884824	12.010557
C	5.7708413	6.1878059	10.799098	**C**	20.327364	7.388267	4.571092
H	6.7322501	6.6366597	11.027002	**H**	20.640422	7.514817	5.608599
C	9.2122572	0.4640897	14.465008	**C**	20.877517	7.120326	2.231141
H	8.7834889	−0.539143	14.504968	**H**	21.621092	7.036102	1.43707
P	2.0462771	2.1469788	15.622849	**C**	18.30383	0.119903	11.223825
P	8.3211178	4.142248	12.741409	**C**	18.57804	−2.225979	11.736777
P	2.2359744	0.0738272	12.301182	**C**	17.736126	−2.553753	10.674931
Fe	−0.351838	0.7422595	10.135852	**H**	19.263421	−3.286761	7.762271
Fe	1.5076244	5.4168301	16.484	**H**	17.016848	0.579785	9.551415
Fe	5.2347682	4.2516093	11.213052	**H**	18.526551	1.167853	11.431974
F	1.7728606	3.511382	9.8626117	**H**	17.525999	−3.602869	10.452341
F	−1.188468	3.7165907	13.513204	**H**	19.540161	−0.62714	12.832752
F	2.5277318	6.6133513	13.344372	**H**	19.016927	−3.01733	12.34673

1a				**1a^F**			
C	1.459258	11.302974	0.932511	**C**	7.342704	5.009595	15.473738
P	1.548058	11.779801	4.427859	**F**	7.388104	3.712115	15.815504
Fe	0.997119	14.192681	2.015427	**C**	10.612564	3.596896	13.845926
C	1.478992	12.739307	0.665036	**F**	10.961298	4.826267	13.407506
C	0.348306	13.510128	0.21526	**C**	11.605873	2.810478	14.425403
H	−0.6391	13.103445	0.024663	**F**	12.866267	3.260367	14.536573
C	2.145254	14.952959	0.484373	**C**	5.059618	−0.904768	12.514898
H	2.739988	15.860549	0.534456	**F**	5.048284	−0.237425	13.683238
C	2.588458	13.641619	0.836416	**C**	0.834104	5.303942	13.455435
H	3.575613	13.363425	1.188082	**C**	0.461399	−0.992554	10.292547
C	−1.358978	9.536832	4.725203	**H**	−0.042964	−1.895524	10.622188
H	−1.340637	10.616682	4.632005	**C**	3.045785	0.931165	16.225906
C	0.933688	13.39964	3.900398	**C**	−0.053699	−4.372904	14.244461
C	4.822526	8.708483	4.797757	**F**	−0.742676	−5.403105	14.751106
H	5.413045	9.606054	4.957157	**N**	0.029489	4.297441	13.065489
C	0.707518	15.662343	3.422364	**C**	5.263616	0.008985	16.699389
H	0.932131	16.716365	3.283566	**F**	6.562915	0.208451	16.962686
C	1.607938	14.670011	3.920841	**C**	5.189547	−2.317630	10.132393
H	2.633926	14.825946	4.239526	**F**	5.253650	−3.028342	8.994783
C	0.860927	11.682645	6.130419	**C**	0.875291	1.615161	18.441351
C	3.317825	12.171931	4.74611	**F**	2.149402	1.585610	18.882120
C	−0.616359	12.440356	7.90638	**C**	3.303780	4.700961	15.573096
H	−1.319134	13.179978	8.293702	**H**	3.421494	4.584767	14.500548
C	−1.146483	7.250373	1.515905	**C**	−1.457414	1.317789	18.978910
H	−0.344695	6.521274	1.46054	**F**	−2.419030	1.036042	19.865405
C	−0.295942	11.31681	8.668915	**C**	1.840947	0.874886	10.250835
H	−0.753189	11.173141	9.647683	**H**	2.494151	1.684168	10.562706
C	1.17171	10.54896	6.90376	**C**	6.306173	−1.208855	11.964858
H	1.861745	9.797898	6.514449	**F**	7.441667	−0.843476	12.574965
C	0.605277	10.373322	8.164881	**C**	2.599086	3.797386	16.451208
H	0.858748	9.489263	8.752028	**C**	0.581777	1.929297	17.107684
C	3.810853	12.586911	5.991849	**C**	5.131727	2.033251	11.312432
H	3.125609	12.704468	6.832014	**H**	4.678938	1.427201	10.533927
C	1.84144	3.784199	1.250382	**C**	0.329343	3.762012	11.865931
H	1.979915	3.570064	0.189605	**C**	1.413151	−2.188323	13.158298

C	5.173707	12.842294	6.161428	**N**	1.395401	4.094157	11.116767
H	5.54725	13.159068	7.136593	**C**	0.511493	5.960929	14.721147
C	−0.979204	8.675646	1.37266	**C**	3.856061	−1.275965	11.903889
C	4.211646	12.011436	3.674403	**C**	5.305598	5.076555	9.594856
H	3.837707	11.650321	2.712511	**H**	5.947670	4.772242	8.773498
C	5.569829	12.28535	3.842563	**N**	1.931512	5.715590	12.789686
H	6.25583	12.160284	3.002712	**C**	−1.183785	1.695956	12.149408
C	6.056125	12.696991	5.086956	**H**	−0.950783	1.505455	13.189774
H	7.12018	12.897139	5.221377	**C**	1.420225	−0.245237	11.059940
C	3.807127	8.56491	1.234563	**C**	0.618351	7.354738	16.570981
C	3.713999	4.212406	6.097162	**H**	0.883114	8.173490	17.233679
C	5.131108	9.067739	1.496406	**C**	−0.288723	5.380513	15.768265
H	5.389036	10.112455	1.62841	**H**	−0.830749	4.447205	15.675895
C	5.2505	6.755145	1.369846	**C**	5.433524	3.275389	13.242615
H	5.637193	5.740968	1.409341	**H**	5.266947	3.745319	14.203657
C	−0.246954	8.657727	4.560429	**C**	2.202154	5.027878	11.664549
H	0.750195	8.965551	4.268249	**C**	8.985502	1.893389	14.214238
C	3.88633	7.127924	1.164335	**F**	7.733817	1.413546	14.188030
H	3.038534	6.469685	1.013585	**C**	0.322856	−0.364504	9.015406
C	3.038302	7.314729	4.285504	**H**	−0.344972	−0.681984	8.219584
H	2.061724	6.964822	3.969666	**C**	0.082813	−2.063950	13.584560
C	1.501698	4.316176	3.970844	**F**	−0.525928	−0.863274	13.516252
H	1.369092	4.509112	5.036859	**C**	−0.601620	2.744608	11.364716
C	3.431075	8.678072	4.465597	**C**	4.408688	1.094449	16.494081
H	2.802958	9.547801	4.292659	**F**	4.959382	2.319730	16.578543
C	2.82055	3.362857	8.625398	**C**	3.487956	5.273594	11.019112
H	2.472647	3.033655	9.605503	**C**	1.989036	−3.454972	13.332175
C	5.298376	7.35887	4.814565	**F**	3.276980	−3.699828	13.018831
H	6.317762	7.036421	5.007792	**C**	−2.063306	0.947011	11.311448
C	4.193557	6.481892	4.503682	**H**	−2.626541	0.066848	11.605657
C	−5.405925	10.241657	9.122341	**C**	−1.134891	2.647782	10.029461
H	−6.308223	10.650473	9.580062	**H**	−0.879469	3.302498	9.202057
C	3.659204	2.844424	6.415333	**C**	−1.787643	1.614362	17.655496
H	3.967734	2.106512	5.670856	**F**	−3.071873	1.610466	17.268915
C	3.206587	2.421964	7.664711	**C**	2.582682	−0.388923	16.163027
H	3.160968	1.356005	7.893501	**F**	1.269119	−0.625026	15.930592
C	−4.190721	9.549939	7.130738	**C**	6.657449	3.330488	12.493632
C	2.952934	4.008362	2.065843	**C**	11.276269	1.535680	14.892840
H	3.957562	3.962373	1.641561	**F**	12.216720	0.761741	15.449075
C	6.016326	7.948445	1.580955	**C**	3.961359	−2.016511	10.717271
H	7.079531	7.992232	1.798829	**F**	2.868229	−2.516498	10.116255
C	−5.349066	10.062563	7.741085	**C**	−2.049051	1.544839	10.007424
H	−6.210367	10.328217	7.123363	**H**	−2.606297	1.200984	9.140774
C	0.389502	4.084597	3.159247	**C**	3.708109	5.841439	16.329735
H	−0.612254	4.10834	3.591208	**H**	4.209634	6.717449	15.931407
C	−3.165718	9.360082	9.324463	**C**	7.010699	5.911286	16.485357
H	−2.310825	9.075777	9.9401	**F**	6.760407	5.484654	17.730722
C	−2.530139	6.999779	1.774794	**C**	2.557232	4.418773	17.752663
H	−2.979719	6.02697	1.952026	**H**	2.083753	4.014588	18.639520
C	−3.097629	9.203435	7.937234	**C**	1.179836	0.784275	8.986174
H	−2.185461	8.820635	7.479302	**H**	1.267033	1.497850	8.172222
C	−3.2171	8.258537	1.809311	**C**	6.368399	−1.905589	10.758336
H	−4.271793	8.395482	2.03009	**F**	7.555695	−2.196232	10.211904
C	−2.26464	9.29661	1.566628	**C**	1.072384	7.190083	15.223825
H	−2.448222	10.365558	1.557504	**H**	1.738500	7.844544	14.671449
C	−3.498428	12.065783	5.508119	**C**	3.955135	4.658574	9.803362
H	−3.113873	11.831796	6.501369	**H**	3.368448	3.992290	9.180231
C	−2.52337	8.74244	5.013759	**C**	1.276083	−4.535363	13.858196

C	2.796438	4.298475	3.429045	**F**	1.868104	−5.731379	13.998965
C	−0.038509	12.62598	6.647674	**C**	3.242450	5.670256	17.673576
H	−0.291426	13.50792	6.059639	**H**	3.362833	6.382157	18.484786
C	−0.70161	7.315659	4.750382	**C**	−0.656060	−3.121168	14.107263
H	−0.097949	6.419241	4.651985	**F**	−1.929951	−2.941082	14.493001
C	−4.314034	9.883174	9.921018	**C**	4.569896	6.052207	11.565860
H	−4.363115	10.007831	11.003728	**H**	4.524117	6.615080	12.491873
C	−2.107546	7.360184	5.019306	**C**	7.532482	6.794310	13.907322
H	−2.76068	6.508408	5.188044	**F**	7.809494	7.283448	12.682448
C	3.328721	5.148768	7.067748	**C**	6.920606	7.272278	16.187991
H	3.366159	6.213517	6.835689	**F**	6.575310	8.145982	17.142962
C	−4.554258	11.365062	3.44948	**C**	7.178293	7.719036	14.890812
H	−5.017842	10.583962	2.844125	**F**	7.092072	9.027806	14.605252
C	−4.075533	11.049908	4.729625	**C**	3.407058	−1.491829	16.363600
C	0.555673	3.827219	1.795333	**F**	2.910922	−2.741415	16.312015
H	−0.314046	3.648931	1.161536	**C**	−0.211106	6.233975	16.907831
C	−4.452439	12.665902	2.950466	**H**	−0.682925	6.057112	17.869860
H	−4.828546	12.896353	1.95247	**C**	6.461025	2.562206	11.287960
C	−3.408039	13.368166	5.015505	**H**	7.192913	2.426277	10.496806
H	−2.953114	14.148893	5.626723	**C**	7.615466	5.418489	14.159729
C	−3.886546	13.671661	3.737581	**C**	−0.769798	1.905841	16.746717
H	−3.819343	14.691623	3.357008	**F**	−1.139961	2.165207	15.477769
N	0.255006	10.707233	1.012291	**C**	4.763400	−1.291106	16.629048
N	2.645644	10.672326	1.049021	**F**	5.576133	−2.339950	16.809608
C	2.563834	9.330164	1.175053	**C**	−0.117479	1.314848	19.374204
P	4.314261	4.669966	4.415498	**F**	0.200615	1.027354	20.646184
Fe	4.510037	7.794946	2.978282	**C**	9.283856	3.168437	13.715720
N	1.415625	8.632142	1.234982	**C**	4.495748	2.481320	12.515577
C	0.290743	9.372949	1.200291	**H**	3.471695	2.269032	12.816807
P	−4.224426	9.303043	5.305088	**C**	5.683459	5.934057	10.678560
C	0.76765	14.870802	0.094244	**H**	6.660543	6.384022	10.818118
H	0.139567	15.705709	−0.203344	**C**	9.962349	1.075183	14.786050
Fe	−1.720031	8.216588	3.213576	**F**	9.645544	−0.140548	15.255884
C	−0.529957	15.01595	3.094234	**P**	1.845634	2.284250	15.798310
H	−1.403688	15.493294	2.660085	**P**	8.155330	4.303649	12.779554
C	−0.391046	13.618566	3.37216	**P**	2.268590	−0.633391	12.623796
H	−1.13787	12.850001	3.198705	**Fe**	−0.165319	0.941772	10.510261
C	2.888211	4.724795	8.324876	**Fe**	1.680950	5.612565	16.335019
H	2.590566	5.464357	9.070217	**Fe**	5.114104	4.081915	11.382352

$[1a(Au)]^+_{open}$				**$[1a(Au)]^+_{closed}$**			
C	7.3772256	4.4523549	15.38644	**C**	2.571527	11.421766	−2.887881
H	7.5450679	3.383894	15.522155	**H**	2.602232	12.293919	−3.542975
C	10.133352	2.8379024	14.164693	**C**	−1.617497	10.566229	2.407519
H	10.572372	3.8381546	14.156538	**C**	2.486166	9.050454	1.817798
C	10.785343	1.8034814	14.833954	**C**	3.463858	14.670304	0.872043
H	11.728662	1.9984298	15.345703	**C**	5.325231	13.703815	−0.653217
C	4.419687	−0.801441	13.359765	**H**	4.719427	13.441797	−1.512569
H	4.0387973	−0.478383	14.329137	**C**	1.977338	15.734721	2.23556
C	0.8169464	4.995499	13.513789	**C**	−1.444848	12.211035	0.107162
C	0.412977	−0.834286	9.9818745	**C**	−2.687351	12.688995	−0.443968
H	−0.072546	−1.729111	10.357518	**H**	−3.46138	13.211261	0.10927
C	3.9224334	1.1307865	16.57966	**C**	4.563348	10.911779	1.319738
C	−0.670045	−3.781033	13.917412	**C**	−0.692121	11.607445	−0.963207
H	−1.277137	−4.617114	14.265927	**H**	0.290671	11.160774	−0.873166
N	0.0551972	3.9828935	13.047284	**C**	6.64548	11.207743	2.296821
C	6.3319178	0.880663	16.55845	**H**	7.423931	11.482839	3.002355
H	7.3253927	1.3064391	16.416396	**C**	1.078954	13.879704	5.592117

C	5.4222095	−1.587432	10.873206	**C**	0.63358	17.890214	4.961574
H	5.8138569	−1.888372	9.9010638	**H**	−0.129357	18.474037	5.468092
C	1.5288395	1.4803283	18.772429	**C**	1.70205	16.501564	3.444554
H	2.5640176	1.5946579	19.097073	**C**	2.499464	9.18591	−1.216443
C	3.4595066	4.7521079	15.613595	**H**	2.477867	8.309541	−0.569738
H	3.5817819	4.5823812	14.548216	**C**	4.834093	14.26629	0.581294
C	−0.783368	0.9696695	19.276434	**C**	5.962068	14.453568	1.454438
H	−1.553487	0.7057068	20.00187	**H**	5.910765	14.853274	2.459212
C	1.7127486	1.1041432	9.8746701	**C**	1.558451	14.59016	6.750289
H	2.3138881	1.9616667	10.162064	**H**	2.557477	14.512245	7.16725
C	5.751515	−1.187344	13.2365	**C**	1.320927	15.016581	0.172924
H	6.3923165	−1.168787	14.117264	**C**	2.410433	9.027512	−2.601127
C	2.9198066	3.8171605	16.572204	**H**	2.315004	8.026704	−3.023837
C	1.1935999	1.6500292	17.419969	**C**	−0.634001	15.238769	6.364107
C	5.0429171	2.1493866	10.774207	**H**	−1.584493	15.759034	6.43699
H	4.5883464	1.6503492	9.9246837	**C**	2.63609	16.820238	4.496919
C	0.2690278	3.68612	11.74564	**H**	3.660379	16.472117	4.558585
C	0.8917279	−1.640671	13.026861	**C**	1.410463	11.065563	5.590581
N	1.272468	4.1722315	10.996873	**C**	−0.282345	14.290021	5.35676
C	0.4729934	5.5434331	14.824932	**H**	−0.918395	13.941694	4.55201
C	3.5779168	−0.810841	12.237733	**C**	5.567062	10.523017	0.361863
C	5.148975	5.421928	9.5215342	**H**	5.372314	10.174464	−0.647359
H	5.7717226	5.255191	8.647764	**C**	−0.624242	14.740233	−2.992865
N	1.8554116	5.5420734	12.858764	**H**	−0.781851	14.454039	−4.028594
C	−1.37454	1.6873788	11.758177	**C**	−2.851129	15.663886	2.936093
H	−1.211361	1.3781355	12.785261	**H**	−2.656257	16.732716	2.834376
C	1.3051362	0.0188624	10.735115	**C**	−1.468576	11.710907	−2.156897
C	0.3737542	6.9480959	16.666753	**H**	−1.158	11.377959	−3.142854
H	0.4996454	7.8072035	17.318967	**C**	0.514725	11.110195	6.667961
C	−0.178626	4.8371737	15.894158	**H**	0.119679	12.066262	7.010413
H	−0.540553	3.8177949	15.835813	**C**	3.524217	8.257925	2.32742
C	5.3487254	3.1152937	12.861626	**H**	4.548567	8.629425	2.32096
H	5.1844132	3.4662661	13.873739	**C**	2.640879	11.590761	−1.504867
C	2.1061044	5.0206764	11.641163	**H**	2.684186	12.594928	−1.075096
C	8.3672931	1.3175778	13.516751	**C**	2.615868	10.469702	−0.661462
H	7.4180865	1.1206478	13.017692	**C**	−1.927368	14.741009	2.44525
C	0.2835938	−0.275182	8.6731176	**H**	−0.991561	15.085019	1.997159
H	−0.343466	−0.665677	7.8770558	**C**	−1.898507	8.981269	4.222355
C	−0.228477	−1.406004	13.836645	**H**	−1.747048	8.717722	5.268526
H	−0.476871	−0.38414	14.128761	**C**	3.659172	12.804748	5.280352
C	−0.707125	2.7877333	11.119624	**C**	−2.695384	12.379129	−1.838389
C	5.2004116	1.6847623	16.415876	**H**	−3.47777	12.645716	−2.543267
H	5.3105527	2.7437878	16.180302	**C**	0.459292	17.158295	3.750974
C	3.3638115	5.3815709	11.0012	**H**	−0.438399	17.102139	3.148522
C	1.2367388	−2.95383	12.675099	**C**	1.915768	9.828352	5.161576
H	2.1191668	−3.139449	12.061247	**H**	2.609019	9.781562	4.322181
C	−2.237944	1.0719796	10.80262	**C**	1.538917	8.652857	5.807276
H	−2.851707	0.1920979	10.970331	**H**	1.942057	7.700944	5.463513
C	−1.178438	2.8553262	9.7582694	**C**	6.846678	10.708755	0.968935
H	−0.852739	3.5802053	9.0191754	**H**	7.806946	10.543069	0.48884
C	−1.117026	1.1201228	17.927907	**C**	−1.430382	10.205889	3.751031
H	−2.145736	0.97316	17.597693	**H**	−0.919102	10.884145	4.433584
C	3.7851409	−0.232194	16.888284	**C**	−2.182798	13.366347	2.562709
H	2.7919878	−0.668855	17.005573	**C**	−1.574905	15.405051	−2.151292
C	6.5698487	3.2811232	12.12126	**H**	−2.576215	15.710827	−2.439995
C	10.2388	0.515268	14.835618	**C**	2.453011	10.14346	−3.440342
H	10.755835	−0.298337	15.345712	**H**	2.391635	10.017111	−4.521895
C	4.0826989	−1.211338	10.992314	**C**	1.171615	8.558991	1.828046

H	3.4355276	−1.210315	10.115039	**H**	0.356401	9.168907	1.439785
C	−2.129034	1.8012317	9.5734795	**C**	0.329397	14.990637	−0.895447
H	−2.652242	1.5743839	8.6493041	**C**	−4.267043	13.860822	3.700903
C	3.6956854	5.9842162	16.290559	**H**	−5.175168	13.513139	4.194693
H	4.0646697	6.8916329	15.826287	**C**	7.133443	14.03585	0.758013
C	7.0224549	5.247538	16.476191	**H**	8.143684	14.031932	1.156613
H	6.8864694	4.7940603	17.459246	**C**	−3.357983	12.929893	3.193588
C	2.8256785	4.4963214	17.846427	**H**	−3.564369	11.864646	3.290423
H	2.4357127	4.0748487	18.766742	**C**	−4.01977	15.22921	3.567549
C	1.0853793	0.9106545	8.6058722	**H**	−4.734884	15.95474	3.957047
H	1.1614585	1.581505	7.7554611	**C**	0.544913	14.475911	−2.221498
C	6.2587498	−1.571112	11.991754	**H**	1.449023	13.984695	−2.558144
H	7.3078685	−1.851568	11.891618	**C**	−0.998257	15.553541	−0.855148
C	0.8135354	6.8590495	15.308575	**H**	−1.461272	16.016992	0.008051
H	1.3262054	7.6224037	14.732788	**C**	1.975163	17.682798	5.420894
C	3.8069538	4.9629869	9.6942817	**H**	2.404356	18.083616	6.334455
H	3.2100544	4.4010854	8.9838717	**C**	5.241053	11.33897	2.517771
C	0.4541786	−4.019709	13.120974	**H**	4.764169	11.699415	3.421253
H	0.7252164	−5.040396	12.849441	**C**	0.899963	7.288051	2.329936
C	3.3082108	5.8288683	17.660557	**H**	−0.125448	6.92019	2.327906
H	3.3366255	6.6023062	18.422463	**C**	−2.544838	8.097185	3.352947
C	−1.010452	−2.473915	14.276645	**H**	−2.907144	7.136281	3.720462
H	−1.880641	−2.28727	14.906601	**C**	0.499608	15.426002	7.220231
C	4.4563232	6.0791579	11.63589	**H**	0.560338	16.117929	8.055468
H	4.4390242	6.4913013	12.638882	**C**	3.245323	6.988856	2.842526
C	7.3834805	6.400787	13.960568	**H**	4.057821	6.377796	3.237654
H	7.5582406	6.8591991	12.985732	**C**	6.741456	13.574812	−0.541113
C	6.8521503	6.6248005	16.310876	**H**	7.403768	13.163322	−1.297078
H	6.5948615	7.2498268	17.16676	**C**	4.196174	12.031408	6.321161
C	7.0237522	7.1992666	15.048995	**H**	3.597168	11.251043	6.789076
H	6.904607	8.2756	14.915869	**C**	5.737353	14.040634	5.144061
C	4.9211995	−1.027791	17.042284	**H**	6.340356	14.827057	4.687209
H	4.8117297	−2.084156	17.289511	**C**	1.936379	6.500889	2.841215
C	−0.225252	5.6970453	17.030581	**H**	1.723415	5.507646	3.238429
H	−0.626304	5.4406972	18.00649	**C**	−2.269019	9.67978	1.538579
C	6.3687614	2.6828881	10.824946	**H**	−2.421262	9.951518	0.49438
H	7.1025646	2.6606125	10.024301	**C**	4.441093	13.806055	4.684989
C	7.5648208	5.0182863	14.115379	**H**	4.043214	14.37955	3.84379
C	−0.129877	1.4550523	17.00075	**C**	5.502146	12.259301	6.760275
H	−0.377584	1.5643145	15.942788	**H**	5.913585	11.650274	7.566015
C	6.1941922	−0.473675	16.872656	**C**	0.129099	9.927086	7.304631
H	7.0811617	−1.09767	16.987358	**H**	−0.568385	9.969125	8.142129
C	0.5392091	1.1442935	19.696306	**C**	6.273403	13.268097	6.178084
H	0.8011876	1.0132002	20.746607	**H**	7.290394	13.449728	6.527694
C	8.9093622	2.6110762	13.5101	**C**	−2.725094	8.446434	2.01245
C	4.4131437	2.4309155	12.027278	**H**	−3.230729	7.761457	1.330695
H	3.3781075	2.217696	12.288832	**C**	0.641882	8.699427	6.878955
C	5.5474387	6.1060186	10.715709	**H**	0.342894	7.778801	7.381669
H	6.5279709	6.5348572	10.897118	**Au**	1.335025	12.127313	2.43058
C	9.0357633	0.2770652	14.169108	**Fe**	5.801284	12.479052	0.918588
H	8.6115435	−0.728349	14.160931	**Fe**	0.98447	15.889683	5.277097
P	2.4486256	2.1379236	16.206899	**Fe**	−1.086695	13.570368	−1.36798
P	8.1303782	4.044605	12.652102	**N**	3.228186	15.267652	2.058565
P	1.8610985	−0.2323	12.41293	**N**	2.543164	14.513965	−0.098463
Fe	−0.289658	1.0764395	10.118148	**N**	0.986989	15.628202	1.3255
Fe	1.7292715	5.4290166	16.403139	**P**	−0.985867	12.18646	1.8423
Fe	5.0022088	4.1668296	11.143022	**P**	1.937955	12.576398	4.706061
Au	1.8840099	1.4030256	14.076796	**P**	2.787138	10.722605	1.14171

$[1b(Au)]^{+}_{open}$				$[1b(Au)]^{+}_{closed}$			
C	7.2187038	4.7373937	15.247319	**C**	3.2323614	11.361714	−3.052615
H	7.2280705	3.6817033	15.515382	**H**	3.7966355	12.0489	−3.684972
C	9.764646	2.8200168	14.787191	**C**	−1.673334	10.768009	2.6146127
H	10.056694	3.8501805	14.999527	**C**	2.3244885	9.0922774	1.5724914
C	10.299144	1.7840573	15.553293	**C**	3.5755058	14.641813	1.0095669
H	11.001235	2.012755	16.356284	**C**	5.6915375	13.87466	−0.307202
C	4.4948779	−0.66322	13.311214	**H**	5.2721093	13.821745	−1.307385
H	4.1413558	−0.256157	14.258342	**C**	1.8044034	15.74966	2.2843379
C	0.7551229	5.0507902	13.527474	**C**	−1.506878	12.237923	0.1915326
C	0.3684836	−1.018724	10.078736	**C**	−2.724599	12.697298	−0.433955
H	−0.130146	−1.858779	10.551218	**H**	−3.489526	13.305352	0.0368472
C	3.9264997	1.2469243	16.497828	**C**	4.5133383	10.868949	1.2314983
C	−0.47552	−3.691103	14.275159	**C**	−0.784796	11.469493	−0.78713
H	−1.042405	−4.513346	14.712912	**H**	0.1833815	11.012275	−0.636884
C	−0.050083	4.0647814	12.93999	**C**	6.5251787	10.933982	2.3922212
C	6.3457638	1.0802173	16.47063	**H**	7.253731	11.093972	3.181427
H	7.32574	1.5400816	16.335161	**C**	1.1780135	13.836995	5.6175088
C	5.4272284	−1.658447	10.873493	**C**	−0.018479	17.659286	4.9448796
H	5.7913755	−2.041542	9.9196903	**H**	−0.901836	18.058059	5.4347999
C	1.4818449	1.4027768	18.646503	**C**	1.3536118	16.50056	3.4610581
H	2.5060397	1.5390629	18.996264	**C**	1.8451346	9.5724541	−1.419076
C	3.4198024	4.867984	15.733315	**H**	1.3223491	8.8498319	−0.793014
H	3.6312902	4.7179055	14.678651	**C**	4.984476	14.250685	0.8932874
C	−0.817843	0.7817792	19.081105	**C**	5.9469441	14.237683	1.9631744
H	−1.589352	0.451966	19.777509	**H**	5.7362743	14.413829	3.0128351
C	1.7120942	0.8610549	9.7538483	**C**	1.5976547	14.591851	6.7747484
H	2.3997565	1.6793075	9.9417954	**H**	2.6045749	14.630876	7.1761063
C	5.822558	−1.060206	13.184609	**C**	1.3419458	14.888902	0.0406264
H	6.4889905	−0.962011	14.039863	**C**	1.7485681	9.4737416	−2.808639
C	2.8355925	3.8881538	16.614804	**H**	1.1446424	8.679069	−3.248299
C	1.1647294	1.6290166	17.298006	**C**	−0.67397	14.94537	6.4781823
C	5.1801116	2.1118156	10.703335	**H**	−1.682571	15.332119	6.5895178
H	4.7493405	1.619087	9.8371484	**C**	2.1753178	17.082691	4.4948414
C	0.2280747	3.5946934	11.644984	**H**	3.2588461	17.040493	4.5517707
C	0.9864942	−1.585525	13.156956	**C**	1.691533	11.046132	5.5340427
C	1.3668915	4.0619104	10.979705	**C**	−0.230287	14.071146	5.4393753
C	0.4082487	5.5900992	14.846559	**H**	−0.837849	13.669514	4.6401119
C	3.6209573	−0.770049	12.220376	**C**	5.5745407	10.506618	0.3216603
C	5.3205732	5.4162101	9.4818308	**H**	5.4524099	10.244771	−0.723811
H	5.9389872	5.2707065	8.6012934	**C**	−0.360347	14.133749	−3.212115
C	1.8890687	5.5021447	12.839496	**H**	−0.458334	13.646653	−4.177774
C	−1.369682	1.5556554	11.666297	**C**	−3.253265	15.750502	2.4004068
H	−1.192161	1.2405579	12.69062	**H**	−3.37997	16.690387	1.8608895
C	1.2973741	−0.119726	10.725749	**C**	−1.551476	11.444359	−1.992005
C	0.2450598	6.9833602	16.705372	**H**	−1.250754	10.970737	−2.921798
H	0.3383882	7.8443026	17.360666	**C**	1.0193692	11.032642	6.7646716
C	−0.230089	4.8639259	15.913722	**H**	0.7175468	11.969794	7.2317286
H	−0.542734	3.8262435	15.873339	**C**	3.3208989	8.1530398	1.8746949
C	5.4246457	3.0741113	12.800066	**H**	4.3721468	8.4199303	1.7689978
H	5.2185018	3.4373203	13.800934	**C**	3.317125	11.472283	−1.664767
C	2.2398344	4.9817114	11.586047	**H**	3.9685213	12.217267	−1.213952
C	8.4973542	1.2176236	13.496773	**C**	2.6162294	10.587606	−0.831443
H	7.7808888	0.9887701	12.707289	**C**	−2.370357	14.787318	1.9122896
C	0.2179539	−0.58439	8.7251265	**H**	−1.836203	14.957165	0.9805649
H	−0.438721	−1.032934	7.9855394	**C**	−1.782704	9.2184205	4.4808074
C	−0.088531	−1.319875	14.016044	**H**	−1.474748	8.9434686	5.4891656

H	−0.338524	−0.28593	14.25921	**C**	3.813663	12.918274	5.2362984
C	−0.711976	2.6574488	11.014725	**C**	−2.74377	12.207465	−1.775278
C	5.1859772	1.8459004	16.348182	**H**	−3.514633	12.411722	−2.512873
H	5.2553906	2.9129352	16.136569	**C**	−0.008021	16.854093	3.7650814
C	3.5208979	5.3383826	10.964472	**H**	−0.889133	16.527532	3.2225844
C	1.3357604	−2.913036	12.86828	**C**	2.0694639	9.8318416	4.9412589
H	2.1842289	−3.123427	12.215821	**H**	2.5732788	9.8281812	3.975905
C	−2.234327	0.9166345	10.724622	**C**	1.7928215	8.6202677	5.5734116
H	−2.839271	0.0339294	10.90897	**H**	2.0931276	7.6877626	5.0964679
C	−1.190183	2.6895505	9.6554335	**C**	6.807209	10.550738	1.0414858
H	−0.889272	3.4101821	8.9005227	**H**	7.7916882	10.361126	0.623331
C	−1.134364	0.9914942	17.736368	**C**	−1.292099	10.393028	3.9117955
H	−2.15161	0.8262416	17.380101	**H**	−0.6015	11.014716	4.4796633
C	3.8357891	−0.125643	16.778836	**C**	−2.205744	13.563347	2.5779976
H	2.8586563	−0.600568	16.879866	**C**	−1.30495	15.032907	−2.622856
C	6.6798962	3.2099605	12.108181	**H**	−2.238568	15.364098	−3.067843
C	9.9494743	0.4564314	15.28389	**C**	2.4332361	10.371255	−3.630605
H	10.381128	−0.354747	15.871302	**H**	2.3627438	10.286479	−4.715354
C	4.0908291	−1.273623	10.99849	**C**	0.9748409	8.7375133	1.7187926
H	3.4191794	−1.349917	10.143453	**H**	0.1923571	9.4644935	1.5066615
C	−2.127884	1.6217972	9.4826201	**C**	0.4479362	14.73831	−1.112571
H	−2.646392	1.3732606	8.5613115	**C**	−3.834275	14.286868	4.2295175
C	3.6063267	6.0714689	16.477963	**H**	−4.415038	14.076777	5.1284597
H	4.0026698	7.0008521	16.083285	**C**	7.2232233	13.887988	1.4252639
C	6.8252771	5.6909174	16.185104	**H**	8.1423397	13.772558	1.9920668
H	6.5002128	5.3757081	17.177494	**C**	−2.963468	13.314562	3.7331824
C	2.6684395	4.5057035	17.913061	**H**	−2.882412	12.356278	4.2456277
H	2.2338032	4.0382089	18.790128	**C**	−3.976795	15.510464	3.5719656
C	1.0443271	0.5684756	8.5244187	**H**	−4.663646	16.264541	3.9572429
H	1.1222593	1.1440545	7.606741	**C**	0.7081858	13.942936	−2.283546
C	6.2940538	−1.54993	11.963535	**H**	1.5476454	13.270248	−2.42499
H	7.3392321	−1.8439	11.858437	**C**	−0.816027	15.399568	−1.33125
C	0.6948582	6.9109089	15.348475	**H**	−1.29391	16.106255	−0.659486
H	1.1734039	7.7097299	14.789646	**C**	1.3316083	17.799301	5.3983951
C	3.9749256	4.9611894	9.6471689	**H**	1.6581088	18.337284	6.283443
H	3.397908	4.4220169	8.9020353	**C**	5.116545	11.139362	2.509209
C	0.6029641	−3.960947	13.42684	**H**	4.5901324	11.465023	3.3957984
H	0.8783152	−4.992203	13.203814	**C**	0.6226804	7.4589954	2.1492546
C	3.149797	5.8484827	17.817337	**H**	−0.430786	7.2030936	2.2585634
H	3.1331625	6.5845929	18.615704	**C**	−2.64636	8.3977529	3.750706
C	−0.820433	−2.369608	14.571021	**H**	−3.024771	7.4739403	4.1899681
H	−1.653526	−2.156568	15.241456	**C**	0.4550957	15.271291	7.2966376
C	4.6212625	6.0208997	11.605949	**H**	0.4541886	15.947535	8.1467471
H	4.642021	6.4059496	12.620836	**C**	2.9648585	6.8775373	2.3196329
C	7.682691	6.4881633	13.652817	**H**	3.7450513	6.1534387	2.5577782
H	8.0585262	6.8030793	12.677859	**C**	7.0656619	13.660888	0.0211095
C	6.8501325	7.0494301	15.853907	**H**	7.8465098	13.360105	−0.6711
H	6.5589846	7.7977797	16.592412	**C**	4.6376609	11.877465	5.6925632
C	7.272938	7.4467086	14.58334	**H**	4.2529353	10.85956	5.7503527
H	7.312383	8.5057481	14.324778	**C**	5.6297881	14.486305	5.6302674
C	4.9997783	−0.882931	16.920954	**H**	6.0032782	15.511485	5.6259655
H	4.9265432	−1.947341	17.146143	**C**	1.618293	6.5271448	2.4541833
C	−0.321909	5.7157669	17.055804	**H**	1.3460313	5.5288787	2.7990278
H	−0.726476	5.4408647	18.02515	**C**	−2.543141	9.9438366	1.8861534
C	6.5160821	2.6129837	10.805491	**H**	−2.841944	10.223801	0.8762555
H	7.2810306	2.5723663	10.035181	**C**	4.321943	14.225794	5.2214399
C	7.6516339	5.1219481	13.968657	**H**	3.6663595	15.043292	4.9312551
C	−0.144266	1.4100035	16.84726	**C**	5.9521149	12.137996	6.0854861

H	−0.37745	1.5650698	15.791707	**H**	6.5784443	11.317338	6.4372776
C	6.2530804	−0.283404	16.760724	**C**	0.7306377	9.8163611	7.3882501
H	7.16185	−0.877724	16.858956	**H**	0.2036961	9.8130277	8.3432633
C	0.4900901	0.9830893	19.533354	**C**	6.4564431	13.439604	6.0482732
H	0.7395248	0.8074134	20.580196	**H**	7.4808394	13.641154	6.3626401
C	8.8450807	2.5521672	13.756797	**C**	−3.021015	8.7601729	2.4536322
C	4.5072748	2.4099933	11.930658	**H**	−3.69389	8.1216035	1.8798712
H	3.4550477	2.2323441	12.146586	**C**	1.1193784	8.6104555	6.7976873
C	5.7171222	6.0708601	10.689527	**H**	0.8937585	7.6638736	7.2902947
H	6.6933935	6.5000334	10.887091	**Au**	1.3607157	12.208343	2.3934773
C	9.054987	0.1800097	14.248243	**Fe**	5.8741014	12.386924	1.1013589
H	8.7896111	−0.854717	14.024322	**Fe**	0.7869104	15.822536	5.3391787
P	2.4262493	2.2189737	16.134932	**Fe**	−1.067165	13.3624	−1.456168
P	8.2443218	3.9320545	12.690618	**C**	3.1267699	15.29724	2.164997
P	1.9011913	−0.204265	12.405702	**C**	2.6701828	14.447603	−0.044145
Fe	−0.292651	0.9064568	10.050267	**C**	0.925999	15.53932	1.2118151
Fe	1.6403482	5.498215	16.463445	**P**	−1.017687	12.329823	1.9177571
Fe	5.1684267	4.1280325	11.075924	**P**	2.0933694	12.612586	4.6738401
Au	1.9028006	1.5352278	13.972903	**P**	2.7355697	10.779526	0.9901441
H	1.5959163	3.6699313	9.9906284	**H**	3.8375285	15.495334	2.9620068
H	−0.957111	3.7336511	13.446065	**H**	3.0093338	13.986143	−0.96713
H	2.5275035	6.2500408	13.307341	**H**	−0.084487	15.931846	1.2795327

$1b_{open,\ rotated}$				**$[1b(Au)]^{+}_{open,\ rotated}$**			
C	11.697710	−5.238792	0.138518	**C**	1.650149	6.536562	6.343440
Fe	14.045016	6.787964	4.308186	**H**	1.138781	7.500343	6.328525
Fe	13.064036	−1.152038	2.752151	**C**	3.103936	9.144117	4.323966
Fe	18.534846	2.543682	1.599376	**H**	3.730014	8.388351	3.843688
P	17.758851	−0.606861	2.297160	**C**	2.356111	10.023276	3.541967
P	11.186966	−4.002775	2.672872	**H**	2.396771	9.950737	2.454240
P	17.079874	7.176603	2.853874	**C**	5.063783	0.250650	13.347594
C	16.781632	3.087102	0.698565	**H**	4.561293	0.656777	14.226933
C	14.844896	4.308531	1.671629	**C**	1.366084	5.310410	13.487925
H	15.279029	5.231939	1.289750	**C**	1.136234	−0.498864	9.810458
C	13.188323	3.165841	3.008070	**H**	0.614169	−1.297563	10.327441
H	12.318050	3.186163	3.664356	**C**	3.166060	0.903992	16.528309
C	15.645580	5.662027	4.839261	**C**	0.548554	−3.197664	14.129652
H	15.880476	4.704841	4.380662	**H**	0.078345	−4.045043	14.629506
C	17.730948	4.171736	0.654197	**C**	0.572017	4.399490	12.759820
H	17.588064	5.145895	1.115680	**C**	5.347712	0.159220	17.271198
C	13.786395	−2.864575	1.913950	**H**	6.333301	0.388125	17.678241
H	14.387165	−3.599886	2.437765	**C**	6.351092	−0.793539	11.095435
C	18.615833	0.910312	2.814620	**H**	6.853824	−1.197189	10.215965
C	14.976652	1.914057	1.967241	**C**	0.297967	1.307892	18.025842
H	15.497661	0.967191	1.811618	**H**	1.181098	1.255056	18.664283
C	13.696148	4.360798	2.478868	**C**	3.519787	4.634254	16.293839
C	17.385031	1.970352	0.017748	**H**	3.985443	4.523807	15.317831
H	16.932573	0.988975	−0.095266	**C**	−2.072973	0.947515	17.690855
C	18.899789	3.723261	−0.038062	**H**	−3.043249	0.638092	18.080528
H	19.801958	4.303472	−0.208616	**C**	2.523321	1.329932	9.391836
C	17.982785	2.026465	3.478661	**H**	3.230184	2.141487	9.534445
H	16.954468	2.049968	3.830194	**C**	6.410888	−0.098325	13.414487
C	13.130196	5.658587	2.872965	**H**	6.956124	0.041607	14.348137
C	14.267567	−1.723591	1.196952	**C**	2.574930	3.709045	16.876105
H	15.310167	−1.428571	1.094214	**C**	0.418055	1.742053	16.696977
C	13.386376	0.732720	3.484899	**C**	3.896512	9.494725	10.463030
C	13.503734	6.947980	2.347581	**H**	4.290243	10.079687	11.289459
H	14.187912	7.113684	1.521075	**C**	0.947053	4.004798	11.459378

C	19.147006	−1.504101	1.494487	**C**	1.770558	−1.016062	12.866279
C	12.346007	−2.848633	1.884439	**C**	2.147860	4.482002	10.922355
C	15.501775	3.097540	1.422881	**C**	0.895074	5.845691	14.769982
C	19.948017	1.332029	2.453170	**C**	4.349239	0.066813	12.152486
H	20.670028	0.726947	1.914076	**C**	6.234581	6.973845	10.736142
C	18.917065	3.109058	3.532763	**H**	7.081604	7.636063	10.888963
H	18.733927	4.092847	3.953552	**C**	2.582621	5.732970	12.939937
C	16.074132	6.949004	4.348920	**C**	−0.761215	2.071643	11.124929
C	17.099182	9.015592	2.773007	**H**	−0.770946	1.690886	12.142211
C	18.686341	2.361163	−0.433768	**C**	2.076276	0.416078	10.413699
H	19.395042	1.727336	−0.958948	**C**	0.600454	7.232080	16.621504
C	14.259320	−0.225079	4.115461	**H**	0.708902	8.055372	17.321324
H	15.343155	−0.197957	4.099569	**C**	−0.070651	5.242826	15.652767
C	13.833291	1.940893	2.774893	**H**	−0.556851	4.284701	15.505754
C	13.457683	−1.219070	4.757675	**C**	2.589029	8.041611	9.217237
H	13.834365	−2.089195	5.285968	**H**	1.822711	7.327080	8.933288
C	20.100062	−2.240645	2.213758	**C**	2.993530	5.325806	11.659179
H	20.011909	−2.318755	3.298342	**C**	2.264380	10.205704	6.329356
C	20.125785	2.682528	2.891699	**H**	2.221134	10.278614	7.416571
H	21.010827	3.294027	2.745569	**C**	1.016182	−0.149986	8.430846
C	16.128237	9.642363	1.976398	**H**	0.361731	−0.630819	7.709745
H	15.431281	9.031784	1.400125	**C**	0.481075	−0.892465	13.406767
C	13.132536	−0.993440	0.713499	**H**	−0.034313	0.067060	13.359171
H	13.166083	−0.051441	0.172665	**C**	0.048597	3.164751	10.656372
C	14.693307	7.287420	6.192274	**C**	4.435569	1.194356	17.045691
H	14.098672	7.770583	6.962536	**H**	4.710095	2.225969	17.268766
C	18.766187	6.804867	3.484002	**C**	4.256150	5.791806	11.085717
C	12.857884	7.964958	3.118773	**C**	2.442920	−2.241452	12.958839
H	12.966383	9.036264	2.977274	**H**	3.451063	−2.341291	12.556412
C	13.222644	−5.847175	3.504404	**C**	−1.509396	1.552087	10.023097
H	13.265337	−6.177180	2.465462	**H**	−2.186950	0.703969	10.053109
C	18.008556	9.810194	3.486482	**C**	−0.210564	3.308786	9.246875
H	18.772429	9.334243	4.102739	**H**	0.256400	4.039783	8.592821
C	17.528185	−1.543509	3.855643	**C**	−1.953941	1.359976	16.361033
C	14.803571	5.873086	5.976609	**H**	−2.828621	1.372501	15.709898
H	14.305459	5.095996	6.549304	**C**	2.813864	−0.426534	16.242853
C	11.948261	−1.678526	1.137034	**H**	1.831604	−0.657025	15.827939
H	10.923225	−1.368008	0.954484	**C**	3.676375	8.479230	8.377978
C	17.938229	11.203030	3.413843	**C**	1.565939	11.004095	4.150730
H	18.652473	11.810518	3.972121	**H**	0.988280	11.698287	3.539294
C	15.477242	7.952428	5.196553	**C**	4.997354	−0.457066	11.024561
H	15.591098	9.024660	5.072616	**H**	4.444622	−0.601370	10.095929
C	12.320478	−4.836540	3.872873	**C**	−1.172464	2.322036	8.863572
C	19.262936	−1.417828	0.098761	**H**	−1.556392	2.163204	7.860089
H	18.513318	−0.862693	−0.468034	**C**	3.681083	5.722697	17.204930
C	12.081213	−0.887523	4.528797	**H**	4.304548	6.597378	17.045323
H	11.217672	−1.465062	4.845661	**C**	0.917946	5.357012	6.197371
C	11.065214	−5.317942	1.387581	**H**	−0.165732	5.403000	6.076923
C	17.824353	−1.036032	5.128786	**C**	2.155162	4.248020	18.149361
H	18.345263	−0.082033	5.220832	**H**	1.427879	3.803219	18.820555
C	12.035538	0.312886	3.749596	**C**	1.871329	0.968166	8.172732
H	11.138614	0.799926	3.376985	**H**	1.979294	1.482350	7.224122
C	19.788896	6.642004	2.534577	**C**	7.057291	−0.617559	12.288132
H	19.564031	6.778522	1.474419	**H**	8.113856	−0.882687	12.339180
C	20.323996	−2.036619	−0.565596	**C**	1.305593	7.084773	15.385955
H	20.405204	−1.959334	−1.650932	**H**	2.025160	7.788212	14.978012
C	12.264909	−4.441645	5.217885	**C**	5.216792	6.680553	11.697374
H	11.550377	−3.674269	5.519863	**H**	5.171292	7.081971	12.705281

C	16.852275	−2.772552	3.754303	**C**	1.830671	−3.327061	13.589541
H	16.608438	−3.168606	2.766350	**H**	2.361648	−4.276787	13.663709
C	16.048889	11.034642	1.914349	**C**	2.842407	5.486416	18.342170
H	15.285642	11.508196	1.294873	**H**	2.721542	6.151803	19.192002
C	16.471962	−3.474562	4.894650	**C**	−0.129165	−1.977959	14.033025
C	21.365261	6.096089	4.286523	**H**	−1.126297	−1.867000	14.460134
H	22.371309	5.811750	4.597677	**C**	4.707240	5.550136	9.736667
C	19.062287	6.604471	4.841063	**H**	4.191529	4.962059	8.984686
H	18.273530	6.718044	5.585845	**C**	3.693498	5.252549	6.456348
C	12.236600	5.904973	3.979550	**H**	4.782592	5.216429	6.526998
H	11.797955	5.149148	4.623584	**C**	1.572487	4.121170	6.185465
C	16.755156	−2.951747	6.161490	**H**	0.997019	3.204263	6.050560
H	16.437669	−3.489534	7.055951	**C**	2.962561	4.069722	6.317205
C	14.052957	−6.440513	4.457780	**H**	3.485850	3.112418	6.282958
H	14.746345	−7.227852	4.157002	**C**	3.727837	−1.452239	16.471073
C	21.153679	−2.869897	1.548601	**H**	3.448381	−2.480778	16.242564
H	21.888561	−3.442249	2.117137	**C**	−0.246799	6.090568	16.787750
C	17.436080	−1.737591	6.274790	**H**	−0.889244	5.888254	17.639444
H	17.663584	−1.328329	7.260523	**C**	4.483751	9.378559	9.164303
C	12.071469	7.319216	4.127624	**H**	5.396286	9.860298	8.824550
H	11.474962	7.814409	4.888288	**C**	3.046339	6.496866	6.482646
C	13.997482	−6.028954	5.793159	**C**	−0.710529	1.753795	15.865726
H	14.645206	−6.494969	6.537254	**H**	−0.602014	2.067649	14.825187
C	13.103304	−5.023944	6.170876	**C**	4.998218	−1.161234	16.980456
H	13.047872	−4.701997	7.211924	**H**	5.714233	−1.965404	17.152326
C	21.271165	−2.764799	0.159089	**C**	−0.947006	0.918398	18.520147
H	22.096204	−3.256207	−0.358583	**H**	−1.038229	0.581983	19.553353
C	16.955173	11.818527	2.633731	**C**	3.056260	9.217635	5.726888
H	16.900714	12.906732	2.579891	**C**	2.728704	8.665928	10.496838
C	10.752369	−7.375869	−0.504628	**H**	2.084969	8.500189	11.356881
C	20.353950	6.248620	5.238111	**C**	5.918857	6.277932	9.526608
H	20.569620	6.086720	6.295366	**H**	6.475036	6.332411	8.595313
C	21.080838	6.300217	2.932461	**C**	1.526607	11.095757	5.543402
H	21.865214	6.177925	2.183862	**H**	0.915691	11.861724	6.023651
C	11.538169	−6.260631	−0.802252	**P**	2.029293	2.239980	16.028541
C	10.115347	−7.462044	0.738186	**P**	4.084765	8.015154	6.666922
C	10.262221	−6.436410	1.671136	**P**	2.573467	0.452779	12.131255
H	15.928038	−4.414914	4.799484	**Fe**	0.508729	1.440734	9.640630
H	12.323049	−4.376181	−0.094701	**Fe**	1.721388	5.512674	16.611087
H	12.036565	−6.185662	−1.770332	**Fe**	4.378939	7.535956	10.048286
H	9.754804	−6.503243	2.636613	**Au**	2.094126	2.079784	13.719089
H	10.631878	−8.174126	−1.238383	**H**	2.424753	4.183424	9.913009
H	9.495984	−8.328304	0.976642	**H**	−0.406213	4.108645	13.143336
				H	3.214935	6.408941	13.514351

$[1c(Au)]^+_{open}$				**$[1c(Au)]^+_{closed}$**			
C	7.1823035	4.6698648	15.236198	**C**	2.4496027	10.658412	−2.856271
H	7.178547	3.6055461	15.465973	**H**	2.8398717	11.241666	−3.691417
C	9.7410656	2.7839455	14.709053	**C**	−1.442345	10.244299	1.9408068
H	10.044396	3.8108728	14.921639	**C**	2.9048327	8.9931853	2.0901148
C	10.282139	1.7398833	15.458547	**C**	3.721847	14.802326	0.8447092
H	11.001252	1.957948	16.249323	**C**	5.4126122	13.765564	−0.864545
C	4.499657	−0.760188	13.367377	**H**	4.7472279	13.588883	−1.698698
H	4.125449	−0.394041	14.323813	**C**	2.3048283	16.098106	2.4337551
C	0.6923035	5.1402563	13.514642	**C**	−1.336082	12.29786	−0.011268
C	0.3799287	−1.052505	10.111163	**C**	−2.616149	12.633152	−0.590462
H	−0.131718	−1.881023	10.590169	**H**	−3.503608	12.925944	−0.039027
C	3.9380051	1.2392684	16.534392	**C**	4.6814552	10.921567	1.1099999

C	−0.466439	−3.721397	14.295385	**C**	−0.443434	11.974131	−1.096821
H	−1.039976	−4.539542	14.732133	**H**	0.6004069	11.706937	−0.993022
C	−0.060031	4.1389832	12.888471	**C**	6.8488902	11.13929	1.9196442
C	6.3553008	1.0561492	16.479632	**H**	7.6908023	11.382515	2.5612108
H	7.3363665	1.5050041	16.317577	**C**	0.7560895	14.173998	5.3496283
C	5.4856009	−1.660725	10.913307	**C**	1.4423359	18.200122	5.4272305
H	5.8709966	−2.006147	9.9535531	**H**	0.8486148	18.913713	5.9909834
C	1.4790959	1.4736055	18.676798	**C**	2.1837593	16.809273	3.7140288
H	2.4999877	1.6210937	19.031723	**C**	1.4679116	9.1650916	−0.709351
C	3.3978099	4.8604652	15.649439	**H**	1.0776219	8.5747436	0.1184199
H	3.5806115	4.6850692	14.59395	**C**	5.0442563	14.311284	0.426823
C	−0.82403	0.8646827	19.109118	**C**	6.2663388	14.379609	1.1973532
H	−1.602062	0.5574777	19.8086	**H**	6.3587254	14.720809	2.2184579
C	1.7534523	0.802575	9.771143	**C**	0.8679323	14.697085	6.693919
H	2.4479533	1.6150579	9.9454499	**H**	1.6141051	14.409108	7.4274628
C	5.8266862	−1.16348	13.256966	**C**	1.3113241	15.230975	0.3226828
H	6.4719089	−1.108477	14.13208	**C**	1.0126336	8.9142818	−2.003599
C	2.8616967	3.8953675	16.576739	**H**	0.2739661	8.1295165	−2.169466
C	1.17402	1.6564578	17.318856	**C**	−0.906276	15.76683	5.6515829
C	5.1316143	2.1979024	10.597221	**H**	−1.728053	16.447704	5.4534306
H	4.7045959	1.7437414	9.7083875	**C**	3.0246964	16.609162	4.8752056
C	0.2040985	3.6445417	11.60196	**H**	3.8455546	15.908084	4.9556646
C	1.0115993	−1.626667	13.180479	**C**	0.9656182	11.355377	5.5306208
C	1.3313817	4.1809547	10.96762	**C**	−0.341815	14.853793	4.7121977
C	0.3639729	5.6255717	14.861383	**H**	−0.661881	14.706926	3.6888603
C	3.6527546	−0.815405	12.250827	**C**	5.5974933	10.495617	0.0785615
C	5.3570139	5.5579856	9.5086293	**H**	5.321292	10.127721	−0.903565
H	5.9866383	5.4360152	8.6325092	**C**	−0.841667	15.287659	−2.758211
C	1.7962722	5.6076763	12.784344	**H**	−1.044368	15.136302	−3.814425
C	−1.33195	1.5642125	11.66101	**C**	−3.472041	14.96088	2.9579259
H	−1.164793	1.289743	12.696818	**H**	−3.793322	15.930423	2.5744339
C	1.323997	−0.163543	10.749756	**C**	−1.171272	12.090865	−2.318857
C	0.2107287	6.9212164	16.79017	**H**	−0.760821	11.94304	−3.312947
H	0.2986729	7.7533127	17.482341	**C**	−0.240292	11.448396	6.2400699
C	−0.218035	4.8274699	15.914005	**H**	−0.748595	12.408795	6.3210902
H	−0.516321	3.7908842	15.829992	**C**	4.0863698	8.2665661	2.306674
C	5.3687449	3.080311	12.730933	**H**	5.0467231	8.6694641	1.9904345
H	5.1600224	3.4050044	13.74459	**C**	2.9016939	10.920198	−1.562045
C	2.2226036	5.1049983	11.543643	**H**	3.6302893	11.708627	−1.387324
C	8.4345304	1.2002047	13.433565	**C**	2.4175092	10.172313	−0.477439
H	7.6996517	0.9809985	12.658231	**C**	−2.591178	14.181634	2.2072989
C	0.236241	−0.625158	8.7543304	**H**	−2.226588	14.538631	1.2479008
H	−0.428017	−1.068971	8.0186444	**C**	−1.708647	8.3178664	3.3993139
C	−0.097797	−1.352292	13.992353	**H**	−1.603534	7.8722154	4.3886718
H	−0.370649	−0.316012	14.198187	**C**	3.33545	12.94312	5.3644271
C	−0.694513	2.662427	10.979109	**C**	−2.505992	12.50499	−2.007738
C	5.1987424	1.8248907	16.348895	**H**	−3.290404	12.724727	−2.726459
H	5.270049	2.8841201	16.101707	**C**	1.2001749	17.802358	4.07776
C	3.5241102	5.4581382	10.952436	**H**	0.4036406	18.171955	3.4435101
C	1.386324	−2.955985	12.936467	**C**	1.6165121	10.114891	5.4278574
H	2.2594599	−3.170941	12.318992	**H**	2.5470413	10.03095	4.8644012
C	−2.193248	0.8940176	10.741063	**C**	1.0729123	8.9861742	6.037952
H	−2.789436	0.0118156	10.953541	**H**	1.5885819	8.0299038	5.9529453
C	−1.171263	2.6467049	9.6176022	**C**	6.9261537	10.638028	0.5809037
H	−0.8715	3.3369167	8.8359821	**H**	7.8380426	10.438653	0.0251988
C	−1.127855	1.0299835	17.755321	**C**	−1.292692	9.633794	3.1987081
H	−2.141472	0.8528396	17.394681	**H**	−0.822386	10.171128	4.0215719
C	3.8412543	−0.12324	16.858368	**C**	−2.171844	12.925832	2.6704828

H	2.8625465	−0.587464	16.989079	**C**	−1.764259	15.771762	−1.783242
C	6.6312096	3.2292516	12.054551	**H**	−2.793393	16.068397	−1.962533
C	9.9173912	0.4166237	15.186719	**C**	1.5012191	9.6575612	−3.081026
H	10.354747	−0.40187	15.759606	**H**	1.1447977	9.4564869	−4.09177
C	4.1490717	−1.270668	11.021089	**C**	1.6830566	8.4516663	2.5103251
H	3.4973919	−1.308064	10.148418	**H**	0.7631815	9.0170809	2.377039
C	−2.096986	1.5650383	9.48023	**C**	0.2431847	15.279626	−0.689118
H	−2.6112	1.2838044	8.5659848	**C**	−3.528155	13.25182	4.6577863
C	3.6013194	6.0831287	16.355933	**H**	−3.893771	12.878722	5.6151881
H	3.9659809	7.0060128	15.919055	**C**	7.3480233	13.922623	0.3882661
C	6.8049517	5.5954131	16.207695	**H**	8.3837956	13.841669	0.7043956
H	6.474102	5.2508578	17.188443	**C**	−2.653677	12.467319	3.9061386
C	2.7403723	4.5422047	17.86569	**H**	−2.359951	11.49302	4.2881358
H	2.3470745	4.0926066	18.771197	**C**	−3.940674	14.501604	4.190205
C	1.0800979	0.5135567	8.5455944	**H**	−4.627224	15.109326	4.780303
H	1.1662773	1.0849356	7.6262994	**C**	0.3847026	14.979	−2.098533
C	6.3247929	−1.606777	12.028328	**H**	1.2628365	14.571392	−2.580719
H	7.3699105	−1.90553	11.936941	**C**	−1.107921	15.772896	−0.518561
C	0.623728	6.9314177	15.421385	**H**	−1.541298	16.12998	0.4048272
H	1.0720502	7.768383	14.898872	**C**	2.5658915	17.465216	5.9179641
C	3.9995729	5.1318994	9.623155	**H**	2.9782421	17.518835	6.9210558
H	3.4300214	4.6448788	8.8430497	**C**	5.4713347	11.317212	2.2491853
C	0.6456307	−3.998851	13.494322	**H**	5.0774243	11.65944	3.1991731
H	0.9401923	−5.031818	13.306665	**C**	1.632842	7.1946293	3.1106543
C	3.2040028	5.8870512	17.717958	**H**	0.6687972	6.7892998	3.4181163
H	3.2121077	6.6415432	18.49912	**C**	−2.22797	7.5760974	2.3355507
C	−0.837736	−2.397363	14.545213	**H**	−2.541527	6.5428891	2.488162
H	−1.698528	−2.178751	15.177751	**C**	−0.164125	15.670282	6.8722743
C	4.6369608	6.0799362	11.645363	**H**	−0.324677	16.266981	7.7657136
H	4.6513094	6.4221434	12.671866	**C**	4.0347704	7.0181394	2.9296659
C	7.6764033	6.4669419	13.704657	**H**	4.9591038	6.4641867	3.0976506
H	8.0598285	6.8111481	12.742831	**C**	6.8212753	13.542923	−0.882897
C	6.8532075	6.9640583	15.924895	**H**	7.3843361	13.126686	−1.713017
H	6.5722343	7.6903255	16.688756	**C**	3.5983242	12.61186	6.7028953
C	7.2842737	7.3985908	14.669619	**H**	2.8079522	12.190548	7.3252931
H	7.3426217	8.465221	14.448762	**C**	5.6421624	13.640341	5.092871
C	5.0026915	−0.883616	17.007648	**H**	6.4398825	14.028352	4.4588277
H	4.9260027	−1.939937	17.267228	**C**	2.809729	6.4744159	3.3255611
C	−0.304893	5.6216655	17.094918	**H**	2.7748692	5.4936377	3.8013749
H	−0.676756	5.2867254	18.058365	**C**	−1.957013	9.4919844	0.8744973
C	6.4716104	2.6806441	10.729658	**H**	−2.062814	9.9438238	−0.110658
H	7.242426	2.6605328	9.964412	**C**	4.3664292	13.443353	4.5620679
C	7.6193736	5.0910802	13.970775	**H**	4.1622924	13.663194	3.5146473
C	−0.130145	1.4205129	16.862038	**C**	4.8753024	12.804953	7.2309435
H	−0.355872	1.542805	15.800717	**H**	5.0760908	12.544791	8.2708757
C	6.2574663	−0.297476	16.812814	**C**	−0.788012	10.310306	6.8386243
H	7.1636612	−0.894561	16.918627	**H**	−1.72664	10.388114	7.3885707
C	0.4793904	1.0817127	19.567259	**C**	5.8968252	13.32593	6.4296588
H	0.7188516	0.9405807	20.621618	**H**	6.8935569	13.475086	6.8460919
C	8.7997018	2.5296495	13.694655	**C**	−2.334889	8.1619713	1.0718992
C	4.4513134	2.4572049	11.82976	**H**	−2.729586	7.586	0.2340175
H	3.3981727	2.2717972	12.036345	**C**	−0.132472	9.0802818	6.7415801
C	5.7468759	6.1432446	10.750524	**H**	−0.557224	8.1961741	7.2185235
H	6.7290065	6.5376063	10.9862	**Au**	1.4069014	12.073501	2.375202
C	9.0004255	0.1540889	14.167676	**Fe**	5.9468266	12.446605	0.6168403
H	8.7232927	−0.876989	13.94294	**Fe**	1.0816349	16.175403	5.3131014
P	2.4454023	2.2142699	16.152536	**Fe**	−1.127841	13.869019	−1.300526
P	8.1974157	3.9308717	12.659099	**C**	3.5360739	15.593327	1.9932138

P	1.9321667	−0.252642	12.425442	**C**	2.5591502	14.631182	0.0741242
Fe	−0.255385	0.8807992	10.066399	**C**	1.2308022	15.904435	1.5530166
Fe	1.6426438	5.4902109	16.439806	**P**	−0.926213	11.987198	1.7092961
Fe	5.1418593	4.2009903	11.0428	**P**	1.6672644	12.794408	4.6462879
Au	1.954874	1.4731076	14.003579	**P**	2.913904	10.611146	1.2268361
F	1.5895283	3.749012	9.709386	**F**	4.6288125	15.931826	2.7200691
F	−1.16239	3.6753676	13.528433	**F**	2.661937	13.872059	−1.044203
F	2.5223016	6.6058638	13.343772	**F**	0.0374449	16.439495	1.9071389

$[1a^F(Au)]^+_{open}$				**$[1a^F(Au)]^+_{closed}$**			
C	7.4430184	4.5603742	15.124225	**C**	2.3775013	10.897376	−3.014399
F	7.5064766	3.2196441	15.228351	**F**	1.854697	11.818394	−3.836567
C	10.581593	3.6185525	13.261029	**C**	−1.667691	10.255316	2.1679014
F	10.81871	4.936534	13.093362	**C**	2.4662556	8.8307405	1.6368368
C	11.630073	2.8200611	13.713809	**C**	3.5998271	14.811209	0.6698687
F	12.836031	3.344457	13.963111	**C**	5.0794418	13.351345	−0.864535
C	4.3346451	−1.315427	13.486488	**H**	4.3036932	13.026278	−1.54685
F	3.6302282	−1.395775	14.637334	**C**	2.3905704	16.134953	2.0630888
C	0.8482625	5.162999	13.591705	**C**	−1.587384	12.44819	0.3616522
C	0.4829319	−0.751962	9.9288835	**C**	−2.8093	13.077135	−0.07221
H	0.0406886	−1.710882	10.176872	**H**	−3.515482	13.610755	0.5528214
C	3.2159442	0.6441238	17.023277	**C**	4.643091	10.777031	1.4151194
C	−0.34881	−4.310621	13.516372	**C**	−0.97983	11.841149	−0.799362
F	−0.985499	−5.431238	13.843574	**H**	−0.064493	11.264803	−0.792833
N	0.0476445	4.1483081	13.203811	**C**	6.5259781	11.519704	2.5413582
C	5.4327039	−0.225325	17.577125	**H**	7.1704935	12.021816	3.2564912
F	6.7517019	−0.037515	17.67173	**C**	1.0053958	14.313333	5.1473076
C	5.8185821	−1.268409	11.15551	**C**	1.572302	18.358974	4.9538661
F	6.5292716	−1.255431	10.023704	**H**	0.9604371	19.055558	5.5194499
C	0.795301	1.888826	18.812279	**C**	2.3251486	16.945604	3.2793381
F	2.0151564	1.9215502	19.382814	**C**	3.4671688	9.0157006	−1.285275
C	3.4125484	4.2665864	15.407842	**F**	4.0336787	8.0700212	−0.512368
H	3.3309019	3.9863365	14.363044	**C**	4.8656306	14.185458	0.2907622
C	−1.59467	1.7871039	19.114719	**C**	6.1425421	14.400548	0.9152354
F	−2.657562	1.7483317	19.913582	**H**	6.3040045	14.976629	1.8195244
C	1.7068117	1.2355084	10.066193	**C**	0.9675263	14.969633	6.4338696
H	2.2898849	2.0684157	10.444586	**H**	1.594086	14.741596	7.2890765
C	5.6931525	−1.606752	13.543596	**C**	1.418781	15.270032	0.2012242
F	6.2725874	−1.931714	14.705475	**C**	3.4501806	8.7657766	−2.65845
C	2.8958142	3.5146758	16.525511	**F**	3.9681801	7.6337703	−3.145201
C	0.6642626	1.8854414	17.415924	**C**	−0.668611	15.91802	5.0892482
C	5.017641	2.1826291	10.761553	**H**	−1.439463	16.593507	4.731342
H	4.5217414	1.670576	9.943695	**C**	3.2451317	16.868169	4.3865533
C	0.2276425	3.7563628	11.925998	**H**	4.1384242	16.258311	4.4072691
C	1.0053577	−1.923397	12.821785	**C**	1.3175051	11.434276	5.5350321
N	1.2057839	4.1918045	11.113341	**C**	0.0092754	14.930564	4.3115359
C	0.6282056	5.7312403	14.920024	**H**	−0.109799	14.742226	3.250887
C	3.6764889	−0.972958	12.296353	**C**	5.8039499	10.349499	0.6720888
C	5.0107163	5.395992	9.4124852	**H**	5.8096968	9.7906555	−0.256278
H	5.5973745	5.1985847	8.5203188	**C**	−0.831666	14.997592	−2.752823
N	1.8642946	5.664791	12.869061	**H**	−1.092567	14.706154	−3.76603
C	−1.261694	1.6389007	12.09466	**C**	−3.484177	14.850076	3.7729329
H	−0.995465	1.3502567	13.106052	**F**	−3.778296	16.136076	3.532527
C	1.3730341	0.0195132	10.766839	**C**	−1.8284	12.080031	−1.919022
C	0.921672	7.0068682	16.831817	**H**	−1.628587	11.775688	−2.942095
H	1.2464739	7.7876904	17.512942	**C**	0.0949961	11.363034	6.2095853
C	−0.048126	5.0753022	16.005146	**F**	−0.706219	12.438558	6.3194695
H	−0.594777	4.1464142	15.907721	**C**	3.225202	8.0497598	2.5167111

C	5.4321534	3.1957906	12.807138	**F**	4.3659956	8.5086375	3.0499397
H	5.3216767	3.5529455	13.823382	**C**	2.4128806	11.118501	−1.638051
C	2.0582058	5.080388	11.671774	**C**	2.9378535	10.195067	−0.733603
C	9.1124583	1.7442382	13.207694	**C**	−2.567661	14.180992	2.9673961
F	7.9070292	1.1649394	13.018259	**F**	−1.986613	14.901663	1.9907151
C	0.292708	−0.019115	8.7193833	**C**	−1.464826	8.0113118	3.144331
H	−0.346281	−0.317922	7.8939165	**F**	−0.778462	7.1518073	3.9121696
C	−0.030393	−1.931927	13.76737	**C**	3.5292476	13.165466	5.6074709
F	−0.427838	−0.798639	14.374409	**C**	−2.955276	12.838961	−1.470294
C	−0.738284	2.7802333	11.398402	**H**	−3.761168	13.214253	−2.094216
C	4.6040433	0.8069936	17.133592	**C**	1.2897024	17.878569	3.6368478
F	5.1938808	1.963453	16.791597	**H**	0.4392015	18.13526	3.0139713
C	3.2908666	5.4022951	10.96529	**C**	2.0869506	10.265091	5.5068084
C	1.3210059	−3.15243	12.216945	**F**	3.278077	10.272596	4.8672675
F	2.2696589	−3.220372	11.268009	**C**	1.6796265	9.0764558	6.1018268
C	−2.153605	0.9493355	11.21817	**F**	2.4421582	7.9785183	6.0303002
H	−2.690186	0.0331463	11.445177	**C**	6.9579253	10.805722	1.3783262
C	−1.331418	2.8007956	10.084748	**H**	7.9869886	10.672022	1.0577727
H	−1.129886	3.5427029	9.3186847	**C**	−0.978054	9.2937379	2.9165356
C	−1.759761	1.769992	17.726559	**C**	−2.202568	12.841451	3.1650929
F	−2.985338	1.7144463	17.198463	**C**	−1.673195	15.716407	−1.841532
C	2.6969028	−0.618588	17.34302	**H**	−2.681322	16.065274	−2.045607
F	1.3805295	−0.870699	17.173729	**C**	2.8978331	9.709268	−3.530306
C	6.5962121	3.3732884	11.986788	**F**	2.8797421	9.4803353	−4.842131
C	11.406952	1.4539016	13.907752	**C**	1.321258	8.2352673	1.0911689
F	12.394985	0.6668828	14.340851	**F**	0.540239	8.9369862	0.2341278
C	4.4513398	−0.988815	11.127204	**C**	0.3133675	15.233735	−0.754974
F	3.9098245	−0.749742	9.9233211	**C**	−3.695587	12.869751	5.1195863
C	−2.209604	1.6746759	9.9834891	**F**	−4.21661	12.227939	6.1683424
H	−2.795112	1.4042581	9.1098856	**C**	7.1320177	13.738104	0.1287542
C	3.9574737	5.4818963	15.91372	**H**	8.1951118	13.697695	0.3473909
H	4.3740811	6.2804328	15.308956	**C**	−2.783642	12.221608	4.2852892
C	7.1873313	5.2701011	16.297104	**F**	−2.479004	10.95718	4.6321788
F	7.0226264	4.6325479	17.464318	**C**	−4.056974	14.192409	4.8615958
C	3.1184735	4.2908681	17.724392	**F**	−4.915026	14.82697	5.6581243
H	2.852609	4.0059236	18.735098	**C**	0.3878494	14.689838	−2.084145
C	1.0497325	1.1938254	8.8001856	**H**	1.2363255	14.156356	−2.492926
H	1.0754258	1.9810221	8.0532214	**C**	−0.974445	15.857786	−0.607422
C	6.4447669	−1.579789	12.364387	**H**	−1.325431	16.36439	0.2829017
F	7.7390488	−1.877795	12.388013	**C**	2.7739547	17.730495	5.4155881
C	1.2241757	6.9372683	15.436006	**H**	3.2323374	17.873035	6.389677
H	1.8175574	7.6379989	14.858569	**C**	5.1050812	11.504897	2.5633288
C	3.6824919	4.931893	9.6609281	**H**	4.4529267	11.935452	3.306884
H	3.0630914	4.3361586	8.999221	**C**	0.9493755	6.925791	1.3730974
C	0.6676158	−4.336848	12.555434	**F**	−0.145321	6.3890756	0.814569
F	0.9948708	−5.486447	11.961348	**C**	−2.681414	7.6261234	2.5784093
C	3.7774364	5.4965688	17.335937	**F**	−3.151216	6.396533	2.76811
H	4.0661131	6.3007962	18.005594	**C**	−0.078284	15.939389	6.3939705
C	−0.701941	−3.101438	14.12217	**H**	−0.347714	16.612908	7.2022261
F	−1.681711	−3.069431	15.030099	**C**	2.8564607	6.7414414	2.8435978
C	4.4008683	6.1344871	11.522421	**F**	3.6040989	6.0214203	3.6841524
H	4.4105389	6.5990831	12.502029	**C**	6.4759549	13.089844	−0.967894
C	7.4932646	6.5895435	13.873573	**H**	6.9569929	12.476766	−1.72449
F	7.6508147	7.2769314	12.727156	**C**	3.6564592	12.863311	6.9748166
C	7.072083	6.6610831	16.245053	**F**	2.6167822	12.40616	7.698552
F	6.7928616	7.3504115	17.357269	**C**	5.8655619	13.919114	5.6682428
C	7.2165607	7.32759	15.026444	**F**	6.9183892	14.443444	5.0239536
F	7.0903922	8.6603827	14.975233	**C**	1.7184136	6.1743379	2.2671169

C	3.4990089	−1.661522	17.796231	**F**	1.3621511	4.9269839	2.5679719
F	2.9661286	−2.853505	18.086821	**C**	−2.910398	9.8483077	1.6535737
C	0.146754	5.852581	17.18442	**F**	−3.715798	10.705029	1.0096486
H	−0.219656	5.6113943	18.177702	**C**	4.6590311	13.721666	4.999162
C	6.3292443	2.751301	10.714069	**F**	4.6025806	14.108228	3.7167057
H	7.0044471	2.7336195	9.863424	**C**	4.850739	13.05076	7.6734667
C	7.6150182	5.1939013	13.884623	**F**	4.924875	12.749985	8.9739065
C	−0.636886	1.8163407	16.901005	**C**	−0.34552	10.183473	6.8141192
C	4.8779885	−1.462146	17.915855	**F**	−1.520155	10.150695	7.4525843
F	5.6613348	−2.454384	18.333535	**C**	5.967551	13.573932	7.0165926
C	−0.308455	1.8465168	19.662155	**F**	7.1098421	13.759853	7.6756054
F	−0.146518	1.8574304	20.987593	**C**	−3.404488	8.55292	1.8257253
C	9.2999574	3.1146584	12.995136	**F**	−4.584641	8.2089569	1.302021
C	4.4637849	2.4665706	12.052448	**C**	0.4459482	9.0340057	6.7576341
H	3.4619279	2.2123126	12.398472	**F**	0.0256458	7.9018018	7.3220397
C	5.4521683	6.1345513	10.557675	**Au**	1.4046764	12.012867	2.3223314
H	6.4317912	6.5845267	10.682847	**Fe**	5.7556034	12.380126	0.8234806
C	10.142785	0.9159198	13.654362	**Fe**	1.3255044	16.318032	4.9309321
F	9.923547	−0.390669	13.865024	**Fe**	−1.218284	13.860878	−1.085708
P	2.1187427	1.9324004	16.3181	**N**	3.5835369	15.593653	1.7654385
P	8.0923709	4.3411682	12.309816	**N**	2.5539	14.638012	−0.154329
P	1.9321278	−0.409199	12.395147	**N**	1.2668852	15.997415	1.3261605
Fe	−0.27946	1.0966486	10.356518	**P**	−1.030078	11.987663	2.0135628
Fe	1.9718479	5.3020643	16.36844	**P**	1.9730747	12.902825	4.6304352
Fe	4.950757	4.202837	11.085946	**P**	2.9097053	10.532645	1.081073
Au	1.8370228	1.121114	14.156427	**F**	1.9267522	12.277164	−1.182756
F	−0.853568	1.8081377	15.573497	**F**	0.1843444	9.6058737	3.522852